

Identification of Hybrid Dynamical Models for Human Movement via Switched System Optimal Control

Ram Vasudevan



Electrical Engineering and Computer Sciences
University of California at Berkeley

Technical Report No. UCB/EECS-2014-38

<http://www.eecs.berkeley.edu/Pubs/TechRpts/2014/EECS-2014-38.html>

May 1, 2014

Copyright © 2014, by the author(s).
All rights reserved.

Permission to make digital or hard copies of all or part of this work for personal or classroom use is granted without fee provided that copies are not made or distributed for profit or commercial advantage and that copies bear this notice and the full citation on the first page. To copy otherwise, to republish, to post on servers or to redistribute to lists, requires prior specific permission.

**Identification of Hybrid Dynamical Models for Human Movement via Switched
System Optimal Control**

by

Ramanarayan Vasudevan

A dissertation submitted in partial satisfaction of the
requirements for the degree of
Doctor of Philosophy

in

Engineering – Electrical Engineering and Computer Sciences

in the

Graduate Division

of the

University of California, Berkeley

Committee in charge:

Professor Ruzena K. Bajcsy, Chair
Professor Francesco Borrelli
Professor Claire J. Tomlin

Fall 2012

**Identification of Hybrid Dynamical Models for Human Movement via Switched
System Optimal Control**

Copyright 2012
by
Ramanarayan Vasudevan

Abstract

Identification of Hybrid Dynamical Models for Human Movement via Switched System
Optimal Control

by

Ramanarayan Vasudevan

Doctor of Philosophy in Engineering – Electrical Engineering and Computer Sciences

University of California, Berkeley

Professor Ruzena K. Bajcsy, Chair

The empirical observation of human locomotion has found considerable utility in the diagnosis of numerous neuromuscular pathologies. Unfortunately without the construction of a dynamical system model of the measured gait, the effectualness of these observations is restricted to just the existing diagnostic variety rather than the prediction of potential instabilities in gait or guiding the construction of user specific prosthetics. In order to construct a dynamical system model of an observed gait in an automated fashion, one requires a family of representations rich enough to describe the dynamics of gait and an automated procedure to select a particular representation capable of describing a given observation from this family.

The goal of this thesis is to address these two problems. First, a hybrid dynamical system representation is introduced that is shown to be capable of describing the discontinuities in dynamics that occur during locomotion. In particular, such a representation is constructible from observation given an unconstrained Lagrangian which is intrinsic to the biped after the identification of the sequence of contact points that are enforced during the observed motion. Second, a specific hybrid dynamical system representation is shown to be constructible from observed data by optimally switching between the set of vector fields corresponding to all possible combinations of contact point enforcements.

At this point an algorithm for the computation of an optimal control of constrained nonlinear switched dynamical systems is devised. The control parameter for such systems include a continuous-valued input and discrete-valued input, where the latter corresponds to the mode of the switched system that is active at a particular instance in time. The presented approach, which this thesis proves converges to local minimizers of the constrained optimal control problem, first relaxes the discrete-valued input, performs traditional optimal control, and then projects the constructed relaxed discrete-valued input back to a pure discrete-valued input by employing an extension of the classical Chattering Lemma. This algorithm is extended by formulating a computationally implementable algorithm that works by discretizing the time interval over which the switched dynamical system is defined. Impor-

tantly, this thesis proves that the implementable algorithm constructs a sequence of points by recursive application that converge to the local minimizers of the original constrained optimal control problem. Four simulation experiments are included to validate the theoretical developments and illustrate its superiority when compared to standard mixed integer optimization techniques.

The thesis concludes by applying the presented algorithm to perform the identification of a hybrid dynamical system representation of two classes of gaits. The first is a synthetic gait generated by the application of feedback linearization to a classical robotic bipedal model. For this synthetic observation, the presented identification scheme is able to correctly identify the correct model. The second set of gaits is one constructed from motion capture observations of 9 subjects during a flat ground walking experiment. For each subject, the presented identification scheme determines a distinct hybrid dynamical system representation. Surprisingly, the identified models for each participant share an identical discrete structure, or an identical sequence of contact point enforcements.

“The miracle of the appropriateness
of the language of mathematics
for the formulation of the
laws of physics is a wonderful gift
that we neither understand nor deserve.”

-Eugene Wigner

Contents

Contents	ii
List of Figures	iv
List of Tables	vii
1 Introduction	1
1.1 Applications of Automated Identification of Locomotion	3
1.2 Steps Required for Automated Identification	4
1.3 Contributions and Organization	8
I A Conceptual Algorithm for Hybrid Dynamical System Identification	10
2 The Identification Problem	11
2.1 Norms and Function Spaces	11
2.2 From Constraints to Models	12
2.3 The Switched System Optimal Control Problem	18
3 A Conceptual Algorithm for Switched System Optimal Control	25
3.1 Directional Derivatives	25
3.2 The Weak Topology on the Optimization Space and Local Minimizers	27
3.3 An Optimality Condition	28
3.4 Choosing a Step Size and Projecting the Relaxed Discrete Input	30
3.5 Switched System Optimal Control Algorithm	33
4 Proving the Convergence of the Conceptual Algorithm	35
4.1 Continuity	35
4.2 Derivation of Algorithm Terms	38
4.3 Approximating Relaxed Inputs	48
4.4 Convergence of the Algorithm	52

II An Implementable Algorithm for Hybrid Dynamical System Identification	58
5 An Implementable Algorithm	59
5.1 Discretized Optimization Space	59
5.2 Discretized Trajectories, Cost, Constraint, and Optimal Control Problem . .	61
5.3 Local Minimizers and a Discretized Optimality Condition	62
5.4 Choosing a Discretized Step Size and Projecting the Discretized Relaxed Discrete Input	65
5.5 An Implementable Switched System Optimal Control Algorithm	66
6 Proving the Convergence of the Implementable Algorithm	69
6.1 Continuity and Convergence of the Discretized Components	69
6.2 Derivation of the Implementable Algorithm Terms	75
6.3 Convergence of the Implementable Algorithm	89
III Results	97
7 Examples	98
7.1 Constrained Switched Linear Quadratic Regulator (LQR)	101
7.2 Double Tank System	102
7.3 Quadrotor Helicopter Control	103
7.4 Bevel-Tip Flexible Needle	104
8 Identification of Bipedal Locomotion	106
8.1 Identification from Synthetically Generated Gait	106
8.2 Identification of Human Gait from Motion Capture Data	111
9 Discussion and Concluding Remarks	120
Bibliography	122

List of Figures

1.1	An illustration from [21] of the hand calculations required in order to measure joint angle evolution in the lower extremities for a patient wearing a prosthetic.	2
1.2	An example of a sequence of constraint enforcements. The red dots indicate the constraints enforced in each discrete phase (or domain)	5
1.3	An illustration of the type of tracking achieved by using the methodology presented in [49, 50]. The green circles are the points being tracked and the green lines are drawn in during post-processing.	6
2.1	An illustration of the placement of coordinate systems used during the derivation of the Lagrangian.	14
3.1	An illustration of the application of pulse width modulation (drawn in black) to a one dimensional signal (drawn in black) at two different frequencies. A sawtooth signal at the appropriate frequency is constructed (drawn in a black dotted line) and the value of the signal at the sampling times is projected onto the sawtooth. The pulse width modulation is set equal to zero for the amount of time equal to the projection onto the sawtooth and equal to one for the remainder of the sampling time.	32
7.1	Optimal trajectories for each of the considered optimization algorithms where the point $(1, 1, 1)$ is drawn in green, and where the trajectory is drawn in blue when in mode 1, in purple when in mode 2, and in red when in mode 3.	101
7.2	Optimal trajectories for each of the considered optimization algorithms where $x_1(t)$ is drawn using points and $x_2(t)$ is drawn using stars and where each state trajectory is drawn in blue when in mode 1 and in purple when in mode 2. . . .	102
7.3	Optimal trajectories for each of the considered optimization algorithms where the point $(6, 1)$ is drawn in green, where the trajectory is drawn in blue when in mode 1, in purple when in mode 2, and in red when in mode 3, and where the quadrotor is drawn in black and the normal direction to the frame is drawn in gray.	104
7.4	The optimal trajectory and discrete inputs drawn in cyan generated by Algorithm 2 where the point $(-2, 3.5, 10)$ is drawn in green and obstacles are drawn in grey.	105

8.1	The parameterized kneed compass gait biped model and the associated hybrid system on a cycle model, \mathcal{H}_{CG} , used to generate the synthetic gait illustrated in Figure 8.2a. The specific choice of parameters used during the identification presented in this thesis are in Table 8.1. The constraints enforced within each mode of \mathcal{H}_{CG} are drawn in red and the coordinates of the configuration space of the biped are labeled within each mode.	107
8.2	The gaits generated synthetically via feedback linearization for the kneed compass biped model, \mathcal{H}_{CG} , in Figure 8.1b and as a result of the application of Algorithm 2 to the data illustrated in Figure 8.3. The left leg is drawn in blue, the right leg is drawn in red, and the ground is drawn in black.	108
8.3	The tracking data for 3 of the 5 joints for the gait drawn in Figure 8.2a. The trajectory while the left foot is fixed to the ground (i.e. the $[lf]$ mode) is drawn in blue, and the trajectory while the right foot is fixed to the ground (i.e. the $[rf]$ mode) is drawn in red.	109
8.4	Illustrations of the experimental setup (left) and sensor placement on each leg (right). Each subject in the experiment was required to wear a suit where the sensors (red LEDs) were fastened in place. Each sensor was placed at the joints as illustrated with the red dots on the right lateral (middle) and anterior aspects (right) of the right leg. Sensors are placed identically on the left leg. The same sensors drawn from different views are connected with red arrows (right) and the labeled black arrows are used to illustrate the diversity of subjects in Table 8.3.	112
8.5	The original data is illustrated for the height (in millimeters) of the heel and toe for each leg for all 12 trials for a single individual, and the postprocessed data is illustrated after it has been shifted (drawn at the bottom of the plot) and averaged (drawn at the top of the plot). In each plot the different colors corresponds to different sensor.	113
8.6	A portion of the observed data that is tracked during the application of Algorithm 2 in order to determine a domain specification.	114
8.7	An illustration of the parameters (left), degrees of freedom (right), and contact points of interest (drawn in pink on the right) for the Biped with Torso, Knees, and Feet that is used in order to construct a hybrid system on cycle model of gait for the observed flat ground walking for each of the participants of the motion capture experiment.	115
8.8	The domain specification or sequence of constraint enforcements constructed by application of Algorithm 2 for all 9 participants in the flat ground walking experiment. The red dots indicate the constraints enforced in each mode. Notice that there are in fact 8 different modes visited during two steps, but these other 4 modes can be constructed by simply relabeling the left and right leg in each mode and are not included due to space limitations.	118

- 8.9 The domain specifications in each row for the 9 subjects that participated in the flat ground walking experiment in the order listed in Table 8.3. Comparing with the domain specification illustrated in Figure 8.8 the first through fourth columns correspond to $[lt]$ and $[rt]$, $[lt, rh]$ and $[rt, lh]$, $[lh, rh, rt]$ and $[rh, lh, lt]$, and $[lh, lt]$ and $[rh, rt]$, respectively. Each illustration is a snapshot of the subject's dynamics in the mode and above each plot is the percentage of the total gait spent within that mode. 119

List of Tables

7.1	The dynamics of each of the modes of the switched system examples considered in Chapter 7. The parameters employed during the application of Algorithm 2 are defined explicitly in Chapter 7.	98
7.2	The cost function used for each of the examples during the implementation of Algorithm 2.	99
7.3	The initialization parameters used for each of the examples during the implementation of Algorithm 2 and the MIP described in [25].	99
7.4	The algorithmic parameters used for each of the examples during the implementation of Algorithm 2.	100
7.5	The computation time and the result for each of the examples as a result of the application of Algorithm 2 and the MIP described in [25].	100
8.1	The specific values chosen for the parameters illustrated in Figure 8.1a.	107
8.2	The algorithmic parameters used for the Kneed Compass Gait Switched System Model during the implementation of Algorithm 2.	110
8.3	Table describing each of the subjects. The subject number is in the left column and the l_f, l_h, l_c, l_t measurements correspond to the lengths illustrated in Figure 8.4. The measurement in column 4 is the the only measurement that was self-reported.	111
8.4	Table describing the choice of parameters illustrated in Figure 8.7a for each of the 9 subjects in Table 8.3 as a percentage of their total weight using the formula described in Table 6 in [17] and as function of measured lengths.	116
8.5	The algorithmic parameters used for the switched system model of the Biped with Torso, Knees, and Feet during the implementation of Algorithm 2 for each of the 9 participants in the flat ground walking experiment.	117

Acknowledgments

It has been a great privilege to work with Ruzena Bajcsy. She found a position for me at Berkeley when others could not. She gave me enough freedom to explore my interests and make mistakes which have served me well. Her inclination to ask “hard” questions and persevere in the face of great skepticism and adversity will always be a tremendous inspiration to me during my own research.

I would like to express gratitude to Claire Tomlin, Francesco Borrelli, and Pravin Varaiya for providing numerous useful discussions that were helpful in guiding the focus of this thesis. I am also indebted to Claire and Shankar Sastry for allowing me to work with their students and allowing me to present my research during their group meetings. I am also grateful to have had the opportunity to work with Aaron Ames whose insights into bipedal walking were critical during the development of this thesis.

I also must thank several other collaborators who helped develop results in this dissertation both directly and indirectly. Parvez Ahammad taught me about presenting engineering research when I began and his beliefs have guided me since. Edgar Lobaton whose creativity has always left me dumbstruck patiently taught me algebra and guided my research in computer vision. Humberto Gonzalez’s help was crucial in writing this thesis. In addition to the numerous math classes we have taken together, we have spent the better part of several years working on the results presented herein. Although there were numerous arguments and many frustrating hours spent in 337 Cory, it has been a true privilege to work with Humberto. Sam Burden’s geometric insights were tremendously helpful in understanding locomotion. Maryam Kamgarpour’s ability to identify mistakes in proofs was simultaneously disheartening and incredibly important. Victor Shia’s interest in learning about locomotion was what made writing down the dynamics of human locomotion feasible. Avital Steinitz’s enthusiasm for engineering was helpful in keeping me motivated when the results were not necessarily compelling. I owe Rishi Patel and Andrew Wales a great debt for pulling me away from my work and helping me maintain my sanity.

I am grateful for the emotional support of my family. My sister, Kriththika, was always willing to buy me dinner and listen to me talk about my successes, failures, and interests. My mother, Uma, and my father, Srinivasan, always listened to me rant about my current state of affairs without judging me too harshly. Their frequent words of encouragement were what made completion of graduate school possible.

Chapter 1

Introduction

Human locomotion has been studied at great length for many millennia for numerous reasons. Archaeologists, for example, have speculated that cave drawings from the Paleolithic Era (approximately 33,000 BCE) that depict humans and animals in motion were likely motivated by dire survival questions related to the ability to efficiently move from place to place, escape predators, and hunt for food [4]. Greek philosophers from 500–300 BCE analyzed and described human movement driven by a need to place harmony to the universe [51].

More recently, during the 1940s there was an urgent need for an improved understanding of locomotion in order to treat injured World War II veterans. At the University of California, the meticulous measurements of Eberhart [20] and Inman et al. [39], illustrated the potential of kinematic analysis of human locomotion in diagnosing physical ailment. Their work, as illustrated in Figure 1.1, required careful hand calculation of joint evolution over a set of images captured by a series of cameras that took multiple pictures in rapid succession. These careful kinematic measurements in 2D were used to quantify “normal” human movement and were used during corrective prosthetic design.

Advancements in sensing technology, like motion capture systems, have provided new avenues for the automation of these kinematic measurements. Motivated by the substantial empirical evidence that patients develop adaptive changes in gait patterns as a result of neuromuscular pathologies that can be detected by comparing joint angle measurement over time [8, 73, 90], many biomechanists have employed these systems that require careful application of markers to joints, to diagnose numerous neuromuscular disorders. Perry et al. [62] and Sutherland [79], for example, have been pioneers in the application of this type of gait measurement and subsequent joint angle analysis to assist in the diagnosis of patients with cerebral palsy.

Although fruitful, this line of research that exploits kinematic measurements has two principal shortcomings. First, it requires careful sensor placement on the patient being observed, which is time-consuming, difficult to do accurately, and adversely affects the patient’s gait. Second, these approaches make no attempt to fit a dynamic model to the observed gait, which limits their predictive potential. Quantitatively answering questions about the

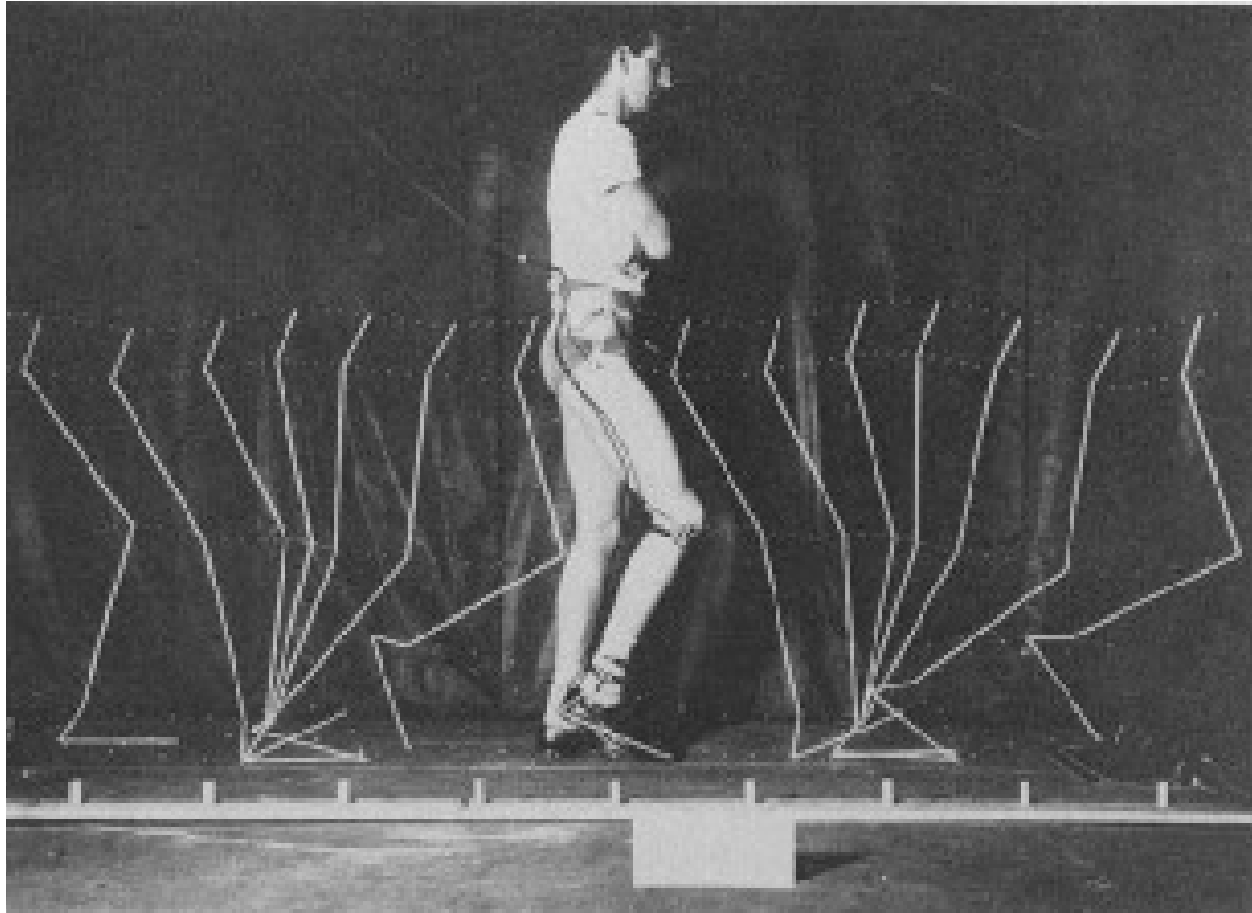


Figure 1.1: An illustration from [21] of the hand calculations required in order to measure joint angle evolution in the lower extremities for a patient wearing a prosthetic.

effectiveness of a particular prosthetic design in comparison to another or predicting instabilities in gait employing just the aforementioned kinematic techniques is impossible. However, as described below for the particular case of quantitatively predicting gait instability, such questions are straightforward to answer given a dynamical system model of locomotion.

The biomechanics community has appreciated this second deficiency in particular and has begun trying to fit dynamic models to observed kinematic trajectories. These methods utilize classical dynamical system models to track observed kinematic trajectories by applying traditional optimal control techniques [44], applying simulated annealing [59], restricting torque actuation patterns [60, 61, 67], or performing heuristic step-by-step pseudo-inverse computations [18, 81, 98]. Unfortunately, classical dynamical system models are incapable of describing locomotion due to the discontinuities in dynamics inherent in human movement.

The goal of this work is to address this deficiency by constructing a framework capable

of identifying a dynamical system description of human locomotion in an automated fashion. In order to accomplish this goal, three separate tasks must be fulfilled. First, a technique that tracks a participant, without being burdensome, while making guarantees about the accuracy of the measurement is required. Second, a mathematical construct rich enough to describe the dynamics of locomotion must be formalized. Finally, an algorithm that takes the tracking data and identifies a mathematical model capable of explaining the observed data is necessary. Though admittedly the principal focus of this thesis is to address the latter two tasks, Section 1.2 describes recent work that addresses each of these problems.

1.1 Applications of Automated Identification of Locomotion

Before describing our approach to address each of these tasks, we briefly digress to detail the utility of constructing a dynamical system description of locomotion. The applications of such an automated identification procedure are numerous, but this section describes how such a formulation can be used to measure instabilities in gait and devise anthropomorphic gait in bipedal robots.

Measuring Instabilities in Gait

Amongst those over the age of 65 falls are the leading cause of injury death [43]. For those who survive a fall, the direct medical costs of falls in 2006 totaled over \$28.2 billion dollars [76]. Frighteningly in addition to the ever increasing size of the overall population, the percentage of the population over the age of 65 is growing dramatically from approximately 10% to 20% in less than 20 years [45]. Given this impending crisis, the development of techniques capable of quantifying stability has never been more important.

Many biomechanists have begun devising various biologically inspired measures to evaluate the stability of a given gait. Several have considered measures corresponding to stride speed, stride length, step width, and double support time [36, 53]. Others have considered measures that are functions of the center of mass or the center of pressure [10]. Unfortunately, a recent study has illustrated that all of these existing measures have little correlation with the actual probability of falling [13]. In fact, the same study argues that the correct way to measure the stability of a particular locomotive pattern is to quantify its basin of attraction. In fact, if this region of attraction is quantified, then a sensitivity to disturbance immediately follows which corresponds directly to the robustness of the gait.

Recently, new insights into Sum of Squares Programming for a limit cycle have illustrated how the measurement of a region of attraction is possible for hybrid dynamical systems [55]; however, the application of this technique to human locomotion demands a hybrid dynamical description of the gait of interest. By utilizing the algorithm presented in this thesis to autonomously construct a hybrid dynamical description of gait, this recent

insight can be applied to quantitatively determine for the first time the stability of observed human locomotion.

Robotics

Since its inception, robotic walking research has spent considerable effort attempting to generate anthropomorphic gait. The construction of a controller in order to generate human-like walking requires the determination of the sequence of constraint enforcements during locomotion. In each phase of walking the control objectives may be, and often are, dramatically different. For example, for the specific discrete phases given in Figure 1.2, it might be desirable to design a control law that transitions from domain $[lh, lt]$ to domain $[lt]$ (i.e. a controller that forces the heel to lift). Knowing that such a controller is desirable (or even needed at all) is purely a function of knowing the sequence of constraint enforcements. In essence, the sequence of constraint enforcement directly affects the nature of walking.

Currently, there exists a fractured landscape in the bipedal walking community when one considers this sequence of constraint enforcements. Traditionally, most models of bipedal robots have employed a single domain model [2, 33, 80, 94], which assumes an instantaneous double support phase and usually excludes the presence of feet (models of this form began with the so-called compass gait biped, which did not have knees or feet). Adding feet to the bipedal robot results in the need to extend the potential sequence of constraint enforcements beyond a single phase, which is typically done by either adding a phase where the heel is off the ground or a double support phase where both feet are on the ground, or any combination thereof [16, 72, 82].

This lack of consistency among models in the literature motivates the desire to determine if there does in fact exist a single “universal” sequence of constraint enforcements that should be used when modeling bipedal robots, especially when the goal is to obtain human-like bipedal walking. As is illustrated in Chapter 8 after the application of the system identification procedure presented in this thesis on human data, there is considerable empirical evidence for just such a “universal” sequence of constraint enforcements.

1.2 Steps Required for Automated Identification

This section describes how this thesis formulates the three tasks required in order to identify a model capable of describing locomotion.

Markerless Tracking with Guarantees

Though it is considered here only briefly, markerless tracking from cameras is in fact a fundamental problem in computer vision. This type of tracking is usually done by employing local photometric descriptors. Traditionally these descriptors are constructed in order to be invariant to a specific class of transformations while remaining robust to noise.

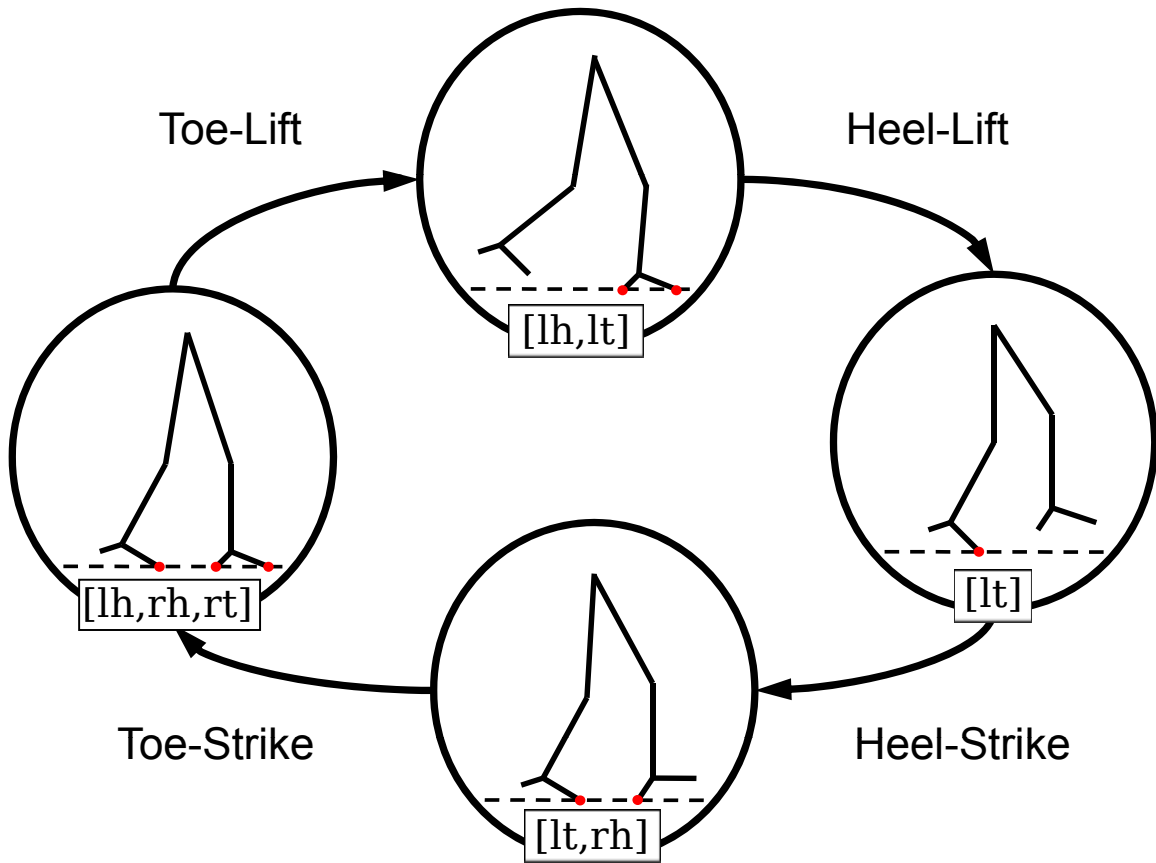


Figure 1.2: An example of a sequence of constraint enforcements. The red dots indicate the constraints enforced in each discrete phase (or domain)

Most popular local descriptors such as complex filters [71], gradient location and orientation histograms [57], shape contexts [6], scale invariant feature transforms [52], spin images [40], and steerable filters [27] are constructed with the goal of remaining invariant under affine transformations as this is what occurs when a viewpoint changes relative to a rigid object with locally planar regions. Unfortunately these descriptors are only verified empirically to be invariant to affine transformations. Even more troublingly, the class of affine transformations are only a subset of continuous deformations which describe how non-rigid objects transform, such as a human during locomotion or a cloth being folded.

We recently wrote several recent papers to address these deficiencies of existing photometric descriptors by devising a notion of topological invariance under the assumption of locally bounded deformation [49, 50]. As illustrated in Figure 1.3, this notion of topological invariance, which significantly outperforms existing descriptors, allows for the construction of a distinct, provably invariant descriptor that can be employed to perform markerless tracking

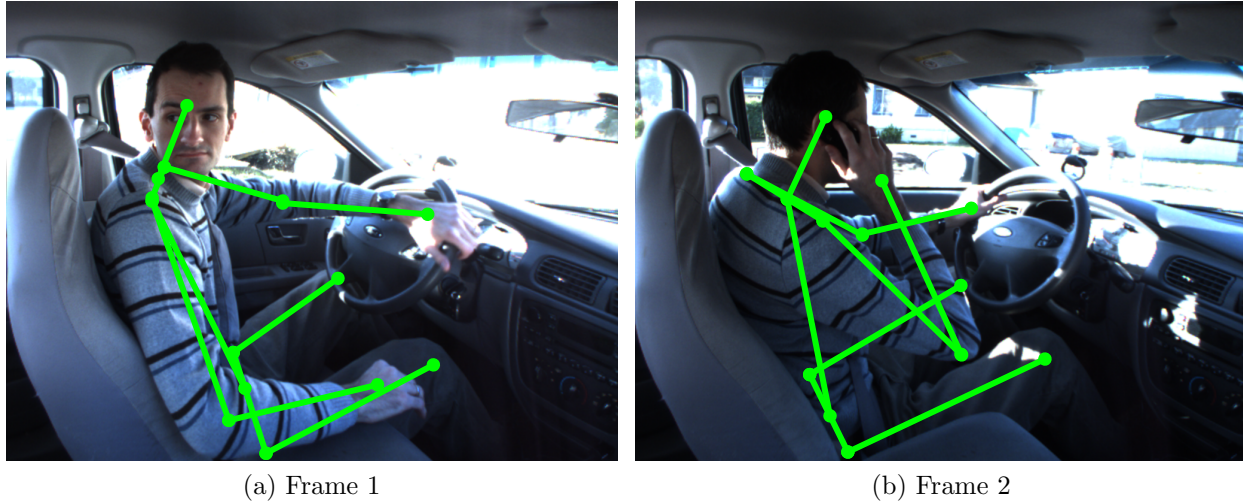


Figure 1.3: An illustration of the type of tracking achieved by using the methodology presented in [49, 50]. The green circles are the points being tracked and the green lines are drawn in during post-processing.

of human movement from cameras.

Representing Locomotion

As described earlier, due to the discontinuities that arise in dynamics during locomotion, classical dynamical systems are incapable of describing human motion. In this thesis, hybrid dynamical models that describe the interaction between continuous-time dynamics and discrete-event dynamics are utilized in order to describe human motion [11]. Such systems have been used in a variety of modeling applications including automobiles and locomotives employing different gears [37, 69], biological systems [28], situations where a control module has to switch its attention among a number of subsystems [48, 68, 91], manufacturing systems [15] and situations where a control module has to collect data sequentially from a number of sensory sources [12, 22].

These hybrid dynamical models have even been used in the robotics community to describe bipedal locomotion [34]. In Chapter 2 we formalize these hybrid dynamical models and illustrate how a quantitative description of human locomotion is completely specified by an unconstrained Lagrangian for a biped and a sequence of contact point enforcements. More importantly, in Chapter 2, we show that given a set of potential contact points, one can in fact write down a set of potential vector fields describing the dynamics of human locomotion while satisfying that set of contact points. One can then attempt to identify a hybrid dynamical model for gait from given tracking data by switching between this set of potential vector fields.

Identifying a Model

In fact, this optimal tracking problem is a switched system optimal control problem. The control parameter for such systems has both a discrete component corresponding to the schedule of discrete modes of the switched system visited and two continuous components corresponding to the duration of time spent in each mode in the mode schedule and the continuous input. The determination of an optimal control for this class of hybrid systems is particularly challenging due to the combinatorial nature of calculating an optimal mode schedule.

Prior Work on Switched System Optimal Control

There has been considerable interest in devising algorithms to perform optimal control of such systems. Even Branicky et al.'s seminal work which presented many of the theoretical underpinnings of hybrid systems includes a set of sufficient conditions for the optimal control of such systems using quasi-variational inequalities [11]. Though compelling from a theoretical perspective, the application of this set of conditions to the construction of a numerical optimal control algorithm for hybrid dynamical systems requires the application of value iterations which is particularly difficult in the context of switched systems, wherein the switching between different discrete modes is specified by a discrete-valued input signal.

The algorithms to solve the switched system optimal control problem in particular can be divided into two distinct groups according to whether they do or do not rely on the Maximum Principle [63, 66, 78]. Given the difficulty of the problem, both groups of approaches sometimes employ similar tactics during algorithm construction. A popular such tactic is one formalized by Xu et al. who proposed a bi-level optimization scheme that at a low level optimized the continuous components of the problem while keeping the mode schedule fixed and at a high level modified the mode schedule [97].

We begin by describing the algorithms for switched system optimal control that rely on the Maximum Principle. One of the first such algorithms, presented by Alamir et al., applied the Maximum Principle directly to a discrete time switched dynamical system [1]. In order to construct such an algorithm for a continuous time switched dynamical system, Shaikh et al. employed the bi-level optimization scheme proposed by Xu et al. and applied the Maximum Principle to perform optimization at the lower level and applied the Hamming distance to compare different possible nearby mode schedules [74].

Given the algorithm that we construct in this paper, the most relevant of the approaches that rely on the Maximum Principle is the one proposed by Benghea et al. who relax the discrete-valued input and treat it as a continuous-valued input over which they can apply the Maximum Principle to perform optimal control [7]. A search through all possible discrete valued inputs is required in order to find one that approximates the trajectory of the switched system due to the application of the constructed relaxed discrete-valued input. Though such a search is expensive, the existence of a discrete-valued input that approximates the behavior of the constructed relaxed discrete-valued input is proven by the Chattering Lemma [9].

Unfortunately this combinatorial search is unavoidable by employing the Chattering Lemma since it provides no means to construct a discrete-valued input that approximates a relaxed discrete-valued input with respect to the trajectory of the switched system. Summarizing, those algorithms that rely on the Maximum Principle construct powerful necessary conditions for optimality. Unfortunately their numerical implementation for nonlinear switched systems is fundamentally restricted due to their reliance on approximating strong or needle variations with arbitrary precision as explained in [56].

Next, we describe the algorithms that do not rely on the Maximum Principle but rather employ weak variations. Several have focused on the optimization of autonomous switched dynamical systems (i.e. systems without a continuous input) by fixing the mode sequence and working on devising first [23] and second order [41] numerical optimal control algorithms to optimize the amount of time spent in each mode. In order to extend these optimization techniques, Axelsson et al. employed the bi-level optimization strategy proposed by Xu et al., and after performing optimization at the lower-level by employing a first order numerical optimal control algorithm to optimize the amount of time spent in each mode while keeping the mode schedule fixed, they modified the mode sequence by employing a single mode insertion technique [5].

There have been two major extensions to Axelsson et al.’s algorithm. First, Wardi et al., extend the approach by performing several single mode insertions at each iteration [92]. Second, we extended Axelsson et al.’s approach to make it applicable to constrained switched dynamical systems with a continuous-valued input [30, 31]. Though these single mode insertion techniques avoid the computational expense of considering all possible mode schedules during the high-level optimization, this improvement comes at the expense of restricting the possible modifications of the existing mode schedule, which may introduce undue local minimizers, and at the expense of requiring a separate optimization for each of the potential mode schedule modifications, which is time consuming.

1.3 Contributions and Organization

In this thesis, we begin in Chapter 2 by formalizing hybrid dynamical systems and detailing how the identification of a mathematical description of human locomotion can be understood as a switched system optimal control problem. Then, inspired by the potential of the Chattering Lemma, we devise a first order numerical optimization algorithm for the optimal control of constrained nonlinear switched systems. Our approach to solve this problem, which is described in Chapter 3, first relaxes the optimal control problem by treating the discrete-valued input to be continuous-valued. After this optimization is complete, an extension of the Chattering Lemma that we devise, allows us to design a projection that takes the computed relaxed discrete-valued input back to a “pure” discrete-valued input while controlling the quality of approximation of the trajectory of the switched dynamical system generated by applying the projected discrete-valued input rather than the relaxed discrete-valued input.

In Chapter 4, we prove that the sequence of points generated by recursive application of our first order numerical optimal control algorithm converge to a point that satisfies a necessary condition for optimality of the constrained nonlinear switched system optimal control problem. We then describe in Chapter 5 how our algorithm can be formulated in order to make numerical implementation feasible. In fact, we prove in Chapter 6 that the sequence of points generated by the recursive application of this numerically implementable algorithm converge to a point that satisfies a necessary condition for optimality of the constrained nonlinear switched system optimal control problem.

In Chapter 7, we implement this algorithm and compare its performance to a commercial mixed integer optimization algorithm on 4 separate problems and illustrate its superior performance with respect to speed and quality of constructed minimizer. Finally, in Chapter 8, we detail the performance of our algorithm in performing automated identification of locomotion on 2 examples. The first example is a synthetic one for which we know the ground truth data and the second is a 9 person human walking experiment. From the data constructed from this experiment, we identify a single universal sequence of switched systems visited by *all* the participants during walking. In addition to the aforementioned publications, portions of this thesis have appeared in [3, 84, 87]. Other portions are currently in the review process [85, 86] and in the preparation process [88].

Part I

A Conceptual Algorithm for Hybrid Dynamical System Identification

Chapter 2

The Identification Problem

In this chapter, we define hybrid systems and illustrate how a sequence of constraint enforcements in addition to an unconstrained Lagrangian is sufficient to fully describe locomotion. Next, we formulate the switched system optimal control problem. We conclude by describing how the identification of a hybrid system description of locomotion can be cast as a switched system optimal control problem. Before proceeding with this analysis, we define the function spaces and norms used throughout this thesis.

2.1 Norms and Function Spaces

This thesis focuses on functions with finite L^2 -norm and finite bounded variation. To formalize this notion, we require a norm. For each $x \in \mathbb{R}^n$, $p \in \mathbb{N}$, and $p > 0$, we let $\|x\|_p$ denote the p -norm of x . For each $A \in \mathbb{R}^{n \times m}$, $p \in \mathbb{N}$, and $p > 0$, we let $\|A\|_{i,p}$ denote the induced p -norm of A .

Given these definitions, we say a function, $f : [0, 1] \rightarrow \mathcal{Y}$, where $\mathcal{Y} \subset \mathbb{R}^n$, belongs to $L^2([0, 1], \mathcal{Y})$ with respect to the Lebesgue measure on $[0, 1]$ if:

$$\|f\|_{L^2} = \left(\int_0^1 \|f(t)\|_2^2 dt \right)^{\frac{1}{2}} < \infty. \quad (2.1)$$

We say a function, $f : [0, 1] \rightarrow \mathcal{Y}$, where $\mathcal{Y} \subset \mathbb{R}^n$, belongs to $L^\infty([0, 1], \mathcal{Y})$ with respect to the Lebesgue measure on $[0, 1]$ if:

$$\|f\|_{L^\infty} = \inf \{ \alpha \geq 0 \mid \|f(x)\|_2 \leq \alpha \text{ for almost every } x \in [0, 1] \} < \infty. \quad (2.2)$$

In order to define the space of functions of finite bounded variation, we first define the total variation of a function. Given P , the set of all finite partitions of $[0, 1]$, we define the *total variation* of $f : [0, 1] \rightarrow \mathcal{Y}$ by:

$$\|f\|_{BV} = \sup \left\{ \sum_{j=0}^{m-1} \|f(t_{j+1}) - f(t_j)\|_1 \mid \{t_k\}_{k=0}^m \in P \right\}. \quad (2.3)$$

Note that the total variation of f is not a norm but rather a seminorm, i.e. it does not separate points. Regardless, we use the norm symbol for the total variation throughout this paper. We say that f is of *bounded variation* if $\|f\|_{BV} < \infty$, and we define $BV([0, 1], \mathcal{Y})$ to be the set of all functions of bounded variation from $[0, 1]$ to \mathcal{Y} .

There is an important connection between the functions of bounded variation and weak derivatives, which we rely on throughout our analysis. Given $f : [0, 1] \rightarrow \mathcal{Y}$, we say that f has a *weak derivative* if there exists a Radon signed measure μ over $[0, 1]$ such that, for each smooth bounded function v ,

$$\int_0^1 f(t)\dot{v}(t)dt = - \int_0^1 v(t)d\mu(t). \quad (2.4)$$

Moreover, we say that $\dot{f} = \frac{d\mu(t)}{dt}$, where the derivative is taken in the Radon–Nikodym sense, is the weak derivative of f . Note that \dot{f} is in general a distribution. Perhaps the most common example of weak derivative is the Dirac Delta, which is the weak derivative of the Step Function. The following result is fundamental in our analysis of functions of bounded variation:

Theorem 1 (Exercise 5.1 in [99]). *If $f \in BV([0, 1], \mathcal{Y})$, then f has a weak derivative, denoted \dot{f} . Moreover,*

$$\|f\|_{BV} = \int_0^1 \|\dot{f}(t)\|_1 dt. \quad (2.5)$$

We omit the proof of this result since it is beyond the scope of this paper. More details about the functions of bounded variation and weak derivatives can be found in Sections 3.5 and 9 in [26] and Section 5 in [99].

2.2 From Constraints to Models

In this section, we introduce a definition of a hybrid system applicable to gait description.

Hybrid Systems on a Cycle

Since steady state locomotion is periodic, we define a subclass of hybrid systems, *hybrid systems on a cycle*, in order to describe gait. In order to define this subclass, we begin by defining a directed graph. A *graph* is a tuple $G = (V, E)$, where V is a set of *vertices* and $E \subset V \times V$ is a set of *edges*; an edge $e \in E$ can be written as $e = (i, j)$ and the source of e , denoted $\text{source}(e)$, is i , and the target of e , denoted $\text{target}(e)$, is j .

A *directed cycle* (or just a cycle) is a graph $\ell = (V, E)$ such that the edges and vertices can be written as:

$$\begin{aligned} V &= \{v_0, v_1, \dots, v_{p-1}\}, \\ E &= \{e_0 = (v_0, v_1), \dots, e_{p-1} = (v_{p-1}, v_0)\}. \end{aligned} \quad (2.6)$$

Since in the case of a cycle, the edges are completely determined by the vertices, we denote a cycle by:

$$\ell : v_0 \rightarrow v_1 \rightarrow \cdots \rightarrow v_{p-1}$$

Example 1. *The domain graph pictured in Figure 1.2 has an underlying graph that is a directed cycle. In particular, there are 4 vertices and edges, which results in the cycle:*

$$\ell_u : [lh, lt] \rightarrow [lt] \rightarrow [lt, rh] \rightarrow [lt, rh, rt]. \quad (2.7)$$

Utilizing the notion of a directed cycle, we can define a subclass of hybrid systems of interest in this thesis:

Definition 1. *A hybrid system on a cycle is a tuple*

$$\mathcal{H} = (\ell, \mathcal{D}, U, S, \Delta, f), \quad (2.8)$$

where

- $\ell = (V, E)$ is a directed cycle,
- $\mathcal{D} = \{D_v\}_{v \in V}$ is a set of domains where $D_v \subset \mathbb{R}^n$ is compact,
- $U \subset \mathbb{R}^m$ is the set of admissible controls and is bounded and convex,
- $S = \{S_e\}_{e \in E}$ is a set of guards, where $S_e \subseteq D_e$ is a closed subset,
- $\Delta = \{\Delta_e\}_{e \in E}$ is a set of reset maps, where $\Delta_e : \mathbb{R}^n \rightarrow \mathbb{R}^n$ is a smooth map,
- $f : \mathbb{R} \times \mathbb{R}^n \times U \times V \rightarrow \mathbb{R}^n$, where $f(\cdot, \cdot, \cdot, v)$ is a vector field on vertex $v \in V$ (i.e. $\dot{x}(t) = f(t, x(t), u(t), v)$ for $t \in \mathbb{R}$, $x(t) \in D_v$, and $u(t) \in U$)

Given an initial condition inside of a particular vertex, an *execution* of a hybrid system on a cycle evolves as a standard dynamical system until a guard is reached. In this case a “jump” occurs via an application of the reset map to a new domain of the system as specified by the target of the edge that indexes the guard that has been reached. The evolution then continues as a standard dynamical system and the process is repeated.

Hybrid Systems from Constraints

The remainder of this section discusses how a Lagrangian for a biped together with a sequence of active constraints allows one to explicitly construct a hybrid model of the system. We begin with a biped in 3 dimensions; however, note that the discussion that follows is also applicable in the 2 dimensional case.

We first construct a Lagrangian for a biped when no assumptions on ground contact are made. As in Figure 2.1, let R_0 be a fixed inertial or world frame, and R_b be a reference frame attached to the body of the biped which is specified by a position in \mathbb{R}^3 and an orientation

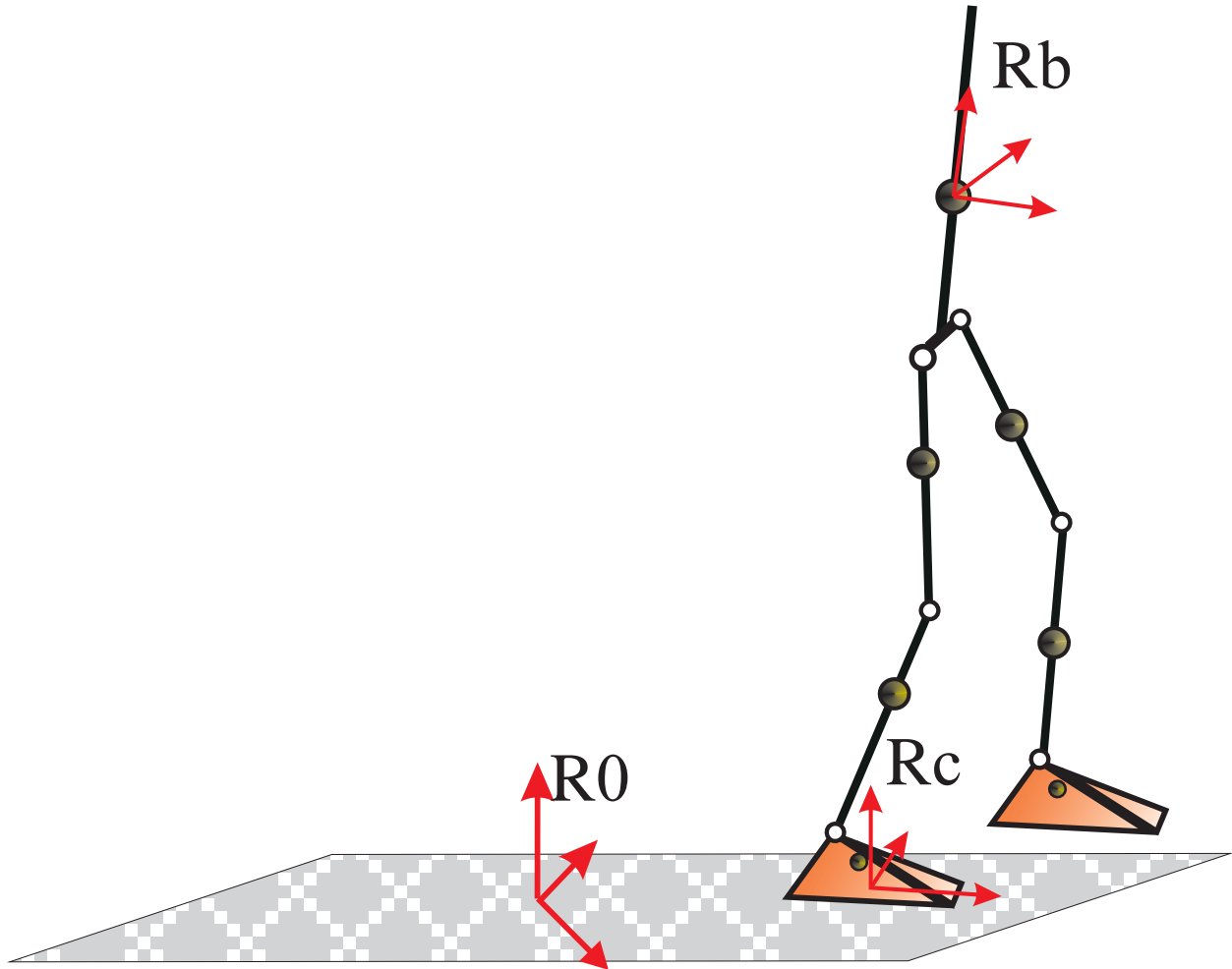


Figure 2.1: An illustration of the placement of coordinate systems used during the derivation of the Lagrangian.

in $SO(3)$. Consider a configuration space for the biped P_r that is usually specified by a collection of relative angles between successive links. Concatenating the description of the body frame and the configuration space, we define the *generalized configuration space* $P = \mathbb{R}^3 \times SO(3) \times P_r$. The evolution of the *generalized coordinates* for the biped are then given by $p : [0, \infty) \rightarrow P$.

Unconstrained Equations of Motion

Letting TP denote the tangent space of the generalized configuration space as defined in Chapter 3 of [47], the Lagrangian of the biped, $\mathcal{L} : TP \rightarrow \mathbb{R}$, can be stated in terms of kinetic and potential energies as:

$$\mathcal{L}(p(t), \dot{p}(t)) = T(p(t), \dot{p}(t)) - V(p(t)), \quad (2.9)$$

where $(p(t), \dot{p}(t)) \in TP$. The Euler-Lagrange Equation yields the equations of motion. Though the ensuing analysis follows for general multi-link systems, we focus on the case of rigid body systems since the examples of locomotion identification we consider in Chapter 8 are all restricted to the rigid body variety. In particular, the equations of motion for rigid body systems can be stated as follows:

$$M(p(t))\ddot{p}(t) + C(p(t), \dot{p}(t)) = N(p(t))u(t), \quad (2.10)$$

where $M(p(t)) \in \mathbb{R}^{|P| \times |P|}$ is the inertia matrix, $u(t) \in \mathbb{R}^m$ is an admissible vector of actuations, $N(p(t)) \in \mathbb{R}^{|P| \times m}$ is the actuator distribution matrix, $C(p(t), \dot{p}(t)) \in \mathbb{R}^{|P|}$ contains the Coriolis, gravity terms and non-conservative forces grouped into a single vector and $|P|$ is the dimension of the generalized configuration space [58]. Though the formulas for these matrices are not described here since it falls beyond the scope of this thesis, their construction for multi-link rigid body systems, like the bipeds considered in this thesis, only requires knowledge of the masses and lengths of the various component links. In fact, given these masses and lengths, the construction of this vector field can be done symbolically entirely inside of Mathematica [96].

Contact Points and Constraints

The continuous dynamics of the hybrid system on a cycle depend on which constraints are enforced at any given time, while the discrete dynamics depend on the change in constraints. Constraints and their enforcement are dictated by the number of contact points of the system with the ground or itself. Specifically, we define *the set of contact points* as $\mathcal{C} = \{c_1, c_2, \dots, c_k\}$, where each c_i is a specific type of contact possible in the biped, either with the ground or with the biped itself (such as the knee locking).

Example 2. *In the instance of a biped with just foot contact, we can consider 4 contact points of interest:*

$$\mathcal{C} = \{lh, lt, rh, rt\}, \quad (2.11)$$

where *lh* and *lt* indicate the left heel and toe, and *rh* and *rt* indicate right heel and toe, respectively.

Contact points introduce a *holonomic constraint* on the system that must be held constant for a contact point to be maintained. Each of these holonomic constraints can be described by a vector-valued function $g_c : P \rightarrow \mathbb{R}^{n_c}$ for $c \in \mathcal{C}$ and $n_c \in \mathbb{N}$ and satisfaction of this constraint can be described by $g_c(p(t)) = \text{constant} \in \mathbb{R}^{n_c}$.

Example 3. *Consider again the biped with just foot contact, as in Example 2. To describe the set of holonomic constraints, consider a reference frame R_c at the contact point $c \in \{lh, lt, rh, rt\}$ such that the axis of rotation about this point (either the heel or toe) is in the z direction (the axis pointing up) as illustrated in Figure 2.1. The holonomic constraint can*

then be written as:

$$g_c(p(t)) = \begin{bmatrix} p_c(p(t)) \\ \varphi_{c,x} \\ \varphi_{c,y} \end{bmatrix}, \quad (2.12)$$

where $p_c(p(t))$ is the position of the contact point given the generalized coordinate $p(t) \in P$ and $\varphi_{c,x}, \varphi_{c,y} \in \mathcal{S}^1$ describe the orientation of reference frame R_c relative to R_0 by specifying the rotation about the x and y axis of R_0 , respectively.

Observe that in this previous example, if $g_c(p(t)) = \text{constant}$ then the foot contact point is fixed but allowed to rotate about the heel or toe depending upon the specific type of foot contact. It is useful to express the collection of all holonomic constraints in a single matrix $g(p(t)) \in \mathbb{R}^{N \times |\mathcal{C}|}$ where $N = \sum_{c \in \mathcal{C}} n_c$, and $|\mathcal{C}|$ denotes the cardinality of \mathcal{C} . In the instance of Example 3, this can be written as:

$$g(p(t)) = \begin{bmatrix} g_{lh}(p(t)) & \Theta_{nih} & \Theta_{nih} & \Theta_{nih} \\ \Theta_{nit} & g_{lt}(p(t)) & \Theta_{nit} & \Theta_{nit} \\ \Theta_{nrh} & \Theta_{nrh} & g_{rhh}(p(t)) & \Theta_{nrh} \\ \Theta_{nrt} & \Theta_{nrt} & \Theta_{nrt} & g_{rt}(p(t)), \end{bmatrix} \quad (2.13)$$

where Θ_{n_c} denotes the column vector of all zeros of size $n_c \in \mathbb{N}$.

The second class of constraints that are important during the construction of a hybrid system on a cycle description of human locomotion are *unilateral constraints*, h_c for $c \in \mathcal{C}$. These are scalar valued functions, $h_c : P \rightarrow \mathbb{R}$, that dictate the set of admissible configurations of the system; that is $h_c(p(t)) \leq 0$ implies that the configuration of the system is not violating the unilateral constraint for the contact point c .

Example 4. *In the case of foot contact, assuming that biped is walking on flat ground, the unilateral constraints are the height of a contact point above the ground:*

$$h_c(p(t)) = -p_{c,z}(p(t)) \leq 0, \quad (2.14)$$

where $p_{c,z}(p(t))$ is the position of the z -coordinate of the contact point.

These can be put in the form of a matrix $h(p(t)) \in \mathbb{R}^{|\mathcal{C}| \times |\mathcal{C}|}$ in the same manner as holonomic constraints where $|P|$ denotes the dimension of the generalized configuration space P .

Domain Specification

For a particular periodic sequence of contact point enforcements, we can associate a directed cycle. We call this association the *domain specification*. To define this formally, we assign to each vertex in the directed cycle a binary vector describing which contact points are active in that vertex:

Definition 2. Let $\ell = (V, E)$ be a cycle and $\mathcal{C} = \{c_1, c_2, \dots, c_k\}$ a set of contact points. A domain specification is a function $\mathcal{B} : \ell \rightarrow \mathbb{Z}_2^k$ such that $[B(v)]_i = 1$ if c_i is enforced in v and $[B(v)]_i = 0$ otherwise.

Example 5. In the case of the domain graph ℓ_u given in Example 1 and set of contact points $\mathcal{C} = \{lh, lt, rh, rt\}$, the domain specification is given by $\mathcal{B}_u : \ell_u \rightarrow \mathbb{Z}_2^4$ where $\mathcal{B}_u([lh, lt])$, $\mathcal{B}_u([lt])$, $\mathcal{B}_u([lt, rh])$ and $\mathcal{B}_u([lt, rh, rt])$ are given by:

$$\mathcal{B}_u(\ell) : \begin{bmatrix} 1 \\ 1 \\ 0 \\ 0 \end{bmatrix} \rightarrow \begin{bmatrix} 0 \\ 1 \\ 0 \\ 0 \end{bmatrix} \rightarrow \begin{bmatrix} 0 \\ 1 \\ 1 \\ 0 \end{bmatrix} \rightarrow \begin{bmatrix} 0 \\ 1 \\ 1 \\ 1 \end{bmatrix}.$$

Hybrid System Construction

Now, we demonstrate that given a Lagrangian and a domain specification, a hybrid system on a cycle can be explicitly constructed. Observe that since the Lagrangian is intrinsic to the biped being considered, this implies that a domain specification alone dictates the mathematical model that describes a particular locomotion pattern for that biped.

Continuous Dynamics

Each of the domains of the hybrid system on a cycle can be defined as equal to the tangent space of the generalized configuration space of the unconstrained biped. The vector field in each mode is constructed by imposing the constraints as specified by the domain specification, \mathcal{B} . For the vertex $v \in V$, the holonomic constraints that are imposed are given by:

$$g_v(p(t)) = g(p(t))\mathcal{B}(v), \quad (2.15)$$

where the domain specification dictates which constraints are enforced.

Differentiating the holonomic constraint yields a *kinematic constraint*:

$$\mathcal{K}_v(p(t))\dot{p}(t) = 0, \quad (2.16)$$

where $\mathcal{K}_v(p(t)) = \text{RowBasis}\left(\frac{\partial g_v(q(t))}{\partial p}\right)$ is a basis for the row space of the Jacobian (this removes any redundant constraints so that \mathcal{K}_v has full row rank). The kinematic constraint yields the *constrained dynamics* in that vertex:

$$M(p(t))\ddot{p}(t) + C(p(t), \dot{p}(t)) = N(p(t))u(t) + \mathcal{K}_v(p(t))F_v(p(t), \dot{p}(t)), \quad (2.17)$$

which enforces the holonomic constraint; here M , C and N are as in Equation (2.10) and $F_v(p(t), \dot{p}(t))$ is a *wrench* (or a Lagrange multiplier) that ensures that the holonomic constraint is maintained [58]. Differentiating the kinematic constraint, we have:

$$\mathcal{K}_v(p(t))\ddot{p}(t) + \dot{\mathcal{K}}_v(p(t))\dot{p}(t) = 0. \quad (2.18)$$

Letting $x(t) = (p(t), \dot{p}(t))$, Equations (2.17) and (2.18) specify the wrench and a vector field that can be written as $f(t, x(t), u(t), v)$ for the vertex $v \in V$.

We make several important observations. Notice that *only* the holonomic constraints rather than the unilateral constraints appear in the constrained vector field. Moreover, notice that the actual position to be maintained by the contact point as determined by the holonomic constraint *never* appears inside of the vector field.

Discrete Dynamics

We now construct the guards and reset maps for a hybrid system on a cycle using the domain specification. For the vertex $v \in V$ and from the wrench $F_v(p(t), \dot{p}(t))$, one can ensure that the contact point is enforced by considering the following inequalities:

$$F_v(p(t), \dot{p}(t)) \preceq 0, \quad (2.19)$$

These are coupled with the unilateral constraint in each mode, $h_v(p(t)) = h(p(t))\mathcal{B}(v)$, to yield the set of admissible configurations:

$$A_v(p(t), \dot{p}(t)) = \begin{bmatrix} F_v(p(t), \dot{p}(t)) \\ h_v(p(t)) \end{bmatrix} \preceq 0. \quad (2.20)$$

The guard is just the boundary of the domain with the additional assumption that the set of admissible configurations is decreasing, i.e., the vector field is pointed outside of the domain, or for an edge $e = (v, v') \in E$,

$$S_e = \{(p(t), \dot{p}(t)) \in TP : A_v(p(t), \dot{p}(t)) = 0 \text{ and } \dot{A}_v(p(t), \dot{p}(t)) \preceq 0\}. \quad (2.21)$$

The reset map can be defined as equal to the identity.

Switched System Optimal Control

The result of this analysis is that given a domain specification and a biped (which determines just the unconstrained Lagrangian), the hybrid model on a cycle for the biped for a specific periodic locomotion is completely determined. Given a set of contact points, one can immediately write down a set of vector fields corresponding to all possible combinations of contact point enforcements. Recall that the constrained vector field does not depend on the specific location at which the holonomic constraint must be maintained. Given tracking data corresponding to locomotion, one can try to identify a hybrid model on a cycle by trying to optimally switch between these different possible vector fields in a manner that minimizes the difference between the observed and generated data.

2.3 The Switched System Optimal Control Problem

In order to formalize this approach, we require several additional definitions.

Optimization Spaces

Given a set of contact points, \mathcal{C} , one can write down the set of all possible vector fields corresponding to the enforcement of all combinations of contact points. Let this set of all possible vector fields be denoted $\mathcal{Q} = \{1, 2, \dots, q\}$. We are then interested in the control of systems whose trajectory is governed by a set of vector fields $f : \mathbb{R} \times \mathbb{R}^n \times \mathbb{R}^m \times \mathcal{Q} \rightarrow \mathbb{R}^n$. Each of these distinct vector fields is called a *mode* of the switched system. To formalize the optimal control problem, we define three spaces: the *pure discrete input space*, \mathcal{D}_p , the *relaxed discrete input space*, \mathcal{D}_r , and the *continuous input space*, \mathcal{U} . Throughout the document, we employ the following convention: given the pure or relaxed discrete input d , we denote its i -th coordinate by d_i .

Before formally defining each space, we require some notation. Let the q -simplex, Σ_r^q , be defined as:

$$\Sigma_r^q = \left\{ (d_1, \dots, d_q) \in [0, 1]^q \mid \sum_{i=1}^q d_i = 1 \right\}, \quad (2.22)$$

and let the corners of the q -simplex, Σ_p^q , be defined as:

$$\Sigma_p^q = \left\{ (d_1, \dots, d_q) \in \{0, 1\}^q \mid \sum_{i=1}^q d_i = 1 \right\}. \quad (2.23)$$

Note that $\Sigma_p^q \subset \Sigma_r^q$. Also, there are exactly as many corners, denoted e_i for $i \in \mathcal{Q}$, of the q -simplex as there are distinct vector fields. Thus, $\Sigma_p^q = \{e_1, \dots, e_q\}$.

Using this notation, we define the pure discrete input space, \mathcal{D}_p , as:

$$\mathcal{D}_p = L^2([0, 1], \Sigma_p^q) \cap BV([0, 1], \Sigma_p^q). \quad (2.24)$$

Next, we define the relaxed discrete input space, \mathcal{D}_r :

$$\mathcal{D}_r = L^2([0, 1], \Sigma_r^q) \cap BV([0, 1], \Sigma_r^q). \quad (2.25)$$

Notice that the discrete input at each instance in time can be written as the linear combination of the corners of the simplex. Given this observation, we employ these corners to index the vector fields (i.e. for each $i \in \mathcal{Q}$ we write $f(\cdot, \cdot, \cdot, e_i)$ for $f(\cdot, \cdot, \cdot, i)$). Finally, we define the continuous input space, \mathcal{U} :

$$\mathcal{U} = L^2([0, 1], U) \cap BV([0, 1], U), \quad (2.26)$$

where $U \subset \mathbb{R}^m$ is a bounded, convex set.

Let $\mathcal{X} = L^\infty([0, 1], \mathbb{R}^m) \times L^\infty([0, 1], \mathbb{R}^q)$ be endowed with the following norm for each $\xi = (u, d) \in \mathcal{X}$:

$$\|\xi\|_{\mathcal{X}} = \|u\|_{L^2} + \|d\|_{L^2}, \quad (2.27)$$

where the L^2 -norm is as defined in Equation (2.1). We combine \mathcal{U} and \mathcal{D}_p to define our *pure optimization space*, $\mathcal{X}_p = \mathcal{U} \times \mathcal{D}_p$, and we endow it with the same norm as \mathcal{X} . Similarly, we combine \mathcal{U} and \mathcal{D}_r to define our *relaxed optimization space*, $\mathcal{X}_r = \mathcal{U} \times \mathcal{D}_r$, and endow it with the \mathcal{X} -norm too. Note that $\mathcal{X}_p \subset \mathcal{X}_r \subset \mathcal{X}$.

Trajectories, Cost, Constraint, and the Optimal Control Problem

Given $\xi = (u, d) \in \mathcal{X}_r$, for convenience throughout the paper we let:

$$f(t, x(t), u(t), d(t)) = \sum_{i=1}^q d_i(t) f(t, x(t), u(t), e_i), \quad (2.28)$$

where $d(t) = \sum_{i=1}^q d_i(t) e_i$. We employ the same convention when we consider the partial derivatives of f . Given $x_0 \in \mathbb{R}^n$, we say that a *trajectory of the system* corresponding to $\xi \in \mathcal{X}_r$ is the solution to:

$$\dot{x}(t) = f(t, x(t), u(t), d(t)), \quad \forall t \in [0, 1], \quad x(0) = x_0, \quad (2.29)$$

and denote it by $x^{(\xi)} : [0, 1] \rightarrow \mathbb{R}^n$, where we suppress the dependence on x_0 in $x^{(\xi)}$ since it is assumed given. To ensure the clarity of the ensuing analysis, it is useful to sometimes emphasize the dependence of $x^{(\xi)}(t)$ on ξ . Therefore, we define the *flow of the system*, $\phi_t : \mathcal{X}_r \rightarrow \mathbb{R}^n$ for each $t \in [0, 1]$ as:

$$\phi_t(\xi) = x^{(\xi)}(t). \quad (2.30)$$

To define the cost function, we assume that we are given a *terminal cost*, $h_0 : \mathbb{R}^n \rightarrow \mathbb{R}$. The *cost function*, $J : \mathcal{X}_r \rightarrow \mathbb{R}$, for the optimal control problem is then defined as:

$$J(\xi) = h_0(x^{(\xi)}(1)). \quad (2.31)$$

Notice that if the problem formulation includes a running cost, $L : \mathbb{R} \times \mathbb{R}^n \times \mathbb{R}^m \rightarrow \mathbb{R}$, then one can extend the existing state vector by introducing a new state, and modifying the cost function to evaluate this new state at the final time, as shown in Section 4.1.2 in [64]. By performing this type of modification, observe that each mode of the switched system can have a different running cost associated with it (i.e. the running cost can be defined as $L(t, x(t), u(t), d(t))$).

Next, we define a family of functions, $h_j : \mathbb{R}^n \rightarrow \mathbb{R}$ for $j \in \mathcal{J} = \{1, \dots, N_c\}$. Given a $\xi \in \mathcal{X}_r$, the state $x^{(\xi)}$ is said to satisfy the constraint if $h_j(x^{(\xi)}(t)) \leq 0$ for each $t \in [0, 1]$ and for each $j \in \mathcal{J}$. We compactly describe all the constraints by defining the *constraint function* $\Psi : \mathcal{X}_r \rightarrow \mathbb{R}$, by:

$$\Psi(\xi) = \max_{j \in \mathcal{J}, t \in [0, 1]} h_j(x^{(\xi)}(t)), \quad (2.32)$$

since $h_j(x^{(\xi)}(t)) \leq 0$ for each t and j if and only if $\psi(\xi) \leq 0$. To ensure the clarity of the ensuing analysis, it is useful to sometimes emphasize the dependence of $h_j(x^{(\xi)}(t))$ on ξ . Therefore, we define *component constraint functions*, $\psi_{j,t} : \mathcal{X}_r \rightarrow \mathbb{R}$ for each $t \in [0, 1]$ and $j \in \mathcal{J}$ as:

$$\psi_{j,t}(\xi) = h_j(\phi_t(\xi)). \quad (2.33)$$

With these definitions, we can state the Switched System Optimal Control Problem:

Switched System Optimal Control Problem.

$$\min_{\xi \in \mathcal{X}_p} \{J(\xi) \mid \Psi(\xi) \leq 0\}. \quad (2.34)$$

Identification via Switched System Optimal Control

Notice in particular that if we are given a set of tracking data corresponding to human locomotion, an unconstrained Lagrangian, and constraints corresponding to the physical configurations of the biped, then the determination of the hybrid system on a cycle model for the gait in question can be computed as a solution to the Switched System Optimal Control Problem.

That is, suppose we are given an unconstrained Lagrangian and a set of contact points of interest, \mathcal{C} . Given this information, we can construct the vector field, $f : \mathbb{R} \times \mathbb{R}^n \times \mathbb{R}^m \times \mathcal{Q} \rightarrow \mathbb{R}^n$ where $\mathcal{Q} = \{1, \dots, 2^{|\mathcal{C}|}\}$ and $|\mathcal{C}|$ denotes the cardinality of \mathcal{C} by applying the construction presented in Section 2.2. Recall again, that these vector fields depend only on the holonomic constraints which are described entirely by the set of contact points of interest. Moreover, they do not depend on the specific location at which the holonomic constraint must be maintained (i.e. the vector field for the $[lt]$ mode is constructed by requiring that the left toe remain fixed rather than requiring that it be fixed on the ground). Suppose we are also given observed data of the continuous state, $x_{obs} : [0, 1] \rightarrow \mathbb{R}^n$, of a hybrid system on a cycle, \mathcal{H} , that we are attempting to identify.

The determination of the domain specification, \mathcal{B} as in Definition 2, can then be thought of as finding the solution to the Switched System Optimal Control Problem as in Equation (2.34), when we choose a running cost equal to:

$$L(t, x(t), u(t), d(t)) = \|x_{obs}(t) - x(t)\|_2^2. \quad (2.35)$$

If some unilateral constraints on physical configurations of the biped are known *a priori* (e.g. the knee of a biped is not allowed to bend beyond the thigh), these can be added as constraints to the Switched System Optimal Control Problem. In addition, it may make sense to penalize certain inputs within certain modes of the switched system and not penalize them within other modes of the switched system during the Switched System Optimal Control (e.g. penalizing an actuation at a joint while it is constrained to the ground may not make sense). This decision can be reflected in the choice of running cost with a straightforward modification of Equation (2.35). Also observe that if some function of the state is observed, the 2-norm of the difference between this observation and the same function applied to the state of the switched system generated during the optimization can be minimized in order to determine a domain specification. These variants of Equation (2.35) are described in more detail in Chapter 8.

Importantly, if the domain specification is determined by solving the Switched System Optimal Control Problem by employing Equation (2.35) or any of the aforementioned variants, then the hybrid system on a cycle immediately follows since the unconstrained Lagrangian was assumed given.

Assumptions and Uniqueness

In order to devise an algorithm to solve Switched System Optimal Control Problem, we make the following assumptions about the dynamics, cost, and constraints:

Assumption 1. For each $i \in \mathcal{Q}$, $f(\cdot, \cdot, \cdot, e_i)$ is differentiable in both x and u . Also, each $f(\cdot, \cdot, \cdot, e_i)$ and its partial derivatives are Lipschitz continuous with constant $L > 0$, i.e. given $t_1, t_2 \in [0, 1]$, $x_1, x_2 \in \mathbb{R}^n$, and $u_1, u_2 \in U$:

- (1) $\|f(t_1, x_1, u_1, e_i) - f(t_2, x_2, u_2, e_i)\|_2 \leq L(|t_1 - t_2| + \|x_1 - x_2\|_2 + \|u_1 - u_2\|_2)$,
- (2) $\left\| \frac{\partial f}{\partial x}(t_1, x_1, u_1, e_i) - \frac{\partial f}{\partial x}(t_2, x_2, u_2, e_i) \right\|_{i,2} \leq L(|t_1 - t_2| + \|x_1 - x_2\|_2 + \|u_1 - u_2\|_2)$,
- (3) $\left\| \frac{\partial f}{\partial u}(t_1, x_1, u_1, e_i) - \frac{\partial f}{\partial u}(t_2, x_2, u_2, e_i) \right\|_{i,2} \leq L(|t_1 - t_2| + \|x_1 - x_2\|_2 + \|u_1 - u_2\|_2)$.

Assumption 2. The functions h_0 and h_j are Lipschitz continuous and differentiable in x for all $j \in \mathcal{J}$. In addition, the derivatives of these functions with respect to x are also Lipschitz continuous with constant $L > 0$, i.e. given $x_1, x_2 \in \mathbb{R}^n$, for each $j \in \mathcal{J}$:

- (1) $|h_0(x_1) - h_0(x_2)| \leq L \|x_1 - x_2\|_2$,
- (2) $\left\| \frac{\partial h_0}{\partial x}(x_1) - \frac{\partial h_0}{\partial x}(x_2) \right\|_2 \leq L \|x_1 - x_2\|_2$,
- (3) $|h_j(x_1) - h_j(x_2)| \leq L \|x_1 - x_2\|_2$,
- (4) $\left\| \frac{\partial h_j}{\partial x}(x_1) - \frac{\partial h_j}{\partial x}(x_2) \right\|_2 \leq L \|x_1 - x_2\|_2$.

If a running cost is included in the problem statement (i.e. if the cost also depends on the integral of a function), then this function must also satisfy Assumption 1. Note that the equations of motion as defined in Equations (2.17) and (2.18) satisfy this assumption. Assumption 2 is a standard assumption on the objectives and constraints and is used to prove the convergence properties of the algorithm defined in the next section. These assumptions lead to the following result:

Lemma 2. There exists a constant $C > 0$ such that, for each $\xi \in \mathcal{X}_r$ and $t \in [0, 1]$,

$$\|x^{(\xi)}(t)\|_2 \leq C, \quad (2.36)$$

where $x^{(\xi)}$ is a solution of Differential Equation (2.29).

Proof. Given $\xi = (u, d) \in \mathcal{X}_r$ and noticing that $|d_i(t)| \leq 1$ for all $i \in \mathcal{Q}$ and $t \in [0, 1]$, we have:

$$\|x^{(\xi)}(t)\|_2 \leq \|x_0\|_2 + \sum_{i=1}^q \int_0^t \|f(s, x^{(\xi)}(s), u(s), e_i)\|_2 ds. \quad (2.37)$$

Next, observe that $\|f(0, x_0, 0, e_i)\|_2$ is bounded for all $i \in \mathcal{Q}$ and $u(s)$ is bounded for each $s \in [0, 1]$ since U is bounded. Then by Assumption 1, we know there exists a $K > 0$ such that for each $s \in [0, 1]$, $i \in \mathcal{Q}$, and $\xi \in \mathcal{X}_r$,

$$\|f(s, x^{(\xi)}(s), u(s), e_i)\|_2 \leq K(\|x^{(\xi)}(s)\|_2 + 1). \quad (2.38)$$

Applying the Bellman-Gronwall Inequality (Lemma 5.6.4 in [64]) to Equation (2.37), we have $\|x^{(\xi)}(t)\|_2 \leq e^{qK}(1 + \|x_0\|_2)$ for each $t \in [0, 1]$. Since x_0 is assumed given and bounded, we have our result. \square

In fact, this implies that the dynamics, cost, constraints, and their derivatives are all bounded:

Corollary 1. *There exists a constant $C > 0$ such that for each $\xi = (u, d) \in \mathcal{X}_r$, $t \in [0, 1]$, and $j \in \mathcal{J}$:*

- (1) a) $\|f(t, x^{(\xi)}(t), u(t), d(t))\|_2 \leq C,$
 b) $\left\|\frac{\partial f}{\partial x}(t, x^{(\xi)}(t), u(t), d(t))\right\|_{i,2} \leq C,$
 c) $\left\|\frac{\partial f}{\partial u}(t, x^{(\xi)}(t), u(t), d(t))\right\|_{i,2} \leq C,$
- (2) a) $|h_0(x^{(\xi)}(t))| \leq C,$
 b) $\left\|\frac{\partial h_0}{\partial x}(x^{(\xi)}(t))\right\|_2 \leq C,$
- (3) a) $|h_j(x^{(\xi)}(t))| \leq C,$
 b) $\left\|\frac{\partial h_j}{\partial x}(x^{(\xi)}(t))\right\|_2 \leq C,$

where $x^{(\xi)}$ is a solution of Differential Equation (2.29).

Proof. The result follows immediately from the continuity of f , $\frac{\partial f}{\partial x}$, $\frac{\partial f}{\partial u}$, h_0 , $\frac{\partial h_0}{\partial x}$, h_j , and $\frac{\partial h_j}{\partial x}$ for each $j \in \mathcal{J}$, as stated in Assumptions 1 and 2, and the fact that each of the arguments to these functions can be constrained to a compact domain, which follows from Lemma 2 and the compactness of U and Σ_r^q . \square

An application of this corollary leads to a fundamental result:

Theorem 3. *For each $\xi \in \mathcal{X}_r$ Differential Equation (2.29) has a unique solution.*

Proof. First let us note that f , as defined in Equation (2.28), is also Lipschitz with respect to its fourth argument. Indeed, given $t \in [0, 1]$, $x \in \mathbb{R}^n$, $u \in U$, and $d_1, d_2 \in \Sigma_r^q$,

$$\begin{aligned} \|f(t, x, u, d_1) - f(t, x, u, d_2)\|_2 &= \left\| \sum_{i=1}^q (d_{1,i} - d_{2,i}) f(t, x, u, e_i) \right\|_2 \\ &\leq Cq \|d_1 - d_2\|_2, \end{aligned} \quad (2.39)$$

where $C > 0$ is as in Corollary 1.

Given that f is Lipschitz with respect to all its arguments, the result follows as a direct extension of the classical existence and uniqueness theorem for nonlinear differential equations (see Section 2.4.1 in [89] for a standard version of this theorem). \square

Therefore, since $x^{(\xi)}$ is unique, it is not an abuse of notation to denote the solution of Differential Equation (2.29) by $x^{(\xi)}$. Next, we develop an algorithm to solve the Switched System Optimal Control Problem.

Chapter 3

A Conceptual Algorithm for Switched System Optimal Control

In this chapter, we describe our optimization algorithm. Our approach proceeds as follows: first, we treat a given pure discrete input as a relaxed discrete input by allowing it to belong \mathcal{D}_r ; second, we perform optimal control over the relaxed optimization space; and finally, we project the computed relaxed input into a pure input. Before describing our algorithm in detail, we begin with a brief digression to motivate why such a roundabout construction is required in order to devise a first order numerical optimal control scheme for the Switched System Optimal Control Problem defined in Equation (2.34).

3.1 Directional Derivatives

To appreciate why the construction of a numerical scheme to find the local minima of the Switched System Optimal Control Problem defined in Equation (2.34) is difficult, suppose that the optimization in the problem took place over the relaxed optimization space rather than the pure optimization space. The Relaxed Switched System Optimal Control Problem is then defined as:

Relaxed Switched System Optimal Control Problem.

$$\min_{\xi \in \mathcal{X}_r} \{J(\xi) \mid \Psi(\xi) \leq 0\}. \quad (3.1)$$

The local minimizers of this problem are then defined as follows:

Definition 3. *Let us denote an ε -ball in the \mathcal{X} -norm centered at ξ by:*

$$\mathcal{N}_{\mathcal{X}}(\xi, \varepsilon) = \{\bar{\xi} \in \mathcal{X}_r \mid \|\xi - \bar{\xi}\|_{\mathcal{X}} < \varepsilon\}. \quad (3.2)$$

We say that a point $\xi \in \mathcal{X}_r$ is a local minimizer of the Relaxed Switched System Optimal Control Problem defined in Equation (3.1) if $\Psi(\xi) \leq 0$ and there exists $\varepsilon > 0$ such that $J(\hat{\xi}) \geq J(\xi)$ for each $\hat{\xi} \in \mathcal{N}_{\mathcal{X}}(\xi, \varepsilon) \cap \{\bar{\xi} \in \mathcal{X}_r \mid \Psi(\bar{\xi}) \leq 0\}$.

Given this definition, a first order numerical optimal control scheme can exploit the vector space structure of the relaxed optimization space in order to define directional derivatives that find local minimizers for this Relaxed Switched System Optimal Control Problem.

To concretize how such an algorithm would work, we introduce some additional notation. Given $\xi \in \mathcal{X}_r$, \mathcal{Y} a Euclidean space, and any function $G : \mathcal{X}_r \rightarrow \mathcal{Y}$, the directional derivative of G at ξ , denoted $DG(\xi; \cdot) : \mathcal{X} \rightarrow \mathcal{Y}$, is computed as:

$$DG(\xi; \xi') = \lim_{\lambda \downarrow 0} \frac{G(\xi + \lambda\xi') - G(\xi)}{\lambda}. \quad (3.3)$$

To understand the connection between directional derivatives and local minimizers, suppose the Relaxed Switched System Optimal Control Problem is unconstrained and consider the first order approximation of the cost J at a point $\xi \in \mathcal{X}_r$ in the $\xi' \in \mathcal{X}$ direction by employing the directional derivative $DJ(\xi; \xi')$:

$$J(\xi + \lambda\xi') \approx J(\xi) + \lambda DJ(\xi; \xi'), \quad (3.4)$$

where $0 \leq \lambda \ll 1$. It follows that if $DJ(\xi; \xi')$, whose existence is proven in Lemma 11, is negative, then it is possible to decrease the cost by moving in the ξ' direction. That is if the directional derivative of the cost at a point ξ is negative along a certain direction, then for each $\varepsilon > 0$ there exists a $\hat{\xi} \in \mathcal{N}_{\mathcal{X}}(\xi, \varepsilon)$ such that $J(\hat{\xi}) < J(\xi)$. Therefore if $DJ(\xi; \xi')$ is negative, then ξ is not a local minimizer of the unconstrained Relaxed Switched System Optimal Control Problem.

Similarly, for the general Relaxed Switched System Optimal Control Problem, consider the first order approximation of each of the component constraint functions, $\psi_{j,t}$ for each $j \in \mathcal{J}$ and $t \in [0, 1]$ at a point $\xi \in \mathcal{X}_r$ in the $\xi \in \mathcal{X}$ direction by employing the directional derivative $D\psi_{j,t}(\xi; \xi')$:

$$\psi_{j,t}(\xi + \lambda\xi') \approx \psi_{j,t}(\xi) + \lambda D\psi_{j,t}(\xi; \xi'), \quad (3.5)$$

where $0 \leq \lambda \ll 1$. It follows that if $D\psi_{j,t}(\xi; \xi')$, whose existence is proven in Lemma 12, is negative, then it is possible to decrease the infeasibility of $\phi_t(\xi)$ with respect to h_j by moving in the ξ' direction. That is if the directional derivatives of the cost and all of the component constraints for all $t \in [0, 1]$ at a point ξ are negative along a certain direction and $\Psi(\xi) = 0$, then for each $\varepsilon > 0$ there exists a $\hat{\xi} \in \{\bar{\xi} \in \mathcal{X}_r \mid \Psi(\bar{\xi}) \leq 0\} \cap \mathcal{N}_{\mathcal{X}}(\xi, \varepsilon)$ such that $J(\hat{\xi}) < J(\xi)$. Therefore, if $\Psi(\xi) = 0$ and $DJ(\xi; \xi')$ and $D\psi_{j,t}(\xi; \xi')$ are negative for all $j \in \mathcal{J}$ and $t \in [0, 1]$, then ξ is not a local minimizer of the Relaxed Hybrid Optimal Control Problem. Similarly, if $\Psi(\xi) < 0$ and $DJ(\xi; \xi')$ is negative, then ξ is not a local minimizer of the Relaxed Hybrid Optimal Control Problem, even if $D\psi_{j,t}(\xi; \xi')$ is greater than zero for all $j \in \mathcal{J}$ and $t \in [0, 1]$.

Returning to the Switched System Optimal Control Problem, it is unclear how to define a directional derivative for the pure discrete input space since it is not a vector space. Therefore, in contrast to the relaxed discrete and continuous input spaces, the construction of a first order numerical scheme for the optimization of the pure discrete input is non-trivial. One could imagine trying to exploit the directional derivatives in the relaxed optimization space in order to construct a first order numerical optimal control algorithm for the Switched

System Optimal Control Problem, but this would require devising some type of connection between points belonging to the pure and relaxed optimization spaces.

3.2 The Weak Topology on the Optimization Space and Local Minimizers

To motivate the type of relationship required between the pure and relaxed optimization space in order to construct a first order numerical optimal control scheme, we begin by describing the Chattering Lemma:

Theorem 4 (Theorem 1 in [7]). *For each $\xi_r \in \mathcal{X}_r$ and $\varepsilon > 0$ there exists a $\xi_p \in \mathcal{X}_p$ such that for each $t \in [0, 1]$:*

$$\|\phi_t(\xi_r) - \phi_t(\xi_p)\|_2 \leq \varepsilon, \quad (3.6)$$

where $\phi_t(\xi_r)$ and $\phi_t(\xi_p)$ are solutions to Differential Equation (2.29) corresponding to ξ_r and ξ_p , respectively.

The theorem as is proven in [9] is not immediately applicable to switched systems, but a straightforward extension as is proven in Theorem 1 in [7] makes that feasible. Note that the theorem as stated in [7], considers only two vector fields (i.e. $q = 2$), but as the author's of the theorem remark, their proof can be generalized to an arbitrary number of vector fields. A particular version of this existence theorem can also be found in Lemma 1 [77].

Theorem 4 says that the behavior of any element of the relaxed optimization space with respect to the trajectory of switched system can be approximated arbitrarily well by a point in the pure optimization space. Unfortunately, the relaxed and pure point as in Theorem 4 need not be near one another in the metric induced by the \mathcal{X} -norm. Therefore, though there exists a relationship between the pure and relaxed optimization spaces, this connection is not reflected in the topology induced by the \mathcal{X} -norm; however, in a particular topology over the relaxed optimization space, a relaxed point and the pure point that approximates it as in Theorem 4 can be made arbitrarily close:

Definition 4. *We say that the weak topology on \mathcal{X}_r induced by Differential Equation (2.29) is the smallest topology on \mathcal{X}_r such that the map $\xi \mapsto x^{(\xi)}$ is continuous. Moreover, an ε -ball in the weak topology centered at ξ is denoted by:*

$$\mathcal{N}_w(\xi, \varepsilon) = \left\{ \bar{\xi} \in \mathcal{X}_r \mid \|x^{(\xi)} - x^{(\bar{\xi})}\|_{L^2} < \varepsilon \right\}. \quad (3.7)$$

A longer introduction to weak topology can be found in Section 3.8 in [70] or Section 2.3 in [46], but before continuing we make an important observation that aids in motivating the ensuing analysis. In order to understand the relationship between the topology generated by the \mathcal{X} -norm on \mathcal{X}_r and the weak topology on \mathcal{X}_r , observe that ϕ_t is Lipschitz continuous for all $t \in [0, 1]$ (this is proven in Corollary 3). Therefore, for any $\varepsilon > 0$ there exists a $\delta > 0$

such that if a pair of points of the relaxed optimization space belong to the same δ -ball in the \mathcal{X} -norm, then the pair of points belong to the same ε -ball in the weak topology on \mathcal{X}_r .

Notice, however, that it is not possible to show that for every $\varepsilon > 0$ that there exists a $\delta > 0$ such that if a pair of points of the relaxed optimization space belong to the same δ -ball in the weak topology on \mathcal{X}_r , then the pair of points belong to the same ε -ball in the \mathcal{X} -norm. More informally, a pair of points may generate trajectories that are near one another in the L^2 -norm while not being near one another in the \mathcal{X} -norm. Since the weak topology, in contrast to the \mathcal{X} -norm induced topology, naturally places points that generate nearby trajectories next to one another, we extend Definition 4 in order to define a weak topology on \mathcal{X}_p which we then use to define a notion of local minimizer for the Switched System Optimal Control Problem:

Definition 5. *We say that a point $\xi \in \mathcal{X}_p$ is a local minimizers of the Switched System Optimal Control Problem defined in Equation (2.34) if $\Psi(\xi) \leq 0$ and there exists $\varepsilon > 0$ such that $J(\hat{\xi}) \geq J(\xi)$ for each $\hat{\xi} \in \mathcal{N}_w(\xi, \varepsilon) \cap \{\bar{\xi} \in \mathcal{X}_p \mid \Psi(\bar{\xi}) \leq 0\}$, where \mathcal{N}_w is as defined in Equation (3.7).*

With this definition of local minimizer, we can exploit Theorem 4, even just as an existence result, along with the notion of directional derivative over the relaxed optimization space to construct a necessary condition for optimality for the Switched System Optimal Control Problem.

3.3 An Optimality Condition

Motivated by the approach undertaken in [64], we define an *optimality function*, $\theta : \mathcal{X}_p \rightarrow (-\infty, 0]$ that determines whether a given point is a local minimizer of the Switched System Optimal Control Problem and a corresponding *descent direction*, $g : \mathcal{X}_p \rightarrow \mathcal{X}_r$:

$$\theta(\xi) = \min_{\xi' \in \mathcal{X}_r} \zeta(\xi, \xi'), \quad g(\xi) = \arg \min_{\xi' \in \mathcal{X}_r} \zeta(\xi, \xi'), \quad (3.8)$$

where

$$\zeta(\xi, \xi') = \begin{cases} \max \left\{ \max_{j \in \mathcal{J}, t \in [0,1]} D\psi_{j,t}(\xi; \xi' - \xi) + \gamma\Psi(\xi), \right. \\ \quad \left. DJ(\xi; \xi' - \xi) \right\} + \|\xi' - \xi\|_{\mathcal{X}} & \text{if } \Psi(\xi) \leq 0, \\ \max \left\{ \max_{j \in \mathcal{J}, t \in [0,1]} D\psi_{j,t}(\xi; \xi' - \xi), \right. \\ \quad \left. DJ(\xi; \xi' - \xi) - \Psi(\xi) \right\} + \|\xi' - \xi\|_{\mathcal{X}} & \text{if } \Psi(\xi) > 0, \end{cases} \quad (3.9)$$

where $\gamma > 0$ is a design parameters. For notational convenience in the previous equation we have left out the natural inclusion of ξ from \mathcal{X}_p to \mathcal{X}_r . Before proceeding, we make two observations. First, note that $\theta(\xi) \leq 0$ for each $\xi \in \mathcal{X}_p$, since we can always choose

$\xi' = \xi$ which leaves the trajectory unmodified. Second, note that at a point $\xi \in \mathcal{X}_p$ the directional derivatives in the optimality function consider directions $\xi' - \xi$ with $\xi' \in \mathcal{X}_r$ in order to ensure that first order approximations constructed as in Equations (3.4) and (3.5) belong to the relaxed optimization space \mathcal{X}_r which is convex (e.g. for $0 < \lambda \ll 1$, $J(\xi) + \lambda DJ(\xi; \xi' - \xi) \approx J((1 - \lambda)\xi + \lambda\xi')$ where $(1 - \lambda)\xi + \lambda\xi' \in \mathcal{X}_r$).

To understand how the optimality function behaves, consider several cases. First, if $\theta(\xi) < 0$ and $\Psi(\xi) = 0$, then there exists a $\xi' \in \mathcal{X}_r$ such that both $DJ(\xi; \xi' - \xi)$ and $D\psi_{j,t}(\xi; \xi' - \xi)$ are negative for all $j \in \mathcal{J}$ and $t \in [0, 1]$. By employing the aforementioned first order approximation, we can show that for each $\varepsilon > 0$ there exists an ε -ball in the \mathcal{X} -norm centered at ξ such that $J(\hat{\xi}) < J(\xi)$ for some $\hat{\xi} \in \{\bar{\xi} \in \mathcal{X}_r \mid \Psi(\bar{\xi}) \leq 0\} \cap \mathcal{N}_{\mathcal{X}}(\xi, \varepsilon)$. As a result and because the cost and each of the component constraint functions are assumed Lipschitz continuous and ϕ_t for all $t \in [0, 1]$ is Lipschitz continuous as is proven in Corollary 3, an application of Theorem 4 allows us to show that for each $\varepsilon > 0$ there exists an ε -ball in the weak topology on \mathcal{X}_p centered at ξ such that $J(\xi_p) < J(\xi)$ for some $\xi_p \in \{\bar{\xi} \in \mathcal{X}_p \mid \Psi(\bar{\xi}) \leq 0\} \cap \mathcal{N}_w(\xi, \varepsilon)$. Therefore, it follows that if $\theta(\xi) < 0$ and $\Psi(\xi) = 0$, then ξ is not a local minimizer of the Switched System Optimal Control Problem.

Second, if $\theta(\xi) < 0$ and $\Psi(\xi) < 0$, then there exists a $\xi' \in \mathcal{X}_r$ such that $DJ(\xi; \xi' - \xi)$ is negative. Though $D\psi_{j,t}(\xi; \xi' - \xi)$ maybe positive for some $j \in \mathcal{J}$ and $t \in [0, 1]$, by employing the aforementioned first order approximation, we can show that for each $\varepsilon > 0$ there exists an ε -ball in the \mathcal{X} -norm centered at ξ such that $J(\hat{\xi}) < J(\xi)$ for some $\hat{\xi} \in \{\bar{\xi} \in \mathcal{X}_r \mid \Psi(\bar{\xi}) \leq 0\} \cap \mathcal{N}_{\mathcal{X}}(\xi, \varepsilon)$. As a result and because the cost and each of the constraint functions are assumed Lipschitz continuous and ϕ_t for all $t \in [0, 1]$ is Lipschitz continuous as is proven in Corollary 3, an application of Theorem 4 allows us to show that for each $\varepsilon > 0$ there exists an ε -ball in the weak topology on \mathcal{X}_p centered at ξ such that $J(\xi_p) < J(\xi)$ for some $\xi_p \in \{\bar{\xi} \in \mathcal{X}_p \mid \Psi(\bar{\xi}) \leq 0\} \cap \mathcal{N}_w(\xi, \varepsilon)$. Therefore, it follows that if $\theta(\xi) < 0$ and $\Psi(\xi) < 0$, then ξ is not a local minimizer of the Switched System Optimal Control Problem. In this case, the addition of the Ψ term in ζ ensures that a direction that reduces the cost does not simultaneously require a decrease in the infeasibility in order to be considered as a potential descent direction.

Third, if $\theta(\xi) < 0$ and $\Psi(\xi) > 0$, then there exists a $\xi' \in \mathcal{X}_r$ such that $D\psi_{j,t}(\xi; \xi' - \xi)$ is negative for all $j \in \mathcal{J}$ and $t \in [0, 1]$. By employing the aforementioned first order approximation, we can show for each $\varepsilon > 0$ there exists an ε -ball in the \mathcal{X} -norm centered at ξ such that $\Psi(\hat{\xi}) < \Psi(\xi)$ for some $\hat{\xi} \in \mathcal{N}_{\mathcal{X}}(\xi, \varepsilon)$. As a result and because each of the constraint functions are assumed Lipschitz continuous and ϕ_t for all $t \in [0, 1]$ is Lipschitz continuous as is proven in Corollary 3, an application of Theorem 4 allows us to show that for each $\varepsilon > 0$ there exists an ε -ball in the weak topology on \mathcal{X}_p centered at ξ such that $\Psi(\xi_p) < \Psi(\xi)$ for some $\xi_p \in \mathcal{N}_w(\xi, \varepsilon)$. Therefore, though it is clear that ξ is not a local minimizer of the Switched System Optimal Control Problem since $\Psi(\xi) > 0$, it follows that if $\theta(\xi) < 0$ and $\Psi(\xi) > 0$, then it is possible to locally reduce the infeasibility of ξ . In this case, the addition of the DJ term in ζ serves as a heuristic to ensure that the reduction in infeasibility does not come at the price of an undue increase in the cost.

These observations are formalized in Theorem 17 where we prove that if ξ is a local

minimizer of the Switched System Optimal Control Problem, then $\theta(\xi) = 0$, or that $\theta(\xi) = 0$ is a necessary condition for the optimality of ξ . To illustrate the importance of θ satisfying this property, recall how the directional derivative of a cost function is employed during unconstrained finite dimensional optimization. Since the directional derivative of the cost function at a point being equal to zero in all directions is a necessary condition for optimality for an unconstrained finite dimensional optimization problem, it is used as a stopping criterion by first order numerical algorithms (Corollary 1.1.3 and Algorithm Model 1.2.23 in [64]). Similarly, by satisfying Theorem 17, θ is a necessary condition for optimality for the Switched System Optimal Control Problem and can therefore be used as a stopping criterion for a first order numerical optimal control algorithm trying to solve the Switched System Optimal Control Problem. Given θ 's importance, we say *a point, $\xi \in \mathcal{X}_p$, satisfies the optimality condition* if $\theta(\xi) = 0$.

3.4 Choosing a Step Size and Projecting the Relaxed Discrete Input

Impressively, Theorem 4 just as an existence result is sufficient to allow for the construction of an optimality function that encapsulates a necessary condition for optimality for the Switched System Optimal Control Problem. Unfortunately, Theorem 4 is unable to describe how to exploit the descent direction, $g(\xi)$, since its proof provides no means to construct a pure input that approximates the behavior of a relaxed input while controlling the quality of the approximation. In this paper, we extend Theorem 4 by devising a scheme that remedies this shortcoming. This allows for the development of a numerical optimal control algorithm for the Switched System Optimal Control Problem that first, performs optimal control over the relaxed optimization space and then projects the computed relaxed control into a pure control.

Before describing the construction of this projection, we describe how the descent direction, $g(\xi)$, can be exploited to construct a point in the relaxed optimization space that either reduces the cost (if the ξ is feasible) or the infeasibility (if ξ is infeasible). Comparing our approach to finite dimensional optimization, the argument that minimizes ζ is a “direction” along which to move the inputs in order to reduce the cost in the relaxed optimization space, but we require an algorithm to choose a step size. We employ a line search algorithm similar to the traditional Armijo algorithm used during finite dimensional optimization in order to choose a step size (Algorithm Model 1.2.23 in [64]). Fixing $\alpha \in (0, 1)$ and $\beta \in (0, 1)$, a step size for a point $\xi \in \mathcal{X}_p$ is chosen by solving the following optimization problem:

$$\mu(\xi) = \begin{cases} \min \left\{ k \in \mathbb{N} \mid J(\xi + \beta^k(g(\xi) - \xi)) - J(\xi) \leq \alpha\beta^k\theta(\xi), \right. \\ \left. \Psi(\xi + \beta^k(g(\xi) - \xi)) \leq \alpha\beta^k\theta(\xi) \right\} & \text{if } \Psi(\xi) \leq 0, \\ \min \left\{ k \in \mathbb{N} \mid \Psi(\xi + \beta^k(g(\xi) - \xi)) - \Psi(\xi) \leq \alpha\beta^k\theta(\xi) \right\} & \text{if } \Psi(\xi) > 0. \end{cases} \quad (3.10)$$

In Lemma 24, we prove that for $\xi \in \mathcal{X}_p$, if $\theta(\xi) < 0$, then $\mu(\xi) < \infty$. Therefore, if $\theta(\xi) < 0$ for some $\xi \in \mathcal{X}_p$, then we can construct a descent direction, $g(\xi)$, and a step size, $\mu(\xi)$, and a new point $(\xi + \beta^{\mu(\xi)}(g(\xi) - \xi)) \in \mathcal{X}_r$ that produces a reduction in the cost (if ξ is feasible) or a reduction in the infeasibility (if ξ is infeasible).

We define the projection that takes this constructed point to a point belonging the pure optimization space while controlling the quality of approximation in two steps. First, we approximate the relaxed input by its N -th partial sum approximation via the Haar wavelet basis. To define this operation, $\mathcal{F}_N : L^2([0, 1], \mathbb{R}) \cap BV([0, 1], \mathbb{R}) \rightarrow L^2([0, 1], \mathbb{R}) \cap BV([0, 1], \mathbb{R})$, we employ the Haar wavelet (Section 7.2.2 in [54]):

$$\lambda(t) = \begin{cases} 1 & \text{if } t \in [0, \frac{1}{2}), \\ -1 & \text{if } t \in [\frac{1}{2}, 1), \\ 0 & \text{otherwise.} \end{cases} \quad (3.11)$$

Letting $\mathbf{1} : \mathbb{R} \rightarrow \mathbb{R}$ be the constant function equal to one and $b_{kj} : [0, 1] \rightarrow \mathbb{R}$ for $k \in \mathbb{N}$ and $j \in \{0, \dots, 2^k - 1\}$, be defined as $b_{kj}(t) = \lambda(2^k t - j)$, the projection \mathcal{F}_N for some $c \in L^2([0, 1], \mathbb{R}) \cap BV([0, 1], \mathbb{R}) \rightarrow L^2([0, 1], \mathbb{R}) \cap BV([0, 1], \mathbb{R})$ is defined as:

$$[\mathcal{F}_N(c)](t) = \langle c, \mathbf{1} \rangle + \sum_{k=0}^N \sum_{j=0}^{2^k-1} \langle c, b_{kj} \rangle \frac{b_{kj}(t)}{\|b_{kj}\|_{L^2}^2}. \quad (3.12)$$

Note that the inner product here is the traditional Hilbert space inner product.

This projection is then applied to each of the coordinates of an element in the relaxed optimization space. To avoid introducing additional notation, we let the coordinate-wise application of \mathcal{F}_N to some relaxed discrete input $d \in \mathcal{D}_r$ be denoted as $\mathcal{F}_N(d)$ and similarly for some continuous input $u \in \mathcal{U}$. Lemma 18 proves that for each $N \in \mathbb{N}$, each $t \in [0, 1]$, and each $i \in \{1, \dots, q\}$, $[\mathcal{F}_N(d)]_i(t) \in [0, 1]$ and $\sum_{i=1}^q [\mathcal{F}_N(d)]_i(t) = 1$ for the projection $\mathcal{F}_N(d)$. Therefore it follows that for each $d \in \mathcal{D}_r$, $\mathcal{F}_N(d) \in \mathcal{D}_r$.

Second, we use pulse width modulation as illustrated for a specific example in Figure 3.1. That is, we project the output of $\mathcal{F}_N(d)$ to a pure discrete input by employing the function $\mathcal{P}_N : \mathcal{D}_r \rightarrow \mathcal{D}_p$ which computes a multi-dimensional pulse width modulation of its argument with frequency 2^{-N} :

$$[\mathcal{P}_N(d)]_i(t) = \begin{cases} 1 & \text{if } t \in \left[2^{-N} \left(k + \sum_{j=1}^{i-1} d_j \left(\frac{k}{2^N} \right) \right), \right. \\ & \left. 2^{-N} \left(k + \sum_{j=1}^i d_j \left(\frac{k}{2^N} \right) \right) \right), \quad k \in \{0, 1, \dots, 2^N - 1\}, \\ 0 & \text{otherwise.} \end{cases} \quad (3.13)$$

Lemma 18 proves that for each $N \in \mathbb{N}$, each $t \in [0, 1]$, and each $i \in \{1, \dots, q\}$, $[\mathcal{P}_N(\mathcal{F}_N(d))]_i(t) \in \{0, 1\}$ and $\sum_{i=1}^q [\mathcal{P}_N(\mathcal{F}_N(d))]_i(t) = 1$. This proves that $\mathcal{P}_N(\mathcal{F}_N(d)) \in \mathcal{D}_p$ for each $d \in \mathcal{D}_r$.

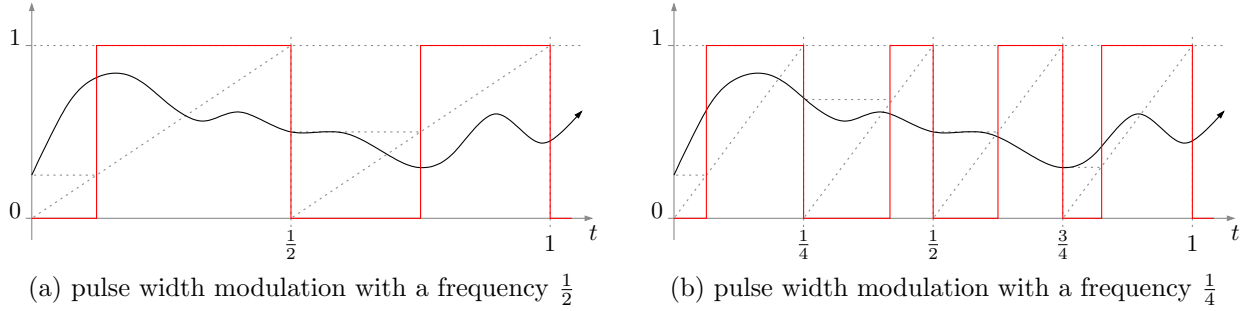


Figure 3.1: An illustration of the application of pulse width modulation (drawn in black) to a one dimensional signal (drawn in black) at two different frequencies. A sawtooth signal at the appropriate frequency is constructed (drawn in a black dotted line) and the value of the signal at the sampling times is projected onto the sawtooth. The pulse width modulation is set equal to zero for the amount of time equal to the projection onto the sawtooth and equal to one for the remainder of the sampling time.

Fixing $N \in \mathbb{N}$, we compose the two projections and define $\rho_N : \mathcal{X}_r \rightarrow \mathcal{X}_p$ as:

$$\rho_N(u, d) = \left(\mathcal{F}_N(u), \mathcal{P}_N(\mathcal{F}_N(d)) \right). \quad (3.14)$$

Critically, as shown in Theorem 21, this projection allows us to extend Theorem 4 by constructing an upper bound that goes to zero as N goes infinity between the error of employing the relaxed control rather than its projection in the solution of Differential Equation (2.29). Therefore in a fashion similar to applying the Armijo algorithm, we choose an $N \in \mathbb{N}$ at which to perform pulse width modulation by performing a line search. Fixing $\bar{\alpha} \in (0, \infty)$, $\bar{\beta} \in \left(\frac{1}{\sqrt{2}}, 1\right)$, and $\omega \in (0, 1)$, a frequency at which to perform pulse width modulation for a point $\xi \in \mathcal{X}_p$ is computed by solving the following optimization problem:

$$\nu(\xi) = \begin{cases} \min \left\{ k \in \mathbb{N} \mid \begin{aligned} &\xi' = \xi + \beta^{\mu(\xi)}(g(\xi) - \xi), \\ &J(\rho_k(\xi')) - J(\xi) \leq (\alpha\beta^{\mu(\xi)} - \bar{\alpha}\bar{\beta}^k)\theta(\xi), \\ &\Psi(\rho_k(\xi')) \leq 0, \\ &\bar{\alpha}\bar{\beta}^k \leq (1 - \omega)\alpha\beta^{\mu(\xi)} \end{aligned} \right\} & \text{if } \Psi(\xi) \leq 0, \\ \min \left\{ k \in \mathbb{N} \mid \begin{aligned} &\xi' = \xi + \beta^{\mu(\xi)}(g(\xi) - \xi), \\ &\Psi(\rho_k(\xi')) - \Psi(\xi) \leq (\alpha\beta^{\mu(\xi)} - \bar{\alpha}\bar{\beta}^k)\theta(\xi), \\ &\bar{\alpha}\bar{\beta}^k \leq (1 - \omega)\alpha\beta^{\mu(\xi)} \end{aligned} \right\} & \text{if } \Psi(\xi) > 0. \end{cases} \quad (3.15)$$

In Lemma 25, we prove that for $\xi \in \mathcal{X}_p$, if $\theta(\xi) < 0$, then $\nu(\xi) < \infty$. Therefore, if $\theta(\xi) < 0$ for some $\xi \in \mathcal{X}_p$, then we can construct a descent direction, $g(\xi)$, a step size, $\mu(\xi)$, a frequency at

which to perform pulse width modulation, $\nu(\xi)$, and a new point $\rho_{\nu(\xi)}(\xi + \beta^{\mu(\xi)}(g(\xi) - \xi)) \in \mathcal{X}_p$ that produces a reduction in the cost (if ξ is feasible) or a reduction in the infeasibility (if ξ is infeasible).

3.5 Switched System Optimal Control Algorithm

Consolidating our definitions, Algorithm 1 describes our numerical method to solve the Switched System Optimal Control Problem. For analysis purposes, we define $\Gamma : \mathcal{X}_p \rightarrow \mathcal{X}_p$ by

$$\Gamma(\xi) = \rho_{\nu(\xi)}(\xi + \beta^{\mu(\xi)}(g(\xi) - \xi)). \quad (3.16)$$

We say $\{\xi_j\}_{j \in \mathbb{N}}$ is a *sequence generated by Algorithm 1* if $\xi_{j+1} = \Gamma(\xi_j)$ for each $j \in \mathbb{N}$. We can prove several important properties about the sequence generated by Algorithm 1. First, in Lemma 26, we prove that if there exists $i_0 \in \mathbb{N}$ such that $\Psi(\xi_{i_0}) \leq 0$, then $\Psi(\xi_i) \leq 0$ for each $i \geq i_0$. That is, if the Algorithm constructs a feasible point, then the sequence of points generated after this feasible point are always feasible. Second, in Theorem 27, we prove $\lim_{j \rightarrow \infty} \theta(\xi_j) = 0$ or that Algorithm 1 converges to a point that satisfies the optimality condition.

Algorithm 1 Optimization Algorithm for the Switched System Optimal Control Problem

Require: $\xi_0 \in \mathcal{X}_p$, $\alpha \in (0, 1)$, $\bar{\alpha} \in (0, \infty)$, $\beta \in (0, 1)$, $\bar{\beta} \in \left(\frac{1}{\sqrt{2}}, 1\right)$, $\gamma \in (0, \infty)$, $\omega \in (0, 1)$.

- 1: Set $j = 0$.
 - 2: Compute $\theta(\xi_j)$ as defined in Equation (3.8).
 - 3: **if** $\theta(\xi_j) = 0$ **then**
 - 4: **return** ξ_j .
 - 5: **end if**
 - 6: Compute $g(\xi_j)$ as defined in Equation (3.8).
 - 7: Compute $\mu(\xi_j)$ as defined in Equation (3.10).
 - 8: Compute $\nu(\xi_j)$ as defined in Equation (3.15).
 - 9: Set $\xi_{j+1} = \rho_{\nu(\xi_j)}(\xi_j + \beta^{\mu(\xi_j)}(g(\xi_j) - \xi_j))$, as defined in Equation (3.14).
 - 10: Replace j by $j + 1$ and go to Line 2.
-

Chapter 4

Proving the Convergence of the Conceptual Algorithm

In this chapter, we derive the various components of Algorithm 1 and prove that Algorithm 1 converges to a point that satisfies our optimality condition. Our argument proceeds as follows: first, we prove the continuity of the state, cost, and constraint, which we employ in latter arguments; second, we construct the components of the optimality function and prove that these components satisfy various properties that ensure that the well-posedness of the optimality function; third, we prove that we can control the quality of approximation between the trajectories generated by a relaxed discrete input and its projection by ρ_N as a function of N ; finally, we prove the convergence of our algorithm.

4.1 Continuity

In this section, we prove the continuity of the state, cost, and constraint. We begin by proving the continuity of the solution to Differential Equation (2.29) with respect to ξ by proving that this mapping is sequentially continuous:

Lemma 5. *Let $\{\xi_j\}_{j=1}^{\infty} \subset \mathcal{X}_r$ be a convergent sequence with limit $\xi \in \mathcal{X}_r$. Then the corresponding sequence of trajectories $\{x^{(\xi_j)}\}_{j=1}^{\infty}$, as defined in Equation (2.29), converges uniformly to $x^{(\xi)}$.*

Proof. For notational convenience, let $\xi_j = (u_j, d_j)$, $\xi = (u, d)$, and ϕ_t as defined in Equation (2.30). We begin by proving the convergence of $\{\phi_t(\xi_j)\}_{j=1}^{\infty}$ to $\phi_t(\xi)$ for each $t \in [0, 1]$. Consider

$$\|\phi_t(\xi_j) - \phi_t(\xi)\|_2 = \left\| \int_0^t \sum_{i=1}^q [d_j]_i(\tau) f(\tau, \phi_\tau(\xi_j), u_j(\tau), e_i) - d_i(\tau) f(\tau, \phi_\tau(\xi), u(\tau), e_i) d\tau \right\|_2. \quad (4.1)$$

Therefore,

$$\begin{aligned} \|\phi_t(\xi_j) - \phi_t(\xi)\|_2 &= \left\| \int_0^t \sum_{i=1}^q ([d_j]_i(\tau) - d_i(\tau)) f(\tau, \phi_\tau(\xi_j), u_j(\tau), e_i) + \right. \\ &\quad + d_i(\tau) (f(\tau, \phi_\tau(\xi_j), u_j(\tau), e_i) - f(\tau, \phi_\tau(\xi), u_j(\tau), e_i)) + \\ &\quad \left. + d_i(\tau) (f(\tau, \phi_\tau(\xi), u_j(\tau), e_i) - f(\tau, \phi_\tau(\xi), u(\tau), e_i)) d\tau \right\|_2. \end{aligned} \quad (4.2)$$

Applying the Triangle Inequality, Assumption 1, Condition 1 in Corollary 1, and the boundedness of d , we have that there exists a $C > 0$ such that

$$\|\phi_t(\xi_j) - \phi_t(\xi)\|_2 \leq \int_0^1 \sum_{i=1}^q C |[d_j]_i(\tau) - d_i(\tau)| + L \|\phi_\tau(\xi_j) - \phi_\tau(\xi)\|_2 + L \|u_j(\tau) - u(\tau)\|_2 d\tau. \quad (4.3)$$

Applying the Bellman-Gronwall Inequality (Lemma 5.6.4 in [64]), we have that

$$\|\phi_t(\xi_j) - \phi_t(\xi)\|_2 \leq e^L \left(\int_0^1 C \|d_j(\tau) - d(\tau)\|_1 + L \|u_j(\tau) - u(\tau)\|_2 d\tau \right). \quad (4.4)$$

Note that $\|u\|_2 \leq \|u\|_1$ for each $u \in \mathbb{R}^m$. Then applying Holder's inequality (Proposition 6.2 in [26]) to the vector valued function, we have:

$$\int_0^1 \|d_j(\tau) - d(\tau)\|_1 d\tau \leq \|d_j - d\|_{L^2}, \quad \text{and} \quad \int_0^1 \|u_j(\tau) - u(\tau)\|_1 d\tau \leq \|u_j - u\|_{L^2}. \quad (4.5)$$

Since the sequence ξ_j converges to ξ , for every $\varepsilon > 0$ we know there exists some j_0 such that for all j greater than j_0 , $\|\xi_j - \xi\|_{\mathcal{X}} \leq \varepsilon$. Therefore $\|\phi_t(\xi_j) - \phi_t(\xi)\|_2 \leq e^L(L + C)\varepsilon$, which proves the convergence of $\{\phi_t(\xi_j)\}_{j=1}^\infty$ to $\phi_t(\xi)$ for each $t \in [0, 1]$ as $j \rightarrow \infty$. Since this bound does not depend on t , we in fact have the uniform convergence of $\{x^{(\xi_j)}\}_{j=1}^\infty$ to $x^{(\xi)}$ as $j \rightarrow \infty$, hence obtaining our desired result. \square

Notice that since \mathcal{X}_r is a metric space, the previous result proves that the function ϕ_t which assigns $\xi \in \mathcal{X}_r$ to $\phi_t(\xi)$ as the solution of Differential Equation (2.29) employing the notation defined in Equation (2.30) is continuous.

Corollary 2. *The function ϕ_t that maps $\xi \in \mathcal{X}_r$ to $\phi_t(\xi)$ as the solution of Differential Equation (2.29) where we employ the notation defined in Equation (2.30) is continuous for all $t \in [0, 1]$.*

In fact, our arguments have shown that this mapping is Lipschitz continuous:

Corollary 3. *There exists a constant $L > 0$ such that for each $\xi_1, \xi_2 \in \mathcal{X}_r$ and $t \in [0, 1]$:*

$$\|\phi_t(\xi_1) - \phi_t(\xi_2)\|_2 \leq L \|\xi_1 - \xi_2\|_{\mathcal{X}}, \quad (4.6)$$

where $\phi_t(\xi)$ is as defined in Equation (2.30).

As a result of this corollary, we immediately have the following results:

Corollary 4. *There exists a constant $L > 0$ such that for each $\xi_1 = (u_1, d_1) \in \mathcal{X}_r$, $\xi_2 = (u_2, d_2) \in \mathcal{X}_r$, and $t \in [0, 1]$:*

- (1) $\|f(t, \phi_t(\xi_1), u_1(t), d_1(t)) - f(t, \phi_t(\xi_2), u_2(t), d_2(t))\|_2 \leq$
 $\leq L(\|\xi_1 - \xi_2\|_{\mathcal{X}} + \|u_1(t) - u_2(t)\|_2 + \|d_1(t) - d_2(t)\|_2),$
- (2) $\left\| \frac{\partial f}{\partial x}(t, \phi_t(\xi_1), u_1(t), d_1(t)) - \frac{\partial f}{\partial x}(t, \phi_t(\xi_2), u_2(t), d_2(t)) \right\|_{i,2} \leq$
 $\leq L(\|\xi_1 - \xi_2\|_{\mathcal{X}} + \|u_1(t) - u_2(t)\|_2 + \|d_1(t) - d_2(t)\|_2),$
- (3) $\left\| \frac{\partial f}{\partial u}(t, \phi_t(\xi_1), u_1(t), d_1(t)) - \frac{\partial f}{\partial u}(t, \phi_t(\xi_2), u_2(t), d_2(t)) \right\|_{i,2} \leq$
 $\leq L(\|\xi_1 - \xi_2\|_{\mathcal{X}} + \|u_1(t) - u_2(t)\|_2 + \|d_1(t) - d_2(t)\|_2),$

where $\phi_t(\xi)$ is as defined in Equation (2.30).

Proof. The proof of Condition 1 follows by the fact that the vector field f is Lipschitz in all its arguments, as shown in the proof of Theorem 3, and applying Corollary 3. The remaining conditions follow in a similar fashion. \square

Corollary 5. *There exists a constant $L > 0$ such that for each $\xi_1, \xi_2 \in \mathcal{X}_r$, $j \in \mathcal{J}$, and $t \in [0, 1]$:*

- (1) $|h_0(\phi_1(\xi_1)) - h_0(\phi_1(\xi_2))| \leq L \|\xi_1 - \xi_2\|_{\mathcal{X}},$
- (2) $\left\| \frac{\partial h_0}{\partial x}(\phi_1(\xi_1)) - \frac{\partial h_0}{\partial x}(\phi_1(\xi_2)) \right\|_2 \leq L \|\xi_1 - \xi_2\|_{\mathcal{X}},$
- (3) $|h_j(\phi_t(\xi_1)) - h_j(\phi_t(\xi_2))| \leq L \|\xi_1 - \xi_2\|_{\mathcal{X}},$
- (4) $\left\| \frac{\partial h_j}{\partial x}(\phi_t(\xi_1)) - \frac{\partial h_j}{\partial x}(\phi_t(\xi_2)) \right\|_2 \leq L \|\xi_1 - \xi_2\|_{\mathcal{X}},$

where $\phi_t(\xi)$ is as defined in Equation (2.30).

Proof. This result follows by Assumption 2 and Corollary 3. \square

Even though it is a straightforward consequence of Condition 1 in Corollary 5, we write the following result to stress its importance.

Corollary 6. *There exists a constant $L > 0$ such that, for each $\xi_1, \xi_2 \in \mathcal{X}_r$:*

$$|J(\xi_1) - J(\xi_2)| \leq L \|\xi_1 - \xi_2\|_{\mathcal{X}} \quad (4.7)$$

where J is as defined in Equation (2.31).

In fact, the Ψ is also Lipschitz continuous:

Lemma 6. *There exists a constant $L > 0$ such that, for each $\xi_1, \xi_2 \in \mathcal{X}_r$:*

$$|\Psi(\xi_1) - \Psi(\xi_2)| \leq L \|\xi_1 - \xi_2\|_{\mathcal{X}} \quad (4.8)$$

where Ψ is as defined in Equation (2.32).

Proof. Since the maximum in Ψ is taken over $\mathcal{J} \times [0, 1]$, which is compact, and the maps $(j, t) \mapsto \psi_{j,t}(\xi)$ are continuous for each $\xi \in \mathcal{X}$, we know from Condition 3 in Corollary 5 that there exists $L > 0$ such that,

$$\begin{aligned} \Psi(\xi_1) - \Psi(\xi_2) &= \max_{(j,t) \in \mathcal{J} \times [0,1]} \psi_{j,t}(\xi_1) - \max_{(j,t) \in \mathcal{J} \times [0,1]} \psi_{j,t}(\xi_2) \\ &\leq \max_{(j,t) \in \mathcal{J} \times [0,1]} \psi_{j,t}(\xi_1) - \psi_{j,t}(\xi_2) \\ &\leq L \|\xi_1 - \xi_2\|_{\mathcal{X}}. \end{aligned} \quad (4.9)$$

By reversing ξ_1 and ξ_2 , and applying the same argument we get the desired result. \square

4.2 Derivation of Algorithm Terms

Next, we formally derive the components of the optimality function and prove the well-posedness of the optimality function. We begin by deriving the formal expression for the directional derivative of the trajectory of the switched system.

Lemma 7. *Let $\xi = (u, d) \in \mathcal{X}_r$, $\xi' = (u', d') \in \mathcal{X}$, and let $\phi_t : \mathcal{X}_r \rightarrow \mathbb{R}^n$ be as defined in Equation (2.30). Then the directional derivative of ϕ_t , as defined in Equation (3.3), is given by*

$$D\phi_t(\xi; \xi') = \int_0^t \Phi^{(\xi)}(t, \tau) \left(\frac{\partial f}{\partial u}(\tau, \phi_\tau(\xi), u(\tau), d(\tau)) u'(\tau) + \sum_{i=1}^q f(\tau, \phi_\tau(\xi), u(\tau), e_i) d'_i(\tau) \right) d\tau, \quad (4.10)$$

where $\Phi^{(\xi)}(t, \tau)$ is the unique solution of the following matrix differential equation:

$$\frac{\partial \Phi}{\partial t}(t, \tau) = \frac{\partial f}{\partial x}(t, \phi_t(\xi), u(t), d(t)) \Phi(t, \tau), \quad t \in [0, 1], \quad \Phi(\tau, \tau) = I. \quad (4.11)$$

Proof. For notational convenience, let $x^{(\lambda)} = x^{(\xi + \lambda \xi')}$, $u^{(\lambda)} = u + \lambda u'$, and $d^{(\lambda)} = d + \lambda d'$. Then, if we define $\Delta x^{(\lambda)} = x^{(\lambda)} - x^{(\xi)}$,

$$\Delta x^{(\lambda)}(t) = \int_0^t f(\tau, x^{(\lambda)}(\tau), u^{(\lambda)}(\tau), d^{(\lambda)}(\tau)) - f(\tau, x^{(\xi)}(\tau), u(\tau), d(\tau)) d\tau, \quad (4.12)$$

thus,

$$\begin{aligned} \Delta x^{(\lambda)}(t) &= \int_0^t f(\tau, x^{(\lambda)}(\tau), u^{(\lambda)}(\tau), d^{(\lambda)}(\tau)) - f(\tau, x^{(\lambda)}(t), u^{(\lambda)}(\tau), d(\tau)) d\tau + \\ &\quad + \int_0^t f(\tau, x^{(\lambda)}(\tau), u^{(\lambda)}(\tau), d(\tau)) - f(\tau, x^{(\xi)}(t), u^{(\lambda)}(\tau), d(\tau)) d\tau + \\ &\quad + \int_0^t f(\tau, x^{(\xi)}(\tau), u^{(\lambda)}(\tau), d(\tau)) - f(\tau, x^{(\xi)}(t), u(\tau), d(\tau)) d\tau, \end{aligned} \quad (4.13)$$

and applying the Mean Value Theorem,

$$\begin{aligned} \Delta x^{(\lambda)}(t) &= \int_0^t \lambda \sum_{i=1}^q d'_i(\tau) f(\tau, x^{(\lambda)}(\tau), u^{(\lambda)}(\tau), e_i) + \\ &\quad + \int_0^t \frac{\partial f}{\partial x}(\tau, x^{(\xi)}(\tau) + \nu_x(\tau) \Delta x^{(\lambda)}(\tau), u^{(\lambda)}(\tau), d(\tau)) \Delta x^{(\lambda)}(\tau) + \\ &\quad + \int_0^t \lambda \frac{\partial f}{\partial u}(\tau, x^{(\xi)}(\tau), u(\tau) + \nu_u(\tau) \lambda u'(\tau), d(\tau)) u'(\tau) dt, \end{aligned} \quad (4.14)$$

where $\nu_u, \nu_x : [0, t] \rightarrow [0, 1]$.

Let $z(t)$ be the unique solution of the following differential equation:

$$\begin{aligned} \dot{z}(\tau) &= \frac{\partial f}{\partial x}(\tau, x^{(\xi)}(\tau), u(\tau), d(\tau)) z(\tau) + \frac{\partial f}{\partial u}(\tau, x^{(\xi)}(\tau), u(\tau), d(\tau)) u'(\tau) + \\ &\quad + \sum_{i=1}^q d'_i(\tau) f(\tau, x^{(\xi)}(\tau), u(\tau), e_i), \quad \tau \in [0, t], \quad z(0) = 0. \end{aligned} \quad (4.15)$$

We want to show that $\lim_{\lambda \downarrow 0} \left\| \frac{\Delta x^{(\lambda)}(t)}{\lambda} - z(t) \right\|_2 = 0$. To prove this, consider the following inequalities that follow from Condition 2 in Assumption 1:

$$\begin{aligned} &\left\| \int_0^t \frac{\partial f}{\partial x}(\tau, x^{(\xi)}(\tau), u(\tau), d(\tau)) z(\tau) + \right. \\ &\quad \left. - \frac{\partial f}{\partial x}(\tau, x^{(\xi)}(\tau) + \nu_x(\tau) \Delta x^{(\lambda)}(\tau), u^{(\lambda)}(\tau), d(\tau)) \frac{\Delta x^{(\lambda)}(\tau)}{\lambda} d\tau \right\|_2 \leq \\ &\leq \int_0^t \left\| \frac{\partial f}{\partial x} \right\|_{L^\infty} \left\| z(\tau) - \frac{\Delta x^{(\lambda)}(\tau)}{\lambda} \right\|_2 d\tau + \\ &\quad + \int_0^t L (\|\nu_x(\tau) \Delta x^{(\lambda)}(\tau)\|_2 + \lambda \|u'(\tau)\|_2) \|z(t)\|_2 d\tau \\ &\leq L \int_0^t \left\| z(\tau) - \frac{\Delta x^{(\lambda)}(\tau)}{\lambda} \right\|_2 d\tau + \\ &\quad + L \int_0^t (\|\Delta x^{(\lambda)}(\tau)\|_2 + \lambda \|u'(\tau)\|_2) \|z(t)\|_2 d\tau, \end{aligned} \quad (4.16)$$

also from Condition 3 in Assumption 1:

$$\begin{aligned} \left\| \int_0^t \left(\frac{\partial f}{\partial u}(\tau, x^{(\xi)}(\tau), u(\tau), d(\tau)) - \frac{\partial f}{\partial u}(\tau, x^{(\xi)}(\tau), u(\tau) + \nu_u(\tau)\lambda u'(\tau), d(\tau)) \right) u'(\tau) \right\|_2 &\leq \\ &\leq L \int_0^t \lambda \|\nu_u(\tau)u'(\tau)\|_2 \|u'(\tau)\|_2 d\tau \leq L \int_0^t \lambda \|u'(\tau)\|_2^2 d\tau, \end{aligned} \quad (4.17)$$

and from Condition 1 in Assumption 1:

$$\begin{aligned} \left\| \int_0^t \sum_{i=1}^q d'_i(\tau) (f(\tau, x^{(\xi)}(\tau), u(\tau), e_i) - f(\tau, x^{(\lambda)}(\tau), u^{(\lambda)}(\tau), e_i)) d\tau \right\|_2 &\leq \\ &\leq L \int_0^t \sum_{i=1}^q d'_i(\tau) (\|\Delta x^{(\lambda)}(\tau)\|_2 + \lambda \|u'(\tau)\|_2) d\tau. \end{aligned} \quad (4.18)$$

Now, using the Bellman-Gronwall Inequality (Lemma 5.6.4 in [64]) and the inequalities above,

$$\begin{aligned} \left\| \frac{\Delta x^{(\lambda)}(t)}{\lambda} - z(t) \right\|_2 &\leq e^{Lt} L \left(\int_0^t (\|\Delta x^{(\lambda)}(\tau)\|_2 + \lambda \|u'(\tau)\|_2) \|z(\tau)\|_2 + \lambda \|u'(\tau)\|_2^2 + \right. \\ &\quad \left. + \sum_{i=1}^q d'_i(\tau) (\|\Delta x^{(\lambda)}(\tau)\|_2 + \lambda \|u'(\tau)\|_2) d\tau \right), \end{aligned} \quad (4.19)$$

but note that every term in the integral above is bounded, and $\Delta x^{(\lambda)}(\tau) \rightarrow 0$ for each $\tau \in [0, t]$ since $x^{(\lambda)} \rightarrow x^{(\xi)}$ uniformly as shown in Lemma 5, thus by the Dominated Convergence Theorem (Theorem 2.24 in [26]) and by noting that $D\phi_t(\xi; \xi')$, as defined in Equation (4.10), is exactly the solution of Differential Equation (4.15) we get:

$$\lim_{\lambda \downarrow 0} \left\| \frac{\Delta x^{(\lambda)}(t)}{\lambda} - z(t) \right\|_2 = \lim_{\lambda \downarrow 0} \frac{1}{\lambda} \|x^{(\xi+\lambda\xi')}(t) - x^{(\xi)}(t) - D\phi_t(\xi; \lambda\xi')\|_2 = 0. \quad (4.20)$$

The result of the Lemma then follows. □

Next, we prove that $D\phi_t$ is bounded by proving that $\Phi^{(\xi)}$ is bounded:

Corollary 7. *There exists a constant $C > 0$ such that for each $t, \tau \in [0, 1]$ and $\xi \in \mathcal{X}_r$:*

$$\|\Phi^{(\xi)}(t, \tau)\|_{i,2} \leq C, \quad (4.21)$$

where $\Phi^{(\xi)}(t, \tau)$ is the solution to Differential Equation (4.11).

Proof. Notice that, since the induced matrix norm is submultiplicative,

$$\|\Phi^{(\xi)}(t, \tau)\|_{i,2} = \left\| \Phi^{(\xi)}(t, \tau) + \int_{\tau}^t \left(\frac{\partial f}{\partial x}(s, x^{(\xi)}(s), u(s), d(s)) \Phi^{(\xi)}(s, \tau) \right) ds \right\|_{i,2} \quad (4.22)$$

$$\leq 1 + \int_{\tau}^t \left\| \frac{\partial f}{\partial x}(s, x^{(\xi)}(s), u(s), d(s)) \right\|_{i,2} \|\Phi^{(\xi)}(t, s)\|_{i,2} ds \quad (4.23)$$

$$\leq e^{qC}, \quad (4.24)$$

where in the last step we employed Condition 1 from Corollary 1 with a constant $C > 0$ and the Bellman-Gronwall Inequality. \square

Corollary 8. *There exists a constant $C > 0$ such that for all $\xi \in \mathcal{X}_r$, $\xi' \in \mathcal{X}$, and $t \in [0, 1]$:*

$$\|D\phi_t(\xi; \xi')\|_2 \leq C \|\xi'\|_{\mathcal{X}}, \quad (4.25)$$

where $D\phi_t$ is as defined in Equation (4.10).

Proof. This result follows by employing the Cauchy-Schwarz Inequality, Corollary 1 and Corollary 7. \square

In fact, we can actually prove the Lipschitz continuity of $\Phi^{(\xi)}$:

Lemma 8. *There exists a constant $L > 0$ such that for each $\xi_1, \xi_2 \in \mathcal{X}_r$ and each $t, \tau \in [0, 1]$:*

$$\|\Phi^{(\xi_1)}(t, \tau) - \Phi^{(\xi_2)}(t, \tau)\|_{i,2} \leq L \|\xi_1 - \xi_2\|_{\mathcal{X}}, \quad (4.26)$$

where $\Phi^{(\xi)}$ is the solution to Differential Equation (4.11).

Proof. Letting $\xi_1 = (u_1, d_1) \in \mathcal{X}_r$ and $\xi_2 = (u_2, d_2) \in \mathcal{X}_r$ and by applying the Triangle Inequality and noticing the induced matrix norm is compatible, observe:

$$\begin{aligned} \|\Phi^{(\xi_1)}(t, \tau) - \Phi^{(\xi_2)}(t, \tau)\|_{i,2} &\leq \int_{\tau}^t \left(\left\| \frac{\partial f}{\partial x}(s, x^{(\xi_2)}(s), u_2(s), d_2(s)) \right\|_{i,2} \|\Phi^{(\xi_1)}(s, \tau) + \right. \\ &\quad \left. - \Phi^{(\xi_2)}(s, \tau)\|_{i,2} \right) ds + \int_{\tau}^t \left(\left\| \frac{\partial f}{\partial x}(s, x^{(\xi_1)}(s), u_1(s), d_1(s)) + \right. \right. \\ &\quad \left. \left. - \frac{\partial f}{\partial x}(s, x^{(\xi_2)}(s), u_2(s), d_2(s)) \right\|_{i,2} \|\Phi^{(\xi_1)}(s, \tau)\|_{i,2} \right) ds. \end{aligned} \quad (4.27)$$

By applying Condition 1 in Corollary 1, Condition 2 in Corollary 4, Corollary 7, the same argument as in Equation (4.5), and the Bellman-Gronwall Inequality (Lemma 5.6.4 in [64]), our desired result follows. \square

A simple extension of our previous argument shows that for all $t \in [0, 1]$, $D\phi_t(\xi; \cdot)$ is Lipschitz continuous with respect to its point of evaluation, ξ .

Lemma 9. *There exists a constant $L > 0$ such that for each $\xi_1, \xi_2 \in \mathcal{X}_r$, $\xi' \in \mathcal{X}$, and $t \in [0, 1]$:*

$$\|D\phi_t(\xi_1; \xi') - D\phi_t(\xi_2; \xi')\|_2 \leq L \|\xi_1 - \xi_2\|_{\mathcal{X}} \|\xi'\|_{\mathcal{X}} \quad (4.28)$$

where $D\phi_t$ is as defined in Equation (4.10).

Proof. Let $\xi_1 = (u_1, d_1)$, $\xi_2 = (u_2, d_2)$, and $\xi' = (u', d')$. Then, by applying the Triangle Inequality, and noticing that the induced matrix norm is compatible, observe:

$$\begin{aligned} \|D\phi_t(\xi_1; \xi') - D\phi_t(\xi_2; \xi')\|_2 &\leq \int_0^t \left(\|\Phi^{(\xi_1)}(t, s) - \Phi^{(\xi_2)}(t, s)\|_{i,2} \cdot \right. \\ &\quad \cdot \left\| \frac{\partial f}{\partial u}(s, x^{(\xi_1)}(s), u_1(s), d_1(s)) \right\|_{i,2} + \|\Phi^{(\xi_2)}(t, s)\|_{i,2} \left\| \frac{\partial f}{\partial u}(s, x^{(\xi_1)}(s), u_1(s), d_1(s)) + \right. \\ &\quad \left. - \frac{\partial f}{\partial u}(s, x^{(\xi_2)}(s), u_2(s), d_2(s)) \right\|_{i,2} \left. \right) \|u'(s)\|_2 ds + \int_0^t \sum_{i=1}^q \left(\|\Phi^{(\xi_1)}(t, s) - \Phi^{(\xi_2)}(t, s)\|_{i,2} \cdot \right. \\ &\quad \cdot \left\| f(s, x^{(\xi_1)}(s), u_1(s), e_i) \right\|_2 + \|\Phi^{(\xi_2)}(t, s)\|_{i,2} \left\| f(s, x^{(\xi_1)}(s), u_1(s), e_i) + \right. \\ &\quad \left. \left. - f(s, x^{(\xi_2)}(s), u_2(s), e_i) \right\|_2 \right) \|d'(s)\| ds. \quad (4.29) \end{aligned}$$

By applying Corollary 7, Condition 1 in Corollary 1, Lemma 8, Conditions 1 and 3 in Corollary 4, together with the boundedness of $u'(s)$ and $d'(s)$, and an argument identical to the one used in Equation (4.5), our desired result follows. \square

Next, we prove that $D\phi_t$ is simultaneously continuous with respect to both of its arguments.

Lemma 10. *For each $t \in [0, 1]$, $\xi \in \mathcal{X}_r$, and $\xi' \in \mathcal{X}$, the map $(\xi, \xi') \mapsto D\phi_t(\xi; \xi')$, as defined in Equation (4.10), is continuous.*

Proof. To prove this result, we can employ an argument identical to the one used in the proof of Lemma 5. First, note that $u(t) \in U$ for each $t \in [0, 1]$. Second, note that $\Phi^{(\xi)}$, f , $\frac{\partial f}{\partial x}$, and $\frac{\partial f}{\partial u}$ are bounded, as shown in Corollary 7 and Condition 1 in Corollary 1. Third, recall that $\Phi^{(\xi)}$, f , and $\frac{\partial f}{\partial u}$ are Lipschitz continuous, as proven in Lemma 8 and Conditions 1 and 3 in Corollary 4, respectively. Finally, the result follows after using an argument identical to the one used in Equation (4.5). \square

We can now construct the directional derivative of the cost J and prove it is Lipschitz continuous.

Lemma 11. *Let $\xi \in \mathcal{X}_r$, $\xi' \in \mathcal{X}$, and J be as defined in Equation (2.31). Then the directional derivative of the cost J in the ξ' direction is:*

$$DJ(\xi; \xi') = \frac{\partial h_0}{\partial x}(\phi_1(\xi)) D\phi_1(\xi; \xi'). \quad (4.30)$$

Proof. The result follows directly by the Chain Rule and Lemma 7. \square

Corollary 9. *There exists a constant $L > 0$ such that for each $\xi_1, \xi_2 \in \mathcal{X}_r$ and $\xi' \in \mathcal{X}$:*

$$|DJ(\xi_1; \xi') - DJ(\xi_2; \xi')| \leq L \|\xi_1 - \xi_2\|_{\mathcal{X}} \|\xi'\|_{\mathcal{X}}, \quad (4.31)$$

where DJ is as defined in Equation (4.30).

Proof. Notice by the Triangle Inequality and the Cauchy-Schwartz Inequality:

$$\begin{aligned} |DJ(\xi_1; \xi') - DJ(\xi_2; \xi')| &\leq \left\| \frac{\partial h_0}{\partial x}(\phi_1(\xi_1)) \right\|_2 \|\mathbb{D}\phi_1(\xi_1; \xi') - \mathbb{D}\phi_1(\xi_2; \xi')\|_2 + \\ &\quad + \left\| \frac{\partial h_0}{\partial x}(\phi_1(\xi_1)) - \frac{\partial h_0}{\partial x}(\phi_1(\xi_2)) \right\|_2 \|\mathbb{D}\phi_1(\xi_2; \xi')\|_2. \end{aligned} \quad (4.32)$$

The result then follows by applying Condition 2 in Corollary 1, Condition 2 in Corollary 5, Corollary 8, and Lemma 9. \square

Next, we prove that DJ is simultaneously continuous with respect to both of its arguments, which is a direct consequence of Lemma 10.

Corollary 10. *For each $\xi \in \mathcal{X}_r$ and $\xi' \in \mathcal{X}$, the map $(\xi, \xi') \mapsto DJ(\xi; \xi')$, as defined in Equation (4.30), is continuous.*

Next, we construct the directional derivative of each of the component constraint functions $\psi_{j,t}$ and prove that each of the component constraints is Lipschitz continuous.

Lemma 12. *Let $\xi \in \mathcal{X}_r$, $\xi' \in \mathcal{X}$, and $\psi_{j,t}$ defined as in Equation (2.33). Then for each $j \in \mathcal{J}$ and $t \in [0, 1]$, the directional derivative of $\psi_{j,t}$, denoted $D\psi_{j,t}$, is given by:*

$$D\psi_{j,t}(\xi; \xi') = \frac{\partial h_j}{\partial x}(\phi_t(\xi)) D\phi_t(\xi; \xi'). \quad (4.33)$$

Proof. The result follows using the Chain Rule and Lemma 7. \square

Corollary 11. *There exists a constant $L > 0$ such that for each $\xi_1, \xi_2 \in \mathcal{X}_r$, $\xi' \in \mathcal{X}$, and $t \in [0, 1]$:*

$$|D\psi_{j,t}(\xi_1; \xi') - D\psi_{j,t}(\xi_2; \xi')| \leq L \|\xi_1 - \xi_2\|_{\mathcal{X}} \|\xi'\|_{\mathcal{X}}, \quad (4.34)$$

where $D\psi_{j,t}$ is as defined in Equation (4.33).

Proof. Notice by the Triangle Inequality and the Cauchy Schwartz Inequality:

$$\begin{aligned} |D\psi_{j,t}(\xi_1; \xi') - D\psi_{j,t}(\xi_2; \xi')| &\leq \left\| \frac{\partial h_j}{\partial x}(\phi_t(\xi_1)) \right\|_2 \|\mathbb{D}\phi_t(\xi_1; \xi') - \mathbb{D}\phi_t(\xi_2; \xi')\|_2 + \\ &\quad + \left\| \frac{\partial h_j}{\partial x}(\phi_t(\xi_1)) - \frac{\partial h_j}{\partial x}(\phi_t(\xi_2)) \right\|_2 \|\mathbb{D}\phi_t(\xi_2; \xi')\|_2. \end{aligned} \quad (4.35)$$

The result then follows by applying Condition 3 in Corollary 1, Condition 4 in Corollary 5, Corollary 8, and Lemma 9. \square

Next, we prove that $D\psi_{j,t}$ is simultaneously continuous with respect to both of its arguments, which follows directly from Lemma 10:

Corollary 12. *For each $\xi \in \mathcal{X}_r$, $\xi' \in \mathcal{X}$, and $t \in [0, 1]$, the map $(\xi, \xi') \mapsto D\psi_{j,t}(\xi; \xi')$, as defined in Equation (4.33), is continuous.*

Given these results, we can begin describing the properties satisfied by the optimality function:

Lemma 13. *Let ζ be defined as in Equation (3.9). Then there exists a constant $L > 0$ such that, for each $\xi_1, \xi_2, \xi' \in \mathcal{X}_r$,*

$$|\zeta(\xi_1, \xi') - \zeta(\xi_2, \xi')| \leq L \|\xi_1 - \xi_2\|_{\mathcal{X}}. \quad (4.36)$$

Proof. To prove the result, first notice that for $\{x_i\}_{i \in \mathcal{I}}, \{y_i\}_{i \in \mathcal{I}} \subset \mathbb{R}$:

$$\left| \max_{i \in \mathcal{I}} x_i \right| \leq \max_{i \in \mathcal{I}} |x_i|, \quad \text{and} \quad \max_{i \in \mathcal{I}} x_i - \max_{i \in \mathcal{I}} y_i \leq \max_{i \in \mathcal{I}} \{x_i - y_i\}. \quad (4.37)$$

Therefore,

$$\left| \max_{i \in \mathcal{I}} x_i - \max_{i \in \mathcal{I}} y_i \right| \leq \max_{i \in \mathcal{I}} |x_i - y_i|. \quad (4.38)$$

Letting $\Psi^+(\xi) = \max\{0, \Psi(\xi)\}$ and $\Psi^-(\xi) = \max\{0, -\Psi(\xi)\}$, observe:

$$\zeta(\xi, \xi') = \max \left\{ DJ(\xi; \xi' - \xi) - \Psi^+(\xi), \max_{j \in \mathcal{J}, t \in [0,1]} D\psi_{j,t}(\xi; \xi' - \xi) - \gamma \Psi^-(\xi) \right\} + \|\xi' - \xi\|_{\mathcal{X}}. \quad (4.39)$$

Employing Equation (4.38):

$$\begin{aligned} |\zeta(\xi_1, \xi') - \zeta(\xi_2, \xi')| &\leq \max \left\{ |DJ(\xi_1; \xi' - \xi_1) - DJ(\xi_2; \xi' - \xi_2)| + |\Psi^+(\xi_2) - \Psi^+(\xi_1)|, \right. \\ &\quad \left. \max_{j \in \mathcal{J}, t \in [0,1]} |D\psi_{j,t}(\xi_1; \xi' - \xi_1) - D\psi_{j,t}(\xi_2; \xi' - \xi_2)| + \gamma |\Psi^-(\xi_2) - \Psi^-(\xi_1)| \right\} + \|\xi' - \xi_1\|_{\mathcal{X}} - \|\xi' - \xi_2\|_{\mathcal{X}}. \end{aligned} \quad (4.40)$$

We show three results that taken together with the Triangle Inequality prove the desired result. First, by applying the Reverse Triangle Inequality:

$$\left| \|\xi' - \xi_1\|_{\mathcal{X}} - \|\xi' - \xi_2\|_{\mathcal{X}} \right| \leq \|\xi_1 - \xi_2\|_{\mathcal{X}}. \quad (4.41)$$

Second,

$$\begin{aligned} |DJ(\xi_1; \xi' - \xi_1) - DJ(\xi_2; \xi' - \xi_2)| &= |DJ(\xi_1; \xi' - \xi_1) - DJ(\xi_2; \xi' - \xi_1) + DJ(\xi_2; \xi_2 - \xi_1)| \\ &\leq |DJ(\xi_1; \xi') - DJ(\xi_2; \xi')| + |DJ(\xi_1; \xi_1) - DJ(\xi_2; \xi_1)| + \\ &\quad + \left| \frac{\partial h_0}{\partial x}(\phi_1(\xi_2)) D\phi_1(\xi_2; \xi_2 - \xi_1) \right| \\ &\leq L \|\xi_1 - \xi_2\|_{\mathcal{X}}, \end{aligned} \quad (4.42)$$

where $L > 0$ and we employed the linearity of DJ , Corollary 9, the fact that ξ' and ξ_1 are bounded since $\xi', \xi_1 \in \mathcal{X}_r$, the Cauchy-Schwartz Inequality, Condition 2 in Corollary 1, and Corollary 8. Notice that by employing an argument identical to Equation (4.42) and Corollary 11, we can assume without loss of generality that $|\mathbb{D}\psi_{j,t}(\xi_1; \xi' - \xi_1) - \mathbb{D}\psi_{j,t}(\xi_2; \xi' - \xi_2)| \leq L \|\xi_1 - \xi_2\|_{\mathcal{X}}$. Finally, notice that by applying Lemma 6, $\Psi^+(\xi)$ and $\Psi^-(\xi)$ are Lipschitz continuous. \square

In fact, ζ satisfies an even more important property:

Lemma 14. *For each $\xi \in \mathcal{X}_p$, the map $\xi' \mapsto \zeta(\xi, \xi')$, as defined in Equation (3.9), is strictly convex.*

Proof. The proof follows after noting that the maps $\xi' \mapsto DJ(\xi; \xi' - \xi)$ and $\xi' \mapsto \frac{\partial h_j}{\partial x}(\phi_t(\xi))\mathbb{D}\phi_t(\xi; \xi' - \xi)$ are affine, hence any maximum among these function is convex, and the map $\xi' \mapsto \|\xi' - \xi\|_{\mathcal{X}}$ is strictly convex since we chose the 2-norm as our finite dimensional norm. \square

The following theorem, which follows as a result of the previous lemma, is fundamental to our result since it shows that g , as defined in Equation (3.8), is a well-defined function. We omit the proof since it is a particular case of a well known result regarding the existence of unique minimizers of strictly convex functions over bounded sets in Hilbert spaces (Proposition II.1.2 in [24]).

Theorem 15. *For each $\xi \in \mathcal{X}_p$, the map $\xi' \mapsto \zeta(\xi, \xi')$, as defined in Equation (3.9), has a unique minimizer.*

Employing these results we can prove the continuity of the optimality function. This result is not strictly required in order to prove the convergence of Algorithm 1 or in order to prove that the optimality function encodes local minimizers of the Switched System Optimal Control Problem, but is useful when we describe the implementation of our algorithm.

Lemma 16. *The function θ , as defined in Equation (3.8), is continuous.*

Proof. First, we show that θ is upper semi-continuous. Consider a sequence $\{\xi_i\}_{i=1}^{\infty} \subset \mathcal{X}_r$ converging to ξ , and $\xi' \in \mathcal{X}_r$ such that $\theta(\xi) = \zeta(\xi, \xi')$, i.e. $\xi' = g(\xi)$, where g is defined as in Equation (3.8). Since $\theta(\xi_i) \leq \zeta(\xi_i, \xi')$ for all $i \in \mathbb{N}$,

$$\limsup_{i \rightarrow \infty} \theta(\xi_i) \leq \limsup_{i \rightarrow \infty} \zeta(\xi_i, \xi') = \zeta(\xi, \xi') = \theta(\xi), \quad (4.43)$$

which proves the upper semi-continuity of θ .

Second, we show that θ is lower semi-continuous. Let $\{\xi'_i\}_{i \in \mathbb{N}}$ such that $\theta(\xi_i) = \zeta(\xi_i, \xi'_i)$, i.e. $\xi'_i = g(\xi_i)$. From Lemma 13, we know there exists a Lipschitz constant $L > 0$ such that for each $i \in \mathbb{N}$, $|\zeta(\xi, \xi'_i) - \zeta(\xi_i, \xi'_i)| \leq L \|\xi - \xi_i\|_{\mathcal{X}}$. Consequently,

$$\theta(\xi) \leq (\zeta(\xi, \xi'_i) - \zeta(\xi_i, \xi'_i)) + \zeta(\xi_i, \xi'_i) \leq L\|\xi - \xi_i\|_{\mathcal{X}} + \theta(\xi_i). \quad (4.44)$$

Taking limits we conclude that

$$\theta(\xi) \leq \liminf_{i \rightarrow \infty} \theta(\xi_i), \quad (4.45)$$

which proves the lower semi-continuity of θ , and our desired result. \square

Finally, we can prove that θ encodes a necessary condition for optimality:

Theorem 17. *Let θ be as defined in Equation (3.8), then:*

- (1) θ is non-positive valued, and
- (2) If $\xi \in \mathcal{X}_p$ is a local minimizer of the Switched System Optimal Control Problem as in Definition 5, then $\theta(\xi) = 0$.

Proof. Notice that $\zeta(\xi, \xi) = 0$, therefore $\theta(\xi) = \min_{\xi' \in \mathcal{X}_r} \zeta(\xi, \xi') \leq \zeta(\xi, \xi) = 0$. This proves Condition 1.

To prove Condition 2, we begin by making several observations. Given $\xi' \in \mathcal{X}_r$ and $\lambda \in [0, 1]$, using the Mean Value Theorem and Corollary 9 we have that there exists $s \in (0, 1)$ and $L > 0$ such that

$$\begin{aligned} J(\xi + \lambda(\xi' - \xi)) - J(\xi) &= DJ(\xi + s\lambda(\xi' - \xi); \lambda(\xi' - \xi)) \\ &\leq \lambda DJ(\xi; \xi' - \xi) + L\lambda^2 \|\xi' - \xi\|_{\mathcal{X}}^2. \end{aligned} \quad (4.46)$$

Letting $\mathcal{A}(\xi) = \{(j, t) \in \mathcal{J} \times [0, 1] \mid \Psi(\xi) = h_j(x^{(\xi)}(t))\}$, similar to the equation above, there exists a pair $(j, t) \in \mathcal{A}(\xi + \lambda(\xi' - \xi))$ and $s \in (0, 1)$ such that, using Corollary 11,

$$\begin{aligned} \Psi(\xi + \lambda(\xi' - \xi)) - \Psi(\xi) &\leq \psi_{j,t}(\xi + \lambda(\xi' - \xi)) - \Psi(\xi) \\ &\leq \psi_{j,t}(\xi + \lambda(\xi' - \xi)) - \psi_{j,t}(\xi) \\ &= D\psi_{j,t}(\xi + s\lambda(\xi' - \xi); \lambda(\xi' - \xi)) \\ &\leq \lambda D\psi_{j,t}(\xi; \xi' - \xi) + L\lambda^2 \|\xi' - \xi\|_{\mathcal{X}}^2. \end{aligned} \quad (4.47)$$

Finally, letting L denote the Lipschitz constant as in Condition 1 in Assumption 2, notice:

$$\begin{aligned} \Psi(\xi + \lambda(\xi' - \xi)) - \Psi(\xi) &= \max_{(j,t) \in \mathcal{J} \times [0,1]} \psi_{j,t}(\xi + \lambda(\xi' - \xi)) - \max_{(j,t) \in \mathcal{J} \times [0,1]} \psi_{j,t}(\xi) \\ &\leq \max_{(j,t) \in \mathcal{J} \times [0,1]} \psi_{j,t}(\xi + \lambda(\xi' - \xi)) - \psi_{j,t}(\xi) \\ &\leq L \max_{t \in [0,1]} \|\phi_t(\xi + \lambda(\xi' - \xi)) - \phi_t(\xi)\|_2. \end{aligned} \quad (4.48)$$

We prove Condition 2 by contradiction. That is, using Definition 5, we assume that $\theta(\xi) < 0$ and show that for each $\varepsilon > 0$ there exists $\hat{\xi} \in \mathcal{N}_w(\xi, \varepsilon) \cap \{\bar{\xi} \in \mathcal{X}_p \mid \Psi(\bar{\xi}) \leq 0\}$ such that $J(\hat{\xi}) < J(\xi)$, where $\mathcal{N}_w(\xi, \varepsilon)$ is as defined in Equation (3.7), hence arriving at a contradiction.

Before arriving at this contradiction, we make three initial observations. First, notice that since $\xi \in \mathcal{X}_p$ is a local minimizer of the Switched System Optimal Control Problem,

$\Psi(\xi) \leq 0$. Second, consider g as defined in Equation (3.8), which exists by Theorem 15, and notice that since $\theta(\xi) < 0$, $g(\xi) \neq \xi$. Third, notice that, as a result of Theorem 4, for each $(\xi + \lambda(g(\xi) - \xi)) \in \mathcal{X}_r$ and $\varepsilon' > 0$ there exists a $\xi_\lambda \in \mathcal{X}_p$ such that

$$\|x^{(\xi_\lambda)} - x^{(\xi + \lambda(g(\xi) - \xi))}\|_{L^\infty} < \varepsilon' \quad (4.49)$$

where $x^{(\xi)}$ is the solution to Differential Equation (2.29).

Now, letting $\varepsilon' = -\frac{\lambda\theta(\xi)}{2L} > 0$ and using Corollary 3:

$$\begin{aligned} \|x^{(\xi_\lambda)} - x^{(\xi)}\|_{L^2} &\leq \|x^{(\xi_\lambda)} - x^{(\xi + \lambda(g(\xi) - \xi))}\|_{L^2} + \|x^{(\xi + \lambda(g(\xi) - \xi))} - x^{(\xi)}\|_{L^2} \\ &\leq \left(-\frac{\theta(\xi)}{2L} + L\|g(\xi) - \xi\|_{\mathcal{X}} \right) \lambda. \end{aligned} \quad (4.50)$$

Next, observe that:

$$\theta(\xi) = \max \left\{ DJ(\xi; g(\xi) - \xi), \max_{(j,t) \in \mathcal{J} \times [0,1]} D\psi_{j,t}(\xi; g(\xi) - \xi) + \gamma\Psi(\xi) \right\} + \|g(\xi) - \xi\|_{\mathcal{X}} < 0. \quad (4.51)$$

Also, by Equations (4.46), (4.49), and (4.51), together with Condition 1 in Assumption 2 and Corollary 3:

$$\begin{aligned} J(\xi_\lambda) - J(\xi) &\leq J(\xi_\lambda) - J(\xi + \lambda(g(\xi) - \xi)) + J(\xi + \lambda(g(\xi) - \xi)) - J(\xi) \\ &\leq L\|\phi_1(\xi_\lambda) - \phi_1(\xi + \lambda(g(\xi) - \xi))\|_2 + \theta(\xi)\lambda + 4A^2L\lambda^2 \\ &\leq L\varepsilon' + \theta(\xi)\lambda + 4A^2L\lambda^2 \\ &\leq \frac{\theta(\xi)\lambda}{2} + 4A^2L\lambda^2, \end{aligned} \quad (4.52)$$

where $A = \max\{\|u\|_2 + 1 \mid u \in U\}$ and we used the fact that $\|\xi - \xi'\|_{\mathcal{X}}^2 \leq 4A^2$ and $DJ(\xi; \xi' - \xi) \leq \theta(\xi)$. Hence for each $\lambda \in \left(0, \frac{-\theta(\xi)}{8A^2L}\right)$,

$$J(\xi_\lambda) - J(\xi) < 0. \quad (4.53)$$

Similarly, using Condition 1 in Assumption 2, together with Equations (4.47), (4.48), and (4.51), we have:

$$\begin{aligned} \Psi(\xi_\lambda) &\leq \Psi(\xi_\lambda) - \Psi(\xi + \lambda(g(\xi) - \xi)) + \Psi(\xi + \lambda(g(\xi) - \xi)) \\ &\leq L \max_{t \in [0,1]} \|\phi_t(\xi_\lambda) - \phi_t(\xi + \lambda(g(\xi) - \xi))\|_2 + \Psi(\xi) + (\theta(\xi) - \gamma\Psi(\xi))\lambda + 4A^2L\lambda^2 \\ &\leq L\varepsilon' + \theta(\xi)\lambda + 4A^2L\lambda^2 + (1 - \gamma\lambda)\Psi(\xi) \\ &\leq \frac{\theta(\xi)\lambda}{2} + 4A^2L\lambda^2 + (1 - \gamma\lambda)\Psi(\xi), \end{aligned} \quad (4.54)$$

where $A = \max \{\|u\|_2 + 1 \mid u \in U\}$ and we used the fact that $\|\xi - \xi'\|_{\mathcal{X}}^2 \leq 4A^2$ and $D\psi_{j,t}(\xi; \xi' - \xi) \leq \theta(\xi) - \gamma\Psi(\xi)$ for each $(j, t) \in \mathcal{J} \times [0, 1]$. Hence for each $\lambda \in \left(0, \min \left\{\frac{-\theta(\xi)}{8A^2L}, \frac{1}{\gamma}\right\}\right)$:

$$\Psi(\xi_\lambda) \leq (1 - \gamma\lambda)\Psi(\xi) \leq 0. \quad (4.55)$$

Summarizing, suppose $\xi \in \mathcal{X}_p$ is a local minimizer of the Switched System Optimal Control Problem and $\theta(\xi) < 0$. For each $\varepsilon > 0$, by choosing any

$$\lambda \in \left(0, \min \left\{\frac{-\theta(\xi)}{8A^2L}, \frac{1}{\gamma}, \frac{2L\varepsilon}{2L^2\|g(\xi) - \xi\|_{\mathcal{X}} - \theta(\xi)}\right\}\right), \quad (4.56)$$

we can construct a $\xi_\lambda \in \mathcal{X}_p$ such that $\xi_\lambda \in \mathcal{N}_w(\xi, \varepsilon)$, by Equation (4.50), such that $J(\xi_\lambda) < J(\xi)$, by Equation (4.53), and $\Psi(\xi_\lambda) \leq 0$, by Equation (4.55). Therefore, ξ is not a local minimizer of the Switched System Optimal Control Problem, which is a contradiction and proves Condition 2. \square

4.3 Approximating Relaxed Inputs

In this section, we prove that the projection operation, ρ_N , allows us to control the quality of approximation between the trajectories generated by a relaxed discrete input and its projection. First, we prove for $d \in \mathcal{D}_r$, $\mathcal{F}_N(d) \in \mathcal{D}_r$ and $\mathcal{P}_N(\mathcal{F}_N(d)) \in \mathcal{D}_p$:

Lemma 18. *Let $d \in \mathcal{D}_r$, \mathcal{F}_N be as defined in Equation (3.12), and \mathcal{P}_N be as defined in Equation (3.13). Then for each $N \in \mathbb{N}$ and $t \in [0, 1]$:*

- (1) $[\mathcal{F}_N(d)]_i(t) \in [0, 1]$,
- (2) $\sum_{i=1}^q [\mathcal{F}_N(d)]_i(t) = 1$,
- (3) $[\mathcal{P}_N(\mathcal{F}_N(d))]_i(t) \in \{0, 1\}$,
- (4) $\sum_{i=1}^q [\mathcal{P}_N(\mathcal{F}_N(d))]_i(t) = 1$.

Proof. Condition 1 follows due to the result in Section 3.3 in [35]. Condition 2 follows since the wavelet approximation is linear, thus,

$$\sum_{i=1}^q [\mathcal{F}_N(d)]_i = \sum_{i=1}^q \left(\langle d_i, \mathbf{1} \rangle + \sum_{k=0}^N \sum_{j=0}^{2^k-1} \langle d_i, b_{kj} \rangle \frac{b_{kj}}{\|b_{kj}\|_{L^2}^2} \right) \quad (4.57)$$

$$= \langle \mathbf{1}, \mathbf{1} \rangle + \sum_{k=0}^N \sum_{j=0}^{2^k-1} \langle \mathbf{1}, b_{kj} \rangle \frac{b_{kj}}{\|b_{kj}\|_{L^2}^2} = \mathbf{1}, \quad (4.58)$$

where the last equality holds since $\langle \mathbf{1}, b_{kj} \rangle = 0$ for each k, j .

Conditions 3 and 4 are direct consequences of the definition of \mathcal{P}_N , since \mathcal{P}_N can only take the values 0 or 1, and only one coordinate is equal to 1 at any given time $t \in [0, 1]$. \square

Recall that in order to avoid the introduction of additional notation, we let the coordinate wise application of \mathcal{F}_N to some relaxed discrete input $d \in \mathcal{D}_r$ be denoted as $\mathcal{F}_N(d)$ and similarly for some continuous input $u \in \mathcal{U}$, but in fact \mathcal{F}_N as originally defined took $L^2([0, 1], \mathbb{R}) \cap BV([0, 1], \mathbb{R})$ to $L^2([0, 1], \mathbb{R}) \cap BV([0, 1], \mathbb{R})$. Next, we prove that the wavelet approximation allows us to control the quality of approximation:

Lemma 19. *Let $f \in L^2([0, 1], \mathbb{R}) \cap BV([0, 1], \mathbb{R})$, then*

$$\|f - \mathcal{F}_N(f)\|_{L^2} \leq \frac{1}{2} \left(\frac{1}{\sqrt{2}} \right)^N \|f\|_{BV}, \quad (4.59)$$

where \mathcal{F}_N is as defined in Equation (3.12).

Proof. Since L^2 is a Hilbert space and the collection $\{b_{kj}\}_{k,j}$ is a basis, then

$$f = \langle f, \mathbb{1} \rangle + \sum_{k=0}^{\infty} \sum_{j=0}^{2^k-1} \langle f, b_{kj} \rangle \frac{b_{kj}}{\|b_{kj}\|_{L^2}^2}. \quad (4.60)$$

Note that $\|b_{kj}\|_{L^2}^2 = 2^{-k}$ and that

$$v_{kj}(t) = \int_0^t b_{kj}(s) ds = \begin{cases} t - j2^{-k} & \text{if } t \in [j2^{-k}, (j + \frac{1}{2})2^{-k}), \\ -t + (j + 1)2^{-k} & \text{if } t \in [(j + \frac{1}{2})2^{-k}, (j + 1)2^{-k}), \\ 0 & \text{otherwise,} \end{cases} \quad (4.61)$$

thus $\|v_{kj}\|_{L^\infty} = 2^{-k-1}$. Now, using integration by parts, and since $f \in BV([0, 1], \mathbb{R})$,

$$|\langle f, b_{kj} \rangle| = \left| \int_{j2^{-k}}^{(j+1)2^{-k}} \dot{f}(t) v_{kj}(t) dt \right| \leq 2^{-k-1} \int_{j2^{-k}}^{(j+1)2^{-k}} |\dot{f}(t)| dt \quad (4.62)$$

Finally, Parseval's Identity for Hilbert spaces (Theorem 5.27 in [26]) implies that

$$\begin{aligned} \|f - \mathcal{F}_N(f)\|_{L^2}^2 &= \sum_{k=N+1}^{\infty} \sum_{j=0}^{2^k-1} \frac{|\langle f, b_{kj} \rangle|^2}{\|b_{kj}\|_{L^2}^2} \\ &\leq \sum_{k=N+1}^{\infty} 2^{-k-2} \sum_{j=0}^{2^k-1} \left(\int_{j2^{-k}}^{(j+1)2^{-k}} |\dot{f}(t)| dt \right)^2 \\ &\leq 2^{-N-2} \|f\|_{BV}^2, \end{aligned} \quad (4.63)$$

as desired. \square

The following lemma is fundamental to find a rate of convergence for the approximation of the solution of differential equations using relaxed inputs:

Lemma 20. *There exists $K > 0$ such that for each $d \in \mathcal{D}_r$ and $f \in L^2([0, 1], \mathbb{R}^q) \cap BV([0, 1], \mathbb{R}^q)$,*

$$|\langle d - \mathcal{P}_N(\mathcal{F}_N(d)), f \rangle| \leq K \left(\left(\frac{1}{\sqrt{2}} \right)^N \|f\|_{L^2} \|d\|_{BV} + \left(\frac{1}{2} \right)^N \|f\|_{BV} \right), \quad (4.64)$$

where \mathcal{F}_N is as defined Equation (3.12) and \mathcal{P}_N is as defined in Equation (3.13).

Proof. To simplify our notation, let $t_k = \frac{k}{2^N}$, $p_{ik} = [\mathcal{F}_N(d)]_i(t_k)$, $S_{ik} = \sum_{j=1}^i p_{jk}$, and

$$A_{ik} = \left[t_k + \frac{1}{2^N} S_{(i-1)k}, t_k + \frac{1}{2^N} S_{ik} \right). \quad (4.65)$$

Also let us denote the indicator function of the set A_{ik} by $\mathbb{1}_{A_{ik}}$. Consider

$$\langle \mathcal{F}_N(d) - \mathcal{P}_N(\mathcal{F}_N(d)), f \rangle = \sum_{k=0}^{2^N-1} \sum_{i=1}^q \int_{t_k}^{t_{k+1}} (p_{ik} - \mathbb{1}_{A_{ik}}(t)) f_i(t) dt. \quad (4.66)$$

Let $w_{ik} : [0, 1] \rightarrow \mathbb{R}$ be defined by

$$w_{ik}(t) = \int_{t_k}^t p_{ik} - \mathbb{1}_{A_{ik}}(s) ds = \begin{cases} p_{ik}(t - t_k) & \text{if } t \in [t_k, t_k + \frac{1}{2^N} S_{(i-1)k}), \\ \frac{1}{2^N} p_{ik} S_{(i-1)k} + (p_{ik} - 1) (t - t_k - \frac{1}{2^N} S_{(i-1)k}) & \text{if } t \in A_{ik}, \\ \frac{1}{2^N} p_{ik} (S_{ik} - 1) + p_{ik} (t - t_k - \frac{1}{2^N} S_{ik}) & \text{if } t \in [t_k + \frac{1}{2^N} S_{ik}, t_{k+1}), \end{cases} \quad (4.67)$$

when $t \in [t_k, t_{k+1}]$, and $w_{ik}(t) = 0$ otherwise. Note that $\|w_{ik}\|_{L^\infty} \leq \frac{p_{ik}}{2^N}$. Thus, using integration by parts,

$$\left| \int_{t_k}^{t_{k+1}} (p_{ik} - \mathbb{1}_{A_{ik}}(t)) f_i(t) dt \right| = \left| \int_{t_k}^{t_{k+1}} w(t) \dot{f}_i(t) dt \right| \leq \frac{p_{ik}}{2^N} \int_{t_k}^{t_{k+1}} |\dot{f}_i(t)| dt, \quad (4.68)$$

and

$$\begin{aligned} |\langle \mathcal{F}_N(d) - \mathcal{P}_N(\mathcal{F}_N(d)), f \rangle| &\leq \frac{1}{2^N} \sum_{k=0}^{2^N-1} \int_{t_k}^{t_{k+1}} \sum_{i=1}^q p_{ik} |\dot{f}_i(t)| dt \\ &\leq \frac{1}{2^N} \|f\|_{BV}. \end{aligned} \quad (4.69)$$

where the last inequality follows by Hölder's Inequality.

Also, by Lemma 19 we have that

$$\|d_i - [\mathcal{F}(d)]_i\|_{L^2} \leq \frac{1}{2} \left(\frac{1}{\sqrt{2}} \right)^N \|d_i\|_{BV}. \quad (4.70)$$

Hence, using Cauchy-Schwartz's Inequality,

$$|\langle d - \mathcal{P}_N(\mathcal{F}_N(d)), f \rangle| \leq \|d - \mathcal{F}_N(d)\|_{L^2} \|f\|_{L^2} + |\langle \mathcal{F}_N(d) - \mathcal{P}_N(\mathcal{F}_N(d)), f \rangle|, \quad (4.71)$$

and the desired result follows from Equations (4.63), (4.69). \square

Note that Lemma 20 does not prove convergence of $\mathcal{P}_N(\mathcal{F}_N(d))$ to d in the weak topology on \mathcal{D}_r . Such a result is indeed true, i.e. $\mathcal{P}_N(\mathcal{F}_N(d))$ does converge in the weak topology to d , and it can be shown using an argument similar to the one used in Lemma 1 in [77]. The reason we chose to prove a weaker result is because in this case we get an explicit rate of convergence, which is fundamental to the construction of our optimization algorithm because it allows us to bound the quality of approximation of the state trajectory.

Theorem 21. *Let ρ_N be defined as in Equation (3.14) and ϕ_t be defined as in Equation (2.30). Then there exists $K > 0$ such that for each $\xi = (u, d) \in \mathcal{X}_r$ and for each $t \in [0, 1]$,*

$$\|\phi_t(\rho_N(\xi)) - \phi_t(\xi)\|_2 \leq K \left(\frac{1}{\sqrt{2}} \right)^N (\|\xi\|_{BV} + 1). \quad (4.72)$$

Proof. To simplify our notation, let us denote $u_N = \mathcal{F}_N(u)$ and $d_N = \mathcal{P}_N(\mathcal{F}_N(d))$, thus $\rho_N(\xi) = (u_N, d_N)$. Consider

$$\|x^{(u_N, d_N)}(t) - x^{(u, d)}(t)\|_2 \leq \|x^{(u_N, d_N)}(t) - x^{(u, d_N)}(t)\|_2 + \|x^{(u, d_N)}(t) - x^{(u, d)}(t)\|_2. \quad (4.73)$$

The main result of the theorem will follow from upper bounds from each of these two parts.

Note that

$$\begin{aligned} \|x^{(u_N, d_N)}(t) - x^{(u, d_N)}(t)\|_2 &\leq \int_0^1 \|f(s, x^{(u_N, d_N)}(s), u_N(s), d_N(s)) + \\ &\quad - f(s, x^{(u, d_N)}(s), u(s), d_N(s))\|_2 ds \end{aligned} \quad (4.74)$$

$$\leq L \int_0^1 \|x^{(u_N, d_N)}(t) - x^{(u, d_N)}(t)\|_2 + \|u_N(s) - u(s)\|_2 ds, \quad (4.75)$$

thus, using Bellman-Gronwall's Inequality (Lemma 5.6.4 in [64]) together with the result in Lemma 19 we get

$$\|x^{(u_N, d_N)}(t) - x^{(u, d_N)}(t)\|_2 \leq \frac{Le^L \sqrt{2}}{2} \left(\frac{1}{\sqrt{2}} \right)^N \|u\|_{BV} \quad (4.76)$$

On the other hand,

$$\begin{aligned} x^{(u, d_N)}(t) - x^{(u, d)}(t) &= \int_0^t \sum_{i=1}^q ([d_N]_i(s) - d_i(s)) f(s, x^{(u, d)}(s), u(s), e_i) ds + \\ &\quad + \int_0^t \sum_{i=1}^q [d_N]_i(s) (f(s, x^{(u, d_N)}(s), u(s), e_i) - f(s, x^{(u, d)}(s), u(s), e_i)) ds, \end{aligned} \quad (4.77)$$

thus,

$$\begin{aligned} \|x^{(u,d_N)}(t) - x^{(u,d)}(t)\|_2 &\leq \left\| \int_0^1 \sum_{i=1}^q ([d_N]_i(s) - d_i(s)) f(s, x^{(u,d)}(s), u(s), e_i) ds \right\|_2 + \\ &\quad + L \int_0^1 \|x^{(u,d_N)}(s) - x^{(u,d)}(s)\|_2 ds. \end{aligned} \quad (4.78)$$

Using Bellman-Gronwall's inequality we get

$$\|x^{(u,d_N)}(t) - x^{(u,d)}(t)\|_2 \leq e^L \left\| \int_0^1 \sum_{i=1}^q ([d_N]_i(s) - d_i(s)) f(t, x^{(u,d)}(s), u(s), e_i) ds \right\|_2. \quad (4.79)$$

Recall that f maps to \mathbb{R}^n , so let us denote the k -th coordinate of f by f_k . Let $v_{ki}(t) = f_k(t, x^{(u,d)}(t), u(t), e_i)$ and $v_k = (v_{k1}, \dots, v_{kq})$, then v_k is of bounded variation. Indeed, by Theorem 1 and Condition 1 in Corollary 1, we have that $\|x^{(\xi)}\|_{BV} \leq C$. Thus, by Condition 1 in Assumption 1 and again using Theorem 1, we get that, for each $i \in \mathcal{Q}$,

$$\|v_{ki}\|_{BV} \leq L(1 + C + \|u\|_{BV}). \quad (4.80)$$

Moreover, Condition 1 in Corollary 1 directly imply that $\|v_{ki}\|_{L^2} \leq C$. Hence, Lemma 20 implies that there exists $K > 0$ such that

$$|\langle d - d_N, v_k \rangle| \leq K \left(\left(\frac{1}{\sqrt{2}} \right)^N C \|d\|_{BV} + q \left(\frac{1}{2} \right)^N (1 + C + \|u\|_{BV}) \right). \quad (4.81)$$

Since Equation (4.81) is satisfied for each $k \in \{1, \dots, n\}$, then after ordering the constants and noting that $2^N \geq 2^{\frac{N}{2}}$ for each $N \in \mathbb{N}$, together with Equation (4.76) we get the desired result. \square

4.4 Convergence of the Algorithm

To prove the convergence of our algorithm, we employ a technique similar to the one prescribed in Section 1.2 in [64]. Summarizing the technique, one can think of an algorithm as discrete-time dynamical system, whose desired stable equilibria are characterized by the stationary points of its optimality function, i.e. points $\xi \in \mathcal{X}_p$ where $\theta(\xi) = 0$, since we know from Theorem 17 that all local minimizers are stationary. Before applying this line of reasoning to our algorithm, we present a simplified version of this argument for a general unconstrained optimization problem. This is done in the interest of clarity. Inspired by the stability analysis of dynamical systems, a sufficient condition for the convergence of our algorithm can be formulated by requiring that the cost function satisfy a notion of sufficient descent with respect to an optimality function:

Definition 6. Let \mathcal{S} be a metric space, and consider the problem of minimizing the cost function $J : \mathcal{S} \rightarrow \mathbb{R}$. We say that a function $\Gamma : \mathcal{S} \rightarrow \mathcal{S}$ has the sufficient descent property with respect to an optimality function $\theta : \mathcal{S} \rightarrow (-\infty, 0]$ if for each $x \in \mathcal{S}$ with $\theta(x) < 0$, there exists a $\delta_x > 0$ and $O_x \subset \mathcal{S}$, a neighborhood of x , such that:

$$J(\Gamma(x')) - J(x') \leq -\delta_x, \quad \forall x' \in O_x. \tag{4.82}$$

Importantly, a function satisfying the sufficient property can be proven to approach the zeros of the optimality function:

Theorem 22 (Theorem 1.2.8 in Polak [64]). Consider the problem of minimizing a cost function $J : \mathcal{S} \rightarrow \mathbb{R}$. Suppose that \mathcal{S} is a metric space and a function $\Gamma : \mathcal{S} \rightarrow \mathcal{S}$ has the sufficient descent property with respect to an optimality function $\theta : \mathcal{S} \rightarrow (-\infty, 0]$, as described in Definition 6. Let $\{x_j\}_{j \in \mathbb{N}}$ be a sequence such that, for each $j \in \mathbb{N}$:

$$x_{j+1} = \begin{cases} \Gamma(x_j) & \text{if } \theta(x_j) < 0, \\ x_j & \text{if } \theta(x_j) = 0. \end{cases} \tag{4.83}$$

Then every accumulation point of $\{x_j\}_{j \in \mathbb{N}}$ belongs to the set of zeros of the optimality function θ .

Theorem 22, as originally stated in [64], requires \mathcal{S} to be a Euclidean space, but the result as presented here can be proven without requiring this property using the same original argument. Though Theorem 22 proves that the accumulation point of a sequence generated by Γ converges to a stationary point of the optimality function, it does not prove the existence of the accumulation point. This is in general not a problem for finite-dimensional optimization problems since the level sets of the cost function are usually compact, thus every sequence produced by a descent method has at least one accumulation point. On the other hand, infinite-dimensional problems, such as optimal control problems, do not have this property, since bounded sets may not be compact in infinite-dimensional vector spaces. Thus, even though Theorem 22 can be applied to both finite-dimensional and infinite-dimensional optimization problems, the result is much weaker in the latter case.

The issue mentioned above has been addressed several times in the literature [5, 65, 92, 93], by formulating a stronger version of sufficient descent:

Definition 7 (Definition 2.1 in [5]). Let \mathcal{S} be a metric space, and consider the problem of minimizing the cost function $J : \mathcal{S} \rightarrow \mathbb{R}$. A function $\Gamma : \mathcal{S} \rightarrow \mathcal{S}$ has the uniform sufficient descent property with respect to an optimality function $\theta : \mathcal{S} \rightarrow (-\infty, 0]$ if for each $C > 0$ there exists a $\delta_C > 0$ such that, for every $x \in \mathcal{S}$ with $\theta(x) < 0$,

$$J(\Gamma(x)) - J(x) \leq -\delta_C. \tag{4.84}$$

A sequence of points generated by an algorithm satisfying this property, under mild assumptions, can be shown to approach the zeros of the optimality function:

Theorem 23 (Proposition 2.1 in [5]). *Consider the problem of minimizing a lower bounded cost function $J : \mathcal{S} \rightarrow [\alpha, \infty)$. Suppose that \mathcal{S} is a metric space and $\Gamma : \mathcal{S} \rightarrow \mathcal{S}$ satisfies the uniform sufficient descent property with respect to an optimality function $\theta : \mathcal{S} \rightarrow (-\infty, 0]$, as stated in Definition 7. Let $\{x_j\}_{j \in \mathbb{N}}$ be a sequence such that, for each $j \in \mathbb{N}$:*

$$x_{j+1} = \begin{cases} \Gamma(x_j) & \text{if } \theta(x_j) < 0, \\ x_j & \text{if } \theta(x_j) = 0. \end{cases} \quad (4.85)$$

Then,

$$\lim_{j \rightarrow \infty} \theta(x_j) = 0. \quad (4.86)$$

Proof. Suppose that $\liminf_{j \rightarrow \infty} \theta(x_j) = -2\varepsilon < 0$. Then there exists a subsequence $\{x_{j_k}\}_{k \in \mathbb{N}}$ such that $\theta(x_{j_k}) < -\varepsilon$ for each $k \in \mathbb{N}$. Definition 7 implies that there exists δ_ε such that

$$J(x_{j_k+1}) - J(x_{j_k}) \leq -\delta_\varepsilon, \quad \forall k \in \mathbb{N}. \quad (4.87)$$

But this is a contradiction, since $J(x_{j+1}) \leq J(x_j)$ for each $j \in \mathbb{N}$, thus $J(x_j) \rightarrow -\infty$ as $j \rightarrow \infty$, contrary to the assumption that J is lower bounded. \square

Note that Theorem 23 does not assume the existence of accumulation points of the sequence $\{x_j\}_{j \in \mathbb{N}}$. Thus, this Theorem remains valid even when the sequence generated by Γ does not have accumulation points. This becomes tremendously useful in infinite-dimensional problems where the level sets of the cost function may not be compact. Though we include these results for the sake of completeness of presentation, our proof of convergence of the sequence of points generated by Algorithm 1 does not make explicit use of Theorem 23. The line of argument is similar, but our approach, as described in Theorem 27, requires special treatment due to the projection operation, ρ_N , as defined in Equation (3.14) and the existence of constraints.

Now, we begin the convergence proof of Algorithm 1 by showing that the Armijo algorithm, as defined in Equation (3.10), terminates after a finite number of steps and its value is bounded.

Lemma 24. *Let $\alpha \in (0, 1)$ and $\beta \in (0, 1)$. For every $\delta > 0$ there exists an $M_\delta^* < \infty$ such that if $\theta(\xi) \leq -\delta$ for $\xi \in \mathcal{X}_p$, then $\mu(\xi) \leq M_\delta^*$, where θ is as defined in Equation (3.8) and μ is as defined in Equation (3.10).*

Proof. Given $\xi' \in \mathcal{X}$ and $\lambda \in [0, 1]$, using the Mean Value Theorem and Corollary 9 we have that there exists $s \in (0, 1)$ such that

$$\begin{aligned} J(\xi + \lambda(\xi' - \xi)) - J(\xi) &= DJ(\xi + s\lambda(\xi' - \xi); \lambda(\xi' - \xi)) \\ &\leq \lambda DJ(\xi; \xi' - \xi) + L\lambda^2 \|\xi' - \xi\|_{\mathcal{X}}^2. \end{aligned} \quad (4.88)$$

Letting $\mathcal{A}(\xi) = \{(j, t) \in \mathcal{J} \times [0, 1] \mid \Psi(\xi) = h_j(x^{(\xi)}(t))\}$, then there exists a pair $(j, t) \in \mathcal{A}(\xi + \lambda(\xi' - \xi))$ and $s \in (0, 1)$ such that, using Corollary 11,

$$\begin{aligned} \Psi(\xi + \lambda(\xi' - \xi)) - \Psi(\xi) &\leq \psi_{j,t}(\xi + \lambda(\xi' - \xi)) - \Psi(\xi) \\ &\leq \psi_{j,t}(\xi + \lambda(\xi' - \xi)) - \psi_{j,t}(\xi) \\ &= \text{D}\psi_{j,t}(\xi + s\lambda(\xi' - \xi); \lambda(\xi' - \xi)) \\ &\leq \lambda \text{D}\psi_{j,t}(\xi; \xi' - \xi) + L\lambda^2 \|\xi' - \xi\|_{\mathcal{X}}^2. \end{aligned} \tag{4.89}$$

Now let us assume that $\Psi(\xi) \leq 0$, and consider g as defined in Equation (3.8). Then

$$\theta(\xi) = \max \left\{ \text{D}J(\xi; g(\xi) - \xi), \max_{(j,t) \in \mathcal{J} \times [0,1]} \text{D}\psi_{j,t}(\xi; g(\xi) - \xi) + \gamma\Psi(\xi) \right\} \leq -\delta, \tag{4.90}$$

and using Equation (4.88),

$$J(\xi + \beta^k(g(\xi) - \xi)) - J(\xi) - \alpha\beta^k\theta(\xi) \leq -(1 - \alpha)\delta\beta^k + 4A^2L\beta^{2k}, \tag{4.91}$$

where $A = \max \{\|u\|_2 + 1 \mid u \in U\}$. Hence, for each $k \in \mathbb{N}$ such that $\beta^k \leq \frac{(1-\alpha)\delta}{4A^2L}$ we have that

$$J(\xi + \beta^k(g(\xi) - \xi)) - J(\xi) \leq \alpha\beta^k\theta(\xi). \tag{4.92}$$

Similarly, using Equations (4.89) and (4.90),

$$\Psi(\xi + \beta^k(g(\xi) - \xi)) - \Psi(\xi) + \beta^k(\gamma\Psi(\xi) - \alpha\theta(\xi)) \leq -\delta\beta^k + 4A^2L\beta^{2k}, \tag{4.93}$$

hence for each $k \in \mathbb{N}$ such that $\beta^k \leq \min \left\{ \frac{(1-\alpha)\delta}{4A^2L}, \frac{1}{\gamma} \right\}$ we have that

$$\Psi(\xi + \beta^k(g(\xi) - \xi)) - \alpha\beta^k\theta(\xi) \leq (1 - \beta^k\gamma) \Psi(\xi) \leq 0. \tag{4.94}$$

If $\Psi(\xi) > 0$ then

$$\max_{(j,t) \in \mathcal{J} \times [0,1]} \text{D}\psi_{j,t}(\xi; g(\xi) - \xi) \leq \theta(\xi) \leq -\delta, \tag{4.95}$$

thus, from Equation (4.89),

$$\Psi(\xi + \beta^k(g(\xi) - \xi)) - \Psi(\xi) - \alpha\beta^k\theta(\xi) \leq -(1 - \alpha)\delta\beta^k + 4A^2L\beta^{2k}. \tag{4.96}$$

Hence, for each $k \in \mathbb{N}$ such that $\beta^k \leq \frac{(1-\alpha)\delta}{4A^2L}$ we have that

$$\Psi(\xi + \beta^k(g(\xi) - \xi)) - \Psi(\xi) \leq \alpha\beta^k\theta(\xi). \tag{4.97}$$

Finally, let

$$M_\delta^* = 1 + \max \left\{ \log_\beta \left(\frac{(1-\alpha)\delta}{4A^2L} \right), \log_\beta \left(\frac{1}{\gamma} \right) \right\}, \tag{4.98}$$

then from Equations (4.92), (4.94), and (4.97), we get that $\mu(\xi) \leq M_\delta^*$ as desired. \square

Next, we show that the determination of the frequency at which to perform pulse width modulation as defined in Equation (3.15) terminates after a finite number of steps.

Lemma 25. *Let $\alpha \in (0, 1)$, $\bar{\alpha} \in (0, \infty)$, $\beta \in (0, 1)$, $\bar{\beta} \in \left(\frac{1}{\sqrt{2}}, 1\right)$, and $\xi \in \mathcal{X}_p$. If $\theta(\xi) < 0$, then $\nu(\xi) < \infty$, where θ is as defined in Equation (3.8) and ν is as defined in Equation (3.15).*

Proof. Throughout the proof, we leave out the natural inclusion taking $\xi \in \mathcal{X}_p$ to $\xi \in \mathcal{X}_r$. To simplify our notation let us denote $M = \mu(\xi)$ and $\xi' = \xi + \beta^M(g(\xi) - \xi)$. Theorem 21 implies that there exists $K > 0$ such that

$$J(\rho_N(\xi')) - J(\xi') \leq KL \left(\frac{1}{\sqrt{2}}\right)^N (\|\xi'\|_{BV} + 1), \quad (4.99)$$

where L is the constant defined in Assumption 2.

Let $\mathcal{A}(\xi) = \{(j, t) \in \{1, \dots, N_c\} \times [0, 1] \mid \Psi(\xi) = h_j(x^{(\xi)}(t))\}$, then for each pair $(j, t) \in \mathcal{A}(\rho_N(\xi'))$ we have that

$$\begin{aligned} \Psi(\rho_N(\xi')) - \Psi(\xi') &= \psi_{j,t}(\rho_N(\xi')) - \Psi(\xi') \\ &\leq \psi_{j,t}(\rho_N(\xi')) - \psi_{j,t}(\xi') \\ &\leq KL \left(\frac{1}{\sqrt{2}}\right)^N (\|\xi'\|_{BV} + 1). \end{aligned} \quad (4.100)$$

Recall that $\bar{\alpha} \in (0, \infty)$, $\bar{\beta} \in \left(\frac{1}{\sqrt{2}}, 1\right)$, and $\omega \in (0, 1)$, hence there exists $N_0 \in \mathbb{N}$ such that, for each $N \geq N_0$,

$$KL \left(\frac{1}{\sqrt{2}}\right)^N (\|\xi'\|_{BV} + 1) \leq -\bar{\alpha}\bar{\beta}^N \theta(\xi). \quad (4.101)$$

Also, there exists $N_1 \geq N_0$ such that, for each $N \geq N_1$,

$$\bar{\alpha}\bar{\beta}^N \leq (1 - \omega)\alpha\beta^M. \quad (4.102)$$

Now suppose that $\Psi(\xi) \leq 0$, then, for each $N \geq N_1$,

$$\begin{aligned} J(\rho_N(\xi')) - J(\xi) &= J(\rho_N(\xi')) - J(\xi') + J(\xi') - J(\xi) \\ &\leq (\alpha\beta^M - \bar{\alpha}\bar{\beta}^N) \theta(\xi), \end{aligned} \quad (4.103)$$

and

$$\begin{aligned} \Psi(\rho_N(\xi')) &= \Psi(\rho_N(\xi')) - \Psi(\xi') + \Psi(\xi') \\ &\leq (\alpha\beta^M - \bar{\alpha}\bar{\beta}^N) \theta(\xi) \\ &\leq 0. \end{aligned} \quad (4.104)$$

Similarly, if $\Psi(\xi) > 0$ then, using the same argument as above, we have that

$$\Psi(\rho_N(\xi')) - \Psi(\xi) \leq (\alpha\beta^M - \bar{\alpha}\bar{\beta}^N) \theta(\xi). \quad (4.105)$$

Therefore, from Equations (4.103), (4.104), and (4.105), it follows that $\nu(\xi) \leq N_1$ as desired. \square

The following lemma proves that, once Algorithm 1 finds a feasible point, every point generated afterwards is also feasible. We omit the proof since it follows directly from the definition of ν in Equation (3.15).

Lemma 26. *Let Γ be defined as in Equation (3.16) and let Ψ be as defined in Equation (2.32). Let $\{\xi_i\}_{i \in \mathbb{N}}$ be a sequence generated by Algorithm 1. If there exists $i_0 \in \mathbb{N}$ such that $\Psi(\xi_{i_0}) \leq 0$, then $\Psi(\xi_i) \leq 0$ for each $i \geq i_0$.*

Employing these preceding results, we can prove the convergence of Algorithm 1 to a point that satisfies our optimality condition by employing an argument similar to the one used in the proof of Theorem 23:

Theorem 27. *Let θ be defined as in Equation (3.8). If $\{\xi_i\}_{i \in \mathbb{N}}$ is a sequence generated by Algorithm 1, then $\lim_{i \rightarrow \infty} \theta(\xi_i) = 0$.*

Proof. If the sequence produced by Algorithm 1 is finite, then the theorem is trivially satisfied, so we assume that the sequence is infinite.

Suppose the theorem is not true, then $\liminf_{i \rightarrow \infty} \theta(\xi_i) = -2\delta < 0$ and therefore there exists $k_0 \in \mathbb{N}$ and a subsequence $\{\xi_{i_k}\}_{k \in \mathbb{N}}$ such that $\theta(\xi_{i_k}) \leq -\delta$ for each $k \geq k_0$. Also, recall that $\nu(\xi)$ was chosen such that, given $\mu(\xi)$,

$$\alpha\beta^{\mu(\xi)} - \bar{\alpha}\bar{\beta}^{\nu(\xi)} \geq \omega\alpha\beta^{\mu(\xi)}, \quad (4.106)$$

where $\omega \in (0, 1)$ is a parameter.

From Lemma 24 we know that there exists M_δ^* , which depends on δ , such that $\beta^{\mu(\xi)} \geq \beta^{M_\delta^*}$. Suppose that the subsequence $\{\xi_{i_k}\}_{k \in \mathbb{N}}$ is eventually feasible, then, by Lemma 26, without loss of generality we can assume that the sequence is always feasible. Thus, given Γ as defined in Equation (3.16),

$$\begin{aligned} J(\Gamma(\xi_{i_k})) - J(\xi_{i_k}) &\leq (\alpha\beta^{\mu(\xi)} - \bar{\alpha}\bar{\beta}^{\nu(\xi)})\theta(\xi_{i_k}) \\ &\leq -\omega\alpha\beta^{\mu(\xi)}\delta \\ &\leq -\omega\alpha\beta^{M_\delta^*}\delta. \end{aligned} \quad (4.107)$$

This inequality, together with the fact that $J(\xi_{i+1}) \leq J(\xi_i)$ for each $i \in \mathbb{N}$, implies that $\liminf_{k \rightarrow \infty} J(\xi_{i_k}) = -\infty$, but this is a contradiction since J is lower bounded, which follows from Condition 1 in Corollary 5.

The case when the sequence is never feasible is analogous after noting that, since the subsequence is infeasible, then $\Psi(\xi_{i_k}) > 0$ for each $k \in \mathbb{N}$, establishing a similar contradiction. \square

Part II

An Implementable Algorithm for Hybrid Dynamical System Identification

Chapter 5

An Implementable Algorithm

In this chapter, we describe how to implement Algorithm 1 given the various algorithmic components derived in the Chapter 4. Numerically computing a solution to the Switched System Optimal Control Problem defined as in Equation (2.34) demands employing some form of discretization. When numerical integration is introduced, the original infinite-dimensional optimization problem defined over function spaces is replaced by a finite-dimensional discrete-time optimal control problem. Changing the discretization precision results in an infinite sequence of such approximating problems.

Our goal is the construction of an implementable algorithm that generates a sequence of points by recursive application that converge to a point that satisfies the optimality condition defined in Equation (3.8). Given a particular choice of discretization precision, at a high level, our algorithm solves a finite dimensional optimization problem and terminates its operation when a discretization improvement test is satisfied. At this point, a finer discretization precision is chosen, and the whole process is repeated, using the last iterate, obtained with the coarser discretization precision as a “warm start.”

In this chapter, we begin by describing our discretization strategy, which allows us to define our discretized optimization spaces. Next, we describe how to construct discretized trajectories, cost, constraints, and optimal control problems. This allows us to define a discretized optimality function, and a notion of *consistent approximation* between the optimality function and its discretized counterpart. We conclude by constructing our numerically implementable optimal control algorithm for constrained switched systems.

5.1 Discretized Optimization Space

To define our discretization strategy, for any positive integer N we first define the N -th *switching time space* as:

$$\mathcal{T}_N = \left\{ (\tau_0, \dots, \tau_k) \subset [0, 1] \mid 0 = \tau_0 \leq \tau_1 \leq \dots \leq \tau_k = 1, |\tau_i - \tau_{i-1}| \leq \frac{1}{2^N} \forall i \in \{1, \dots, k\} \right\}, \quad (5.1)$$

i.e. \mathcal{T}_N is the collection of finite partitions of $[0, 1]$ whose samples have a maximum distance of $\frac{1}{2^N}$. For notational convenience, given $\tau \in \mathcal{T}_N$, we define $|\tau|$ as the cardinality of τ . Importantly, notice that the sets \mathcal{T}_N are nested, i.e. for each $N \in \mathbb{N}$, $\mathcal{T}_{N+1} \subset \mathcal{T}_N$.

We utilize the switching time spaces to define a sequence of finite dimensional subspaces of \mathcal{X}_p and \mathcal{X}_r . Given $N \in \mathbb{N}$, $\tau \in \mathcal{T}_N$, and $k \in \{0, \dots, |\tau| - 1\}$, we define $\pi_{\tau,k} : [0, 1] \rightarrow \mathbb{R}$ that scales the discretization:

$$\pi_{\tau,k}(t) = \begin{cases} 1 & \text{if } t \in [\tau_k, \tau_{k+1}), \\ 0 & \text{otherwise.} \end{cases} \quad (5.2)$$

Using this definition, we define $\mathcal{D}_{\tau,p}$, a subspace of the discrete input space, as:

$$\mathcal{D}_{\tau,p} = \left\{ d \in \mathcal{D}_p \mid d = \sum_{k=0}^{|\tau|-1} \bar{d}_k \pi_{\tau,k}, \bar{d}_k \in \Sigma_p^q \forall k \right\}. \quad (5.3)$$

Similarly, we define $\mathcal{D}_{\tau,r}$, a subspace of the relaxed discrete input space, as:

$$\mathcal{D}_{\tau,r} = \left\{ d \in \mathcal{D}_r \mid d = \sum_{k=0}^{|\tau|-1} \bar{d}_k \pi_{\tau,k}, \bar{d}_k \in \Sigma_r^q \forall k \right\}. \quad (5.4)$$

Finally, we define \mathcal{U}_τ , a subspace of the continuous input space, as:

$$\mathcal{U}_\tau = \left\{ u \in \mathcal{U} \mid u = \sum_{k=0}^{|\tau|-1} \bar{u}_k \pi_{\tau,k}, \bar{u}_k \in U \forall k \right\}. \quad (5.5)$$

Now, we can define the N -th discretized pure optimization space induced by switching vector τ as $\mathcal{X}_{\tau,p} = \mathcal{U}_\tau \times \mathcal{D}_{\tau,p}$, and the N -th discretized relaxed optimization space induced by switching vector τ as $\mathcal{X}_{\tau,r} = \mathcal{U}_\tau \times \mathcal{D}_{\tau,r}$. Similarly, we define a subspace of \mathcal{X} :

$$\mathcal{X}_\tau = \left\{ (u, d) \in \mathcal{X} \mid u = \sum_{k=0}^{|\tau|-1} \bar{u}_k \pi_{\tau,k}, \bar{u}_k \in \mathbb{R}^m \forall k, \text{ and } d = \sum_{k=0}^{|\tau|-1} \bar{d}_k \pi_{\tau,k}, \bar{d}_k \in \mathbb{R}^q \forall k \right\}. \quad (5.6)$$

In order for these discretized optimization spaces to be useful, we need to know to show that we can use a sequence of functions belonging to these finite-dimensional subspaces to approximate any infinite dimensional function. The following lemma proves this result and validates our choice of discretized spaces:

Lemma 28. *Let $\{\tau_k\}_{k \in \mathbb{N}}$ with $\tau_k \in \mathcal{T}_k$.*

- (1) *For each $\xi \in \mathcal{X}_p$ there exists a sequence $\{\xi_k\}_{k \in \mathbb{N}}$, with $\xi_k \in \mathcal{X}_{\tau_k,p}$, such that $\xi_k \rightarrow \xi$ as $k \rightarrow \infty$.*

- (2) For each $\xi \in \mathcal{X}_r$ there exists a sequence $\{\xi_k\}_{k \in \mathbb{N}}$, with $\xi_k \in \mathcal{X}_{\tau_k, r}$, such that $\xi_k \rightarrow \xi$ as $k \rightarrow \infty$.

Proof. We only present an outline of the proof, since the argument is outside the scope of this paper. First, every Lebesgue measurable set in $[0, 1]$ can be arbitrarily approximated by intervals (Theorem 2.40 in [26]). Second, the sequence of partitions $\{\tau_k\}_{k \in \mathbb{N}}$ can clearly approximate any interval. Finally, the result follows since every measurable function can be approximated in the L^2 -norm by integrable simple functions, which are the finite linear combination of indicator functions defined on Borel sets (Theorem 2.10 in [26]). \square

5.2 Discretized Trajectories, Cost, Constraint, and Optimal Control Problem

For a positive integer N , given a switching vector, $\tau \in \mathcal{T}_N$, a relaxed control $\xi = (u, d) \in \mathcal{X}_{\tau, r}$, and an initial condition $x_0 \in \mathbb{R}^n$, the discrete dynamics, denoted by $\{z_\tau^{(\xi)}(\tau_k)\}_{k=0}^{|\tau|} \subset \mathbb{R}^n$, are computed via the Forward Euler Integration Formula:

$$\begin{aligned} z_\tau^{(\xi)}(\tau_{k+1}) &= z_\tau^{(\xi)}(\tau_k) + (\tau_{k+1} - \tau_k) f(\tau_k, z_\tau^{(\xi)}(\tau_k), u(\tau_k), d(\tau_k)), \\ \forall k \in \{0, \dots, |\tau| - 1\}, \quad z_\tau^{(\xi)}(0) &= x_0. \end{aligned} \quad (5.7)$$

Employing these discrete dynamics we can define the *discretized trajectory*, $z_\tau^{(\xi)} : [0, 1] \rightarrow \mathbb{R}^n$, by performing linear interpolation over the discrete dynamics:

$$z_\tau^{(\xi)}(t) = \sum_{k=0}^{|\tau|-1} \left(z_\tau^{(\xi)}(\tau_k) + \frac{t - \tau_k}{\tau_{k+1} - \tau_k} (z_\tau^{(\xi)}(\tau_{k+1}) - z_\tau^{(\xi)}(\tau_k)) \right) \pi_{\tau, k}(t), \quad (5.8)$$

where $\pi_{\tau, k}$ are as defined in Equation (5.2). Note that the definition in Equation (5.8) is valid even if $\tau_k = \tau_{k+1}$ for some $k \in \{0, \dots, |\tau|\}$, which becomes clear after replacing Equation (5.7) in Equation (5.8). For notational convenience, we suppress the dependence on τ in $z_\tau^{(\xi)}$ when it is clear in context.

Employing the trajectory computed via Euler integration, we define the *discretized cost function*, $J_\tau : \mathcal{X}_{\tau, r} \rightarrow \mathbb{R}$:

$$J_\tau(\xi) = h_0(z^{(\xi)}(1)). \quad (5.9)$$

Similarly, we define the *discretized constraint function*, $\psi_\tau : \mathcal{X}_{\tau, r} \rightarrow \mathbb{R}$:

$$\Psi_\tau(\xi) = \max_{j \in \mathcal{J}, k \in \{0, \dots, |\tau|\}} h_j(z^{(\xi)}(\tau_k)). \quad (5.10)$$

Note that these definitions extend easily to points belonging to $\mathcal{X}_{\tau, p}$.

As we did in Section 2.3, we now introduce some additional notation to ensure the clarity of the ensuing analysis. First, for any positive integer N and $\tau \in \mathcal{T}_N$, we define the *discretized flow of the system*, $\phi_{\tau, t} : \mathcal{X}_r \rightarrow \mathbb{R}^n$ for each $t \in [0, 1]$ as:

$$\phi_{\tau, t}(\xi) = z_\tau^{(\xi)}(t). \quad (5.11)$$

Second, for any positive integer N and $\tau \in \mathcal{T}_N$, we define *component constraint functions*, $\psi_{\tau,j,t} : \mathcal{X}_r \rightarrow \mathbb{R}$ for each $t \in [0, 1]$ and each $j \in \mathcal{J}$ as:

$$\psi_{\tau,j,t}(\xi) = h_j(\phi_{\tau,t}(\xi)). \quad (5.12)$$

Notice that the discretized cost function and the discretized constraint function become

$$J_\tau(\xi) = h_0(\phi_{\tau,1}(\xi)), \quad \text{and} \quad \Psi_\tau(\xi) = \max_{j \in \mathcal{J}, k \in \{0, \dots, |\tau|\}} \psi_{\tau,j,\tau_k}(\xi), \quad (5.13)$$

respectively. This notation change is made to emphasize the dependence on ξ .

5.3 Local Minimizers and a Discretized Optimality Condition

Before proceeding further, we make an observation that dictates the construction of our implementable algorithm. Recall how we employ directional derivatives and Theorem 4 in order to construct a necessary condition for optimality for the Switched System Optimal Control Problem. In particular, if at a particular point belonging to the pure optimization space the appropriate directional derivatives are negative, then the point is not a local minimizer of the Relaxed Switched System Optimal Control Problem. An application of Theorem 4 to this point proves that it is not a local minimizer of the Switched System Optimal Control Problem.

Proceeding in a similar fashion, for any positive integer $N \in \mathbb{N}$ and $\tau \in \mathcal{T}_N$, we can define a Discretized Relaxed Switched System Optimal Control Problem:

Discretized Relaxed Switched System Optimal Control Problem Induced by Switching Vector τ .

$$\min_{\xi \in \mathcal{X}_{\tau,r}} \{J_\tau(\xi) \mid \Psi_\tau(\xi) \leq 0\}. \quad (5.14)$$

The local minimizers of this problem are then defined as follows:

Definition 8. Fix $N \in \mathbb{N}$, and $\tau \in \mathcal{T}_N$. Let us denote an ε -ball in the \mathcal{X} -norm centered at ξ induced by switching vector τ by:

$$\mathcal{N}_{\tau,\mathcal{X}}(\xi, \varepsilon) = \{\bar{\xi} \in \mathcal{X}_{\tau,r} \mid \|\xi - \bar{\xi}\|_{\mathcal{X}} < \varepsilon\}. \quad (5.15)$$

We say that a point $\xi \in \mathcal{X}_{\tau,r}$ is a local minimizer of the Relaxed Switched System Optimal Control Problem Induced by Switching Vector τ defined in Equation (5.14) if $\Psi_\tau(\xi) \leq 0$ and there exists $\varepsilon > 0$ such that $J_\tau(\hat{\xi}) \geq J_\tau(\xi)$ for each $\hat{\xi} \in \mathcal{N}_{\tau,\mathcal{X}}(\xi, \varepsilon) \cap \{\bar{\xi} \in \mathcal{X}_{\tau,r} \mid \Psi_\tau(\bar{\xi}) \leq 0\}$.

Given this definition, a first order numerical optimal control scheme can exploit the vector space structure of the discretized relaxed optimization space in order to define discretized

directional derivatives that find local minimizers for this Discretized Relaxed Switched System Optimal Control Problem. Just as in Chapter 3.1, we can employ a first order approximation argument and the existence of the directional derivative of the cost, DJ_τ (proven in Lemma 40), and of each of the component constraints, $D\psi_{\tau,j,\tau_k}$ (proven in Lemma 42), for each $j \in \mathcal{J}$ and $k \in \{0, \dots, |\tau|\}$ in order to elucidate this fact.

Employing these directional derivatives, we can define a discretized optimality function. Fixing a positive integer N and $\tau \in \mathcal{T}_N$, we define a *discretized optimality function*, $\theta_\tau : \mathcal{X}_{\tau,p} \rightarrow (-\infty, 0]$ and a corresponding *discretized descent direction*, $g_\tau : \mathcal{X}_{\tau,p} \rightarrow \mathcal{X}_{\tau,r}$:

$$\theta_\tau(\xi) = \min_{\xi' \in \mathcal{X}_{\tau,r}} \zeta_\tau(\xi, \xi'), \quad g_\tau(\xi) = \arg \min_{\xi' \in \mathcal{X}_{\tau,r}} \zeta_\tau(\xi, \xi'), \quad (5.16)$$

where

$$\zeta_\tau(\xi, \xi') = \begin{cases} \max \left\{ \max_{j \in \mathcal{J}, k \in \{0, \dots, |\tau|\}} D\psi_{\tau,j,\tau_k}(\xi; \xi' - \xi) + \gamma \Psi_\tau(\xi), \right. \\ \quad \left. DJ_\tau(\xi; \xi' - \xi) \right\} + \|\xi' - \xi\|_{\mathcal{X}} & \text{if } \Psi_\tau(\xi) \leq 0, \\ \max \left\{ \max_{j \in \mathcal{J}, k \in \{0, \dots, |\tau|\}} D\psi_{\tau,j,\tau_k}(\xi; \xi' - \xi), \right. \\ \quad \left. DJ_\tau(\xi; \xi' - \xi) - \Psi_\tau(\xi) \right\} + \|\xi' - \xi\|_{\mathcal{X}} & \text{if } \Psi_\tau(\xi) > 0, \end{cases} \quad (5.17)$$

where $\gamma > 0$ is a design parameter as in the original optimality function θ , defined in Equation (3.8). Before proceeding, we make two observations. First, note that $\theta_\tau(\xi) \leq 0$ for each $\xi \in \mathcal{X}_{\tau,p}$, since we can always choose $\xi' = \xi$ which leaves the trajectory unmodified. Second, note that at a point $\xi \in \mathcal{X}_{\tau,p}$ the directional derivatives in the optimality function consider directions $\xi' - \xi$ with $\xi' \in \mathcal{X}_{\tau,r}$ in order to ensure that first order approximations belong to the discretized relaxed optimization space $\mathcal{X}_{\tau,r}$ which is convex (e.g. for $0 < \lambda \ll 1$, $J_\tau(\xi) + \lambda DJ_\tau(\xi; \xi' - \xi) \approx J_\tau((1 - \lambda)\xi + \lambda\xi')$ where $(1 - \lambda)\xi + \lambda\xi' \in \mathcal{X}_{\tau,r}$).

Just as we argued in the infinite dimensional case, we can prove, as we do in Theorem 49, that if $\theta_\tau(\xi) < 0$ for some $\xi \in \mathcal{X}_{\tau,p}$, then ξ is not a local minimizer of the Discretized Relaxed Switched System Optimal Control Problem. Proceeding as we did in Chapter 3, we can attempt to apply Theorem 4 to prove that θ encodes local minimizers by employing the weak topology over the discretized pure optimization space. Unfortunately, Theorem 4 does not prove that the element in the pure optimization space, $\xi_p \in \mathcal{X}_p$, that approximates a particular relaxed control $\xi_r \in \mathcal{X}_{\tau,r} \subset \mathcal{X}_r$ at a particular quality of approximation $\varepsilon > 0$ with respect to the trajectory of the switched system, belongs to $\mathcal{X}_{\tau,p}$. Though the point in the pure optimization space that approximates a particular discretized relaxed control at a particular quality of approximation exists, it may exist at a different discretization precision.

This deficiency of Theorem 4 which is shared by our extension to it, Theorem 21, means that our computationally tractable algorithm, in contrast to our conceptual algorithm, requires an additional step where the discretization precision is allowed to improve. Nevertheless, if we prove that the Discretized Switched System Optimal Control Problem

consistently approximates the Switched System Optimal Control Problem in a manner that is formalized next, then an algorithm that generates a sequence of points by recursive application that converge to a point that is a zero of the discretized optimality function is also converging to a point that is a zero of the original optimality function.

Formally, motivated by the approach taken in [64], we define consistent approximation as:

Definition 9 (Definition 3.3.6 [64]). *The Discretized Relaxed Switched System Optimal Control Problem as defined in Equation (5.14) is a consistent approximation of the Switched System Optimal Control Problem as defined in Equation (2.34) if for any infinite sequence $\{\tau_i\}_{i \in \mathbb{N}}$ and $\{\xi_i\}_{i \in \mathbb{N}}$ such that $\tau_i \in \mathcal{T}_i$ and $\xi_i \in \mathcal{X}_{\tau_i, p}$ for each $i \in \mathbb{N}$, then*

$$\lim_{i \rightarrow \infty} |\theta_{\tau_i}(\xi_i) - \theta(\xi_i)| = 0, \quad (5.18)$$

where θ is as defined in Equation (3.8) and θ_{τ} is as defined in Equation (5.16).

Importantly, if this notion of consistent approximation is satisfied, then a critical result follows:

Theorem 29. *Suppose the Discretized Relaxed Switched System Optimal Control Problem, as defined in Equation (5.14), is a consistent approximation, as in Definition 9, of the Switched System Optimal Control Problem, as defined in Equation (2.34). Let $\{\tau_i\}_{i \in \mathbb{N}}$ and $\{\xi_i\}_{i \in \mathbb{N}}$ be such that $\tau_i \in \mathcal{T}_i$ and $\xi_i \in \mathcal{X}_{\tau_i, p}$ for each $i \in \mathbb{N}$. In this case, if $\lim_{i \rightarrow \infty} \theta_{\tau_i}(\xi_i) = 0$, then $\lim_{i \rightarrow \infty} \theta(\xi_i) = 0$.*

Proof. Arguing by contradiction, suppose there exists a $\delta > 0$ such that $\liminf_{i \rightarrow \infty} \theta(\xi_i) < -\delta$. Then by the super-additivity of the \liminf ,

$$\liminf_{i \rightarrow \infty} \theta_{\tau_i}(\xi_i) - \liminf_{i \rightarrow \infty} \theta(\xi_i) \leq \liminf_{i \rightarrow \infty} \theta_{\tau_i}(\xi_i) - \theta(\xi_i). \quad (5.19)$$

Rearranging terms and applying Definition 9, we have that:

$$\liminf_{i \rightarrow \infty} \theta_{\tau_i}(\xi_i) \leq \liminf_{i \rightarrow \infty} (\theta_{\tau_i}(\xi_i) - \theta(\xi_i)) + \liminf_{i \rightarrow \infty} \theta(\xi_i) < -\delta, \quad (5.20)$$

which contradicts the fact that $\lim_{i \rightarrow \infty} \theta_{\tau_i}(\xi_i) = 0$. Since by Condition 1 in Theorem 17, $\liminf_{i \rightarrow \infty} \theta(\xi_i) \leq \limsup_{i \rightarrow \infty} \theta(\xi_i) \leq 0$, we have our result. \square

To appreciate the importance of this result, observe that if we prove that the Discretized Relaxed Switched System Optimal Control Problem is a consistent approximation of the Switched System Optimal Control Problem, as we do in Theorem 50, and devise an algorithm for the Discretized Relaxed Switched System Optimal Control Problem that generates a sequence of discretized points that converge to a point that is a zero of the discretized optimality function, then the sequence of points generated actually converges to a point that also satisfies the necessary condition for optimality for the Switched System Optimal Control Problem.

5.4 Choosing a Discretized Step Size and Projecting the Discretized Relaxed Discrete Input

Before describing the step in our algorithm where the discretization precision is allowed to increase, we describe how the descent direction can be exploited in order to construct a point in the discretized relaxed optimization space that either reduces the cost (if the original point is feasible) or the infeasibility (if the original point is infeasible). Just as we did in Section 3.4, we employ a line search algorithm similar to the traditional Armijo algorithm used during finite dimensional optimization in order to choose a step size (Algorithm Model 1.2.23 in [64]). Given $N \in \mathbb{N}$, $\tau \in \mathcal{T}_N$, $\alpha \in (0, 1)$, and $\beta \in (0, 1)$, a step size for a point $\xi \in \mathcal{X}_{\tau,p}$, is chosen by solving the following optimization problem:

$$\mu_\tau(\xi) = \begin{cases} \min\{k \in \mathbb{N} \mid J_\tau(\xi + \beta^k(g_\tau(\xi) - \xi)) - J_\tau(\xi) \leq \alpha\beta^k\theta_\tau(\xi), \\ \Psi_\tau(\xi + \beta^k(g_\tau(\xi) - \xi)) \leq \alpha\beta^k\theta_\tau(\xi)\} & \text{if } \Psi_\tau(\xi) \leq 0, \\ \min\{k \in \mathbb{N} \mid \Psi_\tau(\xi + \beta^k(g_\tau(\xi) - \xi)) - \Psi_\tau(\xi) \leq \alpha\beta^k\theta_\tau(\xi)\} & \text{if } \Psi_\tau(\xi) > 0. \end{cases} \quad (5.21)$$

Continuing as we did in Section 3.4, given $N \in \mathbb{N}$ we can apply \mathcal{F}_N defined in Equation (3.12) and \mathcal{P}_N defined in Equation (3.13) to the constructed discretized relaxed discrete input. The pulse width modulation at a particular frequency induces a partition in \mathcal{T}_N according to the times at which the constructed pure discrete input switched. That is, let $\sigma_N : \mathcal{X}_\tau \rightarrow \mathcal{T}_N$ be defined by

$$\sigma_N(u, d) = \{0\} \cup \left\{ \frac{k}{2^N} + \frac{1}{2^N} \sum_{j=1}^i [\mathcal{F}_N(d)]_j \left(\frac{k}{2^N} \right) \right\}_{\substack{i \in \{1, \dots, q\} \\ k \in \{0, \dots, 2^N - 1\}}} . \quad (5.22)$$

Employing this induced partition, we can be more explicit about the range of ρ_N by stating that $\rho_N(\xi) \in \mathcal{X}_{\sigma_N(\xi),p}$ for each $\xi \in \mathcal{X}_\tau$.

Now, given given $N \in \mathbb{N}$, $\tau \in \mathcal{T}_N$, $\bar{\alpha} \in (0, \infty)$, $\bar{\beta} \in \left(\frac{1}{\sqrt{2}}, 1\right)$, $\omega \in (0, 1)$, and $k_{\max} \in \mathbb{N}$, a frequency at which to perform pulse width modulation for a point $\xi \in \mathcal{X}_{\tau,p}$ is computed by solving the following optimization problem::

$$\nu_\tau(\xi, k_{\max}) = \begin{cases} \min\{k \leq k_{\max} \mid \xi' = \xi + \beta^{\mu_\tau(\xi)}(g_\tau(\xi) - \xi), \\ \gamma' = (\alpha\beta^{\mu_\tau(\xi)} - \bar{\alpha}\bar{\beta}^k), \\ J_{\sigma_k(\xi')}(\rho_k(\xi')) - J_\tau(\xi) \leq \gamma'\theta_\tau(\xi), \\ \Psi_{\sigma_k(\xi')}(\rho_k(\xi')) \leq \gamma'\theta_\tau(\xi), \\ \bar{\alpha}\bar{\beta}^k \leq (1 - \omega)\alpha\beta^{\mu_\tau(\xi)}\} & \text{if } \Psi_\tau(\xi) \leq 0, \\ \min\{k \leq k_{\max} \mid \xi' = \xi + \beta^{\mu_\tau(\xi)}(g_\tau(\xi) - \xi), \\ \gamma' = (\alpha\beta^{\mu_\tau(\xi)} - \bar{\alpha}\bar{\beta}^k), \\ \Psi_{\sigma_k(\xi')}(\rho_k(\xi')) - \Psi_\tau(\xi) \leq \gamma'\theta_\tau(\xi), \\ \bar{\alpha}\bar{\beta}^k \leq (1 - \omega)\alpha\beta^{\mu_\tau(\xi)}\} & \text{if } \Psi_\tau(\xi) > 0. \end{cases} \quad (5.23)$$

In the discrete case, as opposed to the original infinite dimensional algorithm, due to the aforementioned shortcomings of Theorem 4 and 21, there is no guarantee that the optimization problem solved in order to determine ν_τ is feasible. Without loss of generality, we say that $\nu_\tau(\xi) = \infty$ for each $\xi \in \mathcal{X}_{\tau,r}$ when there is no feasible solution.

Importantly letting $N_0 \in \mathbb{N}$, $\tau_0 \in \mathcal{T}_{N_0}$, and $\xi \in \mathcal{X}_{\tau,r}$, we prove, in Lemma 53, that if $\theta(\xi) < 0$ then for each $\eta \in \mathbb{N}$ there exists a finite $N \geq N_0$ such that $\nu_{\sigma_N(\xi)}(\xi, N + \eta)$ is finite. That is, if $\theta(\xi) < 0$, then ν_τ is always finite after a certain discretization quality is reached. Observe also that the condition on Ψ_τ when $\Psi_\tau \leq 0$ in the computation of ν_τ is slightly different than corresponding condition on Ψ when $\Psi \leq 0$ in the computation of ν in Equation (3.15). This more demanding condition is required in the discretized situation in order to ensure that the discretized algorithm is able to remain feasible after becoming feasible as the discretization quality is increased.

5.5 An Implementable Switched System Optimal Control Algorithm

Consolidating our definitions, Algorithm 2, describes our numerical method to solve Switched System Optimal Control Problem. Notice that note that at each step of Algorithm 2, $\xi_j \in \mathcal{X}_{\tau_j,p}$. Also, observe the two principal differences between Algorithm 1 and Algorithm 2.

First, as discussed earlier, ν_τ maybe infinite as is checked in Line 10 of Algorithm 2, at which point the discretization precision is increased since we know that if $\theta(\xi) < 0$, then ν_τ is always finite after a certain discretization quality is reached. Second, notice that if θ_τ comes close to zero as is checked in Line 3 of Algorithm 2, the discretization precision is increased. To understand why this additional check is required, remember that our goal in this paper is the construction of an implementable algorithm that constructs a sequence of points by recursive application that converges to a point that satisfies the optimality condition. In particular, θ_τ may come arbitrarily close to zero due to a particular discretization precision that limits the potential descent directions to search amongst, rather than because it is actually close to a local minimizer of the Switched System Optimal Control Problem. This additional step that improves the discretization precision is included in Algorithm 2 to guard against this possibility.

With regards to actual numerical implementation, we make two additional comments. First, a stopping criterion is chosen that terminates the operation of the algorithm if θ_τ is too large. We describe our selection of this parameter in Chapter 7. Second, due to the definitions of DJ_τ and $D\psi_{\tau,j,\tau_k}$ for each $j \in \mathcal{J}$ and $k \in \{0, \dots, |\tau|\}$, the optimization required to solve θ_τ is a quadratic program.

For analysis purposes, we define $\Gamma_\tau : \{\xi \in \mathcal{X}_{\tau,p} \mid \nu_\tau(\xi, k_{\max}) < \infty\} \rightarrow \mathcal{X}_p$ by:

$$\Gamma_\tau(\xi) = \rho_{\nu_\tau(\xi, k_{\max})}(\xi + \beta^{\mu_\tau(\xi)}(g_\tau(\xi) - \xi)). \quad (5.24)$$

We say $\{\xi_j\}_{j \in \mathbb{N}}$ is a sequence generated by Algorithm 2 if $\xi_{j+1} = \Gamma_{\tau_j}(\xi_j)$ for each $j \in \mathbb{N}$. We can prove several important properties about the sequence generated by Algorithm 2. First,

letting $\{N_i\}_{i \in \mathbb{N}}$, $\{\tau_i\}_{i \in \mathbb{N}}$, and $\{\xi_i\}_{i \in \mathbb{N}}$ be the sequences produced by Algorithm 2, then, as we prove in Lemma 55, there exists $i_0 \in \mathbb{N}$ such that, if $\Psi_{\tau_{i_0}}(\xi_{i_0}) \leq 0$, then $\Psi(\xi_i) \leq 0$ and $\Psi_{\tau_i}(\xi_i) \leq 0$ for each $i \geq i_0$. That is, once Algorithm 2 finds a feasible point, every point generated after it remains feasible. Second, as we prove in Theorem 57, $\lim_{j \rightarrow \infty} \theta(\xi_j) = 0$ for a sequence $\{\xi_j\}_{j \in \mathbb{N}}$ generated by Algorithm 2, or Algorithm 2 converges to a point that satisfies the optimality condition.

Algorithm 2 Numerically Tractable Algorithm for the Switched System Optimal Control Problem

Require: $N_0 \in \mathbb{N}$, $\tau_0 \in \mathcal{T}_{N_0}$, $\xi_0 \in \mathcal{X}_{\tau_0, p}$, $\alpha \in (0, 1)$, $\bar{\alpha} \in (0, \infty)$, $\beta \in (0, 1)$, $\bar{\beta} \in \left(\frac{1}{\sqrt{2}}, 1\right)$,
 $\gamma \in (0, \infty)$, $\eta \in \mathbb{N}$, $\Lambda \in (0, \infty)$, $\chi \in \left(0, \frac{1}{2}\right)$, $\omega \in (0, 1)$.

- 1: Set $j = 0$.
 - 2: Compute $\theta_{\tau_j}(\xi_j)$ as defined in Equation (5.16).
 - 3: **if** $\theta_{\tau_j}(\xi_j) > -\Lambda 2^{-\chi N_j}$ **then**
 - 4: Set $\xi_{j+1} = \xi_j$, $N_{j+1} = N_j + 1$, $\tau_{j+1} = \sigma_{N_{j+1}}(\xi_j)$.
 - 5: Replace j by $j + 1$ and go to Line 2.
 - 6: **end if**
 - 7: Compute $g_{\tau_j}(\xi_j)$ as defined in Equation (5.16).
 - 8: Compute $\mu_{\tau_j}(\xi_j)$ as defined in Equation (5.21).
 - 9: Compute $\nu_{\tau_j}(\xi_j, N_j + \eta)$ as defined in Equation (5.23).
 - 10: **if** $\nu_{\tau_j}(\xi_j, N_j + \eta) = \infty$ **then**
 - 11: Set $\xi_{j+1} = \xi_j$, $N_{j+1} = N_j + 1$, $\tau_{j+1} = \sigma_{N_{j+1}}(\xi_{j+1})$.
 - 12: Replace j by $j + 1$ and go to Line 2.
 - 13: **end if**
 - 14: Set $\xi_{j+1} = \rho_{\nu_{\tau_j}(\xi_j, N_j + \eta)}(\xi_j + \beta^{\mu_{\tau_j}(\xi_j)}(g_{\tau_j}(\xi_j) - \xi_j))$, $N_{j+1} = \max\{N_j, \nu_{\tau_j}(\xi_j, N_j + \eta)\}$,
 $\tau_{j+1} = \sigma_{N_{j+1}}(\xi_{j+1})$.
 - 15: Replace j by $j + 1$ and go to Line 2.
-

Chapter 6

Proving the Convergence of the Implementable Algorithm

In this chapter, we derive the various components of Algorithm 2 and prove that Algorithm 2 converges to a point that satisfies our optimality condition. Our argument proceeds as follows: first, we prove the continuity and convergence of the discretized state, cost, and constraints to their infinite dimensional analogues; second, we construct the components of the optimality function and prove the convergence of these discretized components to their infinite dimensional analogues; finally, we prove the convergence of our algorithm.

6.1 Continuity and Convergence of the Discretized Components

In this subsection, we prove the continuity and convergence of the discretized state, cost, and constraint. We begin by proving the boundedness of the linear interpolation of the Euler Integration scheme:

Lemma 30. *There exists a constant $C > 0$ such that for each $N \in \mathbb{N}$, $\tau \in \mathcal{T}_N$, $\xi \in \mathcal{X}_{\tau,r}$, and $t \in [0, 1]$,*

$$\|z^{(\xi)}(t)\|_2 \leq C \tag{6.1}$$

Proof. We begin by showing the result for each $t \in \tau$. By Condition 1 in Assumption 1, together with the boundedness of $\|f(0, x_0, 0, e_i)\|_2$ for each $i \in \mathcal{Q}$, there exists a constant $K > 0$ such that, for each $N \in \mathbb{N}$, $\tau \in \mathcal{T}_N$, $\xi \in \mathcal{X}_{\tau,r}$, $i \in \mathcal{Q}$, and $k \in \{0, \dots, |\tau|\}$,

$$\|f(\tau_k, z^{(\xi)}(\tau_k), u(\tau_k), e_i)\|_2 \leq K(\|z^{(\xi)}(\tau_k)\|_2 + 1). \tag{6.2}$$

Employing Equation (5.7) and the Discrete Bellman-Gronwall Inequality (Exercise 5.6.14 in [64]), we have:

$$\begin{aligned}
 \|z^{(\xi)}(\tau_k)\|_2 &\leq \|x_0\|_2 + \frac{1}{2^N} \sum_{j=0}^k \sum_{i=1}^q \|f(\tau_j, z^{(\xi)}(\tau_j), u(\tau_j), e_i)\|_2 \\
 &\leq (\|x_0\|_2 + 1) \left(1 + \frac{qK}{2^N}\right)^{2^N} \\
 &\leq e^{qK} (\|x_0\|_2 + 1),
 \end{aligned} \tag{6.3}$$

thus obtaining the desired result for each $t \in \tau$.

The result for each $t \in [0, 1]$ follows after observing that, in Equation (5.8), $\left(\frac{t-\tau_k}{\tau_{k+1}-\tau_k}\right) \leq 1$ for each $t \in [\tau_k, \tau_{k+1})$ and $k \in \{0, \dots, |\tau|\}$. \square

In fact, this implies that the dynamics, cost, constraints, and their derivatives are all bounded:

Corollary 13. *There exists a constant $C > 0$ such that for each $N \in \mathbb{N}$, $\tau \in \mathcal{T}_N$, $j \in \mathcal{J}$, and $\xi = (u, d) \in \mathcal{X}_{\tau,r}$:*

- (1) a) $\|f(t, z^{(\xi)}(t), u(t), d(t))\|_2 \leq C$,
 b) $\left\|\frac{\partial f}{\partial x}(t, z^{(\xi)}(t), u(t), d(t))\right\|_{i,2} \leq C$,
 c) $\left\|\frac{\partial f}{\partial u}(t, z^{(\xi)}(t), u(t), d(t))\right\|_{i,2} \leq C$.
- (2) a) $|h_0(z^{(\xi)}(t))| \leq C$,
 b) $\left\|\frac{\partial h_0}{\partial x}(z^{(\xi)}(t))\right\|_2 \leq C$,
- (3) a) $|h_j(z^{(\xi)}(t))| \leq C$,
 b) $\left\|\frac{\partial h_j}{\partial x}(z^{(\xi)}(t))\right\|_2 \leq C$.

Proof. The result follows immediately from the continuity of f , $\frac{\partial f}{\partial x}$, $\frac{\partial f}{\partial u}$, h_0 , $\frac{\partial h_0}{\partial x}$, h_j , and $\frac{\partial h_j}{\partial x}$ for each $j \in \mathcal{J}$, as stated in Assumptions 1 and 2, and the fact that the arguments of these functions can be constrained to a compact domain, which follows from Lemma 30 and the compactness of U and Σ_r^q . \square

Next, we prove that the mapping from the discretized relaxed optimization space to the discretized trajectory is Lipschitz:

Lemma 31. *There exists a constant $L > 0$ such that, for each $N \in \mathbb{N}$, $\tau \in \mathcal{T}_N$, $\xi_1, \xi_2 \in \mathcal{X}_{\tau,r}$ and $t \in [0, 1]$:*

$$\|\phi_{\tau,t}(\xi_1) - \phi_{\tau,t}(\xi_2)\|_2 \leq L\|\xi_1 - \xi_2\|_{\mathcal{X}}, \tag{6.4}$$

where $\phi_{\tau,t}(\xi)$ is as defined in Equation (5.11).

Proof. We first prove this result for each $t \in \tau$. For notational convenience we will define $\Delta\tau_j = \tau_{j+1} - \tau_j$. Letting $\xi_1 = (u_1, d_1)$ and $\xi_2 = (u_2, d_2)$, notice that for $j \in \{0, \dots, |\tau| - 1\}$, by Equation (5.7) and rearranging the terms, there exists $L' > 0$ such that:

$$\begin{aligned} & \left\| \phi_{\tau, \tau_{j+1}}(\xi_1) - \phi_{\tau, \tau_{j+1}}(\xi_2) \right\|_2 - \left\| \phi_{\tau, \tau_j}(\xi_1) - \phi_{\tau, \tau_j}(\xi_2) \right\|_2 \leq \\ & \leq \Delta\tau_j \left\| f(\tau_j, \phi_{\tau, \tau_j}(\xi_1), u_1(\tau_j), d_1(\tau_j)) - f(\tau_j, \phi_{\tau, \tau_j}(\xi_2), u_2(\tau_j), d_2(\tau_j)) \right\|_2 \\ & \leq \frac{L'}{2^N} \left\| \phi_{\tau, \tau_j}(\xi_1) - \phi_{\tau, \tau_j}(\xi_2) \right\|_2 + L' \Delta\tau_j (\|u_1(\tau_j) - u_2(\tau_j)\|_2 + \|d_1(\tau_j) - d_2(\tau_j)\|_2), \end{aligned} \quad (6.5)$$

where the last inequality holds since the vector field f is Lipschitz in all of its arguments, as shown in the proof of Theorem 3, and $\Delta\tau_j \leq \frac{1}{2^N}$ by definition of \mathcal{T}_N .

Summing the inequality in Equation (6.5) for $j \in \{0, \dots, k-1\}$ and noting that $\phi_{\tau, \tau_0}(\xi_1) = \phi_{\tau, \tau_0}(\xi_2)$:

$$\begin{aligned} \left\| \phi_{\tau, \tau_k}(\xi_1) - \phi_{\tau, \tau_k}(\xi_2) \right\|_2 & \leq \frac{L'}{2^N} \sum_{j=0}^{k-1} \left\| \phi_{\tau, \tau_j}(\xi_1) - \phi_{\tau, \tau_j}(\xi_2) \right\|_2 + L' \sum_{j=0}^{k-1} \Delta\tau_j \|u_1(\tau_j) - u_2(\tau_j)\|_2 + \\ & \quad + L' \sum_{j=0}^{k-1} \Delta\tau_j \|d_1(\tau_j) - d_2(\tau_j)\|_2. \end{aligned} \quad (6.6)$$

Using the Discrete Bellman-Gronwall Inequality (Exercise 5.6.14 in [64]) and the fact that $(1 + \frac{L'}{2^N})^{\frac{L'}{2^N}} \leq e^{L'}$,

$$\begin{aligned} \left\| \phi_{\tau, \tau_k}(\xi_1) - \phi_{\tau, \tau_k}(\xi_2) \right\|_2 & \leq L' e^{L'} \left(\sum_{j=0}^{|\tau|-1} \Delta\tau_j \|u_1(\tau_j) - u_2(\tau_j)\|_2 + \sum_{j=0}^{|\tau|-1} \Delta\tau_j \|d_1(\tau_j) - d_2(\tau_j)\|_2 \right) \\ & \leq L' e^{L'} \left(\sqrt{\sum_{j=0}^{|\tau|-1} \Delta\tau_j \|u_1(\tau_j) - u_2(\tau_j)\|_2^2} + \right. \\ & \quad \left. + \sqrt{\sum_{j=0}^{|\tau|-1} \Delta\tau_j \|d_1(\tau_j) - d_2(\tau_j)\|_2^2} \right) \\ & = L \|\xi_1 - \xi_2\|_{\mathcal{X}}, \end{aligned} \quad (6.7)$$

where $L = L' e^{L'}$, and we employed Jensen's Inequality (Equation A.2 in [54]) together the fact that the \mathcal{X} -norm of $\xi \in \mathcal{X}_{\tau, r}$ can be written as a finite sum.

The result for any $t \in [0, 1]$ follows by noting that $\phi_{\tau, t}(\xi)$ is a convex combination of $\phi_{\tau, \tau_k}(\xi)$ and $\phi_{\tau, \tau_{k+1}}(\xi)$ for some $k \in \{0, \dots, |\tau| - 1\}$. \square

As a consequence, we immediately have the following results:

Corollary 14. *There exists a constant $L > 0$ such that for each $N \in \mathbb{N}$, $\tau \in \mathcal{T}_N$, $\xi_1 = (u_1, d_1) \in \mathcal{X}_{\tau,r}$, $\xi_2 = (u_2, d_2) \in \mathcal{X}_{\tau,r}$ and $t \in [0, 1]$:*

- (1)
$$\begin{aligned} & \left\| f(t, \phi_{\tau,t}(\xi_1), u_1(t), d_1(t)) - f(t, \phi_{\tau,t}(\xi_2), u_2(t), d_2(t)) \right\|_2 \leq \\ & \leq L(\|\xi_1 - \xi_2\|_{\mathcal{X}} + \|u_1(t) - u_2(t)\|_2 + \|d_1(t) - d_2(t)\|_2), \end{aligned}$$
- (2)
$$\begin{aligned} & \left\| \frac{\partial f}{\partial x}(t, \phi_{\tau,t}(\xi_1), u_1(t), d_1(t)) - \frac{\partial f}{\partial x}(t, \phi_{\tau,t}(\xi_2), u_2(t), d_2(t)) \right\|_{i,2} \leq \\ & \leq L(\|\xi_1 - \xi_2\|_{\mathcal{X}} + \|u_1(t) - u_2(t)\|_2 + \|d_1(t) - d_2(t)\|_2), \end{aligned}$$
- (3)
$$\begin{aligned} & \left\| \frac{\partial f}{\partial u}(t, \phi_{\tau,t}(\xi_1), u_1(t), d_1(t)) - \frac{\partial f}{\partial u}(t, \phi_{\tau,t}(\xi_2), u_2(t), d_2(t)) \right\|_{i,2} \leq \\ & \leq L(\|\xi_1 - \xi_2\|_{\mathcal{X}} + \|u_1(t) - u_2(t)\|_2 + \|d_1(t) - d_2(t)\|_2), \end{aligned}$$

where $\phi_{\tau,t}(\xi)$ is as defined in Equation (5.11).

Proof. The proof of Condition 1 follows by the fact that the vector field f is Lipschitz in all its arguments, as shown in the proof of Theorem 3, and applying Lemma 31. The remaining conditions follow in a similar fashion. \square

Corollary 15. *There exists a constant $L > 0$ such that for each $N \in \mathbb{N}$, $\tau \in \mathcal{T}_N$, $\xi_1 = (u_1, d_1) \in \mathcal{X}_{r,\tau}$, $\xi_2 = (u_2, d_2) \in \mathcal{X}_{r,\tau}$, $j \in \mathcal{J}$, and $t \in [0, 1]$:*

- (1) $|h_0(\phi_{\tau,1}(\xi_1)) - h_0(\phi_{\tau,1}(\xi_2))| \leq L \|\xi_1 - \xi_2\|_{\mathcal{X}},$
- (2) $\left\| \frac{\partial h_0}{\partial x}(\phi_{\tau,1}(\xi_1)) - \frac{\partial h_0}{\partial x}(\phi_{\tau,1}(\xi_2)) \right\|_2 \leq L \|\xi_1 - \xi_2\|_{\mathcal{X}},$
- (3) $|h_j(\phi_{\tau,t}(\xi_1)) - h_j(\phi_{\tau,t}(\xi_2))| \leq L \|\xi_1 - \xi_2\|_{\mathcal{X}},$
- (4) $\left\| \frac{\partial h_j}{\partial x}(\phi_{\tau,t}(\xi_1)) - \frac{\partial h_j}{\partial x}(\phi_{\tau,t}(\xi_2)) \right\|_2 \leq L \|\xi_1 - \xi_2\|_{\mathcal{X}},$

where $\phi_{\tau,t}(\xi)$ is as defined in Equation (5.11).

Proof. This result follows by Assumption 2 and Lemma 31. \square

Even though it is a straightforward consequence of Condition 1 in Corollary 15, we write the following result to stress its importance.

Corollary 16. *Let $N \in \mathbb{N}$ and $\tau \in \mathcal{T}_N$, then there exists a constant $L > 0$ such that, for each $\xi_1, \xi_2 \in \mathcal{X}_{\tau,r}$:*

$$|J_{\tau}(\xi_1) - J_{\tau}(\xi_2)| \leq L \|\xi_1 - \xi_2\|_{\mathcal{X}} \quad (6.8)$$

where J_{τ} is as defined in Equation (5.9).

In fact, Ψ_{τ} is also Lipschitz continuous:

Lemma 32. *Let $N \in \mathbb{N}$ and $\tau \in \mathcal{T}_N$, then there exists a constant $L > 0$ such that, for each $\xi_1, \xi_2 \in \mathcal{X}_\tau$:*

$$|\Psi_\tau(\xi_1) - \Psi_\tau(\xi_2)| \leq L \|\xi_1 - \xi_2\|_{\mathcal{X}} \quad (6.9)$$

where Ψ_τ is as defined in Equation (5.10).

Proof. Since the maximum in Ψ_τ is taken over $\mathcal{J} \times k \in \{0, \dots, |\tau|\}$, which is compact, and the maps $(j, k) \mapsto \psi_{\tau, j, \tau_k}(\xi)$ are continuous for each $\xi \in \mathcal{X}_\tau$, we know from Condition 3 in Corollary 15 that there exists $L > 0$ such that,

$$\begin{aligned} \Psi_\tau(\xi_1) - \Psi_\tau(\xi_2) &= \max_{(j,k) \in \mathcal{J} \times \{0, \dots, |\tau|\}} \psi_{\tau, j, \tau_k}(\xi_1) - \max_{(j,k) \in \mathcal{J} \times \{0, \dots, |\tau|\}} \psi_{\tau, j, \tau_k}(\xi_2) \\ &\leq \max_{(j,k) \in \mathcal{J} \times \{0, \dots, |\tau|\}} \psi_{\tau, j, \tau_k}(\xi_1) - \psi_{\tau, j, \tau_k}(\xi_2) \\ &\leq L \|\xi_1 - \xi_2\|_{\mathcal{X}}. \end{aligned} \quad (6.10)$$

By reversing ξ_1 and ξ_2 , and applying the same argument we get the desired result. \square

We can now show the rate of convergence of the Euler Integration scheme:

Lemma 33. *There exists a constant $B > 0$ such that for each $N \in \mathbb{N}$, $\tau \in \mathcal{T}_N$, $\xi \in \mathcal{X}_{\tau, r}$, and $t \in [0, 1]$:*

$$\|z_\tau^{(\xi)}(t) - x^{(\xi)}(t)\|_2 \leq \frac{B}{2^N}, \quad (6.11)$$

where $x^{(\xi)}$ is the solution to Differential Equation (2.29) and $z_\tau^{(\xi)}$ is as defined in Difference Equation (5.8).

Proof. Let $\xi = (u, d)$, and recall that the vector field f is Lipschitz continuous in all its arguments, as shown in the proof of Theorem 3. By applying Picard's Lemma (Lemma 5.6.3

in [64]), we have:

$$\begin{aligned}
 \|z^{(\xi)}(t) - x^{(\xi)}(t)\|_2 &\leq e^L \int_0^1 \left\| \frac{dz^{(\xi)}}{ds}(s) - f(s, z^{(\xi)}(s), u(s), d(s)) \right\|_2 ds \\
 &= e^L \sum_{k=0}^{|\tau|-1} \int_{\tau_k}^{\tau_{k+1}} \left\| f(\tau_k, z^{(\xi)}(\tau_k), u(\tau_k), d(\tau_k)) + \right. \\
 &\quad \left. - f\left(s, z^{(\xi)}(\tau_k) + \frac{s - \tau_k}{\tau_{k+1} - \tau_k} (z^{(\xi)}(\tau_{k+1}) + \right. \right. \\
 &\quad \left. \left. - z^{(\xi)}(\tau_k)), u(\tau_k), d(\tau_k)\right) \right\|_2 ds \\
 &\leq Le^L \sum_{k=0}^{|\tau|-1} (1 + \|f(\tau_k, z^{(\xi)}(\tau_k), u(\tau_k), d(\tau_k))\|_2) \left(\int_{\tau_k}^{\tau_{k+1}} |s - \tau_k| ds \right) \\
 &\leq \frac{1}{2^N} Le^L (1 + C) \sum_{k=0}^{|\tau|-1} (\tau_{k+1} - \tau_k) = \frac{B}{2^N},
 \end{aligned} \tag{6.12}$$

where $C > 0$ is as defined in Condition 1 in Corollary 13 and, $B = (1 + C)Le^L$, and we used the fact that $\tau_{k+1} - \tau_k \leq \frac{1}{2^N}$ by definition of \mathcal{T}_N in Equation (5.1). \square

Importantly we can show that we can bound the rate of convergence of this discretized cost function. We omit the proof since it follows easily using Assumption 2 and Lemma 33.

Lemma 34. *There exists a constant $B > 0$ such that for each $N \in \mathbb{N}$, $\tau \in \mathcal{T}_N$, and $\xi \in \mathcal{X}_{\tau, r}$:*

$$|J_\tau(\xi) - J(\xi)| \leq \frac{B}{2^N}, \tag{6.13}$$

where J is as defined in Equation (2.31) and J_τ is as defined in Equation (5.9).

Similarly, we can bound the rate of convergence of this discretized constraint function.

Lemma 35. *There exists a constant $B > 0$ such that for each $N \in \mathbb{N}$, $\tau \in \mathcal{T}_N$, and $\xi \in \mathcal{X}_{\tau, r}$:*

$$|\Psi_\tau(\xi) - \Psi(\xi)| \leq \frac{B}{2^N}, \tag{6.14}$$

where Ψ is as defined in Equation (2.32) and Ψ_τ is as defined in Equation (5.10).

Proof. Let $C > 0$ be as defined in Condition 1 in Corollary 1, and let $L > 0$ be the Lipschitz constant as specified in Assumption 2. Then, using the definition of \mathcal{T}_N in Equation (5.1), for each $k \in \{0, \dots, |\tau| - 1\}$ and $t \in [\tau_k, \tau_{k+1}]$,

$$|h_j(x^{(\xi)}(t)) - h_j(x^{(\xi)}(\tau_k))| \leq L \int_{\tau_k}^t \|f(s, x^{(\xi)}(s), u(s), d(s))\|_2 ds \leq \frac{LC}{2^N}. \tag{6.15}$$

Moreover, Condition 3 in Assumption 2 together Lemma 33 imply the existence of a constant $K > 0$ such that:

$$|h_j(x^{(\xi)}(\tau_k)) - h_j(z^{(\xi)}(\tau_k))| \leq \frac{K}{2^N}. \quad (6.16)$$

Employing the Triangle Inequality on the two previous inequalities, we know there exists a constant $B > 0$ such that, for each $t \in [\tau_k, \tau_{k+1}]$,

$$|h_j(x^{(\xi)}(t)) - h_j(z^{(\xi)}(\tau_k))| \leq \frac{B}{2^N}. \quad (6.17)$$

Let $t' \in \arg \max_{t \in [0,1]} h_j(x^{(\xi)}(t))$, and let $\kappa(t') \in \{0, \dots, |\tau| - 1\}$ such that $t' \in [\tau_{\kappa(t')}, \tau_{\kappa(t')+1}]$. Then,

$$\max_{t \in [0,1]} h_j(x^{(\xi)}(t)) - \max_{k \in \{0, \dots, |\tau|\}} h_j(z^{(\xi)}(\tau_k)) \leq h_j(x^{(\xi)}(t')) - h_j(z^{(\xi)}(\tau_{\kappa(t')})) \leq \frac{B}{2^N}. \quad (6.18)$$

Similarly if $k' \in \arg \max_{k \in \{0, \dots, |\tau|\}} h_j(z^{(\xi)}(\tau_k))$, then

$$\max_{k \in \{0, \dots, |\tau|\}} h_j(z^{(\xi)}(\tau_k)) - \max_{t \in [0,1]} h_j(x^{(\xi)}(t)) \leq h_j(z^{(\xi)}(\tau_{k'})) - h_j(x^{(\xi)}(\tau_{k'})) \leq \frac{B}{2^N}. \quad (6.19)$$

This implies that:

$$\Psi(\xi) - \Psi_\tau(\xi) \leq \max_{j \in \mathcal{J}} \left(\max_{t \in [0,1]} h_j(x^{(\xi)}(t)) - \max_{k \in \{0, \dots, |\tau|\}} h_j(z^{(\xi)}(\tau_k)) \right) \leq \frac{B}{2^N}, \quad (6.20)$$

$$\Psi_\tau(\xi) - \Psi(\xi) \leq \max_{j \in \mathcal{J}} \left(\max_{k \in \{0, \dots, |\tau|\}} h_j(z^{(\xi)}(\tau_k)) - \max_{t \in [0,1]} h_j(x^{(\xi)}(t)) \right) \leq \frac{B}{2^N}, \quad (6.21)$$

which proves the desired result. \square

6.2 Derivation of the Implementable Algorithm Terms

Next, we formally derive the components of the discretized optimality function, prove the well-posedness of the discretized optimality function, and prove the convergence of the discretized optimality function to the optimality function. We begin by deriving the equivalent of Lemma 7 for our discretized formulation.

Lemma 36. *Let $N \in \mathbb{N}$, $\tau \in \mathcal{T}_N$, $\xi = (u, d) \in \mathcal{X}_{\tau, r}$, $\xi' = (u', d') \in \mathcal{X}_\tau$, and $\phi_{\tau, t}$ be as defined in Equation (5.11). Then, for each $k \in \{0, \dots, |\tau|\}$, the directional derivative of ϕ_{τ, τ_k} , as*

defined in Equation (3.3), is given by

$$D\phi_{\tau, \tau_k}(\xi; \xi') = \sum_{j=0}^{k-1} (\tau_{j+1} - \tau_j) \Phi_{\tau}^{(\xi)}(\tau_k, \tau_{j+1}) \left(\frac{\partial f}{\partial u}(\tau_j, \phi_{\tau, \tau_j}(\xi), u(\tau_j), d(\tau_j)) u'(\tau_j) + \sum_{i=1}^q f(\tau_j, \phi_{\tau, \tau_j}(\xi), u(\tau_j), e_i) d'_i(\tau_j) \right), \quad (6.22)$$

where $\Phi_{\tau}^{(\xi)}(\tau_k, \tau_j)$ is the unique solution of the following matrix difference equation:

$$\begin{aligned} \Phi_{\tau}^{(\xi)}(\tau_{k+1}, \tau_j) &= \Phi_{\tau}^{(\xi)}(\tau_k, \tau_j) + (\tau_{k+1} - \tau_k) \frac{\partial f}{\partial x}(\tau_k, \phi_{\tau, \tau_k}(\xi), u(\tau_k), d(\tau_k)) \Phi_{\tau}^{(\xi)}(\tau_k, \tau_j), \\ \Phi_{\tau}^{(\xi)}(\tau_j, \tau_j) &= I, \end{aligned} \quad (6.23)$$

for each $k \in \{0, \dots, |\tau| - 1\}$.

Proof. For notational convenience, let $z^{(\lambda)} = z^{(\xi + \lambda \xi')}$, $u^{(\lambda)} = u + \lambda u'$, and $d^{(\lambda)} = d + \lambda d'$. Also, let us define $\Delta z^{(\lambda)} = z^{(\lambda)} - z^{(\xi)}$, thus, for each $k \in \{0, \dots, |\tau|\}$,

$$\begin{aligned} \Delta z^{(\lambda)}(\tau_k) &= \sum_{j=0}^{k-1} (\tau_{j+1} - \tau_j) \left(f(\tau_j, z^{(\lambda)}(\tau_j), u^{(\lambda)}(\tau_j), d^{(\lambda)}(\tau_j)) - f(\tau_j, z^{(\xi)}(\tau_j), u(\tau_j), d(\tau_j)) \right) \\ &= \sum_{j=0}^{k-1} (\tau_{j+1} - \tau_j) \left(\lambda \sum_{i=1}^q d'_i(\tau_j) f(\tau_j, z^{(\lambda)}(\tau_j), u^{(\lambda)}(\tau_j), e_i) + \right. \\ &\quad \left. + \frac{\partial f}{\partial x}(\tau_j, z^{(\xi)}(\tau_j) + \nu_{x,j} \Delta z^{(\lambda)}(\tau_j), u^{(\lambda)}(\tau_j), d(\tau_j)) \Delta z^{(\lambda)}(\tau_j) + \right. \\ &\quad \left. + \lambda \frac{\partial f}{\partial u}(\tau_j, z^{(\xi)}(\tau_j), u(\tau_j) + \nu_{u,j} \lambda u'(\tau_j), d(\tau_j)) u'(\tau_j) \right), \end{aligned} \quad (6.24)$$

where $\{\nu_{x,j}\}_{j=0}^{|\tau|} \subset [0, 1]$ and $\{\nu_{u,j}\}_{j=0}^{|\tau|} \subset [0, 1]$.

Let $\{y(\tau_k)\}_{k=0}^{|\tau|}$ be recursively defined as follows:

$$\begin{aligned} y(\tau_{k+1}) &= y(\tau_k) + (\tau_{k+1} - \tau_k) \left(\frac{\partial f}{\partial x}(\tau_k, z^{(\xi)}(\tau_k), u(\tau_k), d(\tau_k)) y(\tau_k) + \right. \\ &\quad \left. + \frac{\partial f}{\partial u}(\tau_k, z^{(\xi)}(\tau_k), u(\tau_k), d(\tau_k)) u'(\tau_k) + \sum_{i=1}^q d'_i(\tau_k) f(\tau_k, z^{(\xi)}(\tau_k), u(\tau_k), e_i) \right), \\ y(\tau_0) &= 0. \end{aligned} \quad (6.25)$$

We want to show that $\frac{\Delta z^{(\lambda)}(\tau_k)}{\lambda} \rightarrow y(\tau_k)$ as $\lambda \downarrow 0$. Consider:

$$\begin{aligned} & \left\| \frac{\partial f}{\partial x}(\tau_k, z^{(\xi)}(\tau_k), u(\tau_k), d(\tau_k))y(\tau_k) - \frac{\partial f}{\partial x}(\tau_k, z^{(\xi)}(\tau_k) + \right. \\ & \quad \left. + \nu_{x,k} \Delta z^{(\lambda)}(\tau_k), u^{(\lambda)}(\tau_k), d(\tau_k)) \frac{\Delta z^{(\lambda)}(\tau_k)}{\lambda} \right\|_2 \leq \\ & \leq L \left\| y(\tau_k) - \frac{\Delta z^{(\lambda)}(\tau_k)}{\lambda} \right\|_2 + \\ & \quad + L (\|\Delta z^{(\lambda)}(\tau_k)\|_2 + \lambda \|u'(\tau_k)\|_2) \|y(\tau_k)\|_2, \end{aligned} \quad (6.26)$$

which follows by Assumption 1 and the Triangle Inequality. Also,

$$\begin{aligned} & \left\| \left(\frac{\partial f}{\partial u}(\tau_k, z^{(\xi)}(\tau_k), u(\tau_k), d(\tau_k)) - \frac{\partial f}{\partial u}(\tau_k, z^{(\xi)}(\tau_k), u(\tau_k) + \right. \right. \\ & \quad \left. \left. + \nu_{u,k} \lambda u'(\tau_k), d(\tau_k)) \right) u'(\tau_k) \right\|_2 \leq L \lambda \|u'(\tau_k)\|_2^2, \end{aligned} \quad (6.27)$$

and

$$\begin{aligned} & \left\| \sum_{i=1}^q d'_i(\tau_k) \left(f(\tau_k, z^{(\xi)}(\tau_k), u(\tau_k), e_i) + \right. \right. \\ & \quad \left. \left. - f(\tau_k, z^{(\lambda)}(\tau_k), u^{(\lambda)}(\tau_k), e_i) \right) \right\|_2 \leq L \|\Delta z^{(\lambda)}(\tau_k)\|_2 + L \lambda \|u'(\tau_k)\|_2. \end{aligned} \quad (6.28)$$

Hence, using the Discrete Bellman-Gronwall Inequality (Lemma 5.6.14 in [64]) and the inequalities above,

$$\begin{aligned} \left\| y(\tau_k) - \frac{\Delta z^{(\lambda)}(\tau_k)}{\lambda} \right\|_2 & \leq L e^L \sum_{j=0}^{k-1} (\tau_{j+1} - \tau_j) \left((\|\Delta z^{(\lambda)}(\tau_j)\|_2 + \lambda \|u'(\tau_j)\|_2) \|y(\tau_j)\|_2 + \right. \\ & \quad \left. + \lambda \|u'(\tau_j)\|_2^2 + \|\Delta z^{(\lambda)}(\tau_j)\|_2 + \lambda \|u'(\tau_j)\|_2 \right) \end{aligned} \quad (6.29)$$

where we used the fact that $(1 + \frac{L}{2^N})^{\frac{L}{2^N}} \leq e^L$. But, by Lemma 31, the right-hand side of Equation (6.29) goes to zero as $\lambda \downarrow 0$, thus obtaining that

$$\lim_{\lambda \downarrow 0} \frac{\Delta z^{(\lambda)}(\tau_k)}{\lambda} = y(\tau_k). \quad (6.30)$$

The result of the first part of the Lemma is obtained after noting that $D\phi_{\tau, \tau_k}(\xi; \xi')$ is equal to $y(\tau_k)$ for each $k \in \{0, \dots, |\tau|\}$. □

Next, we prove that $D\phi_{\tau, \tau_k}$ is bounded by proving that Φ^ξ is bounded:

Corollary 17. *There exists a constant $C > 0$ such that for each $N \in \mathbb{N}$, $\tau \in \mathcal{T}_N$, $\xi \in \mathcal{X}_{\tau, r}$, and $k, l \in \{0, \dots, |\tau|\}$:*

$$\|\Phi_\tau^{(\xi)}(\tau_k, \tau_l)\|_{i,2} \leq C, \quad (6.31)$$

where $\Phi_\tau^{(\xi)}(\tau_k, \tau_l)$ is the solution to the Difference Equation (6.23).

Proof. This follows directly from Equation (6.23) and Condition 1 in Corollary 13. \square

Corollary 18. *There exists a constant $C > 0$ such that for each $N \in \mathbb{N}$, $\tau \in \mathcal{T}_N$, $\xi \in \mathcal{X}_{\tau, r}$, $\xi' \in \mathcal{X}_\tau$, and $k \in \{0, \dots, |\tau|\}$:*

$$\|D\phi_{\tau, \tau_k}(\xi; \xi')\|_2 \leq C \|\xi'\|_{\mathcal{X}}, \quad (6.32)$$

where $D\phi_{\tau, \tau_k}(\xi; \xi')$ is as defined in Equation (6.22).

Proof. This follows by the Cauchy-Schwartz Inequality together with Corollary 13 and Corollary 17. \square

We now show that $\Phi_\tau^{(\xi)}$ is in fact Lipschitz continuous.

Lemma 37. *There exists a constant $L > 0$ such that for each $N \in \mathbb{N}$, $\tau \in \mathcal{T}_N$, $\xi_1, \xi_2 \in \mathcal{X}_{\tau, r}$, and $k, l \in \{0, \dots, |\tau|\}$:*

$$\|\Phi_\tau^{(\xi_1)}(\tau_k, \tau_l) - \Phi_\tau^{(\xi_2)}(\tau_k, \tau_l)\|_{i,2} \leq L \|\xi_1 - \xi_2\|_{\mathcal{X}}, \quad (6.33)$$

where $\Phi_\tau^{(\xi)}$ is the solution to Difference Equation (6.23).

Proof. Let $\xi_1 = (u_1, d_1)$ and $\xi_2 = (u_2, d_2)$. Then, using the Triangle Inequality:

$$\begin{aligned} & \left\| \Phi_\tau^{(\xi_1)}(\tau_k, \tau_l) - \Phi_\tau^{(\xi_2)}(\tau_k, \tau_l) \right\|_{i,2} \leq \\ & \leq \sum_{i=0}^{k-1} (\tau_{i+1} - \tau_i) \left(\left\| \frac{\partial f}{\partial x}(\tau_i, z^{(\xi_2)}(\tau_i), u_2(\tau_i), d_2(\tau_i)) \right\|_{i,2} \left\| \Phi_\tau^{(\xi_1)}(\tau_i, \tau_j) + \right. \right. \\ & \quad \left. \left. - \Phi_\tau^{(\xi_2)}(\tau_i, \tau_j) \right\|_{i,2} + \left\| \frac{\partial f}{\partial x}(\tau_i, z^{(\xi_1)}(\tau_i), u_1(\tau_i), d_1(\tau_i)) + \right. \right. \\ & \quad \left. \left. - \frac{\partial f}{\partial x}(\tau_i, z^{(\xi_2)}(\tau_i), u_2(\tau_i), d_2(\tau_i)) \right\|_{i,2} \left\| \Phi_\tau^{(\xi_1)}(\tau_i, \tau_j) \right\|_{i,2} \right). \end{aligned} \quad (6.34)$$

The result follows by applying Condition 1 in Corollary 13, Condition 2 in Corollary 14, the same argument used in Equation (4.5), and the Discrete Bellman-Gronwall Inequality (Exercise 5.6.14 in [64]). \square

A simple extension of our previous argument shows that $D\phi_{\tau,\tau_k}(\xi, \cdot)$ is Lipschitz continuous with respect to its point of evaluation, ξ .

Lemma 38. *There exists a constant $L > 0$ such that for each $N \in \mathbb{N}$, $\tau \in \mathcal{T}_N$, $\xi_1, \xi_2 \in \mathcal{X}_{\tau,r}$, $\xi' \in \mathcal{X}_\tau$, and $k \in \{0, \dots, |\tau|\}$:*

$$\|D\phi_{\tau,\tau_k}(\xi_1; \xi') - D\phi_{\tau,\tau_k}(\xi_2; \xi')\|_2 \leq L \|\xi_1 - \xi_2\|_{\mathcal{X}} \|\xi'\|_{\mathcal{X}}, \quad (6.35)$$

where $D\phi_{\tau,\tau_k}$ is as defined in Equation (6.22).

Proof. Let $\xi_1 = (u_1, d_1)$, $\xi_2 = (u_2, d_2)$, and $\xi' = (u', d')$. Then, applying the Triangle Inequality:

$$\begin{aligned} \left\| D\phi_{\tau,\tau_k}(\xi_1; \xi') - D\phi_{\tau,\tau_k}(\xi_2; \xi') \right\|_2 &\leq \sum_{j=0}^{k-1} (\tau_{j+1} - \tau_j) \left(\left\| \Phi_\tau^{(\xi_1)}(\tau_k, \tau_{j+1}) + \right. \right. \\ &\quad \left. \left. - \Phi_\tau^{(\xi_2)}(\tau_k, \tau_{j+1}) \right\|_{i,2} \left\| \frac{\partial f}{\partial u}(\tau_j, z^{(\xi_1)}(\tau_j), u_1(\tau_j), d_1(\tau_j)) \right\|_{i,2} \|u'(\tau_j)\|_2 + \right. \\ &\quad \left. + \left\| \Phi_\tau^{(\xi_2)}(\tau_k, \tau_{j+1}) \right\|_{i,2} \left\| \frac{\partial f}{\partial u}(\tau_j, z^{(\xi_1)}(\tau_j), u_1(\tau_j), d_1(\tau_j)) + \right. \right. \\ &\quad \left. \left. - \frac{\partial f}{\partial u}(\tau_j, z^{(\xi_2)}(\tau_j), u_2(\tau_j), d_2(\tau_j)) \right\|_{i,2} \|u'(\tau_j)\|_2 + \sum_{i=1}^q \left\| \Phi_\tau^{(\xi_1)}(\tau_k, \tau_{j+1}) + \right. \right. \\ &\quad \left. \left. - \Phi_\tau^{(\xi_2)}(\tau_k, \tau_{j+1}) \right\|_{i,2} \left\| f(\tau_j, z^{(\xi_1)}(\tau_j), u_1(\tau_j), e_i) \right\|_{i,2} |d'_i(\tau_j)| + \right. \\ &\quad \left. + \left\| \Phi_\tau^{(\xi_2)}(\tau_k, \tau_{j+1}) \right\|_{i,2} \left\| f(\tau_j, z^{(\xi_1)}(\tau_j), u_1(\tau_j), e_i) - f(\tau_j, z^{(\xi_2)}(\tau_j), u_2(\tau_j), e_i) \right\|_{i,2} |d'_i(\tau_j)| \right) \end{aligned} \quad (6.36)$$

The result follows by applying Lemma 37, Corollary 17, Condition 1 in Corollary 1, Conditions 1 and 3 in Corollary 14, and the same argument used in Equation (4.5). \square

Employing these results, we can prove that $D\phi_{\tau,\tau_k}(\xi; \xi')$ converges to $D\phi_{\tau_k}(\xi; \xi')$ as the discretization is increased:

Lemma 39. *There exists $B > 0$ such that for each $N \in \mathbb{N}$, $\tau \in \mathcal{T}_N$, $\xi \in \mathcal{X}_{\tau,r}$, $\xi' \in \mathcal{X}_\tau$ and $k \in \{0, \dots, |\tau|\}$:*

$$\|D\phi_{\tau_k}(\xi; \xi') - D\phi_{\tau,\tau_k}(\xi; \xi')\|_2 \leq \frac{B}{2^N}, \quad (6.37)$$

where $D\phi_{\tau_k}$ and $D\phi_{\tau,\tau_k}$ are as defined in Equations (4.10) and (6.22), respectively.

Proof. Let $\xi = (u, d)$, $\xi' = (u', d')$. First, by applying the Triangle Inequality and noticing that the induced matrix norm is compatible, we have:

$$\begin{aligned}
 & \left\| \mathbb{D}\phi_{\tau_k}(\xi; \xi') - \mathbb{D}\phi_{\tau, \tau_k}(\xi; \xi') \right\|_2 \leq \\
 & \leq \sum_{j=0}^{k-1} \int_{\tau_j}^{\tau_{j+1}} \left(\left\| \Phi^{(\xi)}(\tau_k, s) - \Phi_{\tau}^{(\xi)}(\tau_k, \tau_{j+1}) \right\|_{i,2} \left\| \frac{\partial f}{\partial u}(\tau_j, z^{(\xi)}(\tau_j), u(\tau_j), d(\tau_j)) \right\|_{i,2} + \right. \\
 & \quad \left. + \left\| \Phi^{(\xi)}(\tau_k, s) \right\|_{i,2} \left\| \frac{\partial f}{\partial u}(s, x^{(\xi)}(s), u(\tau_j), d(\tau_j)) + \right. \right. \\
 & \quad \left. \left. - \frac{\partial f}{\partial u}(\tau_j, z^{(\xi)}(\tau_j), u(\tau_j), d(\tau_j)) \right\|_{i,2} \right) \|u'(\tau_j)\|_2 ds + \\
 & + \sum_{j=0}^{k-1} \int_{\tau_j}^{\tau_{j+1}} \sum_{i=1}^q \left(\left\| \Phi^{(\xi)}(\tau_k, s) \right\|_{i,2} \left\| f(s, x^{(\xi)}(s), u(\tau_j), e_i) - f(\tau_j, z^{(\xi)}(\tau_j), u(\tau_j), e_i) \right\|_2 + \right. \\
 & \quad \left. + \left\| \Phi^{(\xi)}(\tau_k, s) - \Phi_{\tau}^{(\xi)}(\tau_k, \tau_{j+1}) \right\|_{i,2} \left\| f(\tau_j, z^{(\xi)}(\tau_j), u(\tau_j), e_i) \right\|_2 \right) |d'_i(\tau_l)| ds.
 \end{aligned} \tag{6.38}$$

Second, let $\kappa(t) \in \{0, \dots, |\tau|\}$ such that $t \in [\tau_{\kappa(t)}, \tau_{\kappa(t)+1}]$ for each $t \in [0, 1]$. Then, there exists $K > 0$ such that

$$\begin{aligned}
 \left\| x^{(\xi)}(s) - z^{(\xi)}(\tau_{\kappa(s)}) \right\| & \leq \left\| x^{(\xi)}(s) - z^{(\xi)}(s) \right\| + \left\| z^{(\xi)}(s) - z^{(\xi)}(\tau_{\kappa(s)}) \right\| \\
 & \leq \left\| x^{(\xi)}(s) - z^{(\xi)}(s) \right\| + (s - \tau_{\kappa(s)})C \\
 & \leq \frac{K}{2^N},
 \end{aligned} \tag{6.39}$$

where $C > 0$ is as in Condition 1 in Corollary 13, and we applied Lemma 33 and the definition of \mathcal{T}_N in Equation (5.1).

Third, in a fashion similar to how we defined our discretized trajectory in Equation (5.8), we can define a discretized state transition matrix, $\tilde{\Phi}_{\tau}^{(\xi)}$ for each $k \in \{0, \dots, |\tau|\}$ via linear interpolation on the second argument:

$$\tilde{\Phi}_{\tau}^{(\xi)}(\tau_k, t) = \sum_{j=0}^{|\tau|-1} \left(\Phi_{\tau}^{(\xi)}(\tau_k, \tau_j) + \frac{t - \tau_j}{\tau_{j+1} - \tau_j} (\Phi_{\tau}^{(\xi)}(\tau_k, \tau_{j+1}) - \Phi_{\tau}^{(\xi)}(\tau_k, \tau_j)) \right) \pi_{\tau, j}(t). \tag{6.40}$$

where $\tau_{\tau, j}$ is as defined in Equation (5.2). Then there exists a constant $K' > 0$ such that for each $t \in [0, 1]$:

$$\begin{aligned}
 \left\| \Phi^{(\xi)}(\tau_k, t) - \Phi_{\tau}^{(\xi)}(\tau_k, \tau_{\kappa(t)}) \right\|_{i,2} & \leq \left\| \Phi^{(\xi)}(\tau_k, t) - \tilde{\Phi}_{\tau}^{(\xi)}(\tau_k, t) \right\|_{i,2} + \\
 & \quad + \left\| \tilde{\Phi}_{\tau}^{(\xi)}(\tau_k, t) - \Phi_{\tau}^{(\xi)}(\tau_k, \tau_{\kappa(t)}) \right\|_{i,2} \\
 & \leq \frac{K'}{2^N},
 \end{aligned} \tag{6.41}$$

where the last inequality follows by an argument identical to the one used in the proof of Lemma 33, together with an argument identical to the one used in Equation (6.39).

Finally, the result follows from Equation (6.38) after applying Condition 1 in Corollary 13, Corollary 7, Conditions 1 and 3 in Corollary 14, Equations (6.39) and (6.41), and the same argument as in Equation (4.5). \square

Next, we construct the expression for the directional derivative of the discretized cost function and prove that it is Lipschitz continuous.

Lemma 40. *Let $N \in \mathbb{N}$, $\tau \in \mathcal{T}_N$, $\xi \in \mathcal{X}_{\tau,r}$, $\xi' \in \mathcal{X}_\tau$, and J_τ be defined as in Equation (5.9). Then the directional derivative of the discretized cost J_τ in the ξ' direction is:*

$$DJ_\tau(\xi; \xi') = \frac{\partial h_0}{\partial x}(\phi_{\tau,1}(\xi)) D\phi_{\tau,1}(\xi; \xi'). \quad (6.42)$$

Proof. The result follows using the Chain Rule and Lemma 36. \square

Corollary 19. *There exists a constant $L > 0$ such that for each $N \in \mathbb{N}$, $\tau \in \mathcal{T}_N$, $\xi_1, \xi_2 \in \mathcal{X}_{\tau,r}$, and $\xi' \in \mathcal{X}_\tau$:*

$$|DJ_\tau(\xi_1; \xi') - DJ_\tau(\xi_2; \xi')| \leq L \|\xi_1 - \xi_2\|_{\mathcal{X}} \|\eta\|_{\mathcal{X}}, \quad (6.43)$$

where DJ_τ is as defined in Equation (6.42).

Proof. Notice by the Triangle Inequality and the Cauchy Schwartz Inequality:

$$\begin{aligned} |DJ_\tau(\xi_1; \xi') - DJ_\tau(\xi_2; \xi')| &\leq \left\| \frac{\partial h_0}{\partial x}(\phi_{\tau,1}(\xi_1)) \right\|_2 \|\mathbf{D}\phi_{\tau,1}(\xi_1; \eta) - \mathbf{D}\phi_{\tau,1}(\xi_2; \eta)\|_2 + \\ &\quad + \left\| \frac{\partial h_0}{\partial x}(\phi_{\tau,1}(\xi_1)) - \frac{\partial h_0}{\partial x}(\phi_{\tau,1}(\xi_2)) \right\|_2 \|\mathbf{D}\phi_{\tau,1}(\xi_2; \eta)\|_2. \end{aligned} \quad (6.44)$$

The result then follows by applying Condition 2 in Corollary 13, Condition 2 in Corollary 15, Corollary 18, and Lemma 38. \square

In fact, the discretized cost function converges to the original cost function as the discretization is increased:

Lemma 41. *There exists a constant $B > 0$ such that for each $N \in \mathbb{N}$, $\tau \in \mathcal{T}_N$, $\xi \in \mathcal{X}_{\tau,r}$, and $\xi' \in \mathcal{X}_\tau$:*

$$|DJ_\tau(\xi; \xi') - DJ(\xi; \xi')| \leq \frac{B}{2^N}, \quad (6.45)$$

where DJ is as defined in Equation (4.30) and DJ_τ is as defined in Equation (6.42).

Proof. Notice by the Triangle Inequality and the Cauchy Schwartz Inequality:

$$\begin{aligned} |DJ_\tau(\xi; \xi') - DJ(\xi; \xi')| &\leq \left\| \frac{\partial h_0}{\partial x}(\phi_1(\xi)) \right\|_2 \|\mathbb{D}\phi_1(\xi; \xi') - \mathbb{D}\phi_{\tau,1}(\xi; \xi')\|_2 + \\ &\quad + \left\| \frac{\partial h_0}{\partial x}(\phi_1(\xi)) - \frac{\partial h_0}{\partial x}(\phi_{\tau,1}(\xi)) \right\|_2 \|\mathbb{D}\phi_{\tau,1}(\xi; \xi')\|_2. \end{aligned} \quad (6.46)$$

Then the result follows by applying Condition 2 in Assumption 2, Condition 2 in Corollary 1, Lemma 33, Lemma 39, and Corollary 18. \square

Next, we construct the expression for the directional derivative of the discretized component functions and prove that they are Lipschitz continuous.

Lemma 42. *Let $N \in \mathbb{N}$, $\tau \in \mathcal{T}_N$, $\xi \in \mathcal{X}_{\tau,r}$, $\xi' \in \mathcal{X}_\tau$, $j \in \mathcal{J}$, and ψ_{τ,j,τ_k} be defined as in Equation (5.12). Then the directional derivative of each of the discretized component constraints ψ_{τ,j,τ_k} for each $k \in \{0, \dots, |\tau|\}$ in the ξ' direction is:*

$$D\psi_{\tau,j,\tau_k}(\xi; \xi') = \frac{\partial h_j}{\partial x}(\phi_{\tau,\tau_k}(\xi)) D\phi_{\tau,\tau_k}(\xi; \xi'). \quad (6.47)$$

Proof. The result is a direct consequence of the Chain Rule and Lemma 36. \square

Corollary 20. *There exists a constant $L > 0$ such that for each $N \in \mathbb{N}$, $\tau \in \mathcal{T}_N$, $\xi_1, \xi_2 \in \mathcal{X}_{\tau,r}$, $\xi' \in \mathcal{X}_\tau$, and $k \in \{0, \dots, |\tau|\}$:*

$$|D\psi_{\tau,j,\tau_k}(\xi_1; \xi') - D\psi_{\tau,j,\tau_k}(\xi_2; \xi')| \leq L \|\xi_1 - \xi_2\|_{\mathcal{X}} \|\xi'\|_{\mathcal{X}}, \quad (6.48)$$

where $D\psi_{\tau,j,\tau_k}$ is as defined in Equation (6.47).

Proof. Notice by the Triangle Inequality and the Cauchy Schwartz Inequality:

$$\begin{aligned} |D\psi_{\tau,j,\tau_k}(\xi_1; \xi') - D\psi_{\tau,j,\tau_k}(\xi_2; \xi')| &\leq \left\| \frac{\partial h_j}{\partial x}(\phi_{\tau,\tau_k}(\xi_1)) \right\|_2 \|\mathbb{D}\phi_{\tau,\tau_k}(\xi_1; \xi') - \mathbb{D}\phi_{\tau,\tau_k}(\xi_2; \xi')\|_2 + \\ &\quad + \left\| \frac{\partial h_j}{\partial x}(\phi_{\tau,\tau_k}(\xi_1)) - \frac{\partial h_j}{\partial x}(\phi_{\tau,\tau_k}(\xi_2)) \right\|_2 \|\mathbb{D}\phi_{\tau,\tau_k}(\xi_2; \xi')\|_2. \end{aligned} \quad (6.49)$$

The result then follows by applying Condition 3 in Corollary 13, Condition 4 in Corollary 15, Corollary 18, and Lemma 38. \square

In fact, the discretized component constraint functions converge to the original component constraint function as the discretization is increased:

Lemma 43. *There exists a constant $B > 0$ such that for each $N \in \mathbb{N}$, $\tau \in \mathcal{T}_N$, $\xi \in \mathcal{X}_{\tau,r}$, $\xi' \in \mathcal{X}_\tau$, $j \in \mathcal{J}$, and $k \in \{0, \dots, |\tau|\}$:*

$$|D\psi_{\tau,j,\tau_k}(\xi; \xi') - D\psi_{j,\tau_k}(\xi; \xi')| \leq \frac{B}{2^N}, \quad (6.50)$$

where $D\psi_{j,\tau_k}$ is as defined in Equation (4.33) and $D\psi_{\tau,j,\tau_k}$ is as defined in Equation (6.47).

Proof. Notice by the Triangle Inequality and the Cauchy Schwartz Inequality:

$$\begin{aligned} |\mathrm{D}\psi_{\tau,j,\tau_k}(\xi; \xi') - \mathrm{D}\psi_{j,\tau_k}(\xi; \xi')| &\leq \left\| \frac{\partial h_j}{\partial x}(\phi_{\tau_k}(\xi)) \right\|_2 \|\mathrm{D}\phi_{\tau_k}(\xi; \xi') - \mathrm{D}\phi_{\tau,\tau_k}(\xi; \xi')\|_2 + \\ &\quad + \left\| \frac{\partial h_j}{\partial x}(\phi_{\tau_k}(\xi)) - \frac{\partial h_j}{\partial x}(\phi_{\tau,\tau_k}(\xi)) \right\|_2 \|\mathrm{D}\phi_{\tau,\tau_k}(\xi; \xi')\|_2. \end{aligned} \quad (6.51)$$

The result follows by applying Condition 4 in Assumption 2, Condition 3 in Corollary 1, Lemma 33, Lemma 39, and Corollary 18. \square

Given these results, we can begin describing the properties satisfied by the discretized optimality function:

Lemma 44. *Let $N \in \mathbb{N}$, $\tau \in \mathcal{T}_N$, and ζ_τ be defined as in Equation (5.16). Then there exists a constant $L > 0$ such that, for each $\xi_1, \xi_2, \xi' \in \mathcal{X}_{\tau,r}$,*

$$|\zeta_\tau(\xi_1, \xi') - \zeta_\tau(\xi_2, \xi')| \leq L \|\xi_1 - \xi_2\|_{\mathcal{X}}. \quad (6.52)$$

Proof. Letting $\Psi_\tau^+(\xi) = \max\{0, \Psi_\tau(\xi)\}$ and $\Psi_\tau^-(\xi) = \max\{0, -\Psi_\tau(\xi)\}$, observe:

$$\zeta_\tau(\xi, \xi') = \max\left\{ \mathrm{D}J_\tau(\xi; \xi' - \xi) - \Psi_\tau^+(\xi), \max_{j \in \mathcal{J}, k \in \{0, \dots, |\tau|\}} \mathrm{D}\psi_{\tau,j,\tau_k}(\xi; \xi' - \xi) - \gamma \Psi_\tau^-(\xi) \right\} + \|\xi' - \xi\|_{\mathcal{X}}. \quad (6.53)$$

Employing Equation (4.38):

$$\begin{aligned} |\zeta_\tau(\xi_1, \xi') - \zeta_\tau(\xi_2, \xi')| &\leq \max\left\{ \left| \mathrm{D}J_\tau(\xi_1; \xi' - \xi_1) - \mathrm{D}J_\tau(\xi_2; \xi' - \xi_2) \right| + \left| \Psi_\tau^+(\xi_2) - \Psi_\tau^+(\xi_1) \right|, \right. \\ &\quad \left. \max_{j \in \mathcal{J}, k \in \{0, \dots, |\tau|\}} \left| \mathrm{D}\psi_{\tau,j,\tau_k}(\xi_1; \xi' - \xi_1) - \mathrm{D}\psi_{\tau,j,\tau_k}(\xi_2; \xi' - \xi_2) \right| + \gamma \left| \Psi_\tau^-(\xi_2) - \Psi_\tau^-(\xi_1) \right| \right\} + \\ &\quad + \left| \|\xi' - \xi_1\|_{\mathcal{X}} - \|\xi' - \xi_2\|_{\mathcal{X}} \right|. \end{aligned} \quad (6.54)$$

We show three results that taken together with the Triangle Inequality prove the desired result. First, by applying the Reverse Triangle Inequality:

$$\left| \|\xi' - \xi_1\|_{\mathcal{X}} - \|\xi' - \xi_2\|_{\mathcal{X}} \right| \leq \|\xi_1 - \xi_2\|_{\mathcal{X}}. \quad (6.55)$$

Second,

$$\begin{aligned} \left| \mathrm{D}J_\tau(\xi_1; \xi' - \xi_1) - \mathrm{D}J_\tau(\xi_2; \xi' - \xi_2) \right| &= \left| \mathrm{D}J_\tau(\xi_1; \xi' - \xi_1) - \mathrm{D}J_\tau(\xi_2; \xi' - \xi_1) + \mathrm{D}J_\tau(\xi_2; \xi_2 - \xi_1) \right| \\ &\leq \left| \mathrm{D}J_\tau(\xi_1; \xi') - \mathrm{D}J_\tau(\xi_2; \xi') \right| + \\ &\quad + \left| \mathrm{D}J_\tau(\xi_1; \xi_1) - \mathrm{D}J_\tau(\xi_2; \xi_1) \right| + \\ &\quad + \left| \frac{\partial h_0}{\partial x}(\phi_{\tau,1}(\xi_2)) \mathrm{D}\phi_{\tau,1}(\xi_2; \xi_2 - \xi_1) \right| \\ &\leq L \|\xi_1 - \xi_2\|_{\mathcal{X}}, \end{aligned} \quad (6.56)$$

where $L > 0$ and we employed the linearity of DJ_τ , Corollary 19, the fact that ξ' and ξ_1 are bounded since $\xi', \xi_1 \in \mathcal{X}_{\tau,r}$, the Cauchy-Schwartz Inequality, Condition 2 in Corollary 13, and Corollary 18. Notice that by employing an argument identical to Equation (6.56) and Corollary 20, we can assume without loss of generality that $|D\psi_{\tau,j,\tau_k}(\xi_1; \xi' - \xi_1) - D\psi_{\tau,j,\tau_k}(\xi_2; \xi' - \xi_2)| \leq L \|\xi_1 - \xi_2\|_{\mathcal{X}}$. Finally, notice that by applying Lemma 32, $\Psi_\tau^+(\xi)$ and $\Psi_\tau^-(\xi)$ are Lipschitz continuous. \square

Employing these results, we can prove that $\zeta_\tau(\xi; \xi')$ converges to $\zeta(\xi; \xi')$ as the discretization is increased:

Lemma 45. *There exists a constant $B > 0$ such that for each $N \in \mathbb{N}$, $\tau \in \mathcal{T}_N$, and $\xi, \xi' \in \mathcal{X}_{\tau,r}$:*

$$|\zeta_\tau(\xi, \xi') - \zeta(\xi, \xi')| \leq \frac{B}{2^N}, \quad (6.57)$$

where ζ is as defined in Equation (3.9) and ζ_τ is as defined in Equation (5.17).

Proof. Let $\Psi^+(\xi) = \max\{0, \Psi(\xi)\}$, $\Psi_\tau^+(\xi) = \max\{0, \Psi_\tau(\xi)\}$, $\Psi^-(\xi) = \max\{0, -\Psi(\xi)\}$, and $\Psi_\tau^-(\xi) = \max\{0, -\Psi_\tau(\xi)\}$. Notice that we can then write:

$$\zeta(\xi, \xi') = \max \left\{ DJ(\xi; \xi' - \xi) - \Psi^+(\xi), \max_{j \in \mathcal{J}, t \in [0,1]} D\psi_{j,t}(\xi; \xi' - \xi) - \gamma \Psi^-(\xi) \right\} + \|\xi' - \xi\|_{\mathcal{X}}, \quad (6.58)$$

and similarly for $\zeta_\tau(\xi, \xi')$. Employing this redefinition, notice first that by employing an argument identical to the one used in the proof of Lemma 35 we can show that there exists a $K > 0$ such that for any positive integer N , $\tau \in \mathcal{T}_N$ and $\xi \in \mathcal{X}_{\tau,r}$:

$$|\Psi_\tau^+(\xi) - \Psi^+(\xi)| \leq \frac{K}{2^N}, \quad \text{and} \quad |\Psi_\tau^-(\xi) - \Psi^-(\xi)| \leq \frac{K}{2^N}. \quad (6.59)$$

Let $\kappa(t) \in \{0, \dots, |\tau|\}$ such that $t \in [\tau_{\kappa(t)}, \tau_{\kappa(t)+1}]$ for each $t \in [0, 1]$. Then there exists $K' > 0$ such that,

$$\begin{aligned} \left| D\psi_{j,t}(\xi; \xi' - \xi) - D\psi_{j,\tau_{\kappa(t)}}(\xi; \xi' - \xi) \right| &\leq \left\| \frac{\partial h_j}{\partial x}(\phi_t(\xi)) - \frac{\partial h_j}{\partial x}(\phi_{\tau_{\kappa(t)}}(\xi)) \right\|_2 \|\mathbb{D}\phi_t(\xi; \xi' - \xi)\|_2 + \\ &\quad + \left\| \frac{\partial h_j}{\partial x}(\phi_{\tau_{\kappa(t)}}(\xi)) \right\|_2 \|\mathbb{D}\phi_t(\xi; \xi' - \xi) + \\ &\quad \quad \quad - \mathbb{D}\phi_{\tau_{\kappa(t)}}(\xi; \xi' - \xi)\|_2 \\ &\leq C' \left(\left\| \phi_t(\xi) - \phi_{\tau_{\kappa(t)}}(\xi) \right\|_2 + \right. \\ &\quad \left. + \left\| \mathbb{D}\phi_t(\xi; \xi' - \xi) - \mathbb{D}\phi_{\tau_{\kappa(t)}}(\xi; \xi' - \xi) \right\|_2 \right) \\ &\leq \frac{K'}{2^N}, \end{aligned} \quad (6.60)$$

where $C' > 0$ is a constant obtained after applying Corollary 8, Condition 4 in Assumption 2, and Condition 3 in Corollary 1, and the last inequality follows after noting that both terms can be written as the integral of uniformly bounded functions over an interval of length smaller than 2^{-N} . Thus, by the Triangle Inequality, Lemma 43, and Equation (6.60), we know there exists $B > 0$ such that for each $t \in [0, 1]$:

$$\left| D\psi_{j,t}(\xi; \xi' - \xi) - D\psi_{\tau,j,\tau_{\kappa}(t)}(\xi; \xi' - \xi) \right| \leq \frac{B}{2^N}. \quad (6.61)$$

Moreover, if $t' \in \arg \max_{t \in [0,1]} D\psi_{j,t}(\xi; \xi' - \xi)$, then

$$\max_{t \in [0,1]} D\psi_{j,t}(\xi; \xi' - \xi) - \max_{k \in \{0, \dots, |\tau|\}} D\psi_{\tau,j,\tau_k}(\xi; \xi' - \xi) \leq D\psi_{j,t'}(\xi; \xi' - \xi) - D\psi_{\tau,j,\tau_{\kappa}(t')}(\xi; \xi' - \xi) \leq \frac{B}{2^N}. \quad (6.62)$$

Similarly if $k' \in \arg \max_{k \in \{0, \dots, |\tau|\}} D\psi_{\tau,j,\tau_k}(\xi; \xi' - \xi)$, then

$$\max_{k \in \{0, \dots, |\tau|\}} D\psi_{\tau,j,\tau_k}(\xi; \xi' - \xi) - \max_{t \in [0,1]} D\psi_{j,t}(\xi; \xi' - \xi) \leq D\psi_{\tau,j,\tau_{k'}}(\xi; \xi' - \xi) - D\psi_{j,\tau_{k'}}(\xi; \xi' - \xi) \leq \frac{B}{2^N}. \quad (6.63)$$

Therefore, by Equation (6.62),

$$\begin{aligned} & \max_{j \in \mathcal{J}, t \in [0,1]} D\psi_{j,t}(\xi; \xi' - \xi) - \max_{j \in \mathcal{J}, k \in \{0, \dots, |\tau|\}} D\psi_{\tau,j,\tau_k}(\xi; \xi' - \xi) \leq \\ & \leq \max_{j \in \mathcal{J}} \left(\max_{t \in [0,1]} D\psi_{j,t}(\xi; \xi' - \xi) - \max_{k \in \{0, \dots, |\tau|\}} D\psi_{\tau,j,\tau_k}(\xi; \xi' - \xi) \right) \leq \frac{B}{2^N}. \end{aligned} \quad (6.64)$$

and similarly, by Equation (6.63),

$$\begin{aligned} & \max_{j \in \mathcal{J}, k \in \{0, \dots, |\tau|\}} D\psi_{\tau,j,\tau_k}(\xi; \xi' - \xi) - \max_{j \in \mathcal{J}, t \in [0,1]} D\psi_{j,t}(\xi; \xi' - \xi) \leq \\ & \leq \max_{j \in \mathcal{J}} \left(\max_{k \in \{0, \dots, |\tau|\}} D\psi_{\tau,j,\tau_k}(\xi; \xi' - \xi) - \max_{t \in [0,1]} D\psi_{j,t}(\xi; \xi' - \xi) \right) \leq \frac{B}{2^N}, \end{aligned} \quad (6.65)$$

Employing these results and Equation (4.38), observe that:

$$\begin{aligned} |\zeta_{\tau}(\xi, \xi') - \zeta(\xi, \xi')| & \leq \max \left\{ |DJ_{\tau}(\xi; \xi' - \xi) - DJ(\xi; \xi' - \xi)| + |\Psi^+(\xi) - \Psi_{\tau}^+(\xi)|, \right. \\ & \left. \left| \max_{j \in \mathcal{J}, k \in \{0, \dots, |\tau|\}} D\psi_{\tau,j,\tau_k}(\xi; \xi' - \xi) - \max_{j \in \mathcal{J}, t \in [0,1]} D\psi_{j,t}(\xi; \xi' - \xi) \right| + \gamma |\Psi^-(\xi) - \Psi_{\tau}^-(\xi)| \right\}. \end{aligned} \quad (6.66)$$

Finally, applying Lemma 41 and the inequatlities above, we get our desired result. \square

ζ_{τ} is in fact strictly convex just like its infinite dimensional analogue, and its proof is similar to the proof of Lemma 14, hence we omit its details.

Lemma 46. *Let $N \in \mathbb{N}$, $\tau \in \mathcal{T}_N$, and $\xi \in \mathcal{X}_{\tau,p}$. Then the map $\xi' \mapsto \zeta_\tau(\xi, \xi')$, as defined in Equation (5.17), is strictly convex.*

Theorem 47 is very important since it proves that g_τ , as defined in Equation (5.16), is a well-defined function. Its proof is a consequence of the well-known result that strictly-convex functions in finite-dimensional spaces have unique minimizers.

Theorem 47. *Let $N \in \mathbb{N}$, $\tau \in \mathcal{T}_N$, and $\xi \in \mathcal{X}_{\tau,p}$. Then the map $\xi' \mapsto \zeta_\tau(\xi, \xi')$, as defined in Equation (5.17), has a unique minimizer.*

Employing these results we can prove the continuity of the discretized optimality function. This result is not strictly required in order to prove the convergence of Algorithm 2 or in order to prove that the discretized optimality function encodes local minimizers of the Discretized Relaxed Switched System Optimal Control Problem. However, this is a fundamental result from an implementation point of view, since in practice, a computer only produces approximate results, and continuity gives a guarantee that these approximations are at least valid in a neighborhood of the evaluation point.

Lemma 48. *Let $N \in \mathbb{N}$ and $\tau \in \mathcal{T}_N$, then the function θ_τ , as defined in Equation (5.16), is continuous.*

Proof. First, we show that θ_τ is upper semi-continuous. Consider a sequence $\{\xi_i\}_{i \in \mathbb{N}} \subset \mathcal{X}_{\tau,r}$ converging to $\xi \in \mathcal{X}_{\tau,r}$, and $\xi' \in \mathcal{X}_{\tau,r}$, such that $\theta_\tau(\xi) = \zeta_\tau(\xi, \xi')$, i.e. $\xi' = g_\tau(\xi)$, where g is defined as in Equation (5.16). Since $\theta_\tau(\xi_i) \leq \zeta_\tau(\xi_i, \xi')$ for all $i \in \mathbb{N}$,

$$\limsup_{i \rightarrow \infty} \theta_\tau(\xi_i) \leq \limsup_{i \rightarrow \infty} \zeta_\tau(\xi_i, \xi') = \zeta_\tau(\xi, \xi') = \theta_\tau(\xi), \quad (6.67)$$

which proves the upper semi-continuity of θ_τ .

Second, we show that θ_τ is lower semi-continuous. Let $\{\xi'_i\}_{i \in \mathbb{N}} \subset \mathcal{X}_{\tau,r}$ such that $\theta_\tau(\xi_i) = \zeta_\tau(\xi_i, \xi'_i)$, i.e. $\xi'_i = g_\tau(\xi_i)$. From Lemma 44, we know there exists a Lipschitz constant $L > 0$ such that for each $i \in \mathbb{N}$, $|\zeta_\tau(\xi, \xi'_i) - \zeta_\tau(\xi_i, \xi'_i)| \leq L \|\xi - \xi_i\|_{\mathcal{X}}$. Consequently,

$$\theta_\tau(\xi) \leq (\zeta_\tau(\xi, \xi'_i) - \zeta_\tau(\xi_i, \xi'_i)) + \zeta_\tau(\xi_i, \xi'_i) \leq L \|\xi - \xi_i\|_{\mathcal{X}} + \theta_\tau(\xi_i). \quad (6.68)$$

Taking limits we conclude that

$$\theta_\tau(\xi) \leq \liminf_{i \rightarrow \infty} \theta_\tau(\xi_i), \quad (6.69)$$

which proves the lower semi-continuity of θ_τ , and our desired result. \square

Next, we prove that the local minimizers of the Discretized Relaxed Switched System Optimal Control Problem are in fact zeros of the discretized optimality function.

Theorem 49. *Let $N \in \mathbb{N}$, $\tau \in \mathcal{T}_N$, and θ_τ be defined as in Equation (5.16), then:*

- (1) θ_τ is non-positive valued, and

- (2) If $\xi \in \mathcal{X}_{\tau,p}$ is a local minimizer of the Discretized Relaxed Switched System Optimal Control Problem as in Definition 8, then $\theta_\tau(\xi) = 0$.

Proof. Notice $\zeta_\tau(\xi, \xi) = 0$, therefore $\theta_\tau(\xi) = \min_{\xi' \in \mathcal{X}_{\tau,r}} \zeta_\tau(\xi, \xi') \leq \zeta_\tau(\xi, \xi) = 0$. This proves Condition 1.

To prove Condition 2, we begin by making several observations. Given $\xi' \in \mathcal{X}_{\tau,r}$ and $\lambda \in [0, 1]$, using the Mean Value Theorem and Corollary 19 we have that there exists $s \in (0, 1)$ and $L > 0$ such that

$$\begin{aligned} J_\tau(\xi + \lambda(\xi' - \xi)) - J_\tau(\xi) &= DJ_\tau(\xi + s\lambda(\xi' - \xi); \lambda(\xi' - \xi)) \\ &\leq \lambda DJ_\tau(\xi; \xi' - \xi) + L\lambda^2 \|\xi' - \xi\|_{\mathcal{X}}^2. \end{aligned} \quad (6.70)$$

Letting $\mathcal{A}_\tau(\xi) = \{(j, k) \in \mathcal{J} \times \{0, \dots, |\tau|\} \mid \Psi_\tau(\xi) = h_j(z^{(\xi)}(\tau_k))\}$, similar to the equation above, there exists a pair $(j, k) \in \mathcal{A}(\xi + \lambda(\xi' - \xi))$ and $s \in (0, 1)$ such that, using Corollary 20,

$$\begin{aligned} \Psi_\tau(\xi + \lambda(\xi' - \xi)) - \Psi_\tau(\xi) &\leq \psi_{\tau,j,\tau_k}(\xi + \lambda(\xi' - \xi)) - \Psi(\xi) \\ &\leq \psi_{\tau,j,\tau_k}(\xi + \lambda(\xi' - \xi)) - \psi_{\tau,j,\tau_k}(\xi) \\ &= D\psi_{\tau,j,\tau_k}(\xi + s\lambda(\xi' - \xi); \lambda(\xi' - \xi)) \\ &\leq \lambda D\psi_{\tau,j,\tau_k}(\xi; \xi' - \xi) + L\lambda^2 \|\xi' - \xi\|_{\mathcal{X}}^2. \end{aligned} \quad (6.71)$$

We prove Condition 2 by contradiction. That is we assume $\xi \in \mathcal{X}_{\tau,p}$ is a local minimizer of the Discretized Relaxed Switched System Optimal Control Problem and $\theta_\tau(\xi) < 0$ and show that for each $\varepsilon > 0$ there exists $\hat{\xi} \in \{\bar{\xi} \in \mathcal{X}_{\tau,r} \mid \Psi_\tau(\bar{\xi}) \leq 0\} \cap \mathcal{N}_{\tau,\mathcal{X}}(\xi, \varepsilon)$ such that $J_\tau(\hat{\xi}) < J_\tau(\xi)$, where $\mathcal{N}_{\tau,\mathcal{X}}(\xi, \varepsilon)$ is as defined in Equation (5.15), hence arriving at a contradiction.

Before arriving at this contradiction, we make two more observations. First, notice that since $\xi \in \mathcal{X}_p$ is a local minimizer of the Discretized Relaxed Switched System Optimal Control Problem, $\Psi_\tau(\xi) \leq 0$. Second, consider g_τ as defined in Equation (5.16), which exists by Theorem 47 and notice that since $\theta_\tau(\xi) < 0$, $g_\tau(\xi) \neq \xi$.

Next, observe that:

$$\begin{aligned} \theta_\tau(\xi) &= \max\{DJ_\tau(\xi; g_\tau(\xi) - \xi), \\ &\quad \max_{(j,k) \in \mathcal{J} \times \{0, \dots, |\tau|\}} D\psi_{\tau,j,\tau_k}(\xi; g_\tau(\xi) - \xi) + \gamma\Psi_\tau(\xi)\} + \|g_\tau(\xi) - \xi\|_{\mathcal{X}} < 0. \end{aligned} \quad (6.72)$$

For each $\lambda > 0$ by using Equations (6.70) and (6.72) we have:

$$J_\tau(\xi + \lambda(g_\tau(\xi) - \xi)) - J_\tau(\xi) \leq \theta_\tau(\xi)\lambda + 4A^2L\lambda^2, \quad (6.73)$$

where $A = \max\{\|u\|_2 + 1 \mid u \in U\}$ and we used the fact that $DJ_\tau(\xi; g_\tau(\xi) - \xi) \leq \theta_\tau(\xi)$. Hence for each $\lambda \in \left(0, \frac{-\theta_\tau(\xi)}{4A^2L}\right)$:

$$J_\tau(\xi + \lambda(g_\tau(\xi) - \xi)) - J_\tau(\xi) < 0. \quad (6.74)$$

Similarly, for each $\lambda > 0$ by using Equations (6.71) and (6.72) we have:

$$\Psi_\tau(\xi + \lambda(g_\tau(\xi) - \xi)) \leq \Psi_\tau(\xi) + (\theta_\tau(\xi) - \gamma\Psi_\tau(\xi))\lambda + 4A^2L\lambda^2, \quad (6.75)$$

where, as in Equation (6.73), $A = \max\{\|u\|_2 + 1 \mid u \in U\}$ and we used the fact that $D\psi_{\tau,j,\tau_k}(\xi; g(\xi) - \xi) \leq \theta_\tau(\xi)$. Hence for each $\lambda \in \left(0, \min\left\{\frac{-\theta_\tau(\xi)}{4A^2L}, \frac{1}{\gamma}\right\}\right)$:

$$\Psi_\tau(\xi + \lambda(g_\tau(\xi) - \xi)) \leq (1 - \gamma\lambda)\Psi_\tau(\xi) \leq 0. \quad (6.76)$$

Summarizing, suppose $\xi \in \mathcal{X}_{\tau,p}$ is a local minimizer of the Discretized Relaxed Switched System Optimal Control Problem and $\theta_\tau(\xi) < 0$. For each $\varepsilon > 0$, by choosing any

$$\lambda \in \left(0, \min\left\{\frac{-\theta_\tau(\xi)}{4A^2L}, \frac{1}{\gamma}, \frac{\varepsilon}{\|g_\tau(\xi) - \xi\|_{\mathcal{X}}}\right\}\right), \quad (6.77)$$

we can construct a new point $\hat{\xi} = (\xi + \lambda(g_\tau(\xi) - \xi)) \in \mathcal{X}_{\tau,r}$ such that $\hat{\xi} \in \mathcal{N}_{\tau,\mathcal{X}}(\xi, \varepsilon)$ by our choice of λ , $J_\tau(\hat{\xi}) < J_\tau(\xi)$ by Equation (6.74), and $\Psi_\tau(\hat{\xi}) \leq 0$ by Equation (6.76). Therefore, ξ is not a local minimizer of the Discretized Relaxed Switched System Optimal Control Problem, which is a contradiction and proves Condition 2. \square

Finally, we prove that the Discretized Relaxed Switched System Optimal Control Problem consistently approximates the Switched System Optimal Control Problem:

Theorem 50. *Let $\{\tau_i\}_{i \in \mathbb{N}}$ and $\{\xi_i\}_{i \in \mathbb{N}}$ such that $\tau_i \in \mathcal{T}_i$ and $\xi_i \in \mathcal{X}_{\tau_i,p}$ for each $i \in \mathbb{N}$. Then*

$$\lim_{i \rightarrow \infty} |\theta_{\tau_i}(\xi_i) - \theta(\xi_i)| = 0, \quad (6.78)$$

where θ is as defined in Equation (3.8) and θ_τ is as defined in Equation (5.16). That is, the Discretized Relaxed Switched System Optimal Control Problem as defined in Equation (5.14) is a consistent approximation of the Switched System Optimal Control Problem as defined in Equation (2.34), where consistent approximation is defined as in Definition 9.

Proof. First, by Lemma 45,

$$\limsup_{i \rightarrow \infty} \theta(\xi_i) - \theta_{\tau_i}(\xi_i) \leq \limsup_{i \rightarrow \infty} \zeta(\xi_i, g(\xi_i)) - \zeta_{\tau_i}(\xi_i, g_{\tau_i}(\xi_i)) \leq \limsup_{i \rightarrow \infty} \frac{B}{2^i} = 0, \quad (6.79)$$

where g is as defined in Equation (3.8) and g_τ is as defined in Equation (5.16).

Now, by Condition 2 in Lemma 28, we know there exists a sequence $\{\xi'_i\}_{i \in \mathbb{N}}$, with $\xi'_i \in \mathcal{X}_{\tau_i,r}$ for each $i \in \mathbb{N}$, such that $\lim_{i \rightarrow \infty} \xi'_i = g(\xi)$. Then, by Lemma 45,

$$\begin{aligned} \limsup_{i \rightarrow \infty} \theta_{\tau_i}(\xi_i) - \theta(\xi_i) &\leq \limsup_{i \rightarrow \infty} \zeta_{\tau_i}(\xi_i, \xi'_i) - \zeta(\xi_i, g(\xi)) \\ &\leq \limsup_{i \rightarrow \infty} (\zeta_{\tau_i}(\xi_i, \xi'_i) - \zeta(\xi_i, \xi'_i)) + (\zeta(\xi_i, \xi'_i) - \zeta(\xi_i, g(\xi))) \\ &\leq \limsup_{i \rightarrow \infty} \frac{B}{2^i} + \zeta(\xi_i, \xi'_i) - \zeta(\xi_i, g(\xi)). \end{aligned} \quad (6.80)$$

Employing Equation (4.38):

$$|\zeta(\xi_i, \xi'_i) - \zeta(\xi_i, g(\xi))| \leq \max \left\{ \left| \text{DJ}(\xi_i; \xi'_i - \xi_i) - \text{DJ}(\xi_i; g(\xi) - \xi_i) \right|, \right. \\ \left. \max_{j \in \mathcal{J}, t \in [0,1]} \left| \text{D}\psi_{j,t}(\xi_i; \xi'_i - \xi_i) - \text{D}\psi_{j,t}(\xi_i; g(\xi) - \xi_i) \right| \right\} + \left| \|\xi'_i - \xi_i\|_{\mathcal{X}} - \|g(\xi) - \xi_i\|_{\mathcal{X}} \right|. \quad (6.81)$$

Notice, that by applying the Reverse Triangle Inequality:

$$\left| \|\xi'_i - \xi_i\|_{\mathcal{X}} - \|g(\xi) - \xi_i\|_{\mathcal{X}} \right| \leq \|\xi'_i - g(\xi)\|_{\mathcal{X}}. \quad (6.82)$$

Next, notice:

$$\begin{aligned} \left| \text{DJ}(\xi_i; \xi'_i - \xi_i) - \text{DJ}(\xi_i; g(\xi) - \xi_i) \right| &= \left| \text{DJ}(\xi_i; \xi'_i - g(\xi)) \right| \\ &= \left| \frac{\partial h_0}{\partial x}(\phi_1(\xi_i)) \text{D}\phi_1(\xi_i; \xi'_i - g(\xi)) \right| \\ &\leq L \|\xi'_i - g(\xi)\|_{\mathcal{X}}, \end{aligned} \quad (6.83)$$

where $L > 0$ and we employed the linearity of DJ , Condition 2 in Corollary 1, and Corollary 8. Notice that by employing an argument identical to Equation (6.83), we can assume without loss of generality that $\left| \text{D}\psi_{j,t}(\xi_i; \xi'_i - \xi_i) - \text{D}\psi_{j,t}(\xi_i; g(\xi) - \xi_i) \right| \leq L \|\xi'_i - g(\xi)\|_{\mathcal{X}}$. Therefore:

$$\limsup_{i \rightarrow \infty} \left| \zeta(\xi_i, \xi'_i) - \zeta(\xi_i, g(\xi)) \right| \leq 0. \quad (6.84)$$

From Equation (6.80), we have $\limsup_{i \rightarrow \infty} (\theta_{\tau_i}(\xi_i) - \theta(\xi_i)) \leq 0$. Notice that

$$\limsup_{i \rightarrow \infty} |\theta_{\tau_i}(\xi_i) - \theta(\xi_i)| \geq \liminf_{i \rightarrow \infty} |\theta_{\tau_i}(\xi_i) - \theta(\xi_i)| \geq 0. \quad (6.85)$$

Therefore combining our results, we have $\lim_{i \rightarrow \infty} |\theta_{\tau_i}(\xi_i) - \theta(\xi_i)| = 0$. \square

6.3 Convergence of the Implementable Algorithm

In this subsection, we prove that the sequence of points generated by Algorithm 2 converges to a point that satisfies the optimality condition. We begin by proving that the Armijo algorithm as defined in Equation (5.21) terminates after a finite number of steps.

Lemma 51. *Let $\alpha \in (0, 1)$ and $\beta \in (0, 1)$. For every $\delta > 0$, there exists an $M_\delta^* < \infty$ such that if $\theta_\tau(\xi) \leq -\delta$ for $N \in \mathbb{N}$, $\tau \in \mathcal{T}_N$, and $\xi \in \mathcal{X}_{\tau,p}$, then $\mu_\tau(\xi) \leq M_\delta^*$, where θ_τ is as defined in Equation (5.16) and μ_τ is as defined in Equation (5.21).*

Proof. Given $\xi' \in \mathcal{X}$ and $\lambda \in [0, 1]$, using the Mean Value Theorem and Corollary 19 we have that there exists $s \in (0, 1)$ such that

$$\begin{aligned} J_\tau(\xi + \lambda(\xi' - \xi)) - J_\tau(\xi) &= \text{D}J_\tau(\xi + s\lambda(\xi' - \xi); \lambda(\xi' - \xi)) \\ &\leq \lambda \text{D}J_\tau(\xi; \xi' - \xi) + L\lambda^2 \|\xi' - \xi\|_{\mathcal{X}}^2. \end{aligned} \quad (6.86)$$

Letting $\mathcal{A}_\tau(\xi) = \{(j, i) \in \mathcal{J} \times \{0, \dots, |\tau|\} \mid \Psi_\tau(\xi) = \psi_{\tau, j, \tau_i}(\xi)\}$, then there exists a pair $(j, i) \in \mathcal{A}_\tau(\xi + \lambda(\xi' - \xi))$ and $s \in (0, 1)$ such that, using Corollary 11,

$$\begin{aligned} \Psi_\tau(\xi + \lambda(\xi' - \xi)) - \Psi_\tau(\xi) &\leq \psi_{\tau, j, \tau_i}(\xi + \lambda(\xi' - \xi)) - \Psi_\tau(\xi) \\ &\leq \psi_{\tau, j, \tau_i}(\xi + \lambda(\xi' - \xi)) - \psi_{\tau, j, \tau_i}(\xi) \\ &= \text{D}\psi_{\tau, j, \tau_i}(\xi + s\lambda(\xi' - \xi); \lambda(\xi' - \xi)) \\ &\leq \lambda \text{D}\psi_{\tau, j, \tau_i}(\xi; \xi' - \xi) + L\lambda^2 \|\xi' - \xi\|_{\mathcal{X}}^2. \end{aligned} \quad (6.87)$$

Now let us assume that $\Psi_\tau(\xi) \leq 0$, and consider g_τ as defined in Equation (5.16). Then

$$\theta_\tau(\xi) = \max \left\{ \text{D}J_\tau(\xi; g_\tau(\xi) - \xi), \max_{(j, i) \in \mathcal{J} \times \{0, \dots, |\tau|\}} \text{D}\psi_{\tau, j, \tau_i}(\xi; g_\tau(\xi) - \xi) + \gamma \Psi_\tau(\xi) \right\} \leq -\delta, \quad (6.88)$$

and using Equation (6.86),

$$J_\tau(\xi + \beta^k(g_\tau(\xi) - \xi)) - J_\tau(\xi) - \alpha\beta^k\theta_\tau(\xi) \leq -(1 - \alpha)\delta\beta^k + 4A^2L\beta^{2k}, \quad (6.89)$$

where $A = \max \{\|u\|_2 + 1 \mid u \in U\}$. Hence, for each $k \in \mathbb{N}$ such that $\beta^k \leq \frac{(1-\alpha)\delta}{4A^2L}$ we have that

$$J_\tau(\xi + \beta^k(g_\tau(\xi) - \xi)) - J_\tau(\xi) \leq \alpha\beta^k\theta_\tau(\xi). \quad (6.90)$$

Similarly, using Equations (6.87) and (6.88),

$$\Psi_\tau(\xi + \beta^k(g_\tau(\xi) - \xi)) - \Psi_\tau(\xi) + \beta^k(\gamma\Psi_\tau(\xi) - \alpha\theta_\tau(\xi)) \leq -\delta\beta^k + 4A^2L\beta^{2k}, \quad (6.91)$$

hence for each $k \in \mathbb{N}$ such that $\beta^k \leq \min \left\{ \frac{(1-\alpha)\delta}{4A^2L}, \frac{1}{\gamma} \right\}$ we have that

$$\Psi_\tau(\xi + \beta^k(g_\tau(\xi) - \xi)) - \alpha\beta^k\theta_\tau(\xi) \leq (1 - \beta^k\gamma) \Psi_\tau(\xi) \leq 0. \quad (6.92)$$

If $\Psi_\tau(\xi) > 0$ then

$$\max_{(j, i) \in \mathcal{J} \times \{0, \dots, |\tau|\}} \text{D}\psi_{\tau, j, \tau_i}(\xi; g_\tau(\xi) - \xi) \leq \theta_\tau(\xi) \leq -\delta, \quad (6.93)$$

thus, from Equation (6.87),

$$\Psi_\tau(\xi + \beta^k(g_\tau(\xi) - \xi)) - \Psi_\tau(\xi) - \alpha\beta^k\theta_\tau(\xi) \leq -(1 - \alpha)\delta\beta^k + 4A^2L\beta^{2k}. \quad (6.94)$$

Hence, for each $k \in \mathbb{N}$ such that $\beta^k \leq \frac{(1-\alpha)\delta}{4A^2L}$ we have that

$$\Psi_\tau(\xi + \beta^k(g_\tau(\xi) - \xi)) - \Psi_\tau(\xi) \leq \alpha\beta^k\theta_\tau(\xi). \quad (6.95)$$

Finally, let

$$M_\delta^* = 1 + \max \left\{ \log_\beta \left(\frac{(1-\alpha)\delta}{4A^2L} \right), \log_\beta \left(\frac{1}{\gamma} \right) \right\}, \quad (6.96)$$

then from Equations (6.90), (6.92), and (6.95), we get that $\mu_\tau(\xi) \leq M_\delta^*$ as desired. \square

The proof of the following corollary follows directly from the estimates of M_δ^* in the proof of Lemma 51.

Corollary 21. *Let $\alpha \in (0, 1)$ and $\beta \in (0, 1)$. There exists a $\delta_0 > 0$ and $C > 0$ such that if $\delta \in (0, \delta_0)$ and $\theta_\tau(\xi) \leq -\delta$ for $N \in \mathbb{N}$, $\tau \in \mathcal{T}_N$, and $\xi \in \mathcal{X}_{\tau,p}$, then $\mu_\tau(\xi) \leq 1 + \log_\beta(C\delta)$, where θ_τ is as defined in Equation (5.16) and μ_τ is as defined in Equation (5.21).*

Next, we prove a bound between the discretized trajectory for a point in the discretized relaxed optimization space and the discretized trajectory for the same point after projection by ρ_N that we use in a later argument.

Lemma 52. *Consider ρ_N defined as in Equation (3.14) and σ_N defined as in Equation (5.22). There exists $K > 0$ such that for each $N_0, N \in \mathbb{N}$, $\tau \in \mathcal{T}_{N_0}$, $\xi = (u, d) \in \mathcal{X}_{\tau,\tau}$, and $t \in [0, 1]$:*

$$\|\phi_{\sigma_N(\xi),t}(\rho_N(\xi)) - \phi_{\tau,t}(\xi)\|_2 \leq K \left(\left(\frac{1}{\sqrt{2}} \right)^N (\|\xi\|_{BV} + 1) + \left(\frac{1}{2} \right)^{N_0} \right), \quad (6.97)$$

where $\phi_{\tau,t}$ is as defined in Equation (5.11).

Proof. We prove this argument for $t = 1$, but the argument follows identically for all $t \in [0, 1]$. Using the triangular inequality we have that

$$\begin{aligned} \|\phi_{\sigma_N(\xi),1}(\rho_N(\xi)) - \phi_{\tau,1}(\xi)\|_2 &\leq \|\phi_{\sigma_N(\xi),1}(\rho_N(\xi)) - \phi_1(\rho_N(\xi))\|_2 + \|\phi_1(\rho_N(\xi)) - \phi_1(\xi)\|_2 + \\ &\quad + \|\phi_1(\xi) - \phi_{\tau,1}(\xi)\|_2. \end{aligned} \quad (6.98)$$

Thus, by Theorem 21 and Lemma 33 there exists K_1 , K_2 , and K_3 such that

$$\|\phi_{\sigma_N(\xi),1}(\rho_N(\xi)) - \phi_{\tau,1}(\xi)\|_2 \leq K_1 \left(\frac{1}{\sqrt{2}} \right)^N (\|\xi\|_{BV} + 1) + \frac{K_2}{2^N} + \frac{K_3}{2^{N_0}}, \quad (6.99)$$

hence the result follows after organizing the constants and noting that $2^{\frac{N}{2}} \leq 2^N$ for each $N \in \mathbb{N}$. \square

Using this previous lemma, we can prove that ν_τ is eventually finite for all ξ such that $\theta(\xi) < 0$.

Lemma 53. *Let $N_0 \in \mathbb{N}$, $\tau_0 \in \mathcal{T}_{N_0}$, and $\xi \in \mathcal{X}_{\tau,r}$. If $\theta(\xi) < 0$ then for each $\eta \in \mathbb{N}$ there exists a finite $N \geq N_0$ such that $\nu_{\sigma_N(\xi)}(\xi, N + \eta)$ is finite.*

Proof. Recall ν_τ , as defined in Equation (5.23), is infinity only when the optimization problem it solves is not feasible. To simplify our notation, let $\xi' \in \mathcal{X}_{\sigma_N(\xi),r}$ defined by

$\xi' = \xi + \beta^{\mu_{\sigma_N(\xi)}(\xi)}(g_{\sigma_N(\xi)}(\xi) - \xi)$. Then, using Lemma 52, for $k \in \mathbb{N}$, $k \in [N, N + \eta]$,

$$\begin{aligned} J_{\sigma_k(\xi')}(\rho_k(\xi')) - J_{\sigma_N(\xi)}(\xi') &\leq LK \left(\left(\frac{1}{\sqrt{2}} \right)^k (\|\xi'\|_{BV} + 1) + \left(\frac{1}{2} \right)^N \right) \\ &\leq LK \left(\frac{1}{\sqrt{2}} \right)^N (\|\xi'\|_{BV} + 2) \end{aligned} \quad (6.100)$$

Also, from Theorem 50 we know that for N large enough,

$$\frac{1}{2}\theta(\xi) \geq \theta_{\sigma_N(\xi)}(\xi). \quad (6.101)$$

Thus, given $\delta > \frac{1}{2}\theta(\xi)$, there exists $N^* \in \mathbb{N}$ such that, for each $N \geq N^*$ and $k \in [N, N + \eta]$,

$$\begin{aligned} J_{\sigma_k(\xi')}(\rho_k(\xi')) - J_{\sigma_N(\xi)}(\xi') &\leq -\bar{\alpha}\bar{\beta}^N \frac{1}{2}\theta(\xi) \\ &\leq -\bar{\alpha}\bar{\beta}^N \theta_{\sigma_N(\xi)}(\xi). \end{aligned} \quad (6.102)$$

and at the same time

$$\bar{\alpha}\bar{\beta}^N \leq (1 - \omega)\alpha\beta^{M_\delta^*} \leq (1 - \omega)\alpha\beta^{\mu_{\sigma_N(\xi)}(\xi)}, \quad (6.103)$$

where M_δ^* is as in Lemma 51.

Similarly, given $\mathcal{A}_\tau(\xi) = \{(j, t) \in \mathcal{J} \times [0, 1] \mid \Psi_\tau(\xi) = \psi_{\tau, j, t}(\xi)\}$, let $(j, t) \in \mathcal{A}_{\sigma_N(\xi')}(\xi')$. Thus, for $N \geq N^*$, $k \in [N, N + \eta]$, and using Lemma 52,

$$\begin{aligned} \Psi_{\sigma_k(\xi')}(\rho_k(\xi')) - \Psi_{\sigma_N(\xi)}(\xi') &= \psi_{\sigma_k(\xi'), j, t}(\rho_k(\xi')) - \Psi_{\sigma_N(\xi)}(\xi') \\ &\leq \psi_{\sigma_k(\xi'), j, t}(\rho_k(\xi')) - \psi_{\sigma_N(\xi), j, t}(\xi') \\ &\leq LK \left(\frac{1}{\sqrt{2}} \right)^N (\|\xi'\|_{BV} + 2) \\ &\leq -\bar{\alpha}\bar{\beta}^N \theta_{\sigma_N(\xi)}(\xi). \end{aligned} \quad (6.104)$$

Therefore, for $N \geq N^*$, if $\Psi_{\sigma_N(\xi)}(\xi) \leq 0$, then by Equations (6.102), (6.104), and the inequalities from the computation of $\mu_\tau(\xi)$,

$$J_{\sigma_k(\xi')}(\rho_k(\xi')) - J_{\sigma_N(\xi)}(\xi) \leq (\alpha\beta^{\mu_{\sigma_N(\xi)}(\xi)} - \bar{\alpha}\bar{\beta}^N)\theta_{\sigma_N(\xi)}(\xi), \quad (6.105)$$

$$\Psi_{\sigma_k(\xi')}(\rho_k(\xi')) \leq (\alpha\beta^{\mu_{\sigma_N(\xi)}(\xi)} - \bar{\alpha}\bar{\beta}^N)\theta_{\sigma_N(\xi)}(\xi) \leq 0, \quad (6.106)$$

which together with Equation (6.103) implies that the feasible set is not empty. Similarly, if $\Psi_{\sigma_N(\xi)}(\xi) > 0$, by Equation (6.104),

$$\Psi_{\sigma_k(\xi')}(\rho_k(\xi')) - \Psi_{\sigma_N(\xi)}(\xi) \leq (\alpha\beta^{\mu_{\sigma_N(\xi)}(\xi)} - \bar{\alpha}\bar{\beta}^N)\theta_{\sigma_N(\xi)}(\xi), \quad (6.107)$$

as desired.

Hence for all $N \geq N^*$ the feasible sets of the optimization problems associated with $\nu_{\sigma_N(\xi)}$ are not empty, and therefore $\nu_{\sigma_N(\xi)}(\xi, N + \eta) < \infty$. \square

In fact, the discretization precision constructed by Algorithm 2 increases arbitrarily.

Lemma 54. *Let $\{N_i\}_{i \in \mathbb{N}}$, $\{\tau_i\}_{i \in \mathbb{N}}$, and $\{\xi_i\}_{i \in \mathbb{N}}$ be the sequences generated by Algorithm 2. Then $N_i \rightarrow \infty$ as $i \rightarrow \infty$.*

Proof. Suppose that $N_i \leq N^*$ for all $i \in \mathbb{N}$. Then, by definition of Algorithm 2, there exists $i_0 \in \mathbb{N}$ such that $\theta(\xi_i) \leq -\Lambda 2^{-\chi N_i} \leq -\Lambda 2^{-\chi N^*}$ and $\xi_{i+1} = \Gamma_{\tau_i}(\xi_i)$ for each $i \geq i_0$, where Γ_τ is defined in Equation (5.24).

Moreover, by definition of ν_τ we have that if there exists $i_1 \geq i_0$ such that $\Psi_{\tau_{i_1}}(\xi_{i_1}) \leq 0$, then $\Psi_{\tau_i}(\xi_i) \leq 0$ for each $i \geq i_1$. Let us assume that there exists $i_1 \geq i_0$ such that $\Psi_{\tau_{i_1}}(\xi_{i_1}) \leq 0$, then, using Lemma 51,

$$\begin{aligned} J_{\tau_{i+1}}(\xi_{i+1}) - J_{\tau_i}(\xi_i) &\leq (\alpha \beta^{\mu_{\tau_i}(\xi_i)} - \bar{\alpha} \bar{\beta}^{\nu_{\tau_i}(\xi_i, N_i + \eta)}) \theta(\xi_i) \\ &\leq -\omega \alpha \beta^{M_{\delta'}^*} \delta', \end{aligned} \quad (6.108)$$

for each $i \geq i_1$, where $\delta' = \Lambda 2^{-\chi N^*}$. But this implies that $J_{\tau_i}(\xi_i) \rightarrow -\infty$ as $i \rightarrow \infty$, which is a contradiction since h_0 , and therefore J_{τ_i} , is lower bounded.

The argument is completely analogous in the case where the sequence is perpetually infeasible. Indeed, suppose that $\Psi_{\tau_i}(\xi_i) > 0$ for each $i \geq i_0$, then by Lemma 51,

$$\begin{aligned} \Psi_{\tau_{i+1}}(\xi_{i+1}) - \Psi_{\tau_i}(\xi_i) &\leq (\alpha \beta^{\mu_{\tau_i}(\xi_i)} - \bar{\alpha} \bar{\beta}^{\nu_{\tau_i}(\xi_i, N_i + \eta)}) \theta(\xi_i) \\ &\leq -\omega \alpha \beta^{M_{\delta'}^*} \delta', \end{aligned} \quad (6.109)$$

for each $i \geq i_0$, where $\delta' = \Lambda 2^{-\chi N^*}$. But again this implies that $\Psi_{\tau_i}(\xi_i) \rightarrow -\infty$ as $i \rightarrow \infty$, which is a contradiction since we had assumed that $\Psi_{\tau_i}(\xi_i) > 0$. \square

Next, we prove that if Algorithm 2 find a feasible point, then every point generated afterwards remains feasible.

Lemma 55. *Let $\{N_i\}_{i \in \mathbb{N}}$, $\{\tau_i\}_{i \in \mathbb{N}}$, and $\{\xi_i\}_{i \in \mathbb{N}}$ be the sequences generated by Algorithm 2. Then there exists $i_0 \in \mathbb{N}$ such that, if $\Psi_{\tau_{i_0}}(\xi_{i_0}) \leq 0$, then $\Psi(\xi_i) \leq 0$ and $\Psi_{\tau_i}(\xi_i) \leq 0$ for each $i \geq i_0$, where Ψ_τ is as defined in Equation (5.10).*

Proof. Let $\mathcal{I} \subset \mathbb{N}$ be a subsequence defined by

$$\mathcal{I} = \left\{ i \in \mathbb{N} \mid \theta_{\tau_i}(\xi_i) \leq -\frac{\Lambda}{2^{\chi N_i}} \text{ and } \nu_{\tau_i}(\xi_i, N_i + \eta) < \infty \right\}. \quad (6.110)$$

Note that, by definition of Algorithm 2, $\Psi(\xi_{i+1}) = \Psi(\xi_i)$ for each $i \notin \mathcal{I}$. Now, for each $i \in \mathcal{I}$ such that $\Psi_{\tau_i}(\xi_i) \leq 0$, by definition of ν_τ in Equation (5.23) together with Corollary 21,

$$\begin{aligned} \Psi_{\tau_{i+1}}(\xi_{i+1}) &\leq (\alpha \beta^{\mu_{\tau_i}(\xi_i)} - \bar{\alpha} \bar{\beta}^{\nu_{\tau_i}(\xi_i, N_i + \eta)}) \theta_{\tau_i}(\xi_i) \\ &\leq -\omega \alpha \beta^{\mu_{\tau_i}(\xi_i)} \frac{\Lambda}{2^{\chi N_i}} \\ &\leq -\omega \alpha \beta C \left(\frac{\Lambda}{2^{\chi N_i}} \right)^2, \end{aligned} \quad (6.111)$$

where $C > 0$. By Lemma 35 and the fact that $N_{i+1} \geq N_i$, we have that

$$\begin{aligned}\Psi(\xi_{i+1}) &\leq \frac{B}{2^{N_i}} - \omega\alpha\beta C \left(\frac{\Lambda}{2^{\chi N_i}} \right)^2 \\ &\leq \frac{1}{2^{2\chi N_i}} \left(\frac{B}{2^{(1-2\chi)N_i}} - \omega\alpha\beta C \Lambda^2 \right).\end{aligned}\tag{6.112}$$

Hence, if $\Psi_{\tau_{i_1}}(\xi_{i_1}) \leq 0$ for $i_1 \in \mathbb{N}$ such that N_{i_1} is large enough, then $\Psi(\xi_i) \leq 0$ for each $i \geq i_1$.

Moreover, from Equation (6.112) we get that for each $N \geq N_i$ and each $\tau \in \mathcal{T}_N$,

$$\begin{aligned}\Psi_\tau(\xi_{i+1}) &\leq \frac{1}{2^{2\chi N_i}} \left(\frac{B}{2^{(1-2\chi)N_i}} - \omega\alpha\beta C \Lambda^2 \right) + \frac{B}{2^N} \\ &\leq \frac{1}{2^{2\chi N_i}} \left(\frac{2B}{2^{(1-2\chi)N_i}} - \omega\alpha\beta C \Lambda^2 \right).\end{aligned}\tag{6.113}$$

Thus, if $\Psi_{\tau_{i_2}}(\xi_{i_2}) \leq 0$ for $i_2 \in \mathbb{N}$ such that N_{i_2} is large enough, then $\Psi_\tau(\xi_{i_2}) \leq 0$ for each $\tau \in \mathcal{T}_N$ such that $N \geq N_i$. But note that this is exactly the case when $i_2 + k \notin \mathcal{I}$ for $k \in \{1, \dots, n\}$, thus we can conclude that $\Psi_{\tau_{i_2+k}}(\xi_{i_2+k}) \leq 0$. Also note that the case of $i \in \mathcal{I}$ is trivially satisfied by the definition of ν_τ .

Finally, by setting $i_0 = \max\{i_1, i_2\}$ we get the desired result. \square

Next, we prove θ_τ converges to zero.

Lemma 56. *Let $\{N_i\}_{i \in \mathbb{N}}$, $\{\tau_i\}_{i \in \mathbb{N}}$, and $\{\xi_i\}_{i \in \mathbb{N}}$ be the sequences generated by Algorithm 2. Then $\theta_{\tau_i}(\xi_i) \rightarrow 0$ as $i \rightarrow \infty$, where θ_τ is as defined in Equation (5.16).*

Proof. Let us suppose that $\lim_{i \rightarrow \infty} \theta_{\tau_i}(\xi_i) \neq 0$. Then there exists $\delta > 0$ such that

$$\liminf_{i \rightarrow \infty} \theta_{\tau_i}(\xi_i) < -4\delta,\tag{6.114}$$

and hence, using Theorem 50 and Lemma 54, there exists an infinite subsequence $\mathcal{K} \subset \mathbb{N}$ defined by

$$\mathcal{K} = \{i \in \mathbb{N} \mid \theta_{\tau_i}(\xi_i) < -2\delta \text{ and } \theta(\xi_i) < -\delta\}.\tag{6.115}$$

Let us define a second subsequence $\mathcal{I} \subset \mathbb{N}$ by

$$\mathcal{I} = \left\{ i \in \mathbb{N} \mid \theta_{\tau_i}(\xi_i) \leq -\frac{\Lambda}{2^{\chi N_i}} \text{ and } \nu_{\tau_i}(\xi_i, N_i + \eta) < \infty \right\}.\tag{6.116}$$

Note that by the construction of the subsequence \mathcal{K} , together with Lemma 53, we get that $\mathcal{K} \cap \mathcal{I}$ is an infinite set.

Now we analyze Algorithm 2 by considering the behavior of each step as a function of its membership to each subsequence. First, for each $i \notin \mathcal{I}$, $\xi_{i+1} = \xi_i$, thus $J(\xi_{i+1}) = J(\xi_i)$ and $\Psi(\xi_{i+1}) = \Psi(\xi_i)$. Second, let $i \in \mathcal{I}$ such that $\Psi_{\tau_i}(\xi_i) \leq 0$, then

$$\begin{aligned} J_{\tau_{i+1}}(\xi_{i+1}) - J_{\tau_i}(\xi_i) &\leq (\alpha\beta^{\mu_{\tau_i}(\xi_i)} - \bar{\alpha}\bar{\beta}^{\nu_{\tau_i}(\xi_i, N_i + \eta)}) \theta_{\tau_i}(\xi_i) \\ &\leq -\omega\alpha\beta^{\mu_{\tau_i}(\xi_i)} \frac{\Lambda}{2^{\chi N_i}} \\ &\leq -\omega\alpha\beta C \left(\frac{\Lambda}{2^{\chi N_i}} \right)^2, \end{aligned} \quad (6.117)$$

where $C > 0$ and the last inequality follows from Corollary 21. Recall that $N_{i+1} \geq N_i$, thus using Lemmas 34 and 54 we have that

$$\begin{aligned} J(\xi_{i+1}) - J(\xi_i) &\leq \frac{2B}{2^{N_i}} - \omega\alpha\beta C \left(\frac{\Lambda}{2^{\chi N_i}} \right)^2 \\ &\leq \frac{1}{2^{2\chi N_i}} \left(\frac{2B}{2^{(1-2\chi)N_i}} - \omega\alpha\beta C \Lambda^2 \right), \end{aligned} \quad (6.118)$$

and since $\chi \in (0, \frac{1}{2})$, we get that for N_i large enough $J(\xi_{i+1}) \leq J(\xi_i)$. Similarly, if $\Psi_{\tau_i}(\xi_i) > 0$ then

$$\Psi(\xi_{i+1}) - \Psi(\xi_i) \leq \frac{1}{2^{2\chi N_i}} \left(\frac{2B}{2^{(1-2\chi)N_i}} - \omega\alpha\beta C \Lambda^2 \right), \quad (6.119)$$

thus for N_i large enough, $\Psi(\xi_{i+1}) \leq \Psi(\xi_i)$. Third, let $i \in \mathcal{K} \cap \mathcal{I}$ such that $\Psi_{\tau_i}(\xi_i) \leq 0$, then, by Lemma 51,

$$\begin{aligned} J_{\tau_{i+1}}(\xi_{i+1}) - J_{\tau_i}(\xi_i) &\leq (\alpha\beta^{\mu_{\tau_i}(\xi_i)} - \bar{\alpha}\bar{\beta}^{\nu_{\tau_i}(\xi_i, N_i + \eta)}) \theta_{\tau_i}(\xi_i) \\ &\leq -2\omega\alpha\beta^{M_{2\delta}^*} \delta, \end{aligned} \quad (6.120)$$

thus, by Lemmas 34 and 54, for N_i large enough,

$$J(\xi_{i+1}) - J(\xi_i) \leq -\omega\alpha\beta^{M_{2\delta}^*} \delta. \quad (6.121)$$

Similarly, if $\Psi_{\tau_i}(\xi_i) > 0$, using the same argument and Lemma 35, for N_i large enough,

$$\Psi(\xi_{i+1}) - \Psi(\xi_i) \leq -\omega\alpha\beta^{M_{2\delta}^*} \delta. \quad (6.122)$$

Now let us assume that there exists $i_0 \in \mathbb{N}$ such that N_{i_0} is large enough and $\Psi_{\tau_{i_0}}(\xi_{i_0}) \leq 0$. Then by Lemma 55 we get that $\Psi_{\tau_i}(\xi_i) \leq 0$ for each $i \geq i_0$. But as shown above, either $i \notin \mathcal{K} \cap \mathcal{I}$ and $J(\xi_{i+1}) \leq J(\xi_i)$ or $i \in \mathcal{K} \cap \mathcal{I}$ and Equation (6.121) is satisfied, and since $\mathcal{K} \cap \mathcal{I}$ is an infinite set we get that $J(\xi_i) \rightarrow -\infty$ as $i \rightarrow \infty$, which is a contradiction as J is lower bounded.

On the other hand, if we assume that $\Psi_{\tau_i}(\xi_i) > 0$ for each $i \in \mathbb{N}$, then either $i \notin \mathcal{K} \cap \mathcal{I}$ and $\Psi(\xi_{i+1}) \leq \Psi(\xi_i)$ or $i \in \mathcal{K} \cap \mathcal{I}$ and Equation (6.122) is satisfied, thus implying that $\Psi(\xi_i) \rightarrow -\infty$ as $i \rightarrow \infty$. But this is a contradiction since, by Lemma 35, this would imply that $\Psi_{\tau_i}(\xi_i) \rightarrow -\infty$ as $i \rightarrow \infty$.

Finally, both contradictions imply that $\theta_{\tau_i}(\xi_i) \rightarrow 0$ as $i \rightarrow \infty$ as desired. \square

In conclusion, we can prove that the sequence of points generated by Algorithm 2 converges to a point that is a zero of θ or a point that satisfies our optimality condition.

Theorem 57. *Let $\{N_i\}_{i \in \mathbb{N}}$, $\{\tau_i\}_{i \in \mathbb{N}}$, and $\{\xi_i\}_{i \in \mathbb{N}}$ be the sequences generated by Algorithm 2, then*

$$\lim_{i \rightarrow \infty} \theta(\xi_i) = 0, \quad (6.123)$$

where θ is as defined in Equation (3.8).

Proof. This result follows immediately from Lemma 56 after noticing that the Discretized Relaxed Switched System Optimal Control Problem is a consistent approximation of the Switched System Optimal Control Problem, as is proven in Theorem 50, and applying Theorem 29. \square

Part III

Results

Chapter 7

Examples

In this chapter, we apply Algorithm 2 to calculate an optimal control for 4 switched system examples. Before describing each example, we begin by describing the numerical implementation of Algorithm 2.

First, observe that the analysis presented thus far does not require that the initial and final times of the trajectory of switched system be fixed to 0 and 1, respectively. Instead, the initial and final times of the trajectory of the switched system are treated as fixed parameters t_0 and t_f , respectively. Second, we employ a MATLAB implementation of LSSOL from TOMLAB in order to compute the optimality function at each iteration of the algorithm since it is a quadratic program [38]. Third, for each example we employ a stopping criterion

Example	Mode 1	Mode 2	Mode 3
LQR	$\dot{x}(t) = Ax(t) + \begin{bmatrix} 0.9801 \\ -0.1987 \\ 0 \end{bmatrix} u(t)$	$\dot{x}(t) = Ax(t) + \begin{bmatrix} 0.1743 \\ 0.8601 \\ -0.4794 \end{bmatrix} u(t)$	$\dot{x}(t) = Ax(t) + \begin{bmatrix} 0.0952 \\ 0.4699 \\ 0.8776 \end{bmatrix} u(t)$
Tank	$\dot{x}(t) = \begin{bmatrix} 1 - \sqrt{x_1(t)} \\ \sqrt{x_1(t)} - \sqrt{x_2(t)} \end{bmatrix}$	$\dot{x}(t) = \begin{bmatrix} 2 - \sqrt{x_1(t)} \\ \sqrt{x_1(t)} - \sqrt{x_2(t)} \end{bmatrix}$	N/A
Quadrotor	$\ddot{x}(t) = \begin{bmatrix} \frac{\sin x_3(t)}{M} (u(t) + Mg) \\ \frac{\cos x_3(t)}{M} (u(t) + Mg) - g \\ 0 \end{bmatrix}$	$\ddot{x}(t) = \begin{bmatrix} g \sin x_3(t) \\ g \cos x_3(t) - g \\ \frac{-Lu(t)}{I} \end{bmatrix}$	$\ddot{x}(t) = \begin{bmatrix} g \sin x_3(t) \\ g \cos x_3(t) - g \\ \frac{Lu(t)}{I} \end{bmatrix}$
Needle	$\dot{x}(t) = \begin{bmatrix} \sin(x_5(t))u_1(t) \\ -\cos(x_5(t))\sin(x_4(t))u_1(t) \\ \cos(x_4(t))\cos(x_5(t))u_1(t) \\ \kappa \cos(x_6(t))\sec(x_5(t))u_1(t) \\ \kappa \sin(x_6(t))u_1(t) \\ -\kappa \cos(x_6(t))\tan(x_5(t))u_1(t) \end{bmatrix}$	$\dot{x}(t) = \begin{bmatrix} 0 \\ 0 \\ 0 \\ 0 \\ 0 \\ u_2(t) \end{bmatrix}$	N/A

Table 7.1: The dynamics of each of the modes of the switched system examples considered in Chapter 7. The parameters employed during the application of Algorithm 2 are defined explicitly in Chapter 7.

Example	$L(t, x(t), u(t), d(t))$	$\phi(x^{(\xi)}(t_f))$	t_0	t_f
LQR	$0.01 \cdot (u(t))^2$	$\left\ \begin{bmatrix} x_1(t_f) - 1 \\ x_2(t_f) - 1 \\ x_3(t_f) - 1 \end{bmatrix} \right\ _2^2$	0	2
Tank	$2 \cdot (x_2(t) - 3)^2$	0	0	10
Quadrotor	$5 \cdot (u(t))^2$	$\left\ \begin{bmatrix} \sqrt{5} \cdot (x_1(t_f) - 6) \\ \sqrt{5} \cdot (x_2(t_f) - 1) \\ \sin\left(\frac{x_3(t_f)}{2}\right) \end{bmatrix} \right\ _2^2$	0	7.5
Needle	$0.01 \cdot \left\ \begin{bmatrix} u_1(t) \\ u_2(t) \end{bmatrix} \right\ _2^2$	$\left\ \begin{bmatrix} x_1(t_f) + 2 \\ x_2(t_f) - 3.5 \\ x_3(t_f) - 10 \end{bmatrix} \right\ _2^2$	0	8

Table 7.2: The cost function used for each of the examples during the implementation of Algorithm 2.

that terminates Algorithm 2, if θ_τ gets sufficiently close to zero. Each of these stopping criteria is described when we describe each example.

Next, for the sake of comparison we compare the performance of Algorithm 2 on each of the examples to a traditional Mixed Integer Program (MIP). To perform this comparison,

Example	Initial Continuous Input, $\forall t \in [t_0, t_f]$	Initial Discrete Input, $\forall t \in [t_0, t_f]$
LQR	$u(t) = 0$	$d(t) = \begin{bmatrix} 1 \\ 0 \\ 0 \end{bmatrix}$
Tank	N/A	$d(t) = \begin{bmatrix} 1 \\ 0 \end{bmatrix}$
Quadrotor	$u(t) = 5 \times 10^{-4}$	$d(t) = \begin{bmatrix} 0.33 \\ 0.34 \\ 0.33 \end{bmatrix}$
Needle	$u(t) = \begin{bmatrix} 0 \\ 0 \end{bmatrix}$	$d(t) = \begin{bmatrix} 0.5 \\ 0.5 \end{bmatrix}$

Table 7.3: The initialization parameters used for each of the examples during the implementation of Algorithm 2 and the MIP described in [25].

Example	U	γ	α	β	$\bar{\alpha}$	$\bar{\beta}$	Λ	χ	ω
LQR	$u(t) \in [-20, 20]$	1	0.1	0.87	0.005	0.72	10^{-4}	$\frac{1}{4}$	10^{-6}
Tank	N/A	100	0.01	0.75	0.005	0.72	10^{-4}	$\frac{1}{4}$	10^{-6}
Quadrotor	$u(t) \in [0, 10^{-3}]$	10	0.01	0.80	5×10^{-4}	0.72	10^{-4}	$\frac{1}{4}$	10^{-6}
Needle	$u_1(t) \in [0, 5]$ $u_2(t) \in [-\frac{\pi}{2}, \frac{\pi}{2}]$	100	0.002	0.72	0.001	0.71	10^{-4}	$\frac{1}{4}$	0.05

Table 7.4: The algorithmic parameters used for each of the examples during the implementation of Algorithm 2.

Example	Algorithm 2 Computation Time	Algorithm 2 Final Cost	MIP Computation Time	MIP Final Cost
LQR	9.827[s]	1.23×10^{-3}	753.0[s]	1.89×10^{-3}
Tank	32.38[s]	4.829	119700[s]	4.828
Quadrotor	8.350[s]	0.128	2783[s]	0.165
Needle	62.76[s]	0.302	did not converge	did not converge

Table 7.5: The computation time and the result for each of the examples as a result of the application of Algorithm 2 and the MIP described in [25].

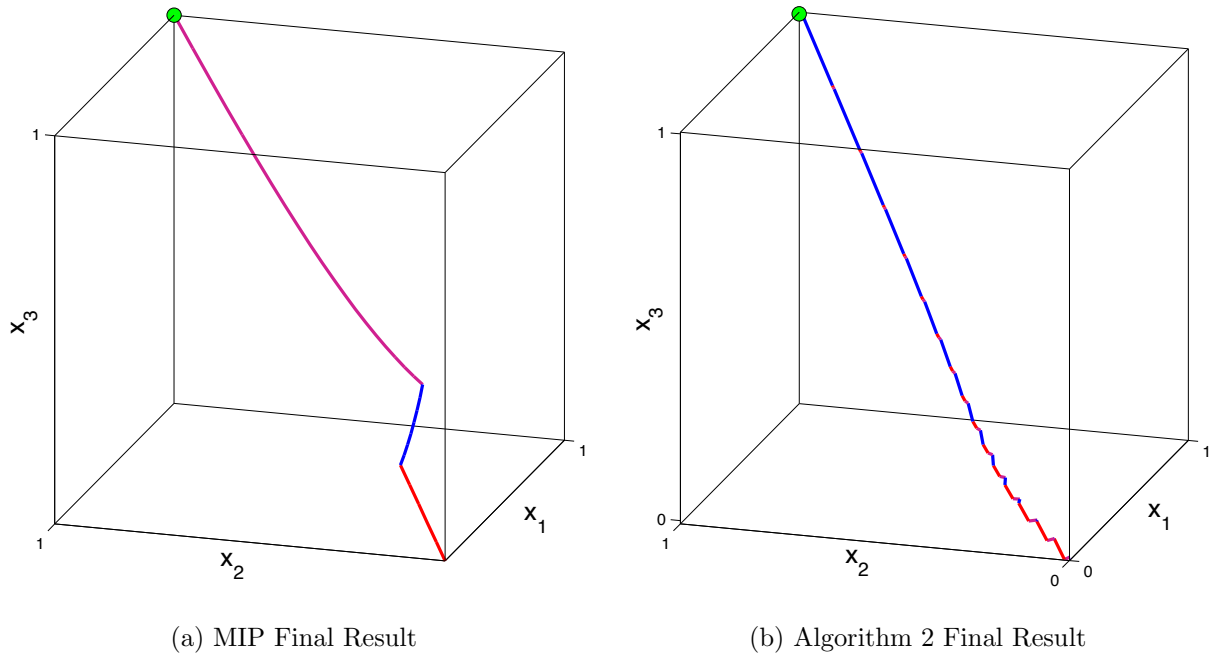


Figure 7.1: Optimal trajectories for each of the considered optimization algorithms where the point $(1, 1, 1)$ is drawn in green, and where the trajectory is drawn in blue when in mode 1, in purple when in mode 2, and in red when in mode 3.

we employ a TOMLAB implementation of a MIP described in [25] which mixes branch and bound steps with sequential quadratic programming steps. Finally, all of our comparisons are performed on an Intel Xeon, 6 core, 3.47 GHz, 100 GB RAM machine.

7.1 Constrained Switched Linear Quadratic Regulator (LQR)

Switched Linear Quadratic Regulator (LQR) examples have been used to illustrate the utility of a variety of proposed optimal control algorithms [23, 97]. We consider an LQR system in 3 dimensions, with 3 discrete modes, and a single continuous input. The dynamics in each mode are as described in Table 7.1 where:

$$A = \begin{bmatrix} 1.0979 & -0.0105 & 0.0167 \\ -0.0105 & 1.0481 & 0.0825 \\ 0.0167 & 0.0825 & 1.1540 \end{bmatrix}. \quad (7.1)$$

The system matrix is purposefully chosen to have 3 unstable eigenvalues and the control matrix in each mode is only able to control along single dimension. Hence, while the system

and control matrix in each mode is not a stabilizable pair, the system and all the control matrices taken together simultaneously is stabilizable and is expected to appropriately switch between the modes to reduce the cost. The objective of the optimization is to have the trajectory of the system at time t_f be at $(1, 1, 1)$ while minimizing the input required to achieve this task. This objective is reflected in the chosen cost function which is described in Table 7.2.

Algorithm 2 and the MIP are initialized at $x_0 = (0, 0, 0)$ with continuous and discrete inputs as described in Table 7.3 with 16 equally spaced samples in time. Algorithm 2 implemented with parameters as given in Table 7.4 took 11 iterations, ended with 48 time samples, and terminated after the optimality condition was bigger than -10^{-2} . The result of both optimization procedures is illustrated in Figure 7.1. The computation time and final cost of both algorithms can be found in Table 7.5. Notice that Algorithm 2 is able to compute a lower cost continuous and discrete input when compared to the MIP and is able to do it more than 75 times faster.

7.2 Double Tank System

To illustrate the performance of Algorithm 2 when there is no continuous input present, we consider a double-tank example. The 2 states of the system correspond to the fluid levels of an upper and lower tank. The output of the upper tank flows into the lower tank, the

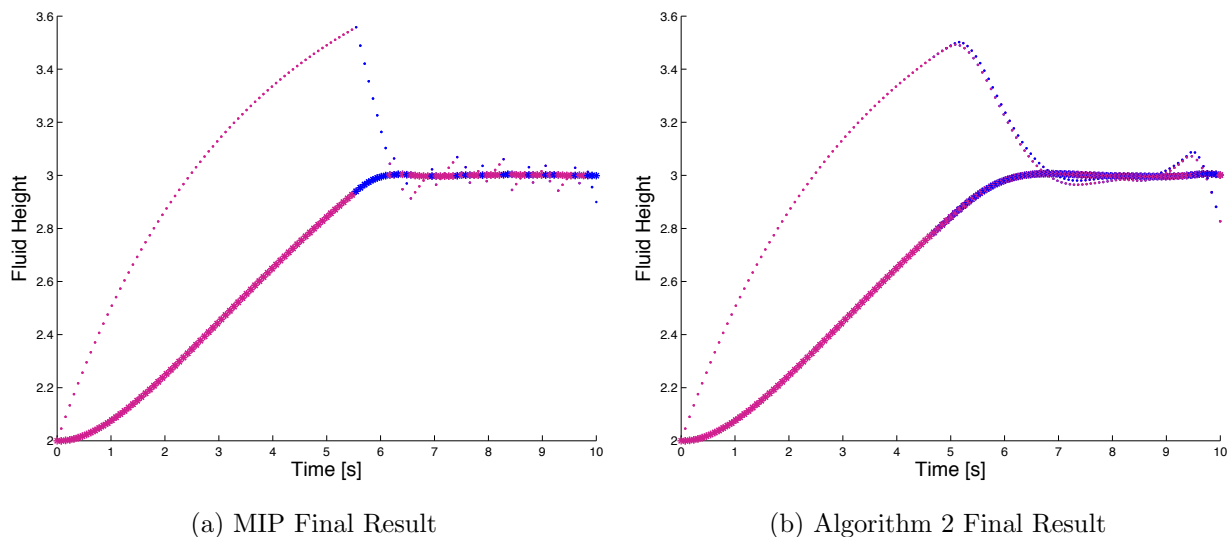


Figure 7.2: Optimal trajectories for each of the considered optimization algorithms where $x_1(t)$ is drawn using points and $x_2(t)$ is drawn using stars and where each state trajectory is drawn in blue when in mode 1 and in purple when in mode 2.

output of the lower tank exits the system, and the flow into the upper tank is restricted to either 1 or 2. The dynamics in each mode are then derived using Toricelli's Law and are described in Table 7.1. The objective of the optimization is to have the fluid level in the lower tank track 3 and this is reflected in the chosen cost function described in Table 7.2.

Algorithm 2 and the MIP are initialized at $x_0 = (2, 2)$ with a discrete input described in Table 7.3 with 128 equally spaced samples in time. Algorithm 2 implemented with parameters as given in Table 7.4 took 67 iterations, ended with 256 time samples, and terminated after the optimality condition was bigger than -10^{-2} . The result of both optimization procedures is illustrated in Figure 7.2. The computation time and final cost of both algorithms can be found in Table 7.5. Notice that Algorithm 2 is able to compute a comparable cost discrete input compared to the MIP and is able to do it nearly 3700 times faster.

7.3 Quadrotor Helicopter Control

Next, we consider the optimal control of a quadrotor helicopter in 2D using a model described in [29]. The evolution of the quadrotor can be defined with respect to a fixed 2D reference frame using six dimensions where the first 3 dimensions represent the position along a horizontal axis, the position along the vertical axis and the roll angle of the helicopter, respectively, and the last 3 dimensions represent the time derivative of the first 3 dimensions. We model the dynamics as a 3 mode switched system (the first mode describes the dynamics of going up, the second mode describes the dynamics of moving to the left, and the third mode describes the dynamics of moving to the right) with a single input as described in Table 7.1 where $L = 0.3050$ meters, $M = 1.3000$ kilograms, $I = 0.0605$ kilogram meters squared, and $g = 9.8000$ meters per second squared. The objective of the optimization is to have the trajectory of the system at time t_f be at position $(6, 1)$ with a zero roll angle while minimizing the input required to achieve this task. This objective is reflected in the chosen cost function which is described in Table 7.2. A state constraint is added to the optimization to ensure that the quadrotor remains above ground.

Algorithm 2 and the MIP are initialized at position $(0, 1)$ with a zero roll angle, with zero velocity, with continuous and discrete inputs as described in Table 7.3, and with 64 equally spaced samples in time. Algorithm 2 implemented with parameters as given in Table 7.4 took 31 iterations, ended with 192 time samples, and terminated after the optimality condition was bigger than -10^{-4} . The result of both optimization procedures is illustrated in Figure 7.3. The computation time and final cost of both algorithms can be found in Table 7.5. Notice that Algorithm 2 is able to compute a lower cost continuous and discrete input when compared to the MIP and is able to do it more than 333 times faster.

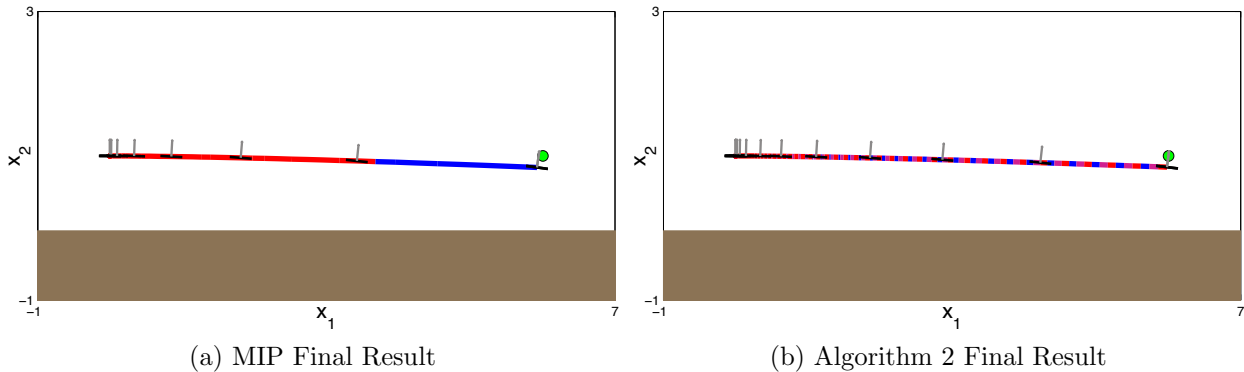


Figure 7.3: Optimal trajectories for each of the considered optimization algorithms where the point $(6, 1)$ is drawn in green, where the trajectory is drawn in blue when in mode 1, in purple when in mode 2, and in red when in mode 3, and where the quadrotor is drawn in black and the normal direction to the frame is drawn in gray.

7.4 Bevel-Tip Flexible Needle

Bevel-tip flexible needles are asymmetric needles that move along curved trajectories when a forward pushing force is applied. The 3D dynamics of such needles has been described in [42] and the path planning in the presence of obstacles has been heuristically considered in [19]. The evolution of the needle can be defined using six dimensions where the first 3 dimensions represent the position of the needle relative to the point of entry and the last 3 dimensions represent the yaw, pitch and roll of the needle relative to the plane, respectively.

As suggested by [19], the dynamics of the needle are naturally modeled as a 2 mode switched system as described in Table 7.1 (the first mode describes the dynamics of going forward while the second mode describes the dynamics of the needle turning) with 2 continuous inputs: u_1 representing the insertion speed and u_2 representing the rotation speed of the needle. κ is the curvature of the needle and is equal to $.22$ inverse centimeters. The objective of the optimization is to have the trajectory of the system at time t_f be at position $(-2, 3.5, 10)$ while minimizing the input required to achieve this task. This objective is reflected in the chosen cost function which is described in Table 7.2. A state constraint is added to the optimization to ensure that the needle remains outside of 3 spherical obstacles centered at $(0, 0, 5)$, $(1, 3, 7)$, and $(-2, 0, 10)$ all with radius 2.

Algorithm 2 and the MIP are initialized at position $(0, 0, 0)$ with continuous and discrete input described in Table 7.3 with 64 equally spaced samples in time. Algorithm 2 implemented with parameters as given in Table 7.4 took 103 iterations, ended with 64 time samples, and terminated after the optimality condition was bigger than -10^{-3} . The MIP was unable to find any solution. The computation time and final cost of both algorithms can be found in Table 7.5. The result of Algorithm 2 is illustrated in Figure 7.4.

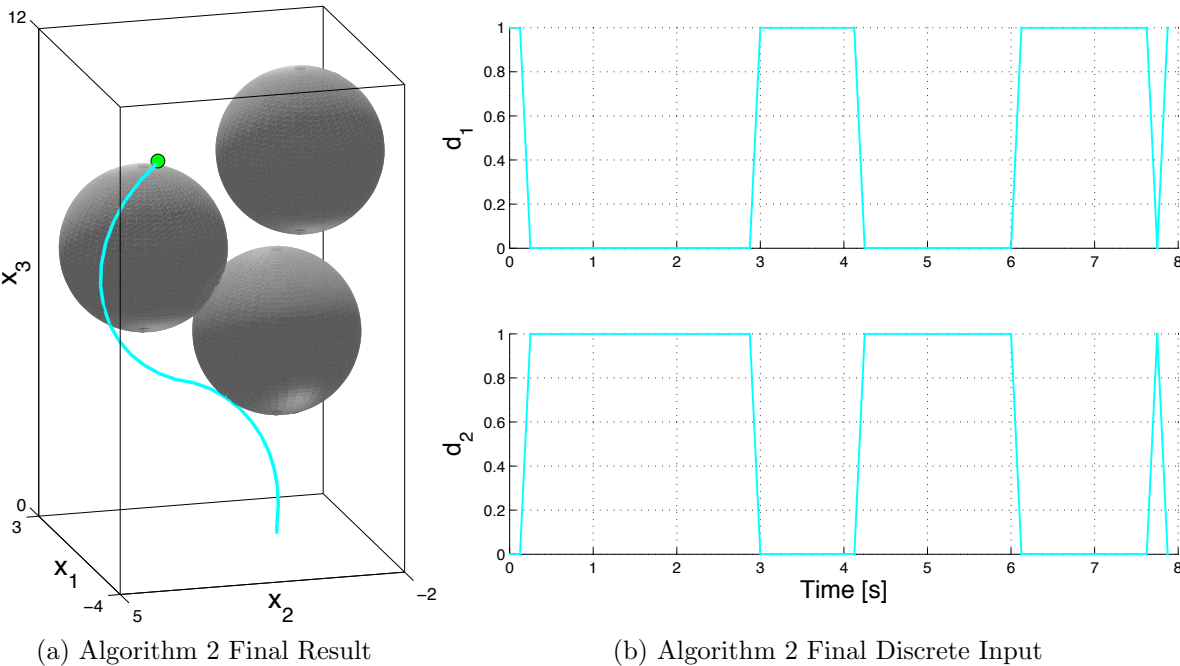


Figure 7.4: The optimal trajectory and discrete inputs drawn in cyan generated by Algorithm 2 where the point $(-2, 3.5, 10)$ is drawn in green and obstacles are drawn in grey.

Chapter 8

Identification of Bipedal Locomotion

In this chapter, we apply Algorithm 2 to identify a hybrid system on a cycle model for bipedal locomotion from tracking data for 2 different examples. The first example is a synthetic one for which we generate ground truth data in order to validate the utility of Algorithm 2 in identifying a model of locomotion. The second example is a 9 subject flat ground motion capture walking experiment for which we attempt to identify a model of locomotion for each participant. In both instances, we illustrate that Algorithm 2 is able to successfully identify the correct hybrid system on a cycle description of the presented locomotion.

8.1 Identification from Synthetically Generated Gait

We begin by constructing a hybrid system model on a cycle, \mathcal{H}_{CG} , for a classical bipedal model that has been considered at length by the robotic walking community [32]. Next, we generate locomotion for this biped by employing feedback linearization. Finally, we apply Algorithm 2 to this generated locomotion and illustrate that we are able to successfully identify \mathcal{H}_{CG} .

A Model for Kneel Compass Gait Biped

The example considered in this section is a 2D rigid body biped with knees and a torso for a total of four links as illustrated in Figure 8.1b. In addition to the torso position and orientation, $(x_{torso}, y_{torso}, \theta_{torso}) \in \mathbb{R}^2 \times \mathbb{S}^1$ with respect to a fixed global coordinate system, the coordinates for the generalized configuration space for this biped are the angle between the upper portion of the legs, $\theta_h \in \mathbb{S}^1$, the angle of the right and left knee with respect to their corresponding upper leg, $\theta_{rk}, \theta_{lk} \in \mathbb{S}^1$, respectively, and the angle of the right and left lower leg with respect to the ground, $\theta_{rf}, \theta_{lf} \in \mathbb{S}^1$, respectively. These different coordinates and their velocities can be assumed to evolve in \mathbb{R}^{16} . Observe that though we employ this over complete representation, this system only has 6 degrees of freedom. We assume full control

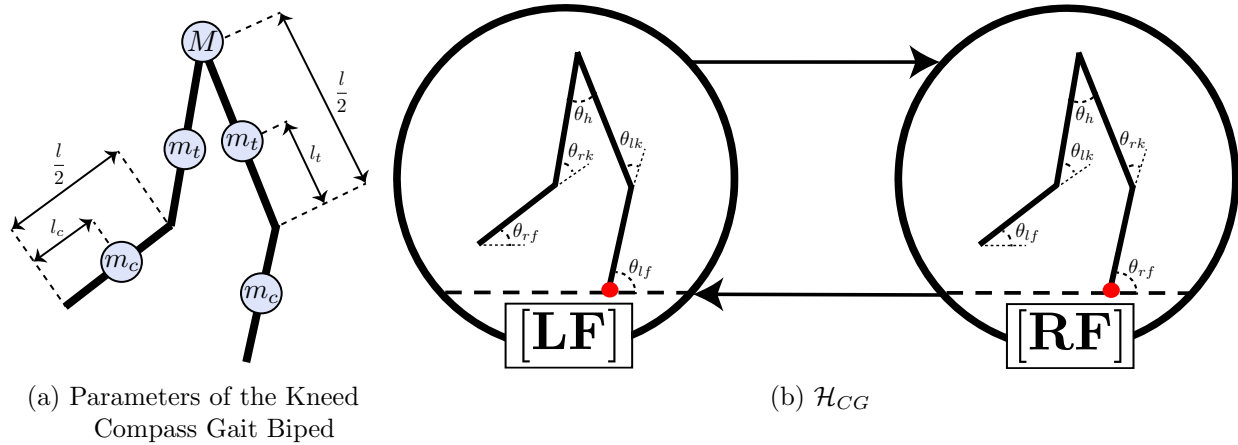


Figure 8.1: The parameterized kneed compass gait biped model and the associated hybrid system on a cycle model, \mathcal{H}_{CG} , used to generate the synthetic gait illustrated in Figure 8.2a. The specific choice of parameters used during the identification presented in this thesis are in Table 8.1. The constraints enforced within each mode of \mathcal{H}_{CG} are drawn in red and the coordinates of the configuration space of the biped are labeled within each mode.

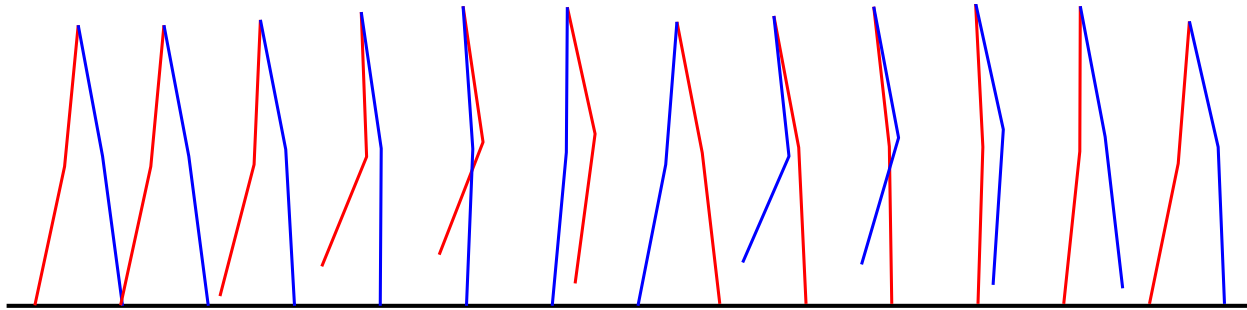
authority, that is the torque at each of the joints, denoted $u = (u_{lf}, u_{rf}, u_{lk}, u_{rk}, u_h) \in \mathbb{R}^5$, is controllable.

We define a hybrid system on a cycle, \mathcal{H}_{CG} , description of locomotion by considering a contact point that fixes the right foot to the ground and another that fixes the left foot to the ground by utilizing the construction presented in Section 2.2. That is, consider a set of contact points $\mathcal{C} = \{lf, rf\}$ and a directed cycle, $\ell_{CG} = [lf] \rightarrow [rf]$. We define the set of domains to be the Euclidean space with dimension equal to the size of the tangent space of the generalized configuration space of the biped which in this case is equal to 16. Next, we define the admissible inputs equal to a bounded subset of \mathbb{R}^5 . This set is formally defined in Table 8.2. The single guard in each mode of the hybrid system corresponds to lifting the constrained foot off the ground. The set of reset maps are set equal to the identity.

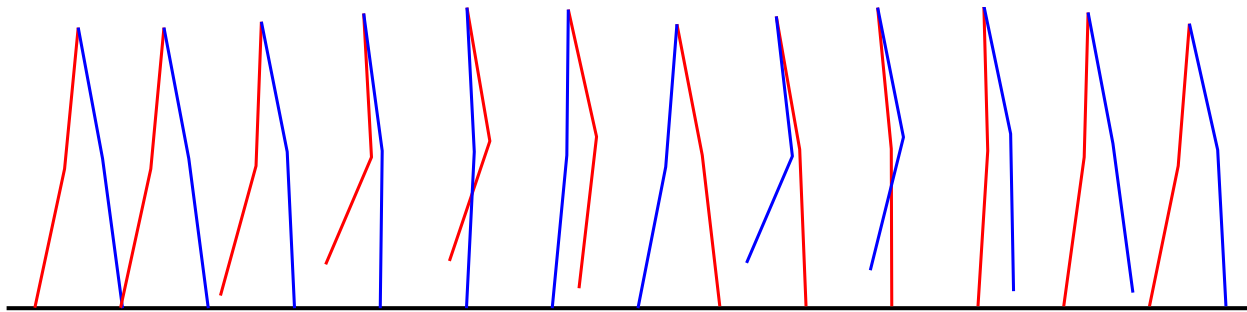
In order to define the vector field in each mode of the system, recall that each of the vector fields is constructed from the unconstrained Lagrangian after noting the holonomic constraint that must be maintained in order to remain within the mode in question. This

M	m_t	m_c	l	l_t	l_c
500g	500g	50g	1m	0.175m	0.375m

Table 8.1: The specific values chosen for the parameters illustrated in Figure 8.1a.



(a) Synthetically Generated Gait Via Feedback Linearization



(b) Gait Generated by Switched System Optimal Control

Figure 8.2: The gaits generated synthetically via feedback linearization for the kneed compass biped model, \mathcal{H}_{CG} , in Figure 8.1b and as a result of the application of Algorithm 2 to the data illustrated in Figure 8.3. The left leg is drawn in blue, the right leg is drawn in red, and the ground is drawn in black.

constrained vector field does not depend on the specific location at which the holonomic constraint must be maintained (i.e. the vector field for the $[lf]$ mode is constructed by requiring that the left foot remain fixed rather than requiring that it be fixed on the ground). Recall that for a rigid body the construction of this vector field as in Equation (2.17) can be done in an automated fashion by just specifying the lengths and masses of the various links drawn in Figure 8.1a. Given the choice of parameters in Table 8.1, we construct the desired vector fields by employing Mathematica [96]. The formulas for these vector fields, as a result, are several pages long without providing any real insight; therefore, we do not include them in this thesis.

Applying Switched System Optimal Control to Identify a Hybrid Model

Utilizing this hybrid system on a cycle model for the kneed compass gait biped, a periodic walk can be constructed by employing feedback linearization as in [75]. The result of this

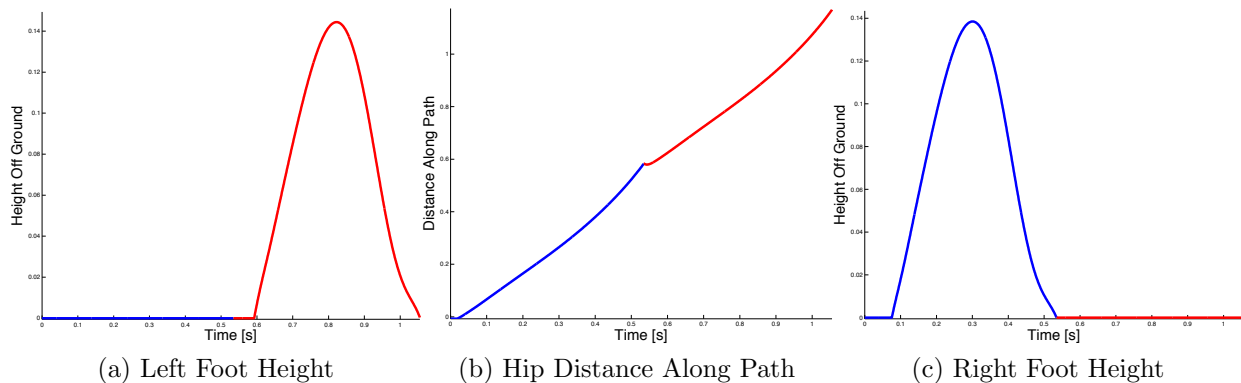


Figure 8.3: The tracking data for 3 of the 5 joints for the gait drawn in Figure 8.2a. The trajectory while the left foot is fixed to the ground (i.e. the $[lf]$ mode) is drawn in blue, and the trajectory while the right foot is fixed to the ground (i.e. the $[rf]$ mode) is drawn in red.

application when the model is initialized with the left foot fixed to the ground (i.e. beginning in the $[lf]$ mode) at time $t_0 = 0$ is a walking gait that begins in the $[lf]$ mode, transitions to the $[rf]$ mode, and then transitions back to the $[lf]$ mode at time $t_f = 1.05$. This is illustrated in Figure 8.2a. From this generated gait, we construct tracking data for each of the joints as illustrated in Figure 8.3.

Our goal is the construction of the hybrid model on a cycle to describe the synthetic locomotion given the tracking data in 2D for each of the 5 joints, denoted $y_{obs} : [t_0, t_f] \rightarrow \mathbb{R}^{10}$, the unconstrained Lagrangian, and the set of contact points of interest, $\mathcal{C} = \{lf, rf\}$. As described in Section 2.2, the identification of this model is complete if we determine the domain specification as in Definition 2. As we showed in Section 2.3, the computation of the domain specification is equivalent to solving the Switched System Optimal Control Problem defined as in Equation (2.34) for the switched system that switches between the vector fields corresponding to the satisfaction of all possible combinations of contact point enforcements.

In order to proceed, we require this switched system vector field. Let $\mathcal{Q} = \{1, \dots, 4\}$ define the set of possible modes of the switched system. Each of the modes can be associated with a possible combination of contact point enforcements in \mathcal{C} by considering the 2-digit binary expansion of the index in \mathcal{Q} associated with the mode in question minus one. For example, the 2-digit binary expansion of mode 1 after subtraction by 1 is 00, which can be associated with none of the contact points being enforced. On the other hand, the 2-digit binary expansion of mode 3 after subtraction by 1 is 10 which can be associated with the enforcement of the rf contact point. Let $\mathcal{B} : \mathcal{Q} \rightarrow \mathbb{Z}_2^2$ denote this operation. Observe that we can then construct a vector field, $f : \mathbb{R} \times \mathbb{R}^n \times \mathbb{R}^m \times \mathcal{Q} \rightarrow \mathbb{R}$ as described earlier for each possible combination of contact point enforcements. Again the computation of this vector field is done in Mathematica and not included in this thesis due to its size.

Proceeding as in Chapter 7, we define a cost, initial condition, and algorithmic param-

U	γ	α	β	$\bar{\alpha}$	$\bar{\beta}$	Λ	χ	ω
$u_i(t) \in [-50, 50],$ $\forall i \in \{lf, rf, lk, rk, h\}$	10	0.1	0.83	0.001	0.72	10^{-4}	$\frac{1}{4}$	10^{-6}

Table 8.2: The algorithmic parameters used for the Knead Compass Gait Switched System Model during the implementation of Algorithm 2.

eters in order to apply Algorithm 2 to identify a domain specification. Before describing our specific choices, recall that the initial and final times can be treated as fixed parameters t_0 and t_f , respectively, during the optimization and that we can employ a stopping criterion to terminate Algorithm 2, if θ_τ gets sufficiently close to zero. We utilize the same implementation of LSSOL from TOMLAB as in Chapter 7 in order to compute the optimality function.

Motivated by Equation (2.35), we choose a running cost as follows:

$$L(t, x(t), u(t), d(t)) = \|y_{obs}(t) - \mathbf{g}(x(t))\|_2^2 + 0.1 \left(\|u_h(t)\|_2^2 + \|u_{lk}(t)\|_2^2 + \|u_{rk}(t)\|_2^2 + \sum_{i=1}^4 \sum_{j=1}^2 (1 - d_i(t)) (1 - [\mathcal{B}(i)]_j) \|u_j(t)\|_2^2 \right), \quad (8.1)$$

where $\mathbf{g} : \mathbb{R}^{16} \rightarrow \mathbb{R}^5$ is the rigid body transformation that takes the continuous state of the switched system to the set of observations (i.e. the rigid body transformation that takes the joint angles of the biped as in Figure 8.1b to the absolute position of the joints), $u_1 = u_{lf}$, and $u_2 = u_{rf}$. Observe that we include a mode dependent penalty that penalizes an input at a particular contact point only if that contact point is not being enforced. For example, expending input at the *lf* joint while the *lf* is constrained is not penalized. We let $\phi(\cdot) = 0$. We also include constraints during the optimization that ensure that each of the joints are kept above the ground.

To challenge Algorithm 2, we initialize the optimization with all of the continuous inputs for all time equal to zero, the discrete input for all time equal to one for the mode corresponding to fixing only the *rf* contact point and zero for the other modes (i.e. $d_3(t) = 1, \forall t \in [t_0, t_f]$), and the initial condition for the continuous state of the switched system equal to the initial condition of the state of the biped that it attempts to mimic. Algorithm 2 is initialized with the parameters in Table 8.2, a stopping criterion equal to 10^{-4} , and 64 equally spaced samples in time.

The gait produced as a result of the optimization is illustrated in Figure 8.2b. Importantly, the optimization produces a pure discrete input that visits the mode corresponding to only the *lf* contact point being enforced and then only the *rf* contact point being enforced, which is identical to the direct cycle component of \mathcal{H}_{CG} that was used to generate the gait in Figure 8.2a.

8.2 Identification of Human Gait from Motion Capture Data

Next, we conduct a 9 subject flat ground walking experiment where the participant’s gait is observed via a motion capture system. We then apply Algorithm 2 on each of the observed gaits and construct a hybrid system on a cycle model for each of the participants.

The Experiment

We begin by describing the experimental setup employed during data collection. The data presented in this thesis is collected using the Phase Space System¹, which computes the 3D position of 19 LED sensors at 480 frames per second using 12 cameras at 1 millimeter level of accuracy. The cameras were calibrated prior to the experiment and were placed to achieve a 1 millimeter level of accuracy for a 4 by 4 by 4 meters cubed sized space. 8 LED sensors were placed on each leg as illustrated in Figure 8.4. 1 LED sensor was placed on the sternum, 1 LED sensor was placed on the back behind the sternum, and 1 LED sensor was placed on the navel. Each sensor was fastened in a manner that ensured that it did not move during the experiment.

Each trial of the experiment required the subject to walk 3 meters along a line drawn on the floor (in Figure 8.4 this line is drawn in blue). To simplify the data analysis, each subject was required to place the right foot at the starting point of the line at the outset of the experiment and was told to walk in a natural manner. Each subject performed 12

¹<http://www.phasespace.com/hardware>

	Sex	Age	Weight	Height	l_f	l_h	l_c	l_t
1	M	30	90.7kg	184cm	14.5cm	8.50cm	43.0cm	44.0cm
2	F	19	53.5kg	164cm	15.0cm	8.00cm	41.0cm	44.0cm
3	M	17	83.9kg	189cm	16.5cm	8.00cm	45.5cm	55.5cm
4	M	22	90.7kg	170cm	14.5cm	9.00cm	43.0cm	39.0cm
5	M	30	68.9kg	170cm	15.0cm	8.00cm	43.0cm	43.0cm
6	M	29	59.8kg	161cm	14.0cm	8.50cm	37.0cm	40.0cm
7	M	26	58.9kg	164cm	14.0cm	9.00cm	39.0cm	41.0cm
8	F	77	63.5kg	163cm	14.0cm	8.00cm	40.0cm	42.0cm
9	F	23	47.6kg	165cm	15.0cm	8.00cm	45.0cm	43.0cm

Table 8.3: Table describing each of the subjects. The subject number is in the left column and the l_f, l_h, l_c, l_t measurements correspond to the lengths illustrated in Figure 8.4. The measurement in column 4 is the the only measurement that was self-reported.

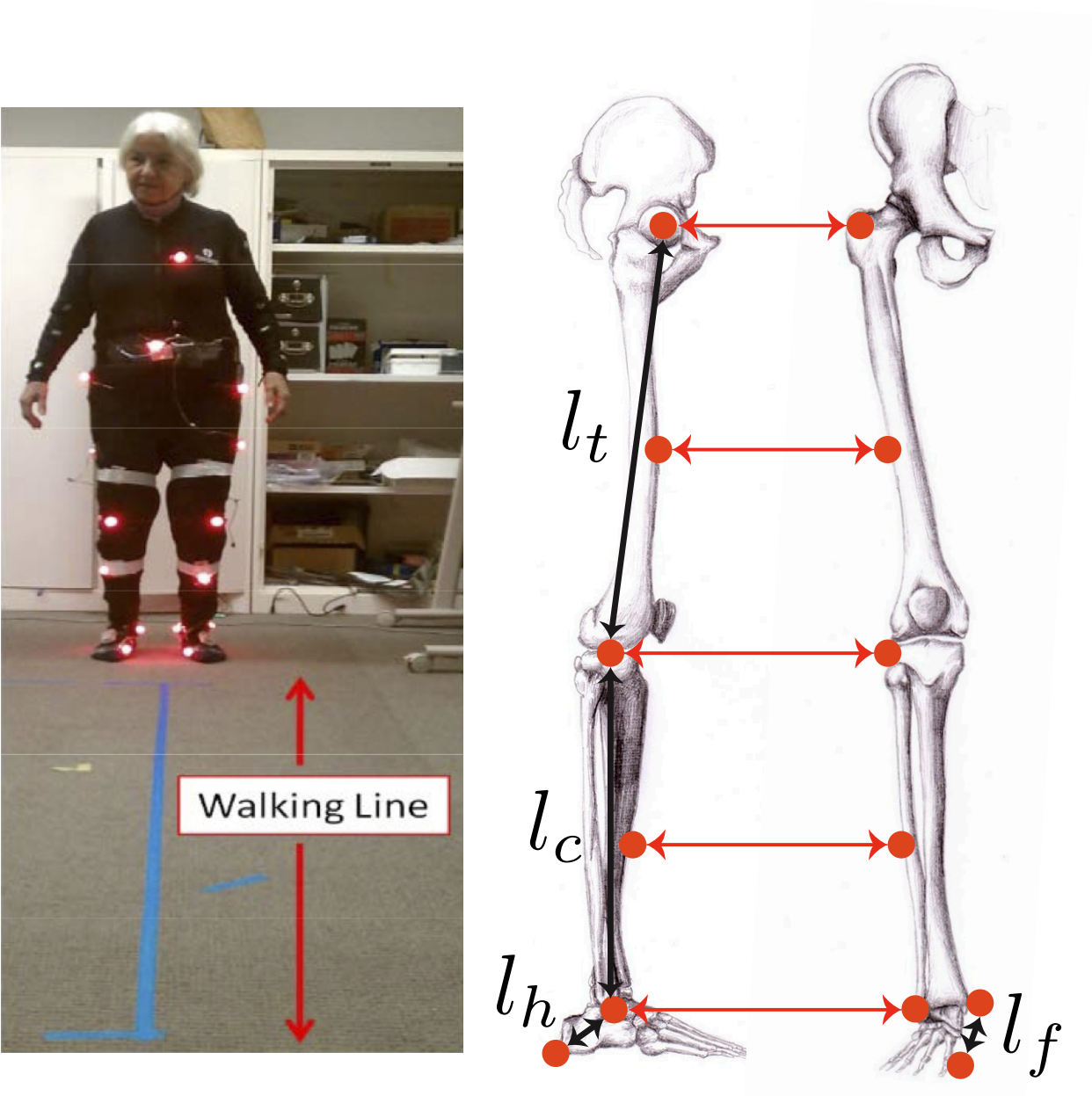


Figure 8.4: Illustrations of the experimental setup (left) and sensor placement on each leg (right). Each subject in the experiment was required to wear a suit where the sensors (red LEDs) were fastened in place. Each sensor was placed at the joints as illustrated with the red dots on the right lateral (middle) and anterior aspects (right) of the right leg. Sensors are placed identically on the left leg. The same sensors drawn from different views are connected with red arrows (right) and the labeled black arrows are used to illustrate the diversity of subjects in Table 8.3.

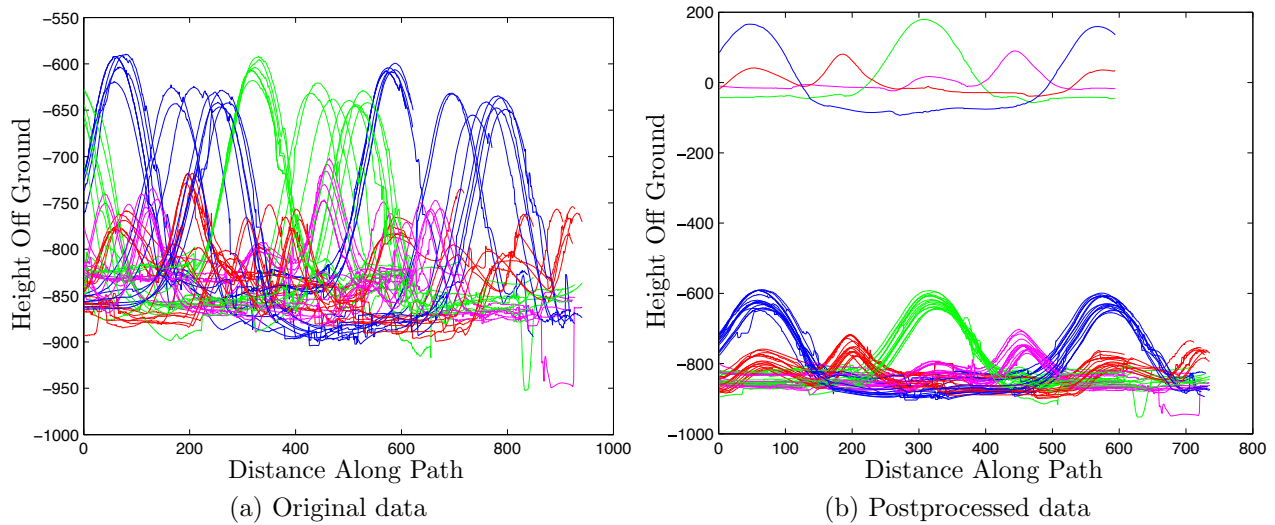


Figure 8.5: The original data is illustrated for the height (in millimeters) of the heel and toe for each leg for all 12 trials for a single individual, and the postprocessed data is illustrated after it has been shifted (drawn at the bottom of the plot) and averaged (drawn at the top of the plot). In each plot the different colors corresponds to different sensor.

such trials, which constituted a single experiment. There were 3 female and 6 male subjects with ages ranging from 17 to 77, heights ranging from 161 to 189 centimeters, and weights ranging from 47.6 to 90.7 kilograms. Table 8.3 describes the measurements of each of the subjects.

Data Processing

In this subsection, we describe how the data is preprocessed in order to make the ensuing analysis tenable. We do this by finding the effective period of the data, rotating the data so that the walking occurs along a 2D plane, and averaging the collected data for each sensor and for each individual over all trials.

Interpolation

Since the motion capture information drops out periodically due to self-occlusions, we begin by finding the effective period of the walking. The data is then interpolated using cubic spline interpolation. The result of this initial data processing is clean data over the course of a few steps (with the number of steps depending upon the individual). From each of the trials, at least 2 steps are isolated (one with the right leg and another with the left leg) by ensuring that the data repeats. If there is no usable data, that trial of walking is dropped.

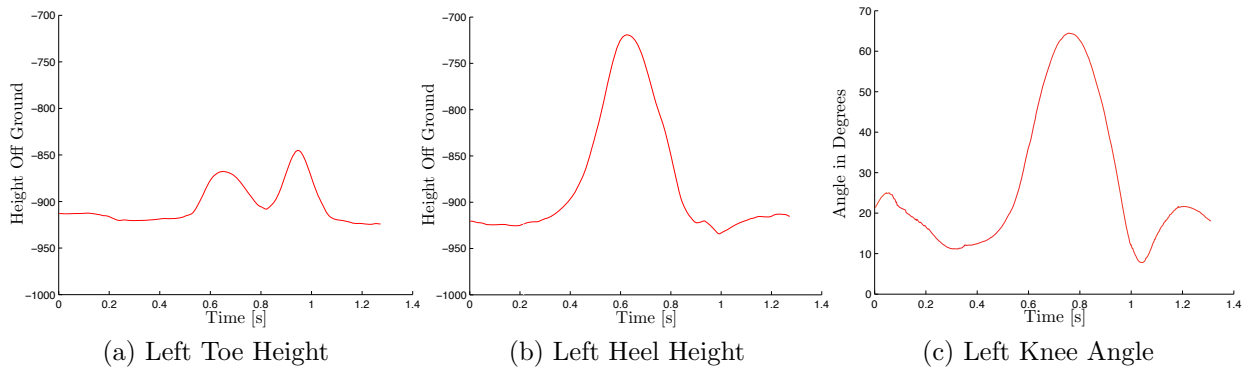


Figure 8.6: A portion of the observed data that is tracked during the application of Algorithm 2 in order to determine a domain specification.

Data Rotation

Using the “clean” 2 step walking data, a series of rotations are employed to ensure that walking only occurs in a 2D plane. This is achieved by considering the sensor on the navel of each subject, which evolves in an approximately linear fashion. By fitting a line to this forward evolution, the direction of the walking is determined.

Averaging

We average the 12 trials from each individual to construct a single trajectory for each of the sensors for each individual. To do this, we begin with the raw data for each sensor (the heel and toe sensor data for each is leg is illustrated in Figure 8.5a), and shift the data to line up each curve since each trial may operate at a different time scale. After shifting the data, we ensure that the sensor data for every trial includes at least 2 steps, one step for each leg, by checking to see if the data is approximately periodic. If this requirement is not satisfied, this trial is removed from the set of trajectories. Finally, all the usable trajectories for properly shifted trials are averaged and used for data analysis. The result of this process is illustrated in Figure 8.5b.

A Switched System Model for the Biped with Torso, Knees and Feet

For each of the 9 joints of the biped drawn in Figure 8.7b, as a result of this aforementioned data processing, we get a set of observations in 2D, $y_{obs} : [t_0, t_f] \rightarrow \mathbb{R}^{18}$ a subset of which are illustrated in Figure 8.6 for one participant. In order to identify a hybrid system on a cycle model for each of the observed gaits, we require an unconstrained Lagrangian and a set of contact points of interest. We perform identification by using a 2D rigid body biped with torso, knees, and feet as illustrated in Figure 8.7b. We focus on contact points associated

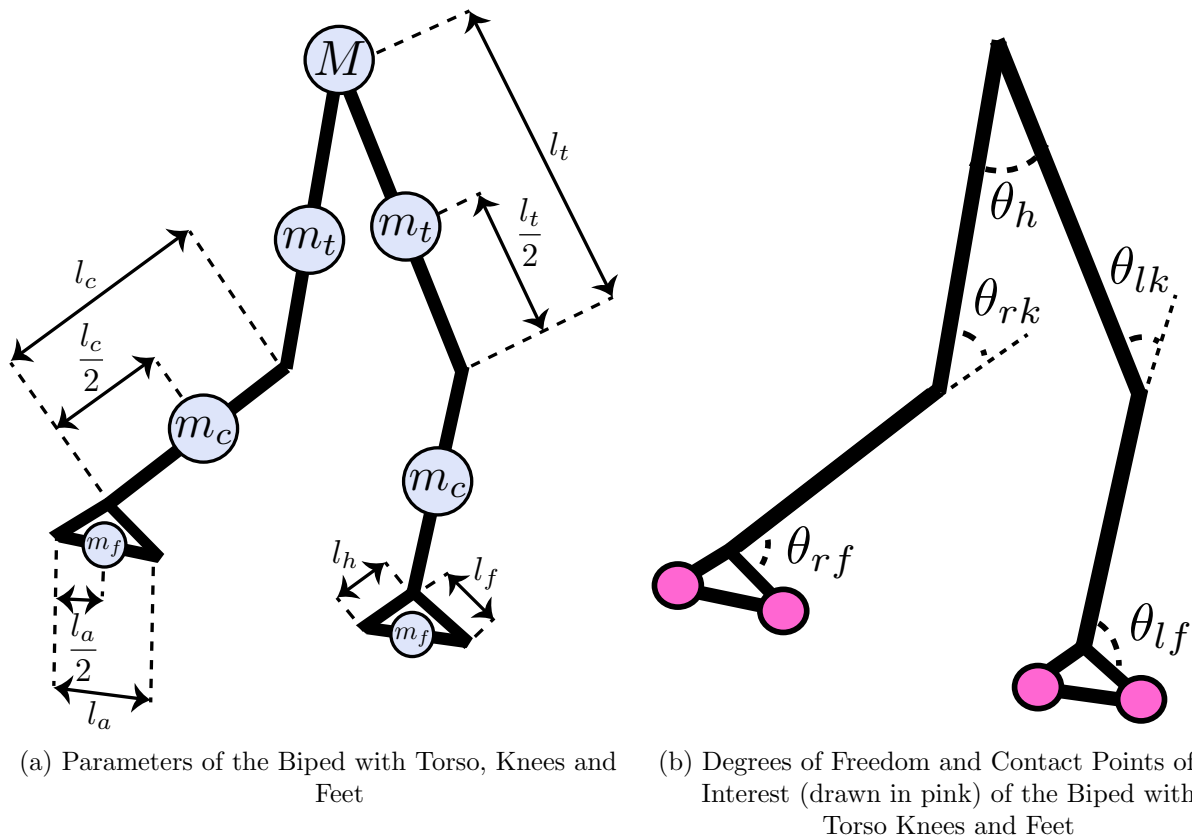


Figure 8.7: An illustration of the parameters (left), degrees of freedom (right), and contact points of interest (drawn in pink on the right) for the Biped with Torso, Knees, and Feet that is used in order to construct a hybrid system on cycle model of gait for the observed flat ground walking for each of the participants of the motion capture experiment.

with the toe and heel on each foot. That is, using the notation defined in Section 2.2, we choose $\mathcal{C} = \{lt, rt, lh, rh\}$.

In addition to the torso position and orientation, $(x_{torso}, y_{torso}, \theta_{torso}) \in \mathbb{R}^2 \times \mathbb{S}^1$ with respect to a fixed global coordinate system, the coordinates for the generalized configuration space for this biped are the angle between the upper portion of the legs, $\theta_h \in \mathbb{S}^1$, the angle of the right and left knee with respect to their corresponding upper leg, $\theta_{rk}, \theta_{lk} \in \mathbb{S}^1$, respectively, and the angle of the right and left ankle with respect to the foot, $\theta_{rf}, \theta_{lf} \in \mathbb{S}^1$, respectively. These different coordinates and their velocities can be assumed to evolve in \mathbb{R}^{16} . Observe that the biped has 8 degrees of freedom. We assume full control authority, that is the torque at each of the joints, denoted $u = (u_{lt}, u_{rt}, u_{lh}, u_{rh}, u_{lf}, u_{rf}, u_{lk}, u_{rk}, u_h) \in \mathbb{R}^9$, is controllable.

As described in Section 2.2, the identification of a hybrid system on a cycle model

for each participant from the observations, y_{obs} , requires the determination of the domain specification as in Definition 2. As we showed in Section 2.3, the computation of the domain specification is equivalent to solving the Switched System Optimal Control Problem defined as in Equation (2.34) for the switched system that switches between the vector fields corresponding to the satisfaction of all possible combinations of contact point enforcements.

For each possible combination of contact point enforcements a vector field must then be constructed. Let $\mathcal{Q} = \{1, \dots, 16\}$ define the set of possible modes of the switched system. Each of the modes can be associated with a possible combination of contact point enforcements in \mathcal{C} by considering the 4-digit binary expansion of the index in \mathcal{Q} associated with the mode in question minus one. For example, the 4-digit binary expansion of mode 1 after subtraction by 1 is 0000, which can be associated with none of the contact points being enforced. On the other hand, the 4-digit binary expansion of mode 8 after subtraction by 1 is 0111 which can be associated with the enforcement of the lt , rt , and lh contact points. Let $\mathcal{B} : \mathcal{Q} \rightarrow \mathbb{Z}_2^4$ denote this operation.

Recall then that we can construct a vector field, $f : \mathbb{R} \times \mathbb{R}^n \times \mathbb{R}^m \times \mathcal{Q} \rightarrow \mathbb{R}$ from the unconstrained Lagrangian after noting the holonomic constraint that must be maintained in order to remain within the mode in question. This constrained vector field does not depend on the specific location at which the holonomic constraint must be maintained (i.e. the vector field for the $[lt]$ mode is constructed by requiring that the left toe remain fixed rather than requiring that it be fixed on the ground). Recall that for a rigid body the construction of this vector field as in Equation (2.17) can be done in an automated fashion by just specifying the lengths and masses of the various links drawn in Figure 8.7a.

We use the measurements in Table 8.3 to guide the determination of these lengths and masses. In particular in order to determine the masses of each of the distinct links, we employ a result from a paper on anatomy that describes the average distribution of mass in humans [17] whose relevant results are summarized in Table 8.4. Given the results in Tables 8.3 and 8.4, we construct the desired vector field, f , which is distinct for each of the different participants by employing Mathematica [96]. Again the formula for this vector field for each of the participants, as a result, is several pages long without providing any insight; therefore, we do not include it in this thesis.

M	m_t	m_c	m_f	l_a
65.2%	11.3%	4.39%	1.71%	$\sqrt{l_h^2 + l_f^2 - \frac{1}{2}l_h l_f}$

Table 8.4: Table describing the choice of parameters illustrated in Figure 8.7a for each of the 9 subjects in Table 8.3 as a percentage of their total weight using the formula described in Table 6 in [17] and as function of measured lengths.

U	γ	α	β	$\bar{\alpha}$	$\bar{\beta}$	Λ	χ	ω
$u_i(t) \in [-50, 50],$ $\forall i \in \{lt, rt, lh, rh, lf, rf, lk, rk, h\}$	10	0.1	0.83	0.001	0.72	10^{-4}	$\frac{1}{4}$	10^{-6}

Table 8.5: The algorithmic parameters used for the switched system model of the Biped with Torso, Knees, and Feet during the implementation of Algorithm 2 for each of the 9 participants in the flat ground walking experiment.

Applying Switched System Optimal Control to Identify a Hybrid Model

Proceeding as in Chapter 7, we define a cost, initial condition, and algorithmic parameters in order to apply Algorithm 2 to identify a domain specification. Before describing our specific choices, recall that the initial and final times can be treated as fixed parameters t_0 and t_f , respectively, during the optimization and that we can employ a stopping criterion to terminate Algorithm 2, if θ_τ gets sufficiently close to zero. We utilize the same implementation of LSSOL from TOMLAB as in Chapter 7 in order to compute the optimality function.

Motivated by Equation (2.35), we choose a running cost as follows:

$$L(t, x(t), u(t), d(t)) = \|y_{obs}(t) - \mathbf{g}(x(t))\|_2^2 + 0.1 \left(\|u_h(t)\|_2^2 + \|u_{lk}(t)\|_2^2 + \|u_{rk}(t)\|_2^2 + \|u_{lf}(t)\|_2^2 + \|u_{rf}(t)\|_2^2 + \sum_{i=1}^{16} \sum_{j=1}^4 (1 - d_i(t)) (1 - [\mathcal{B}(i)]_j) \|u_j(t)\|_2^2 \right), \quad (8.2)$$

where $\mathbf{g} : \mathbb{R}^{16} \rightarrow \mathbb{R}^9$ is the rigid body transformation that takes the continuous state of the switched system to the subset of observations corresponding to the set of joints for each participant (i.e. the rigid body transformation that takes the joint angles of the biped as in Figure 8.7b to the absolute position of the joints), $u_1 = u_{lt}$, $u_2 = u_{rt}$, $u_3 = u_{lh}$, and $u_4 = u_{rh}$. Observe that we include a mode dependent penalty that penalizes an input at a particular contact point only if that contact point is not being enforced. For example, expending input at the lt joint while the lt is constrained is not penalized. We let $\phi(\cdot) = 0$. We also include constraints during the optimization that ensure that each of the joints are kept above the ground.

We initialize Algorithm 2 for each participant with all of the continuous inputs for all time equal to zero, the discrete input for all time equal to one for the mode corresponding to fixing only the lt contact point and zero for the other modes (i.e. $d_2(t) = 1, \forall t \in [t_0, t_f]$), and the initial condition for the continuous state of the switched system equal to the initial condition of the state of the participant whose gait we are attempting to identify. Algorithm 2 is initialized with the parameters in Table 8.5, a stopping criterion equal to 10^{-4} , and 64 equally spaced samples in time.

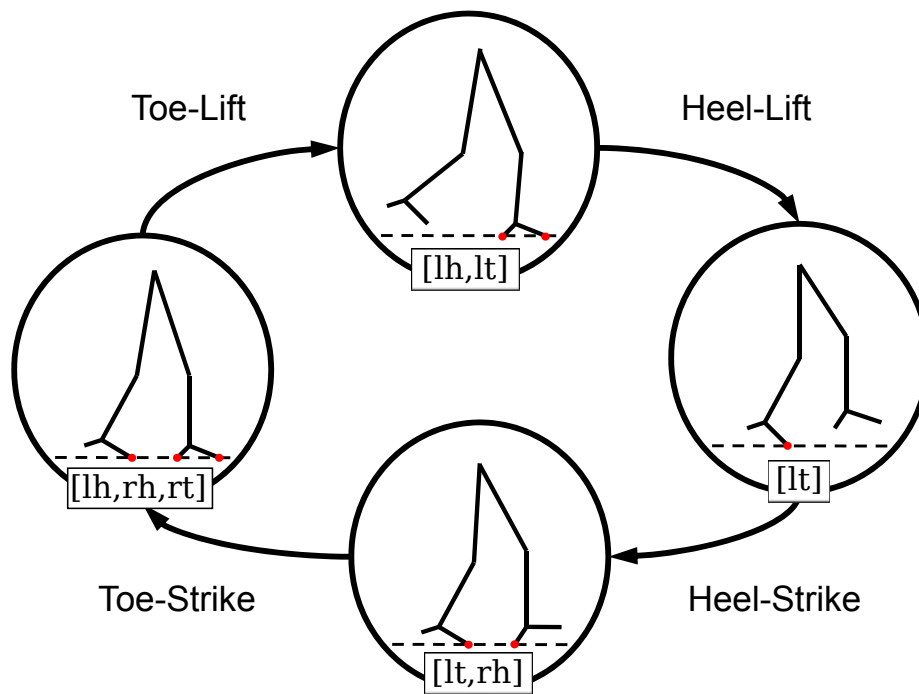


Figure 8.8: The domain specification or sequence of constraint enforcements constructed by application of Algorithm 2 for all 9 participants in the flat ground walking experiment. The red dots indicate the constraints enforced in each mode. Notice that there are in fact 8 different modes visited during two steps, but these other 4 modes can be constructed by simply relabeling the left and right leg in each mode and are not included due to space limitations.

The result of the application of Algorithm 2 to each of the observed trajectories is that the same sequence of modes of the switched system are visited by *all* participants. That is, though the percentage of time spent in each of the distinct modes is different for each participant as illustrated in Figure 8.9, all of the 9 participants in the flat ground walking experiment had the same the domain specification illustrated in Figure 8.8. Importantly, this is the same domain specification that has been empirically observed for normal subjects during flat ground walking experiments [95].

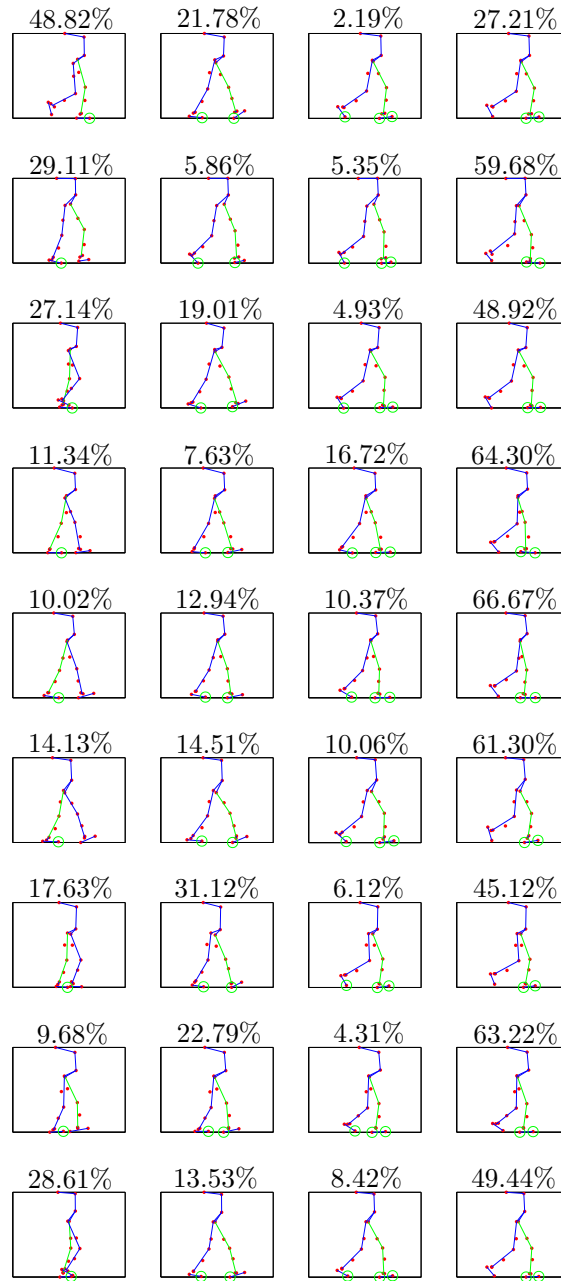


Figure 8.9: The domain specifications in each row for the 9 subjects that participated in the flat ground walking experiment in the order listed in Table 8.3. Comparing with the domain specification illustrated in Figure 8.8 the first through fourth columns correspond to $[lt]$ and $[rt]$, $[lt, rh]$ and $[rt, lh]$, $[lh, rh, rt]$ and $[rh, lh, lt]$, and $[lh, lt]$ and $[rh, rt]$, respectively. Each illustration is a snapshot of the subject's dynamics in the mode and above each plot is the percentage of the total gait spent within that mode.

Chapter 9

Discussion and Concluding Remarks

In this thesis, we devise a technique to perform identification of human locomotion by transforming the problem of identification into a switched system optimal control problem. In particular, we devise a first order numerical optimization algorithm for the optimal control of constrained nonlinear switched systems. The algorithm works by first relaxing the discrete-valued input, performing traditional optimal control, and projecting the computed relaxed discrete-valued input by employing a projection constructed by an extension to the classical Chattering Lemma.

We prove that the sequence of points constructed by recursive application of our algorithm converge to a point that satisfies a necessary condition for optimality of the Switched System Optimal Control Problem. We then devise an implementable algorithm that operates over finite dimensional subspaces of the optimization spaces. We prove the convergence of the sequence of points constructed by recursive application of our computationally tractable algorithm to a point that satisfies a necessary condition for optimality of the Switched System Optimal Control Problem. The utility of the technique in performing identification is illustrated on a synthetic gait and a set of gaits observed during a flat ground walking experiment.

Though this thesis assumes a specific unconstrained Lagrangian, by allowing for optimization over the initial condition, a parameterized unconstrained Lagrangian model can be employed, and the correct lengths and masses of different links of the participant being observed can simultaneously be determined during the identification procedure. Moving forward, in the short term we plan on applying this identification procedure to more complicated locomotion patterns. In addition, we plan on applying the outcome of this identification procedure to measuring the region of attraction of observed gait, which as discussed in the introduction corresponds to a desirable measure of stability of the observed gait.

One challenge remains in order for the broader application of this approach. Even in the instance of a rigid body model, the complexity of the vector fields for 8 link models as constructed by Mathematica is high. More worryingly, the complexity of more realistic, non rigid-body models is considerably higher. Devising modeling tools capable of managing this complexity is critical. Port-Controlled Hamiltonians seem like a potential modeling tool

capable of managing this ever-increasing complexity [83].

Finally, one of the broader goals of this line of investigation is the development of techniques capable of rigorously guiding the design of human specific prosthetics. Although the techniques presented in this thesis after a straightforward extension can be applied to predict instabilities in gait, it is unclear how they can be applied in order to guide the construction of prosthetics. In particular, though a gait with a prosthetic is representable by a hybrid system, the optimal design of a particular prosthetic requires being able to perform optimal control in the presence of autonomous switching. Devising a computationally tractable variational technique for such systems is critical to being able to design such an algorithm. Given such a variational principle, the development of an implementable technique should be straightforward given our recent development of a provably convergent numerical integration scheme [14]. The construction of such an algorithm should fundamentally shift the research in assistive technologies going forward.

Bibliography

- [1] Mazen Alamir and Sid-Ahamed Attia. On solving optimal control problems for switched hybrid nonlinear systems by strong variations algorithms. In *Proceedings of the 6th IFAC Symposium on Nonlinear Control Systems*, number 0, 2004.
- [2] A. D. Ames, R. D. Gregg, and M. W. Spong. A geometric approach to three-dimensional hipped bipedal robotic walking. In *Proceedings of the 45th IEEE Conference on Decision and Control*, San Diego, CA, 2007.
- [3] A.D. Ames, R. Vasudevan, and R. Bajcsy. Human-data based cost of bipedal robotic walking. In *Proceedings of the 14th International Conference on Hybrid Systems: Computation and Control*, pages 153–162, 2011.
- [4] T.P. Andriacchi and E.J. Alexander. Studies of Human Locomotion: Past, Present and Future. *Journal of Biomechanics*, 33(10):1217–1224, 2000.
- [5] Henrik Axelsson, Yorai Y. Wardi, Magnus Egerstedt, and E. I. Verriest. Gradient Descent Approach to Optimal Mode Scheduling in Hybrid Dynamical Systems. *Journal of Optimization Theory and Applications*, 136(2):167–186, November 2008.
- [6] S. Belongie, J. Malik, and J. Puzicha. Shape Matching and Object Recognition Using Shape Contexts. *IEEE Transactions on Pattern Analysis and Machine Intelligence*, 24(4):509–522, 2002.
- [7] Sorin C. Bengea and Raymond A. DeCarlo. Optimal Control of Switching Systems. *Automatica*, 41(1):11–27, January 2005.
- [8] M. Berchuck, TP Andriacchi, BR Bach, and B. Reider. Gait Adaptations by Patients Who Have a Deficient Anterior Cruciate Ligament. *Journal of Bone and Joint Surgery*, 72(6):871, 1990.
- [9] Leonard D. Berkovitz. *Optimal Control Theory*. Springer-Verlag, 1974.
- [10] A. Biswas, E.D. Lemaire, and J. Kofman. Dynamic Gait Stability Index Based on Plantar Pressures and Fuzzy Logic. *Journal of Biomechanics*, 41(7):1574–1581, 2008.

- [11] Michael S. Branicky, Vivek S. Borkar, and Sanjoy K. Mitter. A Unified Framework for Hybrid Control: Model and Optimal Control Theory. *IEEE Transactions on Automatic Control*, 43(1):31–45, 1998.
- [12] Roger Brockett. Stabilization of motor networks. In *Proceedings of the 34th IEEE Conference on Decision and Control*, 1995.
- [13] S.M. Bruijn, D.J.J. Bregman, O.G. Meijer, P.J. Beek, and J.H. van Dieën. The Validity of Stability Measures: A Modelling Approach. *Journal of Biomechanics*, 44(13):2401–2408, 2011.
- [14] Sam Burden, Humberto Gonzalez, Ram Vasudevan, Ruzena Bajcsy, and S. Shankar Sastry. Numerical integration of hybrid dynamical systems via domain relaxation. In *Proceedings of the 50th IEEE Conference in Decision and Control*, pages 3958–3965, 2011.
- [15] Christos G. Cassandras, David L. Pepyne, and Yorai Y. Wardi. Optimal Control of a Class of Hybrid Systems. *IEEE Transactions on Automatic Control*, 46(3):398–415, 2001.
- [16] J.H. Choi and JW Grizzle. Planar bipedal walking with foot rotation. In *American Control Conference*, pages 4909–4916. IEEE, 2005.
- [17] R. Contini, R.J. Drillis, and M. Bluestein. Determination of Body Segment Parameters. *Human Factors: The Journal of the Human Factors and Ergonomics Society*, 5(5):493–504, 1963.
- [18] R.D. Crowninshield and R.A. Brand. A Physiologically Based Criterion of Muscle Force Prediction in Locomotion. *Journal of Biomechanics*, 14(11):793–801, 1981.
- [19] Vincent Duindam, Ron Alterovitz, S. Shankar Sastry, and Ken Goldberg. Screw-based motion planning for bevel-tip flexible needles in 3D environments with obstacles. In *Proceedings of the 2008 IEEE International Conference on Robotics and Automation*, pages 2483–2488, May 2008.
- [20] H.D. Eberhart, V. Inman, et al. Fundamental Studies of Human Locomotion and Other Information Relating to Design of Artificial Limbs. *Report to the National Research Council*, 1947.
- [21] H.D. Eberhart and V.T. Inman. An Evaluation of Experimental Procedures Used in a Fundamental Study of Human Locomotion. *Annals of the New York Academy of Sciences*, 51(7):1213–1228, 1951.
- [22] Magnus Egerstedt and Yorai Y. Wardi. Multi-Process Control Using Queuing Theory. In *Proceedings of the 41st IEEE Conference on Decision and Control*, volume 2, pages 1991–1996, 2002.

- [23] Magnus Egerstedt, Yorai Y. Wardi, and Henrik Axelsson. Transition-Time Optimization for Switched-Mode Dynamical Systems. *IEEE Transactions on Automatic Control*, 51(1):110–115, 2006.
- [24] Ivar Ekeland and Roger Témam. *Convex Analysis and Variational Problems*. Classics in Applied Mathematics. SIAM, 1987.
- [25] R. Fletcher and S. Leyffer. Solving Mixed Integer Nonlinear Programs by Outer Approximation. *Mathematical Programming*, 66(1):327–349, 1994.
- [26] Gerald B. Folland. *Real Analysis: Modern Techniques and Their Applications*. Willey, second edition, 1999.
- [27] W.T. Freeman and E.H. Adelson. The design and use of steerable filters. *IEEE Transactions on Pattern Analysis and Machine Intelligence*, 13(9):891–906, 2002.
- [28] Ronojoy Ghosh and Claire J. Tomlin. Hybrid system models of biological cell network signaling and differentiation. In *Proceedings of the Annual Allerton Conference on Communication Control and Computing*, volume 39, pages 942–951, 2001.
- [29] Jeremy H. Gillula, Gabriel M. Hoffmann, Haomiao Huang, Michael P. Vitus, and Claire J. Tomlin. Applications of Hybrid Reachability Analysis to Robotic Aerial Vehicles. *International Journal of Robotics Research*, 30(3):335–354, 2011.
- [30] Humberto Gonzalez, Ram Vasudevan, Maryam Kamgarpour, S. Shankar Sastry, Ruzena Bajcsy, and Claire J. Tomlin. A descent algorithm for the optimal control of constrained nonlinear switched dynamical systems. In *Proceedings of the 13th International Conference on Hybrid Systems: Computation and Control*, pages 51–60, 2010.
- [31] Humberto Gonzalez, Ram Vasudevan, Maryam Kamgarpour, S. Shankar Sastry, Ruzena Bajcsy, and Claire J. Tomlin. A numerical method for the optimal control of switched systems. In *Proceedings of the 49th IEEE Conference on Decision and Control*, pages 7519–7526. IEEE, 2010.
- [32] A. Goswami, B. Espiau, and A. Keramane. Limit Cycles in a Passive Compass Gait Biped and Passivity-Mimicking Control Laws. *Autonomous Robots*, 4(3):273–286, 1997.
- [33] A. Goswami, B. Thuilot, and B. Espiau. Compass-like biped robot part I : Stability and bifurcation of passive gaits. Rapport de Recherche de l’INRIA, 1996.
- [34] J.W. Grizzle, C. Chevallereau, A.D. Ames, and R.W. Sinnet. 3d bipedal robotic walking: models, feedback control, and open problems. In *IFAC Symposium on Nonlinear Control Systems*, 2010.
- [35] Alfred Haar. Zur Theorie der Orthogonalen Funktionensysteme. *Mathematische Annalen*, 69(3):331–371, 1910.

- [36] J.M. Hausdorff, D.A. Rios, and H.K. Edelberg. Gait Variability and Fall Risk in Community-Living Older Adults: A 1-year Prospective Study. *Archives of Physical Medicine and Rehabilitation*, 82(8):1050–1056, 2001.
- [37] Sven Hedlund and Andres Rantzer. Optimal control of hybrid systems. In *Proceedings of the 38th IEEE Conference on Decision and Control*, Phoenix, Arizona, December 1999.
- [38] K. Holmström. The tomlab optimization environment in matlab. 1999.
- [39] V.T. Inman, H.J. Ralston, and F. Todd. *Human Walking*. Williams & Wilkins, 1981.
- [40] A.E. Johnson and M. Hebert. Using Spin Images for Efficient Object Recognition in Cluttered 3D Scenes. *IEEE Transactions on Pattern Analysis and Machine Intelligence*, 21(5):433–449, 2002.
- [41] E. Johnson and T. Murphey. Second-Order Switching Time Optimization for Non-Linear Time-Varying Dynamic Systems. *IEEE Transactions on Automatic Control*, (99):1–1, 2011.
- [42] Vinutha Kallem and Noah J. Cowan. Image-guided control of flexible bevel-tip needles. In *Proceedings of the 2008 IEEE International Conference on Robotics and Automation*, pages 3015–3020, April 2007.
- [43] P. Kannus, J. Parkkari, S. Niemi, and M. Palvanen. Fall-Induced Deaths Among Elderly People. *American Journal of Public Health*, 95(3):422, 2005.
- [44] M.L. Kaplan and J. H Heegaard. Predictive Algorithms for Neuromuscular Control of Human Locomotion. *Journal of Biomechanics*, 34(8):1077–1083, 2001.
- [45] J.R. Knickman and E.K. Snell. The 2030 Problem: Caring for Aging Baby Boomers. *Health Services Research*, 37(4):849–884, 2002.
- [46] A. Kurdila and M. Zabaranin. *Convex Functional Analysis*. Birkhäuser, 2005.
- [47] John M. Lee. *Introduction to Smooth Manifolds*. Springer, 2002.
- [48] B. Lincoln and A. Rantzer. Optimizing linear system switching. In *Proceedings of the 40th IEEE Conference on Decision and Control*, volume 3, pages 2063–2068, 2001.
- [49] E. Lobaton, R. Vasudevan, R. Alterovitz, and R. Bajcsy. Robust topological features for deformation invariant image matching. In *IEEE International Conference on Computer Vision*, pages 2516–2523. IEEE, 2011.
- [50] E. Lobaton, R. Vasudevan, R. Bajcsy, and R. Alterovitz. Local occlusion detection under deformations using topological invariants. In *European Conference on Computer Vision*, pages 101–114, 2010.

- [51] G. Lorini, D. Bossi, and N. Specchia. The Concept of Movement Prior to Giovanni Alfonso Borelli. *Cappozo A.; M. Marchetti; V. Tosi: Biolocomotion, a Century of Research Using Moving Pictures. Promograph Roma, Italy, 1992.*
- [52] D.G. Lowe. Distinctive Image Features from Scale-Invariant Keypoints. *International Journal of Computer Vision*, 60(2):91–110, 2004.
- [53] B.E. Maki. Gait Changes in Older Adults: Predictors of Falls or Indicators of Fear. *Journal of the American Geriatrics Society*, 45(3):313, 1997.
- [54] Stéphane G. Mallat. *A Wavelet Tour of Signal Processing*. Elsevier, 1999.
- [55] I.R. Manchester. Transverse Dynamics and Regions of Stability for Nonlinear Hybrid Limit Cycles. *Arxiv Preprint arXiv:1010.2241*, 2010.
- [56] David Q. Mayne and Elijah Polak. First-Order Strong Variation Algorithms for Optimal Control. *Journal of Optimization Theory and Applications*, 16(3/4):277–301, 1975.
- [57] K. Mikolajczyk and C. Schmid. A Performance Evaluation of Local Descriptors. *IEEE Transactions on Pattern Analysis and Machine Intelligence*, 27(10):1615–1630, 2005.
- [58] R.M. Murray, Z. Li, and S.S. Sastry. *A Mathematical Introduction to Robotic Manipulation*. CRC, 1994.
- [59] RR Neptune and ML Hull. Evaluation of Performance Criteria for Simulation of Submaximal Steady-State Cycling Using a Forward Dynamic Model. *Journal of Biomechanical Engineering*, 120(3):334, 1998.
- [60] RR Neptune, SA Kautz, and ML Hull. The Effect of Pedaling Rate on Coordination in Cycling. *Journal of Biomechanics*, 30(10):1051–1058, 1997.
- [61] MG Pandy, FC Anderson, and DG Hull. Parameter Optimization Approach for the Optimal Control of Large-Scale Musculoskeletal Systems. *Journal of Biomechanical Engineering*, 114(4):450–460, 1992.
- [62] J. Perry, S. Thorofare, and J.R. Davids. Gait Analysis: Normal and Pathological Function. *Journal of Pediatric Orthopaedics*, 12(6):815, 1992.
- [63] B. Piccoli. Hybrid systems and optimal control. In *Proceedings of the 37th IEEE Conference on Decision and Control*, volume 1, pages 13–18. IEEE, 1998.
- [64] Elijah Polak. *Optimization: Algorithms and Consistent Approximation*. Springer, 1997.
- [65] Elijah Polak and Yorai Y. Wardi. A study of minimizing sequences. *SIAM Journal on Control and Optimization*, 22(4):599–609, 1984.

- [66] Lev S. Pontryagin, Vladimir G. Boltyanskii, Revaz V. Gamkrelidze, and Evgenii F. Mishchenko. *The Mathematical Theory of Optimal Processes*. Interscience Publishers, 1962.
- [67] C.C. Raasch, F.E. Zajac, B. Ma, and W.S. Levine. Muscle Coordination of Maximum-Speed Pedaling. *Journal of Biomechanics*, 30(6):595–602, 1997.
- [68] H. Rehbinder and M. Sanfridson. Scheduling of a Limited Communication Channel for Optimal Control. *Automatica*, 40(3):491–500, 2004.
- [69] M. Rinehart, M. Dahleh, D. Reed, and I. Kolmanovsky. Suboptimal Control of Switched Systems with an Application to the Disc Engine. *IEEE Transactions on Control Systems Technology*, 16(2):189–201, 2008.
- [70] Walter Rudin. *Functional Analysis*. McGraw-Hill, second edition, 1991.
- [71] F. Schaffalitzky and A. Zisserman. Multi-View Matching for Unordered Image Sets. *European Conference on Computer Vision 2002*, pages 414–431, 2002.
- [72] T. Schaub, M. Scheint, M. Sobotka, W. Seiberl, and M. Buss. Effects of compliant ankles on bipedal locomotion. In *Proceedings of the 2009 IEEE International Conference on Robotics and Automation*, pages 2186–2191. IEEE Press, 2009.
- [73] OD Schipplein and TP Andriacchi. Interaction Between Active and Passive Knee Stabilizers During Level Walking. *Journal of Orthopaedic Research*, 9(1):113–119, 1991.
- [74] M. Shahid Shaikh and Peter E. Caines. On the optimal control of hybrid systems: optimization of trajectories, switching times, and location schedules. In *Proceedings of the 6th International Workshop on Hybrid Systems: Computation and Control*, pages 466–481, 2003.
- [75] R.W. Sinnet, M.J. Powell, S. Jiang, and A.D. Ames. Compass gait revisited: A human data perspective with extensions to three dimensions. In *50th IEEE Conference on Decision and Control and European Control Conference*, 2011.
- [76] JA Stevens, PS Corso, EA Finkelstein, and TR Miller. The Costs of Fatal and Non-Fatal Falls Among Older Adults. *Injury Prevention*, 12(5):290–295, 2006.
- [77] Héctor J. Sussmann. The “Bang-Bang” Problem for Certain Control Systems in $GL(n, \mathbb{R})$. *SIAM Journal on Control and Optimization*, 10(3):470, 1972.
- [78] Héctor J. Sussmann. A maximum principle for hybrid optimal control problems. In *Proceedings of the 38th IEEE Conference on Decision and Control*, volume 1, pages 425–430. IEEE, 1999.
- [79] D.H. Sutherland. *Gait Disorders in Childhood and Adolescence*. Williams & Wilkins Baltimore, 1984.

- [80] R. Tedrake, T.W. Zhang, and H.S. Seung. Learning to walk in 20 minutes. In *Proceedings of the Fourteenth Yale Workshop on Adaptive and Learning Systems*, New Haven, Connecticut, USA, 2005.
- [81] D.G. Thelen, F.C. Anderson, and S.L. Delp. Generating Dynamic Simulations of Movement Using Computed Muscle Control. *Journal of Biomechanics*, 36(3):321–328, 2003.
- [82] D. Tlalolini, C. Chevallereau, and Y. Aoustin. Comparison of Different Gaits with Rotation of the Feet for a Planar Biped. *Robotics and Autonomous Systems*, 57(4):371–383, 2009.
- [83] Arjan J. van der Schaft. *L2-Gain and Passivity Techniques in Nonlinear Control*. Springer, 1996.
- [84] Ramanarayan Vasudevan, Aaron Ames, and Ruzena Bajcsy. Persistent Homology for Automatic Determination of Human-Data Based Cost of Bipedal Walking. *Nonlinear Analysis: Hybrid Systems*, to appear 2012.
- [85] Ramanarayan Vasudevan, Humberto Gonzalez, Ruzena Bajcsy, and S. Shankar Sastry. Consistent Approximations for the Optimal Control of Constrained Switched Systems – Part 1. *SIAM Journal on Control and Optimization*, in review.
- [86] Ramanarayan Vasudevan, Humberto Gonzalez, Ruzena Bajcsy, and S. Shankar Sastry. Consistent Approximations for the Optimal Control of Constrained Switched Systems – Part 2. *SIAM Journal on Control and Optimization*, in review.
- [87] Ramanarayan Vasudevan, Gregorij Kurillo, Edgar Lobaton, Tony Bernardin, Oliver Kreylos, Ruzena Bajcsy, and Klara Nahrstedt. High Quality Visualization for Geographically Distributed 3D Teleimmersive Applications. *IEEE Transactions on Multimedia*, 13(3):573–584, 2011.
- [88] Ramanarayan Vasudevan, Victor Shia, Aaron Ames, and Ruzena Bajcsy. Automated Identification of Hybrid Dynamical Models of Human Gait. *IEEE Transactions on Robotics*, in preparation.
- [89] Mathukumalli Vidyasagar. *Nonlinear Systems Analysis*. Classics in Applied Mathematics. SIAM, second edition, 2002.
- [90] M. Wada, S. Imura, K. Nagatani, H. Baba, S. Shimada, and S. Sasaki. Relationship Between Gait and Clinical Results After High Tibial Osteotomy. *Clinical Orthopaedics and Related Research*, 354:180, 1998.
- [91] G. C. Walsh, H. Ye, and L. G. Bushnell. Stability Analysis of Networked Control Systems. *IEEE Transactions on Control Systems Technology*, 10(3):438–446, 2002.

- [92] Yorai Wardi and Magnus Egerstedt. Algorithm for optimal mode scheduling in switched systems. In *Proceedings of the American Control Conference*, pages 4546–4551, 2012.
- [93] Yorai Y. Wardi and Magnus Egerstedt. Optimal control of autonomous switched-mode systems: Conceptual and implementable algorithms. Technical report, 2012.
- [94] E. R. Westervelt, J. W. Grizzle, C. Chevallereau, J.-H. Choi, and B. Morris. *Feedback Control of Dynamic Bipedal Robot Locomotion*. Control and Automation. Boca Raton, FL, June 2007.
- [95] D.A. Winter. Biomechanical Motor Patterns in Normal Walking. *Journal of Motor Behavior*, 15(4):302 – 330, 1983.
- [96] Stephen Wolfram. *The Mathematica Book*. Cambridge University Press, 1999.
- [97] Xuping Xu and Panos J. Antsaklis. Optimal control of switched autonomous systems. In *Proceedings of the 41st IEEE Conference on Decision and Control*, volume 4, pages 4401–4406. IEEE, 2002.
- [98] GT Yamaguchi, DW Moran, and J. Si. A Computationally Dfficient Method for Solving the Redundant Problem in Biomechanics. *Journal of Biomechanics*, 28(8):999–1005, 1995.
- [99] William P. Ziemer. *Weakly Differentiable Functions*. Springer-Verlag, 1989.